ENGINE CHARACTERISATION AND CONTROL FOR VEHICLE APPLICATIONS

by

G.S.GILL

A Thesis submitted to the University of Warwick for the degree of Doctor of Philosophy

June, 1978.

ACKNOWLEDGEMENTS

This thesis is the result of research carried out in the School of Engineering Science, University of Warwick. The author is grateful to the University authorities for providing the necessary facilities.

Thanks are also due to Mr.S.Jacques for his close collaboration in the commissioning of the Ward-Leonard system, and the computer management staff of Control Systems Centre U.M.I.S.T. for allowing the use of their facilities. The author is grateful to Dr.E.P. Ryan for his valuable suggestions during the optimal control design studies.

The author is indebted to his supervisor, Dr.M.T.G.Hughes and Mr.D.Shave for their advice and recommendations. The assistance of Mr.A.Hulme in the operation of Sigma 5 is also acknowledged.

Finally, the author is grateful to Mrs.A.M.Shaw for typing this thesis.

ABSTRACT

The work described in this thesis is concerned with methods of reducing the fuel consumption and emissions of pollutants in automobile engines.

Complex interrelationships between fuel economy and generation of pollutants by the conventional spark ignition engine, make it difficult to achieve significant improvements in both these requirements simultaneously. The alternatives to the spark ignition engine also display similar characteristics. Difficulties are aggravated by the insistence of vehicle owners upon retention or promotion of certain characteristics of the present vehicle. Furthermore, the acceptability of an alternative is also governed by the economic climate of the time.

This thesis investigates an innovative concept of cylinder disabling as a means of improving the part-load efficiency of the conventional spark ignition engine. The concept utilizes the well developed technology of the spark ignition engine, therefore implementation can be considered within the available state of the art. The results of studies show that considerable improvements in part-load efficiency are possible. However, the practical problems associated with applications require further studies.

The instrumentation and development of the test facilities necessary for the investigation of engine behaviour are described. A linearized small signal mathematical model of the test bed is developed. The test bed model is used to apply some of the modern concepts in control theory to solve test bed control problems. As a result it has been shown that sophisticated controls are possible with simple practical realizations.

A method is presented for the measurement of emissions under transient conditions with the available low bandwidth equipment. The transient behaviour of the engine is then investigated by considering the engine as a reactor system. The results of these studies and particularly the behaviour of emissions, is thought to be of significant interest due to the pollutant generating processes involved and the consequences of the results on vehicle simulations.

CONTENTS

CHAPTER 1 INTRODUCTION

1.1. General

This thesis is concerned with a study of automotive engine characteristics with a view to the improvement of engine efficiency through an improved control system.

The study was motivated by the recent concern for the conservation of natural resources. Due to the finite nature of world oil reserves, the liquid fuel oil on which the automobiles of today rely for propulsion falls into the category of a natural resource.

At present the transportation sector accounts for 15 percent of the total United Kingdom energy demand (Ref.1.1). However, the quantities are large enough to warrant a reduction in fuel consumption. The total gasoline delivered in the United Kingdom for cars and motor cycles in 1976 was 14.14 million tonnes (Ref.1.2). This represents approximately 50 percent of the total required by the transportation sector for that year.

Results of recent studies (Ref. 1.3 , 1.4) show that the present day vehicle possesses a potential for improvement of fuel economy through the introduction of changes to its drive train system. The means which may be considered for fuel conservation are listed below and indicate the vast scope of the problem.

1. Changes in engine design
2. Changes in fuels
3. Changes in transmission systems
4. Changes in vehicles.

Initially the author's research project was to investigate methods of characterising automobile engines as a basis for simulation studies of hybrid propulsion systems. At the early stages of the project, an opportunity arose to pursue the possibilities of a technique for controlling the output power of the Otto-cycle engine in a way that offered significant fuel savings at part load. Since this was felt to be of significant potential benefit in vehicles having conventional transmissions, vehicles having continuously variable transmissions and hybrid propulsion systems, the direction of research was amended accordingly.

1.2. Background and Constraints

The transportation system in any developed country is dominated by private automobiles. Automobiles themselves are dominated by the familiar spark ignition or Otto-cycle engine. One of the problems associated with automobiles is the tremendous output of materials and energy residuals. The disposal of residuals-solid, liquid, gaseous and thermal wastes, plus noise, imposes a large cost on the community. The residuals are not "disposed of" but merely dispersed in the environment with further costs imposed on the community in the form of degradation of environmental quality.

The environmental pollution due to vehicle exhaust emissions varies in severity depending upon the geographical or meteorological conditions. The case of Los Angeles is well known. Bitter but valuable experience has resulted in action from the authorities in the United States to control the pollutant levels from vehicles by legislation. The level proposed for 1977-79 by the U.S.Environmental Protection Agency (EPA) are :

Unburnt Hydrocarbons (HC)	:	1.5 grams/mile
Carbon Monoxide (CO)	:	15 grams/mile
Oxides of Nitrogen (NO_x)	:	2.0 grams/mile

In March 1975, the EPA administration recommended the following standards to be enforced from 1982 onwards :-

HC	:	0.41 grams/mile
CO	:	3.4 grams/mile
NO_x	:	2.0 grams/mile

Although only three emittants are controlled by legislation, further definitions of the pollutants emitted by a vehicle may be necessary as the need arises. The need to control these pollutants arises because of their effects on man (Ref.1.5).

Products of combustion from vehicles are many and are well documented (Ref.1.5). Emissions of water and carbon dioxide are not considered to be pollutants . Since carbon dioxide has the potential of affecting the weather (greenhouse effect), it may ultimately be considered a pollutant. The amounts of unburnt hydrocarbons, although insignificant from an energy standpoint, can be objectionable from the point of view of odour, photochemical smog or concievably carcinogenic effects. Hydrocarbons in gaseous form plus oxides of nitrogen combine under the action of sunlight to form photochemical smog. The

smog results in irritation of the eyes and affects the respiratory system. Hydrocarbons also show up as particulate matter.

The toxicity of carbon monoxide occurs because the haemoglobin in the blood has a higher affinity for carbon monoxide than oxygen. The effects are functions of exposure time as well as concentration. The result of exposure is headache → vomitting → collapse → coma and finally death. Oxides of nitrogen also tend to settle on haemoglobin. The most undesirable toxic effect of nitric oxides is their tendency to combine with moisture and form nitric acid in the lungs. The level of sulphur dioxide emissions from automobiles is small compared with that released by burning of coal. However sulphur dioxide when combined with fog can cause smog (London, 1952). Also, when combined with moisture at high temperatures it forms sulphuric acid. Sulphur dioxide also combines with other materials in the atmosphere and settles out as particulate matter. Lead emissions are the results of additives to the fuel and can be controlled at the expense of octane rating of the fuel.

The harmful side effects of automobiles discussed above represent only one view -that of actual operation. The transportation system involves not only a colossal vehicle manufacturing industry but also the petroleum and highway construction activities. Other industries such as steel, lead, glass, rubber and plastics are also utilized by the automotive transportation system. The economy as well as the employment of many people depend heavily on the system. The private car also affects the quality of social and cultural life. Widespread use of the vehicle has resulted in low density connurbation townships which no other system can adequately serve.

The affinity between the owner and the automobile is such that energy and environmental problems cannot be solved by the abolition or serious restriction of automobiles in the foreseeable future.

In recent years considerable work has been done to solve the emissions problem of spark ignition engines (Ref.1.6). Solutions for the reduction of pollutants have unfortunately resulted in a decrease in fuel economy. In the light of this, the recent trend is a search for alternatives to the spark ignition engine. Although the alternatives to the conventional engine are many, they all have their shortcomings as far as applications in the near future are concerned. However, considerable potential is apparent which will require further research and development work to materialize.

Meanwhile improvements in the fuel economy are also possible with some changes to the conventional engine. A fuel saving of 10% across the private automobile fleet would supply enough fuel to keep a 600 MW power station, with a thermal efficiency of 30%, operating for one year. In monetary terms, the reduction in fuel consumption of 10% constitutes an annual saving of 120 million pounds.

1.3. Automotive System Analysis

The evolution of an automobile propulsion system has been controlled by economic constraints and the implementation of desirable qualities into the final product. In the early period (1920's), efforts were devoted to overcome driveability problems associated with the vehicle and the engine. With time, the emphasis shifted towards comfort and performance. The Wankel engine , due to its simplicity (less moving parts) and high power to weight ratios, would have been the ideal power unit at this stage. In recent times pressure has been placed on the

reduction of pollutants with complexities introduced a little later by the need for better fuel economy. Thus the engines and vehicles of the future need to show five characteristics :

1. Fuel economy
2. Low emissions of pollutants
3. Adequate speed and acceleration capabilities
4. Good driveability
5. Comfortable ride.

The importance attached to the above points may not be according to the order in which they are written.

In the case of fuel economy, it is interesting to note that considerable "mileage" can be obtained through changes to the conventional vehicles. One estimate for the American vehicles is shown in table 1 (Ref.1.3) at the end of the present chapter. The figures in the table when coupled with the improvements in fuel economy between 15 - 20 percent due to lean engine operation (Ref.1.4) suggest a considerable potential of the present vehicle system. An optimistic speculation that also considers such items as lubricants and improvements in maintenance, suggests a goal of 50 percent improvement in the fuel economy of European gasoline powered cars (Ref.1.7). The alternative engine systems therefore have to compete with the potential of the conventional system.

The principal elements involved in a consideration of automotive power systems are shown schematically in the following diagram.

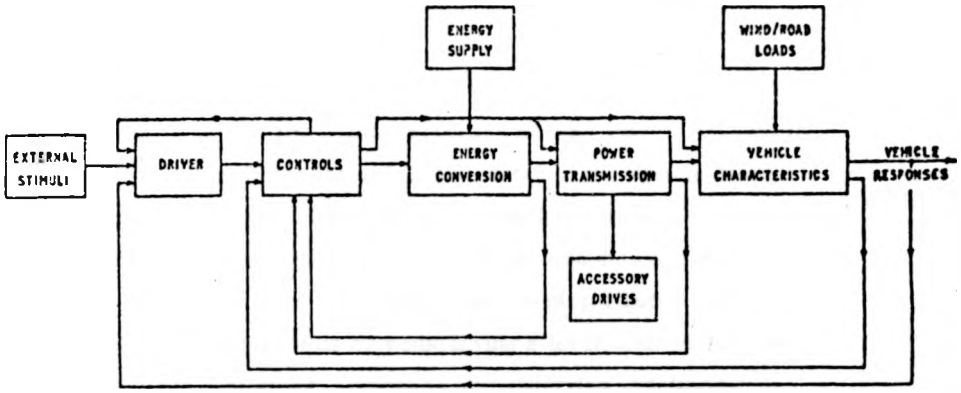

Analysis or simulation of the complete system ideally requires the characterisation of each significant element and of the detailed interconnections between them. The system elements are themselves highly complicated and they interact in complex ways. For example, the insufficient data available permits only a rough estimate of the random fluctuations of external loads on vehicles, resulting from variations in terrain and wind gusts, to be made in specific instances.

An even more difficult problem is the need for characterisation of driving patterns which result from driver responses to "typical" road and traffic conditions. Currently, the combined effects of external stimuli and driving patterns

are represented by vehicle responses , to which pollution levels and fuel consumption are referred in establishing design goals and constraints.

For specific cases such as the one considered in this research study, the characterisation of the vehicle system is simplified by fixing the reference states of the system at an appropriate point. Since the object in this case was to study the effects of engine controls and idealised transmission system on the fuel consumption of the vehicle, the characterisation of the vehicle system was simplified by considering a level road surface and still wind conditions. Further simplification resulted by considering the drive cycles (i.e. a "typical" velocity profile of a vehicle) as a representation of the driving patterns. Hence the problem is transformed from an absolute one, in which the total energy consumption for the production and propulsion of a vehicle would be considered, to a relative one where only the effects of changes to a vehicle drive train are considered.

1.4. Selected Study Elements

The work in this thesis was initiated by a suggestion due to Dr.M.T.G.Hughes. The suggestion was that the conventional spark ignition engine offered a potential for improved fuel economy by reducing the pumping losses. A reduction in pumping losses is realised by disabling a cylinder of an engine. Cylinder disabling is practised by deactivating both the inlet and exhaust valves of a cylinder.

The concept itself is not new. It is believed that it was first introduced in 1916 by the Enger Motor Company on an overhead valve V-12 engine. A manually operated system via an

arrangement of linkages and cams, blocked open the exhaust valves on one of the cylinder banks and shut off the fuel supply to these six cylinders at the same time. It is also believed that during the second world war enterprising individuals practised a form of cylinder disabling by removing the piston and connecting rod assemblies. However, these methods did not realise the full potential of reduction in pumping work and relied more upon the reduction in performance of the vehicle for fuel economy.

The full power of an automobile engine is only utilized during acceleration and high speed cruising. The load on the engine is also high during hill climbing. Under urban stop-go traffic conditions, the mean power required from the engine is low. Thus the operation of the engine is confined to the higher fuel consumption regions resulting in poor fuel economy. In this low efficiency region of the engine, cylinder disabling by reducing the pumping losses increases the efficiency. The idea is similar to a variable displacement engine, the difference being that the displacement is varied in a discrete rather than a continuous manner. With a true continuously variable displacement engine, an added advantage is offered in terms of reduced piston friction which is not realized in the discrete cylinder disabling concept. However, the cylinder disabling method uses the existing well tried engine design, and would require relatively simple modifications. Also, faster response times are possible.

As the processes of interest increase in complexity, the means of understanding of such processes also increase in sophistication. For the assessment of the potential of cylinder disabling an engine test facility was built which allowed

a very fast and accurate communication with the engine (Chapter 3). It must be realized that although accurate measurements can be made on the test bed, any predictions of the vehicle based on these results can only be accurate in the relative sense and not in the absolute sense. This is due to the necessary differences between the engine on the test bed and in the vehicle; such as the length of the exhaust pipe or the air flow meter fitted to the engine intake which can affect the engine performance.

To facilitate rapid testing of the engine without variations due to environmental effects, especially at part engine loads, a two-input two-output controller which controlled the torque and the speed of the engine independently of each other was implemented (Chapter 4). The controller proved to be a useful tool in the determination of optimum engine settings. Modelling of the test bed system, necessary for the design of the controller, also provided a useful insight into the interactions between various elements of the engine test bed system.

Computer simulation has been recognised as a valuable tool in assessing the behaviour of a vehicle with modifications to the drive train. However, the transient behaviour of the engine is little understood. Predictions of pollutant emissions in actual service , based on currently available quasi-static models, are known to yield results with significant error due to the lack of representation of transient effects on pollutant formation. Past work in this field tends to suffer from two important defects :-

1) The dynamics of the exhaust gas analysis system are relatively slow, and thus need to be allowed for in the processing and interpretation of data.

2) The dynamics of pollutant formation in the engine are highly complex, depending on many interacting physical, chemical and thermal processes which at the time of writing are not amenable to detailed computer simulation.

The transient behaviour of the gas analysis system and the engine emissions are discussed in Chapter 5. Also discussed is the behaviour of engine efficiency and the emissions during engine on-off control.

1.5. Arrangement and Contributions of Thesis

This thesis makes the following contributions to the field of test-bed and vehicle system : -

1) Development and application of novel instrumentation and control techniques, such as direct control of fuel-air ratio (Chapter 3), and an independent control of torque and speed (Chapter 4).

The control systems described in Chapter 4 are believed to constitute novel and potential application of existing but advanced control theory. These techniques, perhaps with some further development, could form the basis of highly beneficial developments in test-bed automation in the future.

2. In Chapter 5, a study is made of dynamic modelling techniques for engine pollution production and associated analytical instrumentation under transient engine operation.

3. Investigation, using test bed experiments and computer simulation, of the technique of valve deactivation as a means of improving the part-load efficiency of Otto cycle engines (Chapters 6 and 7).

TABLE 1

Percentage reduction in fuel consumption for small (2100 lb) vehicles over a composite drive cycle (55% EPA urban and 45% EPA highway)

1.	15% reduction in vehicle weight	12%
2.	25% reduction in aerodynamic drag	3%
3.	Improved accessories and accessory drives	1%
4.	Continuously variable transmission	10%
5.	0-60 MPH time increased from 10 to 11 sec	2%

(Source : Ref. 1.3)

References

1.1. "Energy for Road Transport in the United Kingdom." J.Porter and J.W.Fitchie. T.R.R.L. SR 311, 1977.

1.2. "Digest of United Kingdom Energy Statistics." H.M.S.O. 1977.

1.3. "Should we Have a New Engine?" An Automobile Power Systems Evaluation (2 Vols.) Jet Propulsion Laboratory, C.I.T., Aug. 1975.

1.4. Energy Research and Development Administration, Office of Highway Vehicle System, Division of Transportation Energy Conservation, Contractors' Coordination Meeting, Ann Arbor, Mich., May 4-6, 1976. 10th Summary Report, ERDA-76-136.

1.5. "Engine Emissions' Pollution Formation and Measurement." Edited by G.S.Springer and D.J.Patterson. Plenum Press., N.Y., 1973.

1.6. "Current Developments in Spark-Ignition Engines." J.B.Haywood and R.J.Tabaczyniski 1976 S.A.E. 760606

1.7. "Fuel Economy of the Gasoline Engine." D.R.Blackmore and A.Thomas, Macmillan Press, 1977.

CHAPTER 2. AUTOMOTIVE ENGINE SYSTEMS

The subject matter of the present course of study represents an alternative to the conventional vehicle system. It was thought necessary to consider other likely alternatives so as to view the candidacy of cylinder disabling concept in its proper perspective.

A list of alternatives to the conventional vehicle should also contain such items as alternative transportation systems as well as alternative engines or power train systems. However, such an exhaustive list of alternatives covering a wide field can easily prove to be beyond the resources of an individual. A short list on the basis of "likely potential" with respect to fuel economy and exhaust emissions was prepared. Since the object was to obtain some idea about the general state of art, detailed study of each alternative was not undertaken.

2.1. Spark Ignition Engines

Conventional Otto cycle engine

The spark ignition engine employed in most automobiles operates on the four stroke Otto cycle. This engine has been subjected to continuous intensive development for at least 50 to 60 years together with the support technology of fuel supply and maintenance. The improvements achieved over this period have been largely concerned with increase in power to weight ratio, driveability and reliability of the vehicular system. Availability of high octane fuel (lead additives) has given rise to an improvement in specific fuel consumption due to higher compression ratios. However, the recent concern about lead pollution has checked the increase in octane rating of the fuels.

The operation of the engine is idealised by considering the fuel air cycle (Ref. 21) in which the actual properties of the fuel air mixture are considered. The actual cycle exhibits approximately 80% of the indicated work predicted by the fuel air cycle due to heat losses, exhaust blowdown losses, and non-instantaneous combustion losses. Shaft work or the brake power of the engine is lower than the indicated power due to pumping losses and frictional losses. The combined effect of these losses reduces the brake thermal efficiency to a value of about 27% at the point of minimum specific fuel consumption.

Formation of pollutants

There are three main sources of pollutants in most automobiles; fuel tank and carburettor constitute 18% of the total, crankcase vents about 20%, and the rest (62%) are emitted in the exhaust (Ref. 2.2). The evaporative losses from the crankcase vent when led back to the carburettor can easily be burnt. Similarly, the evaporated fuel can be stored and burnt during the engine operation. The primary source of pollutants from an automobile then is the exhaust pipe.

The primary source of energy for vehicle propulsion is derived from crude oil and delivered as hydrocarbon compound. If the hydrocarbon fuel were perfectly combusted only water, nitrogen and carbon dioxide would appear in exhaust gases. Analysis of exhaust gases quickly shows the presence of other species. The products that are considered pollutants and controlled by legislations in certain parts of the world are the oxides of nitrogen, carbon monoxide and unburnt hydrocarbons. The effects of these pollutants are :

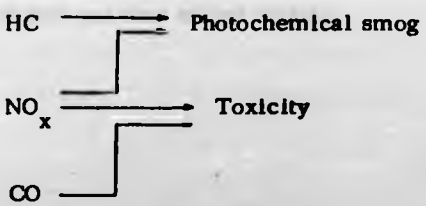

Lead compounds (added to the fuel for better octane requirements) and sulphur present in the fuel also result in emissions of their respective compounds. However, these pollutants can be dealt with by refining of the fuel. Traces of ammonia are always produced in combustion with air but are usually insignificant.

Carbon monoxide (CO) is present in combustion products when there is a deficiency of oxygen on an overall or local basis during the combustion process. "Fuel rich" mixtures therefore increase CO concentration whilst "lean" mixtures reduce the emittant. It is generally assumed that in the post flame combustion products, close to the peak cycle temperatures (2800 K) and pressures (15-40 ATMS), the carbon-oxygen-hydrogen system is equilibrated. As the products expand and cool, oxidation of CO to CO_2 occurs. However, at the lower temperatures the chemical reaction rates are slower, leading to the observed CO in the exhaust gases (Fig. 1).

The principal oxide of nitrogen formed in combustion processes is nitric oxide (NO) and its presence is favoured by high temperatures. Although the temperatures in the post flame products are sufficiently high for large quantities of NO formation, there is insufficient time for the NO to reach equilibrium values. Furthermore, the cooling of the gases during expansion occurs so rapidly that the NO formed has insufficient time to decompose to nitrogen and oxygen. Thus NO is "frozen" and is observed in the exhaust gases (fig. 2).

Unlike nitric oxide and carbon monoxide, hydrocarbons are not expected in high temperature gases. The appearance of hydrocarbons in the products implies that these constituents were never successfully ignited. There are three main conceivable engine conditions that affect the rate of internal heat generation or loss of a parcel of fuel and thus inhibit ignition.

1. The local mixture may be so rich or lean that the reactions are very slow and ignition cannot occur because of heat losses.

2. For isolated elements of fuel, surface to volume ratio may become so large and heat losses consequently so great that ignition cannot occur.

3. Heat losses from fuel air mixture adjacent to a cool surface may prevent ignition.

In an engine the first two items are not of major importance for hydrocarbon formation, but clearly the presence of relatively cool combustion chamber walls can result in heat losses from adjacent mixture. The model of the hydrocarbon formation process based on the quench layer is shown in figure 3 and the hydrocarbons observed in the exhaust gases are shown in figure 4.

Methods of pollutant control

Since all three major pollutants depend upon the fuel-air equivalence ratio (fig.5) the obvious method of control is through this variable. The limiting factor here is the lean burning capability of the engine. The conventional carburettor mixture preparation system which offers a compromise between driveability and economy coupled with simplicity, results in poor homogeneity of mixture and maldistribution of up to 20% (Ref. 2.3) in air fuel ratio between cylinders. Alternative carburettors such as sonic, hot spot, ultrasonic and fuel injection give varying levels of fuel economy (0→22%), obviously influenced by the design of the baseline system used for comparisons. However, the reduction in hydrocarbon and carbon monoxide emissions (50-80%) with these devices suggest an improvement over the conventional system.

Retardation of ignition timing results in reduced peak temperatures in the cylinder and gives higher temperatures through the expansion and the exhaust process. The reduction in peak cylinder temperature results in a reduction in nitricoxide formation. The increase in oxidation activity in the exhaust system due to higher temperatures reduces carbon monoxide and hydrocarbon levels. Changes in the valve timing can be made to increase the residual gases. The trapping of the final portion of exhaust gas which is relatively rich in hydrocarbons not only reduces the hydrocarbon levels in the exhaust but also decreases the nitric oxide formation due to the internal exhaust gas recirculation provided by the increased residual gases in the cylinder.

The control of pollutant formation by adjustments of engine variables can result in adverse effects on driveability and fuel economy which arise on detuning of the engine. This has led to an application of external control devices. Nitric oxide reduction by charge dilution is usually accomplished by exhaust gas recirculation. The dilution of charge reduces the peak cylinder temperature and decreases NO throughput. This method of NO control reduces the power output of the engine. Slower burning rates reduce the engine efficiency and the increased quenching at the cylinder walls increases HC emissions. Because of this, E.G.R. requires ignition retard to reduce HC levels.

Further reductions in emissions can be obtained with a reactor placed in the exhaust system. Such reactors include catalytic converters (reducing for NO and oxidising for CO) and thermal reactors (for HC and CO). The catalytic converters for automobile use consist of an active catalytic material over which the exhaust gases are directed. In a dual bed system the engine is operated "fuel rich" and the exhaust gases containing negligible O_2 are passed over

an NO reduction catalyst. Further downstream air is introduced in the exhaust system before the gases enter a second converter containing an oxidation catalyst for conversion of HC and CO. The function of the reduction converter depends upon the CO/O_2 ratio at the inlet to the converter; therefore a small oxidation converter is sometimes necessary. During cold start transients, the oxidising converter (because it is thermally distant from the engine) cannot do its job properly. Also the downstream converter has to work harder because the engine is operated fuel rich. It is possible to convert all three pollutants simultaneously in a single reactor if the air-fuel ratio of the engine is maintained over a very narrow range about stoichiometric. This has led to the development of so-called "λ-sensor" that responds to changes in the fuel air ratio in the exhaust stream for the application of closed-loop controls. To maintain high catalytic activity, the fuels must be low in concentration of various catalytic poisons such as lead, phosphorus and sulphur. A cause of great concern is the formation of sulphuric acid through the use of catalytic converters.

The oxidation of CO and HC that occurs during the expansion and exhaust stroke can be further enhanced with a thermal reactor. Its function is to promote mixing of gases with secondary air which is injected into the reactor core and also to retain gases at high enough temperature for sufficient time to oxidise CO and HC. However, even with high reactor core gas temperatures complete oxidation is not possible due to incomplete mixing of secondary air. Furthermore "fuel rich" operation of the engine is usually necessary to maintain high reactor core temperature.

The need for exhaust gas emission control therefore results in trade offs with the engine efficiency. Moreover, the pollutant control devices increase the complexity of the system.

Stratified Charge Engines

The promise of low fuel consumption and in latter years the additional promise of low exhaust emissions has accelerated the development of stratified charge engines. As the name implies, the fuel is not distributed uniformly throughout the charge. To achieve satisfactory combustion, 'fuel rich' mixture is created in the vicinity of the spark plug with air or dilute mixture filling the remainder of the cylinder. The concept can be divided into 'open chamber' and 'prechamber' stratified charge engines.

In a prechamber S.C.E. an easily ignitable mixture is set up around the spark plug in a prechamber. The burning jet issuing from the prechamber ignites the lean mixture which has been fed to the main combustion chamber. This prechamber concept sometimes referred to as "jet ignition" was first proposed by Sir Henry Ricardo. The open chamber type of S.C.E. employs a combination of inlet port generated swirl with cup in piston geometry and high pressure timed fuel injection into the combustion chamber to achieve a local fuel rich mixture, whilst the overall fuel air ratio in the chamber is kept lean.

The improvement in efficiency comes from the lower gas temperatures during combustion and expansion which result from lean mixtures used which increases the specific heat ratio and hence the thermal efficiency. Reduced pumping losses and increased compression ratio also increase the efficiency (open chamber). The multifuel capability of the engine is potentially an attractive quality in the light of oil scarcity. The emission characteristics of divided chamber S.C.E. are attractively low, but since the engine is throttled and the compression ratios are relatively low (due to premixed charge), the fuel economy suffers. The open chamber type with its high compression ratio and unthrottled operation gives better fuel economy but can emit smoke and odours (rather like diesels). The reduction of emissions to an acceptable level would require external controls such as E.G.R.

and/or catalytic converters, with some throttling. Therefore trade offs with fuel economy result.

Wankel rotary engine

In the late fifties and early sixties considerable interest was aroused by the development of a rotary engine that operated on the Otto cycle. The major reasons for interest in the Wankel engine are its mechanical simplicity and its high specific output. The disadvantages include the complex geometry of its seals and their durability, the complex housing and combustion chamber shape with large surface to volume ratio which results in high hydrocarbon emissions. The production engine also suffers from poor fuel economy. Due to these problems interest in the Wankel engine has declined significantly in recent years.

Variable displacement engine

The Otto cycle engine exhibits higher efficiency at full throttle than at part throttle due to reduction in throttling losses. The control of power output by throttling the engine can be avoided if the displacement of the engine is varied . Thus higher efficiencies at part loads are realised.

The variation in displacement can be achieved by a swash plate type of mechanism (Ref. 4.4) or by employing linkages between the connecting rod and the crank pin (fig. 6). The variable displacement concept offers considerable fuel savings at part load (fig. 7). The savings in fuel result not only from the lack of throttling but also from the decrease in piston friction due to shorter strokes. The chief disadvantages with these engines are the complexity of the control systems and the slow response times.

2.2. Alternatives to spark ignition engines

The compression ignition engine

The high efficiencies of the diesel engine particularly at part loads are very attractive and make the diesel engine a strong contender as an alternative to the conventional engine. The high efficiency results from the lack of throttling and high compression ratios necessary for compression ignition. The high compression ratios result in poor power to weight ratios. Turbocharging and operation on a two-stroke cycle can improve the power to weight ratio at the expense of added complexities and reduced fuel economy.

There are mainly two types of diesel engines distinguished by the method of combustion. In direct injection (open chamber) diesels the fuel seeks the air and in the indirect injection (prechamber) diesel the air seeks the fuel for combustion. Direct injection diesels have better fuel economy with operation restricted over a narrow speed range. They are noisy and emit smoke more readily than indirect injection diesels.

Although the diesel can meet the 1978 standards for CO and HC with ease, it cannot meet the NO standard. Catalytic methods of NO controls are not applicable to diesels due to high oxygen content in the exhaust. Exhaust gas recirculation reduces NO but the CO and HC increases. Retardation of injection timing has not proved successful. Unregulated emissions such as aldehydes, smoke and particulate emissions pertinent to diesel engines may well be regulated in future. Odour emissions may not be harmful but constitute an obnoxious feature of diesel engines. Although engines are reliable due to initially expensive and robust design, starting and noise are significant problem areas.

In comparing the fuel economy of diesel powered cars with the equivalent gasoline engine vehicle, great care is necessary. The savings normally quoted in the literature are normally based upon equivalent engine capacity or vehicle weight rather than on equivalent vehicle performance. Further anomalies can result because the fuel economy of the gasoline engine is usually sacrificed at full throttle for better performance. A comparison based on equivalent performance plus the comparison of the like with like of the fuel consumption carried out for a number of diesel and gasoline engines shows that on the average the gasoline and diesel engine fuel consumptions are similar (Ref. 2.6).

Stirling engine

Interest has been revived in the Stirling engine due to its potentially high efficiency and low emissions resulting from continuous combustion. Multifuel capability gives the engine a further potential advantage. At the present state the engine requires considerable development to overcome problems such as the sealing of working fluids and control of power output. Advances in materials are necessary to increase the specific power and reduce the costs.

Gas turbine

The gas turbine, due to its simplicity and smooth operation, is thought by many to be the ideal power unit for vehicle applications. Multi fuel capability and good power to weight ratio are additional attractive features. Out of the two possible configurations, namely, the single shaft and twin shaft, the latter is more directly suitable for automotive applications due to its torque speed characteristics.

Although development of the gas turbine has been carried out for many years, high cost and poor part-load efficiency have

delayed its introduction to production vehicles. The chief cause of poor economy is its poor idle fuel consumption. It has a potential as a low emission power unit because it can operate at lean air/fuel ratio. Emission of hydrocarbons is usually not a problem with gas turbines. Smoke emissions can be significant but these can be reduced to low levels with proper injector design. The control of emissions in this case hinges upon the simultaneous control of NO and CO. Combustion temperatures must be high enough to promote oxidation of CO to CO_2 but low enough to decrease the formation of NO.

The main reason for the gas turbine's low efficiency has been the lack of suitable high temperature materials. The use of high temperature ceramics can overcome these problems resulting in a very efficient power unit. The emissions can be reduced by premixing and prevapourising the fuel in a suitably designed combustor. Engine braking, a desirable quality of conventional engines, can be realised in gas turbines by variable geometry nozzles.

The acceptability of the gas turbine as an alternative to the gasoline engine therefore hinges upon the development of suitable materials which is the classical problem with gas turbines.

Rankine cycle engines

Recent developments of rankine cycle engines bring them near to their probable ultimate expectations. The rankine engine can be considered potentially as a very low emission engine. However, Rankine cycles are subject to optimisation for peak efficiency, or reduced size, or reduced cost as a function of the working fluid and design conditions. The best S.F.C. of 0.639 lb/hp.hr which has been achieved (Ref. 2.3) is clearly not adequate. Moreover, the engines require time to build up "steam." These factors make the Rankine cycle unattractive for automotive use.

2.3. Alternative vehicle systems

Electric vehicles

The efficiency range of electric vehicles is limited by the size of the on-board energy storage system. The most common energy storage system is the battery. Available lead acid batteries with low power and energy densities seriously affect the range and performance of the vehicle. Therefore further developments are necessary in this area.

The actual source of energy for charging the batteries would presumably be "off-peak" electricity supplied by the Generating Boards. This would allow a more continuous operation of the generating plants. For long range operation a recharging or replacement networks will be necessary.

Freedom from pollution cannot be claimed for a battery electric vehicle because the source of pollution is merely transferred to the power station. The pollutants may differ in type but may not be less in magnitude or easier to deal with. The energy efficiency of an electric vehicle is a function of range and performance (fig.8). The overall efficiency of the conversion of fuel to propulsion depends heavily upon the efficiencies of energy storage and the propulsion motor together with its control system.

Hybrid vehicle

Hybrid vehicles utilize two or more sources of power for vehicle propulsion such that the combined effect gives the desired characteristics. Commonly a hybrid vehicle consists of a heat engine and an energy storage unit. The energy storage system can be electrochemical, kinetic, thermal or fluidic. The aim is to operate the engine at its best efficiency whilst the energy storage unit supplies the

transient power to or from the vehicle. The energy storage thus acts as a low pass filter that decouples the engine from the vehicle. The system therefore offers a fuel saving potential through efficient engine operation and recuperation of braking energy. Hybrid vehicles can be classified into parallel and series systems. In the series system all of the engine power is converted to electrical energy and is transferred back to mechanical energy at the wheels. The resulting controls for such a system are simple and easy to implement, however the penalty is a reduction in overall efficiency. In the parallel system the power from the prime mover may be used to charge the energy store, propel the vehicle, or both.

The hybrid system requires an energy store with high power and energy densities. Currently lead acid batteries appear to be the favourites due to ease of control, available technology and safety (Ref. 2.7). High speed flywheels offer high power densities but they require special containers to minimize drag losses and to contain the flywheels in the event of accident. An interesting development is the combined use of low speed flywheel and battery pack (Ref. 2.8) that tries to overcome the power and energy density problems. The use of nickel cadmium batteries is another development (Ref. 2.9). Fluidic storage in the form of compressed gas has an advantage in that the waste exhaust heat from the engine can be utilised. Such a potential energy store would necessarily utilise hydrostatic drive systems which are inefficient and noisy. The storage system may also be potentially dangerous in the event of accidents.

As is obvious, the fuel economy of the hybrids may be expected to be best in stop-go driving. This feature makes hybrids suitable for delivery vans as well as private vehicles. Motorway driving does not offer any benefits but reduces the top speed of the vehicle due to the

"dead" load of the energy store. Larger engines used for higher speeds or for towing will result in fuel penalties, particularly if the engine is operated at constant power and speed. This type of engine operation moreover gives integration problems with the energy store. The need therefore is to operate the engine over a range of power levels. One method of varying the power is by on-off operation of the engine such that the operation of the engine is confined to its most efficient regions. Variations in the engine on-off frequency will then result in a control of average power delivered by the engine. However, on-off operation of the engine results in restarting problems of the type investigated in Chapter 5. Further understanding of the individual components of the hybrid power train is necessary to assess its full potential.

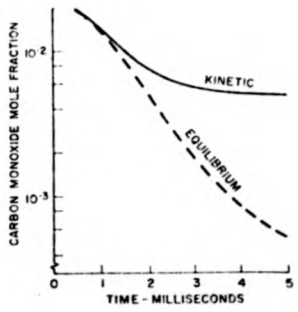

Fig. 1 Carbon monoxide concentration as a function of time following combustion. [REF. 2.2]

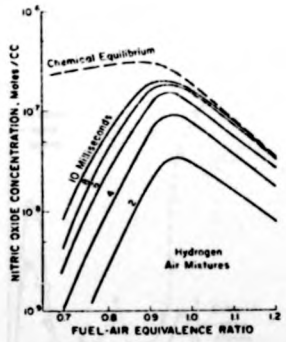

Fig. 2 Nitric oxide concentrations as a function of equivalence ratio and time after combustion. [REF. 2.2]

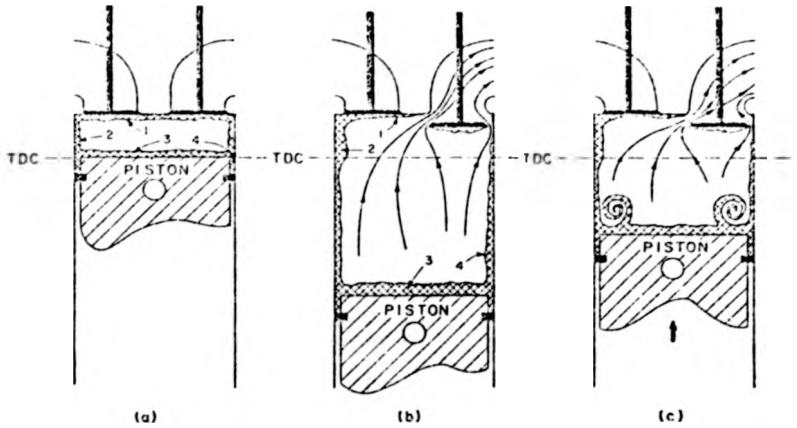

FIG. 3 Schematic summarizing processes important in hydrocarbon emissions. (a) Formation of quench layers 1, 2, 3 and crevice quench 4 as flame is extinguished at cool walls. Not to scale, quench layers are about 0.003 in. thick. (b) Gas in quench volume between piston crown and cylinder wall above the first ring, 4, expands as cylinder pressure falls and is laid along cylinder walls. When exhaust valve opens, head quench layers 1 and 2 exit cylinder. (c) Roll-up of hydrocarbon-rich cylinder wall boundary layer into a vortex as piston moves up cylinder during exhaust stroke.

[REF. 2.10]

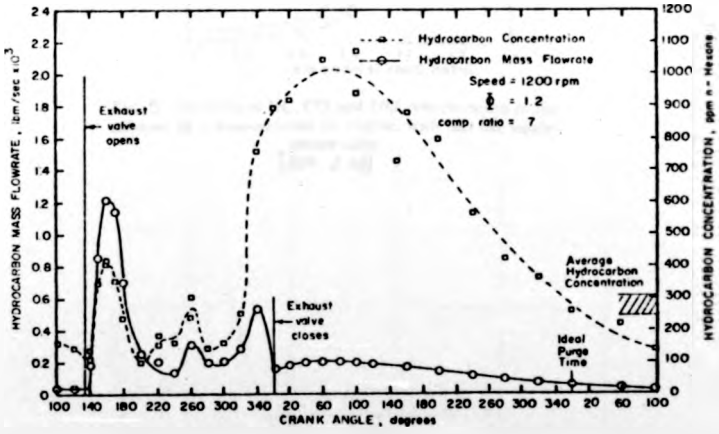

Fig. 4. Hydrocarbon concentration and total hydrocarbon mass flow rate emitted from a single-cylinder spark-ignition engine as a function of crank angle.

[REF. 2.2]

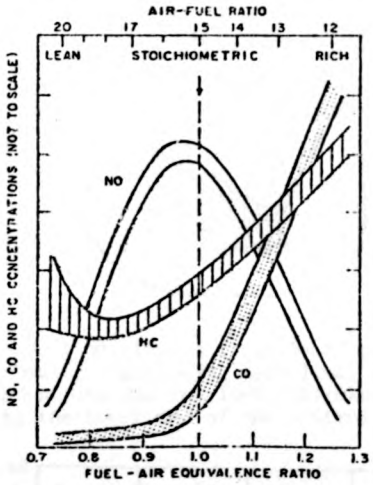

FIG. 5 Variation of HC, CO and NO concentration in the exhaust of a conventional SI engine, with fuel-air equivalence ratio.
[REF. 2.10]

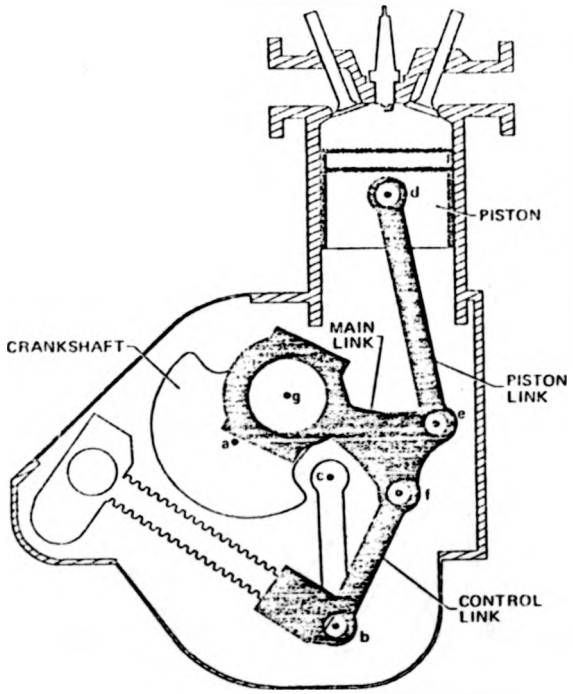

Fig. 6 - Section view of variable displacement engine showing crankshaft, main link, piston link, and stroke control link. Stroke is varied by moving the lower end of the control link [REF. 2.5]

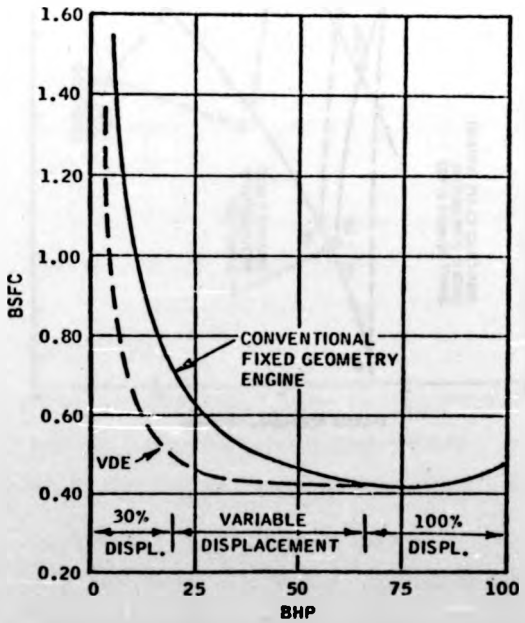

Fig. 7 - Typical bsfc versus power comparison for fixed and VDEs at 1600 rpm [REF. 2.4]

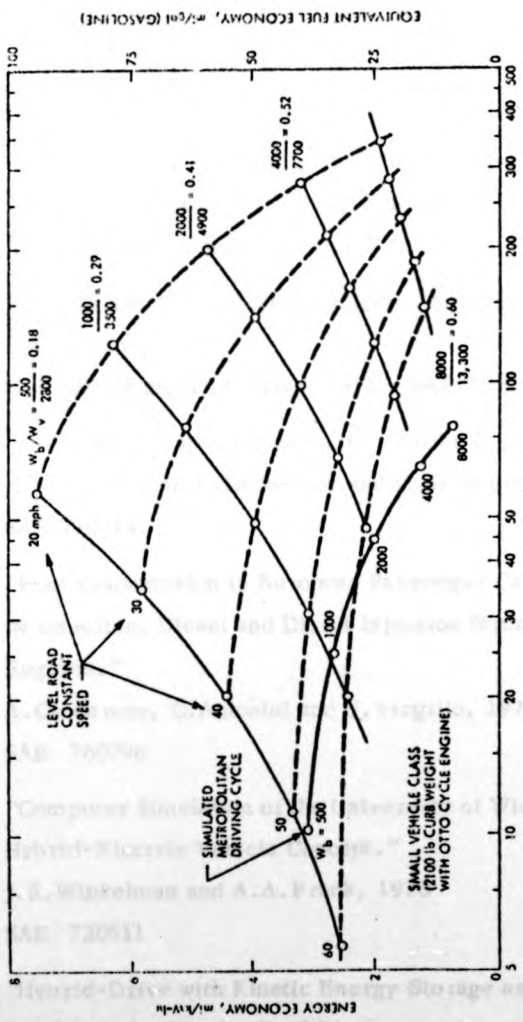

FIG. 8. Energy economy vs range for lead-acid electric car [Ref. 2-3]

References

2.1. "The Internal Combustion Engine in Theory and Practice." Vol.1, second edition, M.I.T. Press, 1966 C.F.Taylor.

2.2. "Engine Emissions. Pollutant Formation and Measurement." G.S.Springer and D.J.Patterson. Plenum Press, New York, 1973.

2.3 "Should we have a New Engine? An Automotive Power Systems Evaluation." Vol.II, Aug. 1975. Jet Propulsion Laboratory, C.I.T.

2.4. "The Variable Displacement Engine: An Advanced Concept Power Plant." H.W.Welsh and C.T.Riley. 1971. SAE 710830.

2.5. "A Variable Displacement Spark Ignition Engine." H.N.Pouliot, W.R.Delameter and C.W.Robinson, 1977 SAE 770114.

2.6. "Fuel Consumption in European Passenger Cards powered by Gasoline, Diesel and Direct Injection Stratified Charge Engines." A.Ciccarone, C.Antonini and U.Virgilio, 1976 SAE 760796

2.7. "Computer Simulation of the University of Wisconsin Hybrid-Electric Vehicle Concept." J.R.Winkelman and A.A.Frank, 1973 SAE 730511

2.8 "Hybrid-Drive with Kinetic Energy Storage as Vehicle Drive." J.Helling. Institut fur Kraftfahrwesen. Proc. 3rd International Electric Vehicle Symposium, Feb.1974

2.9. "Hybrid Vehicle for Fuel Economy." L.E.Unnewehr, J.E.Auiler, L.R.Foote, D.F.Moyer and H.L.Stadler, 1976 SAE 760121.

2.10. "Pollutant Formation and Control in Spark Ignition Engines."
John B. Heywood
Prog. Energy Combst. Sci. Vol.I , 1976, Pergamon Press.

CHAPTER 3 DEVELOPMENT OF THE TEST FACILITY

3.1. The Structure of the Test Facility

Since an engine is a complicated system and not readily amenable to analytic solutions, a test facility was developed to investigate its behaviour experimentally. The test facility consisted of an engine test cell that housed the engine-dynamometer system, together with the transducers and the actuators. The cell contained a cooling water supply for the heat exchangers necessary for the cooling of the engine. An air extraction system was available to prevent a build up of dangerous fumes within the cell. Separate blowers were incorporated to provide control of the air temperature because the existing system was found to be inadequate for prolonged engine tests.

The measurement and control was carried out from the control cell which was located next to the engine cell. Instrumentation and controls were arranged to provide rapid and accurate communication with the engine dynamometer system. The electrical signal levels were made compatible with the school's computer for data logging.

Figures 1 and 2 show the test bed and the control cell respectively.

The Engine

The engine capacity was chosen for its applicability to hybrid propulsion system studies and was representative of the design used to power a large selection of vehicles encountered on the road. The chosen engine was a four cylinder inline unit with a capacity of 875 cc. It had an overhead camshaft and the cylinder head and block was constructed from aluminium.

The engine was mounted on the test bed with an orientation similar to that in the production vehicle. Due to practical constraints a longer than the standard exhaust pipe was connected to the standard exhaust system.

The engine was coupled to the dynamometer by a shaft that had hardy spicer type of end joints. A flexible coupling was designed (Fig. 3) to improve the fatigue life of the transmission shaft. A containment ring was fitted around the shaft as a safety precaution in case of shaft failure.

The Ward-Leonard System

The system consisted of a d.c. generator driven by an auto-synchronous motor. The generator was electrically connected to a d.c. motor, which was coupled to the engine and was used as a regenerative dynamometer (Fig. 4).

Speed control of the engine/dynamometer system was achieved by the control of voltage supplied to the generator field. The control of the generator field voltage was effected by the control of the conduction angle of a thyristor stack arranged for full wave rectification. Although the Ward-Leonard system has inherent speed control due to the back e.m.f. of the dynamometer, the system had in addition a closed loop speed control with integral action to remove steady-state offsets.

The system contained various safety interlocks incorporated for protection, the most important of which was the loop contactor. The loop contactor prevented currents greater than the design value (100A) from flowing through the loop. A particular feature of the control relay scheme was the provision of two methods of shutting down the system. Normal procedure simultaneously

removed the supplies from the dynamometer field, the thyristor unit loop contactor and the ignition system, which allowed the engine dynamometer combination to coast to standstill. The emergency stopping procedure switched off the supply to the generator field and the ignition, but ensured that the loop contactor remained closed with the dynamometer field supply on, thus achieving a rapid deceleration by means of regenerative braking.

The start up and shut down procedures are described in Appendix I.

3.2. Instrumentation

Exhaust gas analysis system

The concern for the pollution of the environment has resulted in extensive studies of engine exhaust emissions. Pollutant formation resulting from any alteration or modifications to the engine power conversion processes are of great interest. With these thoughts in mind, measurement of emissions was considered to be imperative for the proposed course of study. Because of their environmental impact oxides of nitrogen, hydrocarbons and carbon monoxide are considered to be the major pollutants. Therefore these pollutants were of major interest for the present course of engine studies.

The system used can be divided into two parts, one dealing with the sampling and preparation of the exhaust gases and the other with the analysis. The system set-up is shown in Figure 5. The gas sample was drawn from the exhaust pipe via a stainless steel tube. Before passing through a paper filter the sample was cooled in an ice bath and the condensate was removed by a pump. A diaphragm type positive displacement pump set at maximum flow rates was used to draw the sample from the engine exhaust pipe to reduce the time

delays whilst the excess sample was bypassed.

The concentration of carbon monoxide in the exhaust was measured by means of a non-dispersive infrared (NDIR) analyser. The NDIR gas analyser utilizes as its detection principle the absorption of infrared energy by a quantity of the gas to be analysed. "Non-dispersive" refers to the fact that the energy involved is not resolved into discrete spectral levels, but instead involves broad but distinctive absorption regions within infrared. The instrument consists of a sample cell and a reference cell with the infrared energy sources positioned at one end of each cell and a detector charged with carbon monoxide at the other end (Fig.6). The detector consists of two chambers separated by a flexible diaphragm. In operation, the presence of carbon monoxide in the sample cell results in an energy absorption in the cell and thus a reduction in the energy supplied to the detector, whilst the energy absorption in the reference cell is negligible and constant. The difference in the energy received by the detector chambers results in a movement of the diaphragm due to pressure differences. The diaphragm and the adjacent stationary plate form a variable capacitance which is measured and related to the concentration level in the sample cell. Optical filters are used to select the infrared bands of interest to minimize interference with other gases. Stability of drift is obtained by mechanical "chopping" of the infrared light beams.

Nitric oxide (NO) concentration was measured with a chemiluminescence gas analyser. The method utilizes the reaction of NO with ozone to produce NO_2 at an excited state. The excited molecules spontaneously relax to the unexcited state with a release of a discrete quantity of photo energy. Measurement of this energy by a photomultiplier provides a measurement of NO_2 and hence NO.

delays whilst the excess sample was bypassed.

The concentration of carbon monoxide in the exhaust was measured by means of a non-dispersive infrared (NDIR) analyser. The NDIR gas analyser utilizes as its detection principle the absorption of infrared energy by a quantity of the gas to be analysed. "Non-dispersive" refers to the fact that the energy involved is not resolved into discrete spectral levels, but instead involves broad but distinctive absorption regions within infrared. The instrument consists of a sample cell and a reference cell with the infrared energy sources positioned at one end of each cell and a detector charged with carbon monoxide at the other end (Fig.6). The detector consists of two chambers separated by a flexible diaphragm. In operation, the presence of carbon monoxide in the sample cell results in an energy absorption in the cell and thus a reduction in the energy supplied to the detector, whilst the energy absorption in the reference cell is negligible and constant. The difference in the energy received by the detector chambers results in a movement of the diaphragm due to pressure differences. The diaphragm and the adjacent stationary plate form a variable capacitance which is measured and related to the concentration level in the sample cell. Optical filters are used to select the infrared bands of interest to minimize interference with other gases. Stability of drift is obtained by mechanical "chopping" of the infrared light beams.

Nitric oxide (NO) concentration was measured with a chemiluminescence gas analyser. The method utilizes the reaction of NO with ozone to produce NO_2 at an excited state. The excited molecules spontaneously relax to the unexcited state with a release of a discrete quantity of photo energy. Measurement of this energy by a photomultiplier provides a measurement of NO_2 and hence NO.

The instrument used oxygen supply to generate ozone and the excess ozone was destroyed by passing it through an absorber to reduce toxicity of the discharge stream. As indicated above, NO_2 in the sample must be reconverted to NO before it will respond in the measurement. The conversion is carried out by heating the sample at a temperature of $600^{o}F$ and converts approximately 90% of NO_2 into NO. Therefore a check of converter efficiency is essential. However, since NO_2 in the exhaust is only 2 - 3% of the total nitric oxides, measurement of NO only, was undertaken. The schematic of the chemiluminescence analyser is shown in Figure 6.

A flame ionisation detector (FID) was utilized for the measurement of unburnt hydrocarbons. It makes use of the principle that very few ions are present in a flame produced by burning hydrogen. However, if hydrocarbon is introduced the ion flux is increased which is proportional to the hydrocarbon. The basic elements of FID are a burner and collector assembly (Figure 6).
In practice, sample gas is mixed with hydrogen in the burner assembly and the mixture burned in a diffusion flame. Ions that are produced in the flame move to the negatively polarized collector under the influence of an electrical potential applied between the collector plates. At the negative collector the ions receive via a current network, electrons that are collected from the flame zone at the positive collector. Thus a small current flows which after amplification relates to the hydrocarbon present. The detector responds to carbon that is linked with hydrogen, therefore the detector is essentially a carbon counter.

The signal levels out of all the three instruments were amplified and filtered through a second order Butterworth filter with the cut off frequency at 20 Hz. The circuit diagram is shown in Figure 7. Initially the sensitivity of each analysis equipment

was checked by applying the calibrating gas other than the one to which the equipment was sensitive. Each equipment in turn was calibrated by applying a gas of known concentration. The flow rates through each device were fixed at manufacturer's recommended levels and strictly adhered to for actual tests carried out on the engine. This is crucial for the analysers are sensitive to the amount of matter and not the concentrations, e.g. the F.I.D. counts the carbon atoms , therefore an increase in flow rate for a given concentration would result in higher output. In this respect the chemiluminescence analyser did not present any problem, for it had an inbuilt regulating mechanism and NDIR is not very sensitive to "small" changes in flow rates. The F.I.D. response on the other hand, is very sensitive to the fuel and air flow rates as well as the sample flow rates. The flow rate into the detector head of the F.I.D. analyser was monitored by an inclined manometer and regulated by a weighted valve. Finer regulation was obtained by allowing the gas to escape through a paraffin bubbler.

The calibrating gases for gas analysis equipments consisted of the mixture of the constituent gas with nitrogen. Although hexane is the nearest equivalent to gasoline, it was not used as a calibrating gas for the F.I.D. because hexane changes into liquid state inside the storage vessels at room temperatures. In this respect propane has much better characteristics. For the interpretation of propane calibration S.A.E. recommended practice of expressing the results as parts per million of carbon (PPMC) was adopted. That is one ppm propane (C_3H_8) is the equivalent of 3 ppmc hydrocarbons.

The calibration curves are shown in Figure 8. Since the response of CO analyser is non-linear, an equation was fitted to the measured point for ease of computation. The equation is :

$$\% CO = 0.0476\ V^2 + 0.635V$$

The operating pressure for the gas analysis equipment is discussed in Appendix I. The engine emissions data is normally presented as quantity rather than concentration. The conversion from concentration to mass flows is also discussed in Appendix I.

Measurement of Torque

The engine torque was measured at the dynamometer casing with a strain gauge load cell. A shaft torque measurement was considered , but it was thought that high stiffness of the shaft would result in a high signal to noise ratio. For the torque measurement, a stiff load cell was chosen to ensure that the dynamics of the load cell and dynamometer were outside the frequency range of the other components of the test bed system. Tests showed that the natural frequency of the dynamometer casing and load cell was at 25 Hz. The signal from the load cell was amplified using a voltage gain of one thousand. The components of the amplifier were chosen to give a common mode rejection of 60 DB. A second order Butterworth filter was built with a cut-off frequency at 5 Hz to filter the measurement noise.

A permanent lever system was attached to the main test bed frame to facilitate rapid calibration checks of the load cell. Calibration checks were necessary to ensure the absence of hysteresis and dead zone at zero torque in the load cell characteristics.

Measurement of Speed

An A.C. tacho driven by the dynamometer provided a measure of the dynamometer speed. The tacho signal was rectified and filtered via a simple lag with a time constant of 0.05s to obtain a smooth signal. Before rectification the signal was also fed to a speed indicator gauge to provide a visual indication of speed.

An independent means of engine speed measurement was made by utilizing the signal from the toothed disc fitted to the flywheel primarily for ignition timing control. The circuit diagram of the system is shown in Figure 9.

3.3. Measurement and Control Systems

Coolant and Lubricant Temperature Control

For test bed applications, control of engine coolant temperature is vital, since the performance of the engine is strongly dependent upon the operating temperatures. The control of lubricant temperature is also necessary for changes in the lubricant properties due to temperature changes can result in higher frictional losses for a reduction in temperature and a breakdown in lubrication at high temperatures. The normal method of engine coolant temperature control utilizing a thermostat is unsatisfactory, for there is no provision for the removal of steady state off-sets. Therefore it was decided to implement closed-loop temperature control with integral action on both coolant and lubricant temperatures.

A negative coefficient thermistor was used to measure the coolent temperature in the thermostat housing and similarly the oil temperature was measured at the oil gallery. Since the control schemes adopted for coolant and lubricant temperature control were similar, only the coolant temperature control scheme will be discussed.

The system consisted of a motor driven valve, the position of which diverted the flow of engine jacket cooling water to a contra-flow heat exchanger. The valve was driven by a constant speed a.c. reversible motor which was stopped by an electromagnetically operated friction brake as soon as the current to the motor was switched off. A feedback control was implemented on the valve

position to obtain a tight inner control loop. The operation of the motor resulted in a position control of "on-off" type with a dead zone. The dead zone was minimized by implementing large gains in the position control to ensure decisive triggering of the triacs (Fig.10). With the gains chosen, the dead zone was less than 1% of the full travel of the valve.

Initially the frequency response between the valve position and the coolant temperature was measured with the engine operating at mid-power. A feedback gain of 2.5 and an integral time constant of 6.8s were chosen to obtain a gain margin of 10 dB and a phase margin of 90^{o}. The circuit diagram of the temperature measurement and the controller is shown in Figure 10.

Similarly for the oil temperature controller, an integral time constant of 6.8s and a unity gain gave a gain margin of 6.4 dB and a phase margin of 50 degrees.

Ignition timing control

Optimisation studies of the engine and particularly due to the effect of ignition on the pollutant behaviour necessitates some means of ignition timing control. The conventional system, although simple and very reliable, does suffer from inaccuracies resulting from mechanical imperfections. Therefore it was decided to implement an electronic means of ignition timing control. The system consisted of two electromagnetic transducers which monitored the rotation of the crankshaft. A toothed disc with its teeth space by two degrees of the crankshaft rotation was fitted to the flywheel of the engine. The use of the existing starter ring gear was considered. However, it was thought that the resulting inaccuracies due to non-symmetry in the leading and trailing edges of the gear teeth and due to non-symmetry in the teeth warranted the use of a more accurate toothed disc. Two dowels were fitted to the disc spaced by 180 degrees of crankshaft

and a transducer was mounted such that it detected the position of the dowel at 50^{o} deg. B.T.D.C.

The outer transducer (Fig.11) produced a sinewave corresponding to 2 deg. of crankshaft rotation. The signal thus derived was passed via the signal conditioning unit to an AND gate. The signal conditioning circuit was such that the input to the gate was a square wave corresponding to the one degree rotation of the crankshaft. Similarly the output from the inner transducer was also conditioned and fed to the second input of the AND gate via a bistable. Thus, the AND gate was turned on as soon as the piston was detected 50 deg. B.T.D.C. The output from the AND gate was passed via a six bit binary counter and its associated circuitry to a comparator. The comparator compared the demanded timing analogue voltage with the staircase from the binary counter. As the demanded timing equalled the actual timing, a pulse from the comparator triggered the ignition firing circuit. At the same instant the binary counter and the bistable are reset.

The above described system controlled the timing between 50 deg B.T.D.C. to 14 deg A.T.D.C. with an accuracy of $\pm \frac{1}{2}$ deg.

Throttle Position Control

A closed-loop position control was implemented on the throttle position to facilitate static and dynamic testing of the engine. An electro-hydraulic servo system was utilized for the purpose of position control. In such systems, low-power electrical signals are processed to control high-level hydraulic power resulting in a rapid response control system. The alternatives such as pneumatic systems suffer from compressibility problems, hence the action is not positive. Electrical servomotors require gearboxes to provide

and a transducer was mounted such that it detected the position of the dowel at 50^{o} deg. B.T.D.C.

The outer transducer (Fig.11) produced a sinewave corresponding to 2 deg. of crankshaft rotation. The signal thus derived was passed via the signal conditioning unit to an AND gate. The signal conditioning circuit was such that the input to the gate was a square wave corresponding to the one degree rotation of the crankshaft. Similarly the output from the inner transducer was also conditioned and fed to the second input of the AND gate via a bistable. Thus, the AND gate was turned on as soon as the piston was detected 50 deg. B.T.D.C. The output from the AND gate was passed via a six bit binary counter and its associated circuitry to a comparator. The comparator compared the demanded timing analogue voltage with the staircase from the binary counter. As the demanded timing equalled the actual timing, a pulse from the comparator triggered the ignition firing circuit. At the same instant the binary counter and the bistable are reset.

The above described system controlled the timing between 50 deg B.T.D.C. to 14 deg A.T.D.C. with an accuracy of $\pm \frac{1}{2}$ deg.

Throttle Position Control

A closed-loop position control was implemented on the throttle position to facilitate static and dynamic testing of the engine. An electro-hydraulic servo system was utilized for the purpose of position control. In such systems, low-power electrical signals are processed to control high-level hydraulic power resulting in a rapid response control system. The alternatives such as pneumatic systems suffer from compressibility problems, hence the action is not positive. Electrical servomotors require gearboxes to provide

adequate torque for throttle spindle acceleration. The stepping motors on the other hand can provide adequate torque but their output is quantised. The main disadvantage of the hydraulic system is that bulky power supplies and complicated electro-hydraulic valves are necessary. However, the action of control is very rapid and can be very precise.

The system used consisted of a high pressure oil supply unit that supplied oil to the servo valve at relatively constant flow rates, regardless of the discharge pressure. The excess flow was bypassed to the oil reservoir. An oil cooler was found to be necessary to prevent an excessive rise in the oil temperature due to prolonged running of the equipment. The servo valve (Fig. 12) which is vital to the control system chain transforms electrical signals to fluid flow. It consists of an electrically controlled flapper, the position of which modulates the flow out of a nozzle. The change in the flow rate results in a difference in pressure on the end faces of the spool valve. The resulting motion of the spool valve thus controls the flow to the actuator. A mechanical link between the flapper and the spool valve provides a feedback control between the flapper position and the spool valve position. The flow of oil was directed to a double acting actuator linked to the throttle spindle.

The closed loop operation of the throttle position control is described with reference to figure 12. The angular position of the throttle spindle as measured by the feedback potentiometer was compared with the demanded position. The resulting error signal was applied to the flapper valve control, thus causing the position of the throttle to alter. The controller gain was set at a value of 2.0 and integral action to remove steady state errors was not found to be necessary, since the fluid flow was converted to the actuator position, thus providing inherent integral action. The frequency response of the closed loop system (Figure 13) shows the system essentially of second order with ninety degree phase crossover at 27Hz.

Fuel-air ratio control

Any form of serious engine testing requires fuel control of some form. The metering provided by the standard carburettor settings is a compromise between efficiency and performance. For non-standard engine operation necessary for the proposed course of studies, fuel-air ratio control was thought to be vital.

The fuel-air ratio control required a continuous measurement of fuel flow and air flow. A commercially available fuel measurement system that operated on a hot film principle was used. The measurement system gave a linear electrical output for changes in flow rates and was compensated for temperature changes. The system bandwidth extended up to several kHz. The engine carburettor was modified and the flow transducer was fitted between the float chamber and the jets. Initially the system was calibrated for flow rates under a constant head of pressure and when fitted to the engine the values of fuel flow were compared with those obtained by the traditional gravimetric methods . Under typical engine operating conditions, the comparison was within 2%. Although the transducer was compensated for temperature changes, a heat deflector shield was fitted between the transducer and the engine manifolds to prevent large changes in the temperature. Furthermore, the likelihood of vapourisation of fuel whilst flowing through the transducer was reduced by blowing cool air over the transducer and the heat shield.

The measurement of intake air flow was necessary for the implementation of the control scheme and it was also essential for the conversion of emissions data to standard form.

A viscous flow meter was used for air flow measurement because it is not adversely affected by the pulsating flow. The flow meter output (in the form of a pressure head) was proportional to the flow rate. The pressure head was converted to an electrical signal by a micromanometer. A digital thermometer was employed to monitor the temperature of the inlet air flow. Since prolonged engine operation can result in large changes in the air temperature, and hence the performance of the engine, means were provided to blow manually controlled quantities of cool air into the cell. In this manner it was possible to control the inlet air temperature changes.

The operation of the fuel-air ratio control is described with reference to figure 14. The system consisted of an electrical-to-pressure converter, the output pressure of which was applied to the carburettor float chamber. The converter consisted of an externally fed air chamber, the pressure of which was regulated by 'bleeding' air into a separate vacuum chamber. The air flow was regulated by adjusting the opening of an orifice electrically. The settings of the converter were adjusted to give a change in the output pressure within the range of + 15 cm and - 10 cm of water. Higher vacuum levels resulted in a reverse flow through the fuel transducer, resulting in positive feedback.

The control of fuel air ratio was achieved by applying a feedback control on the fuel flow with a proportional-plus-integral action to remove offsets. The fuel-air ratio control then consisted of making the fuel flow proportional to the measured air flow. The constant of proportionality was adjustable and represented the fuel air ratio setting. The frequency response of the fuel flow with respect to the throttle position is shown in figure 15.

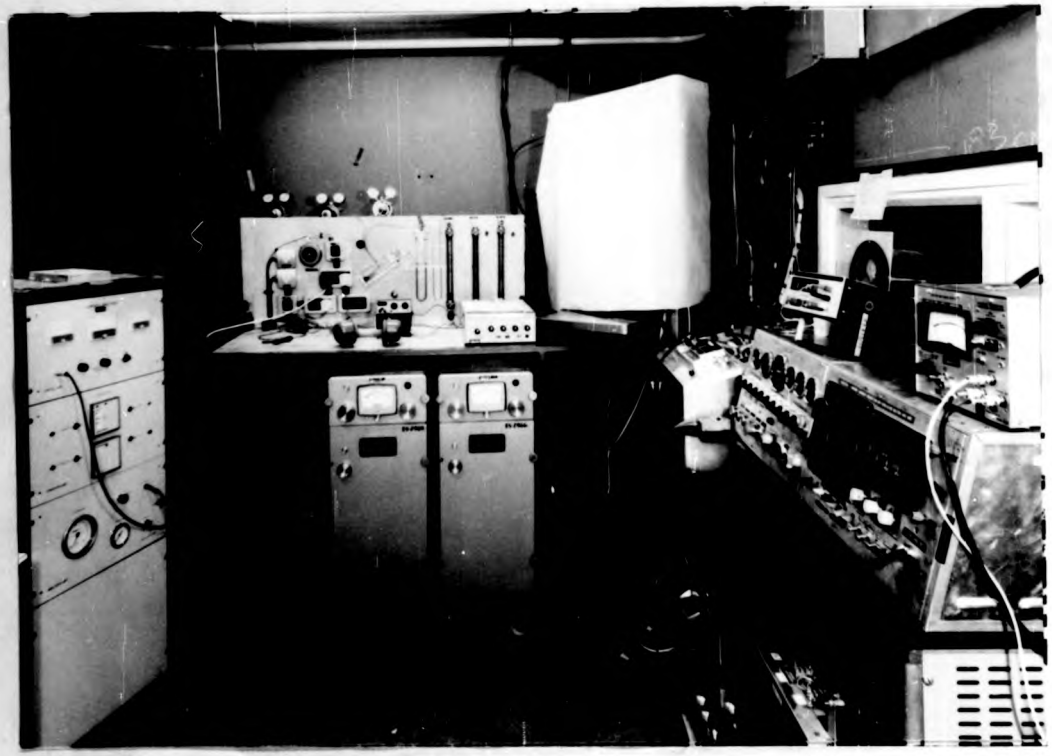

CONTROL CELL

FIG.1

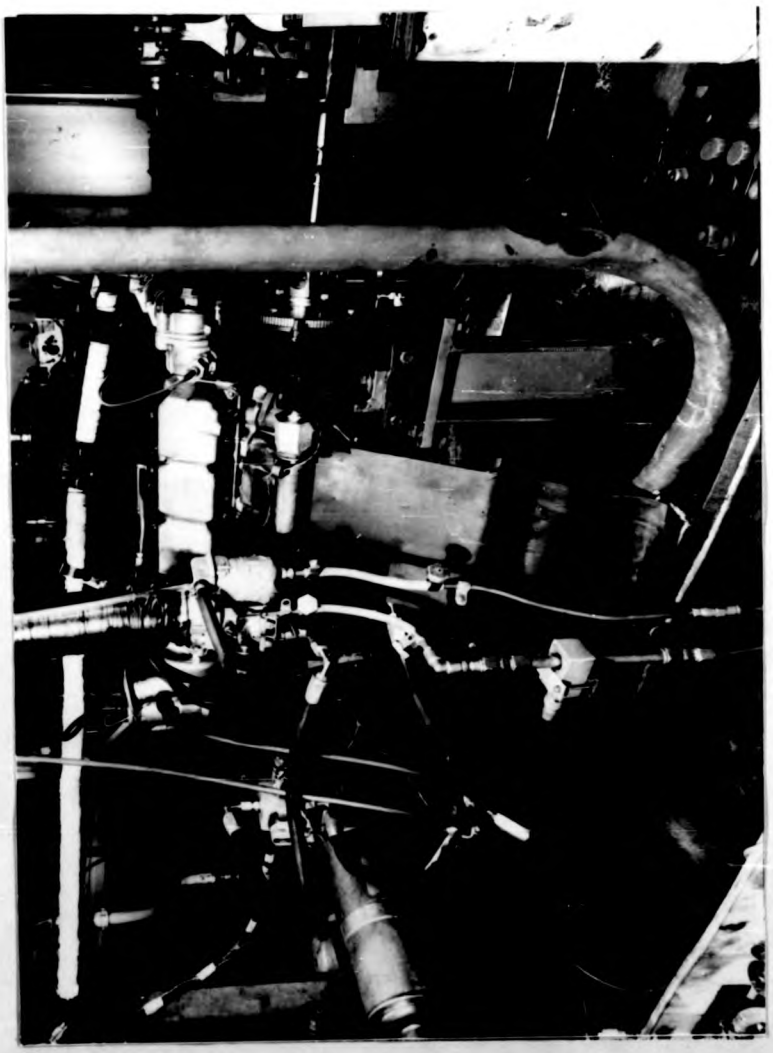

ENGINE TEST BED

FIG.2

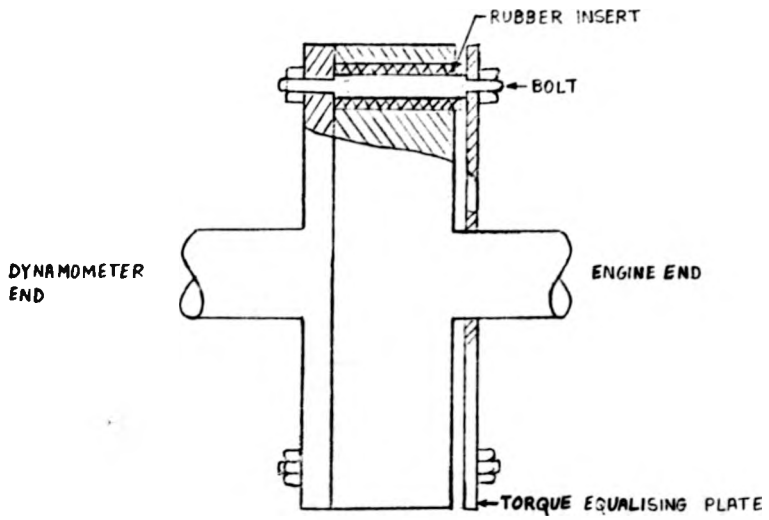

FLEXIBLE COUPLING

FIG.3

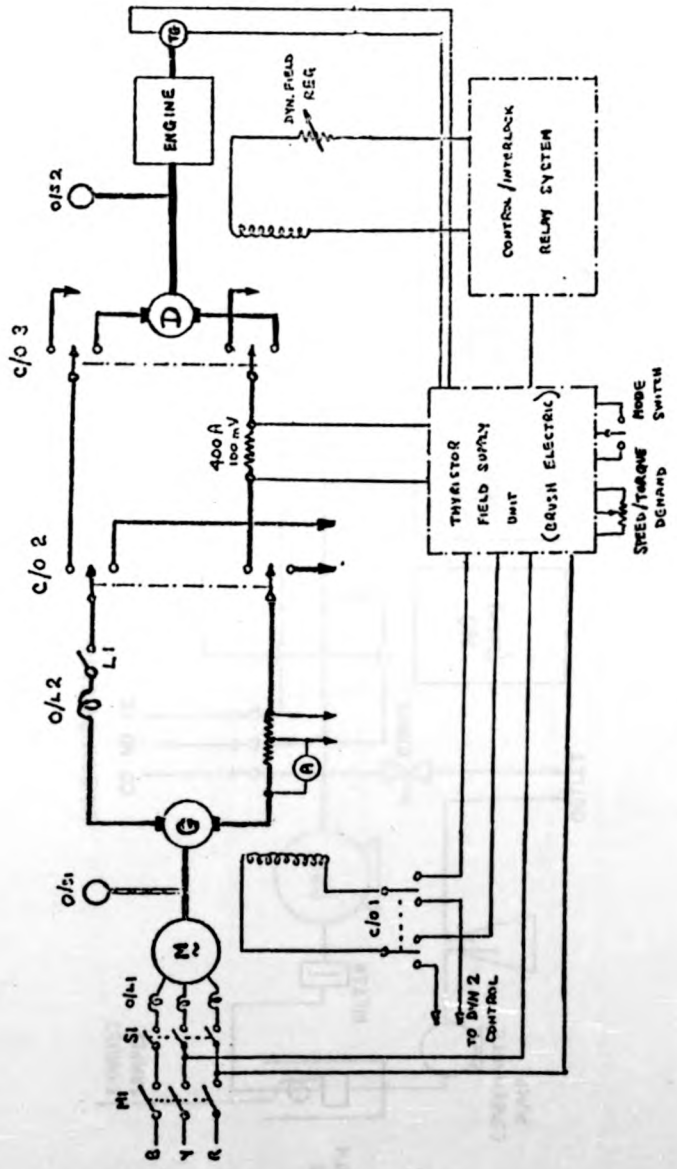

ENGINE WARD-LEONARD SYSTEM

FIG.4

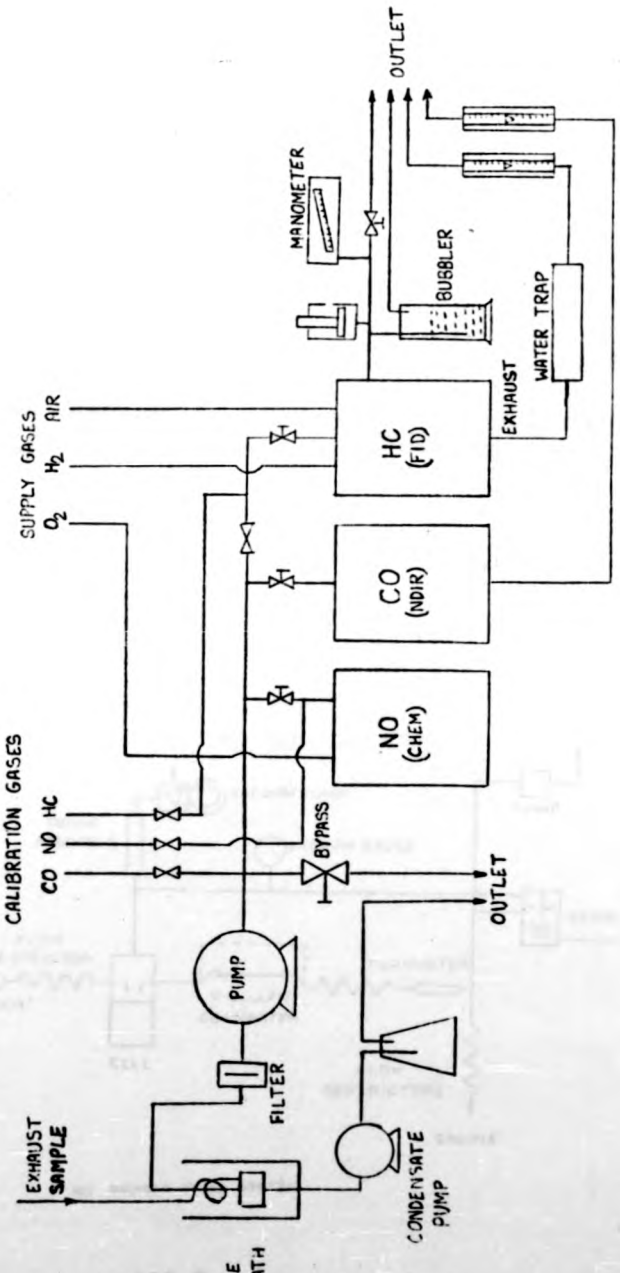

EXHAUST GAS ANALYSIS SYSTEM

FIG.5

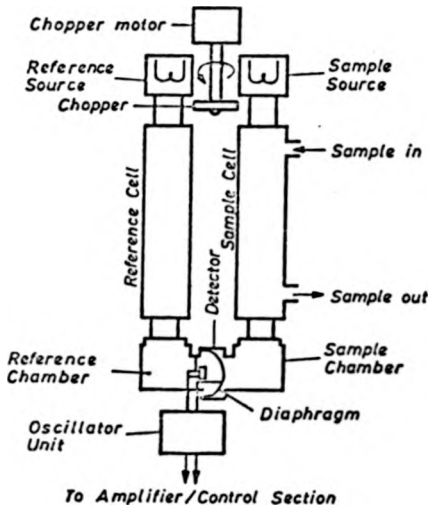

NDIR

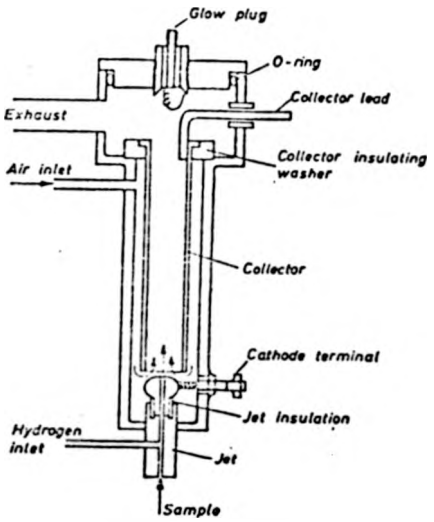

F.I.D

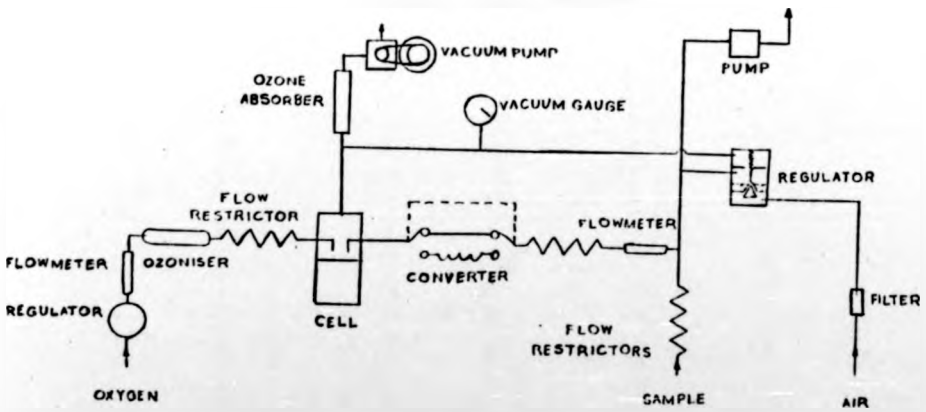

NO ANLYSER FLOW SYSTEM

FIG.6

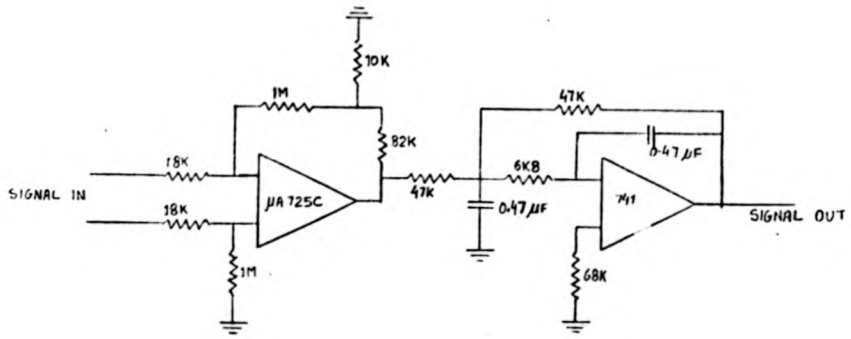

EMISSIONS SIGNAL AMPLIFIER

FIG.7

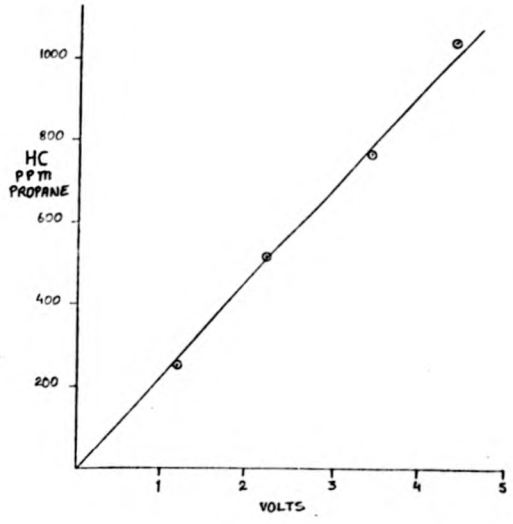

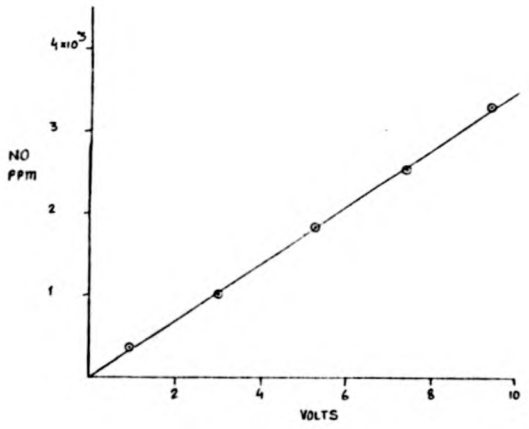

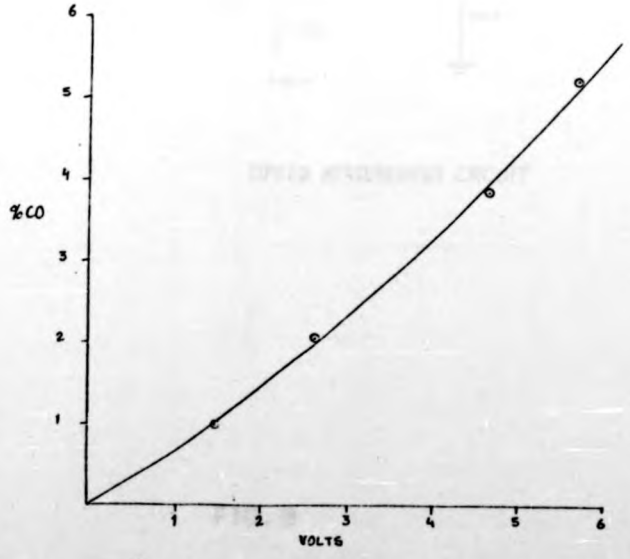

CALIBRATION OF GAS ANALYSERS

FIG. 8

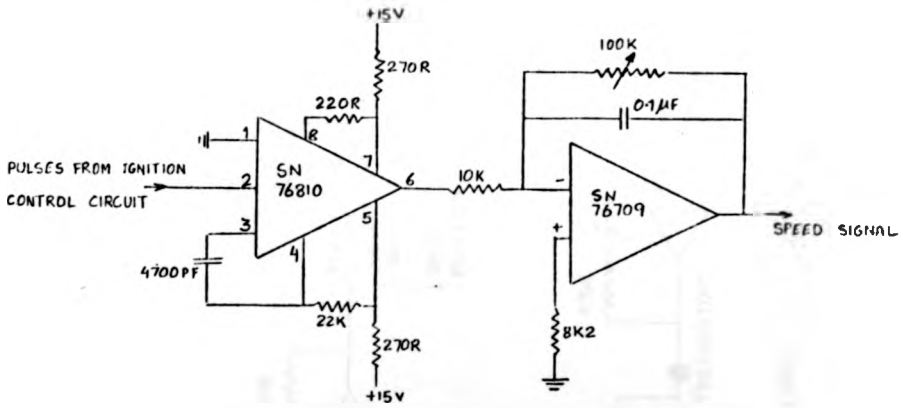

SPEED MEASUREMENT CIRCUIT

FIG. 9

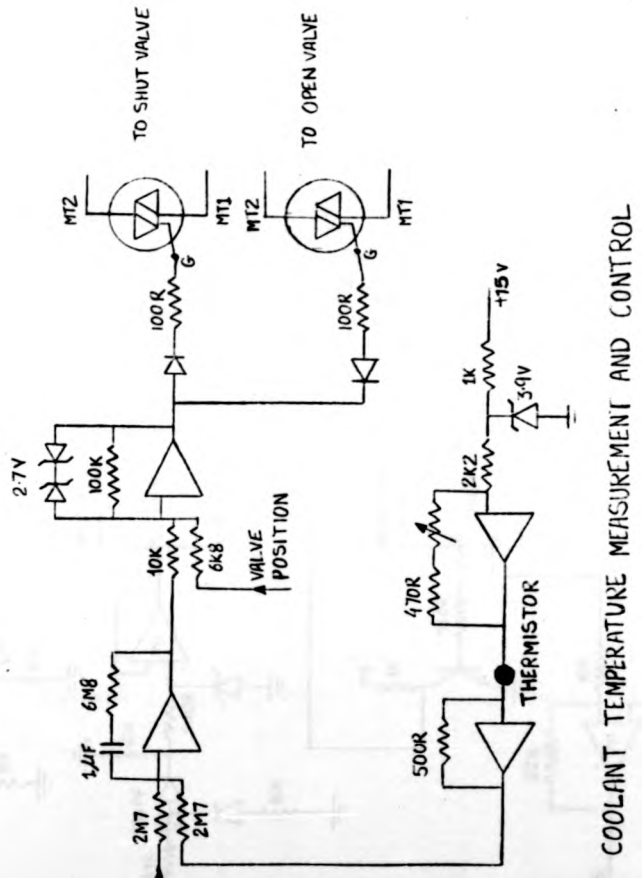

FIG.10 COOLANT TEMPERATURE MEASUREMENT AND CONTROL

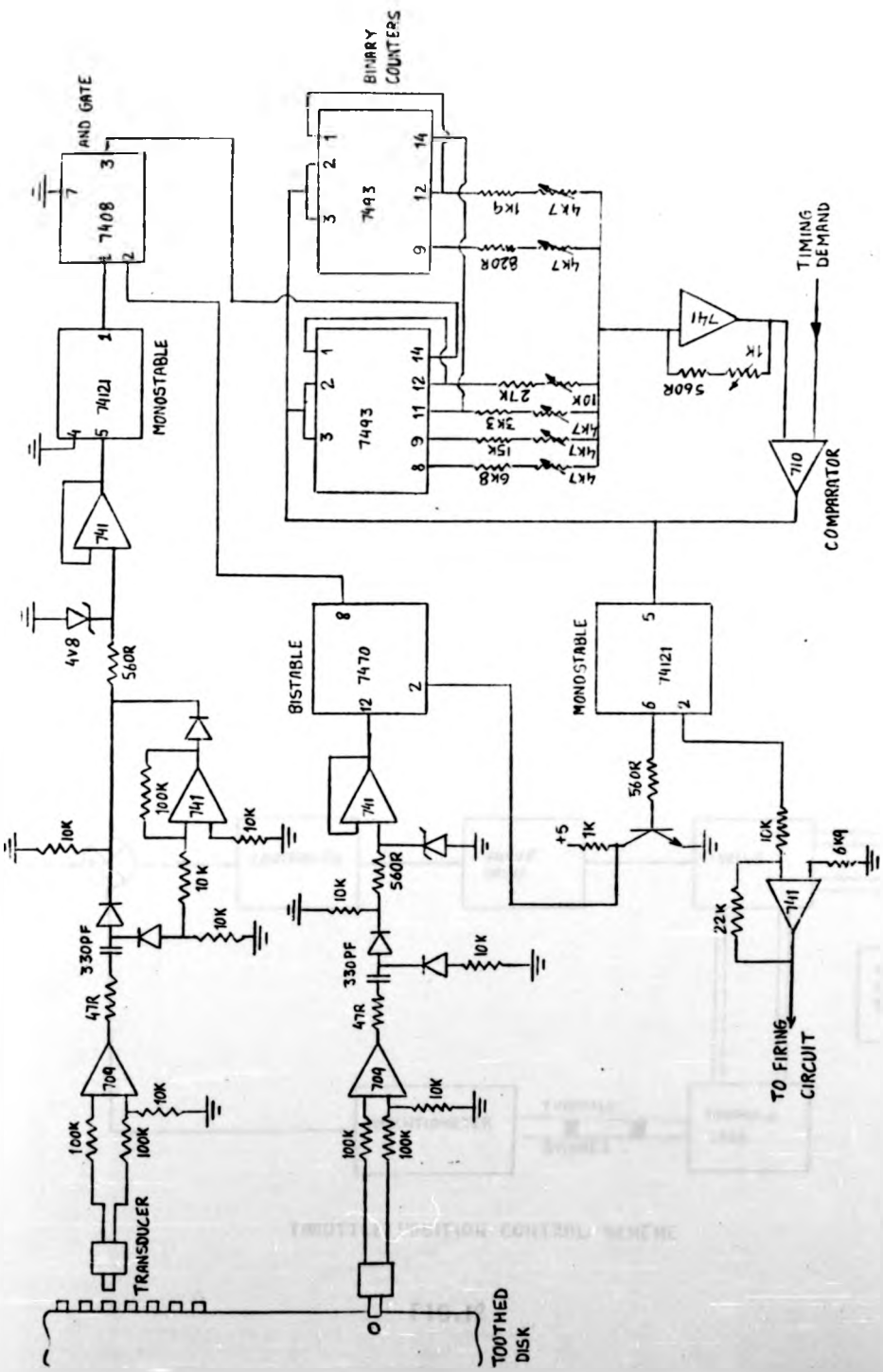

IGNITION TIMING CONTROL CIRCUIT

FIG.11

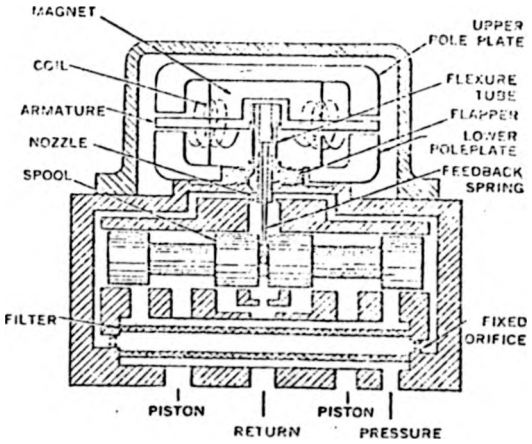

SERVO VALVE

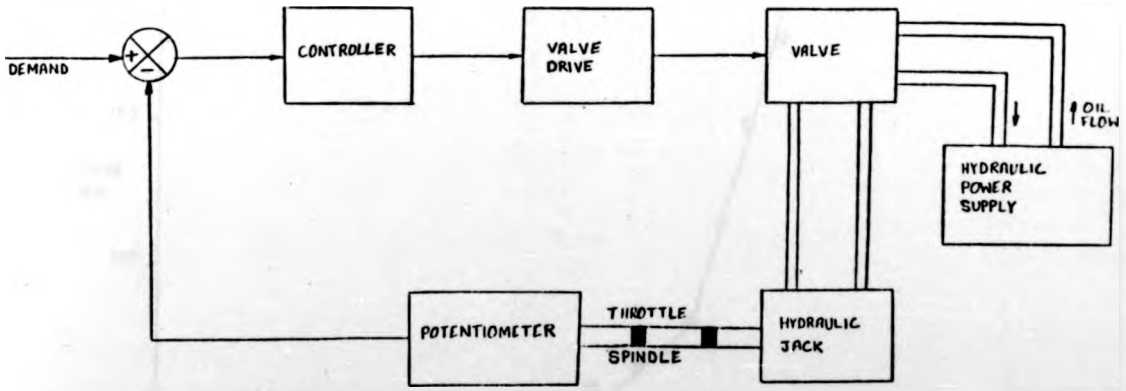

THROTTLE POSITION CONTROL SCHEME

FIG.12

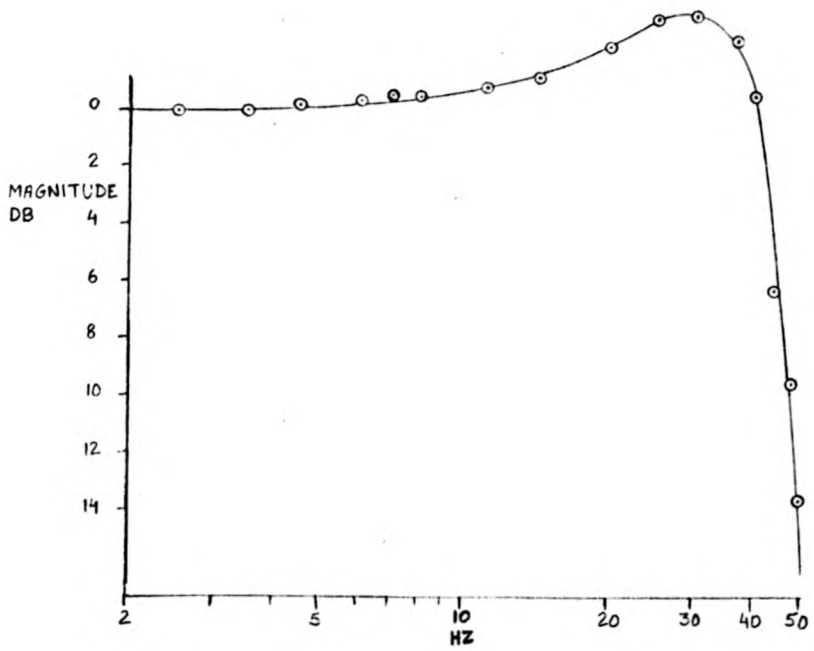

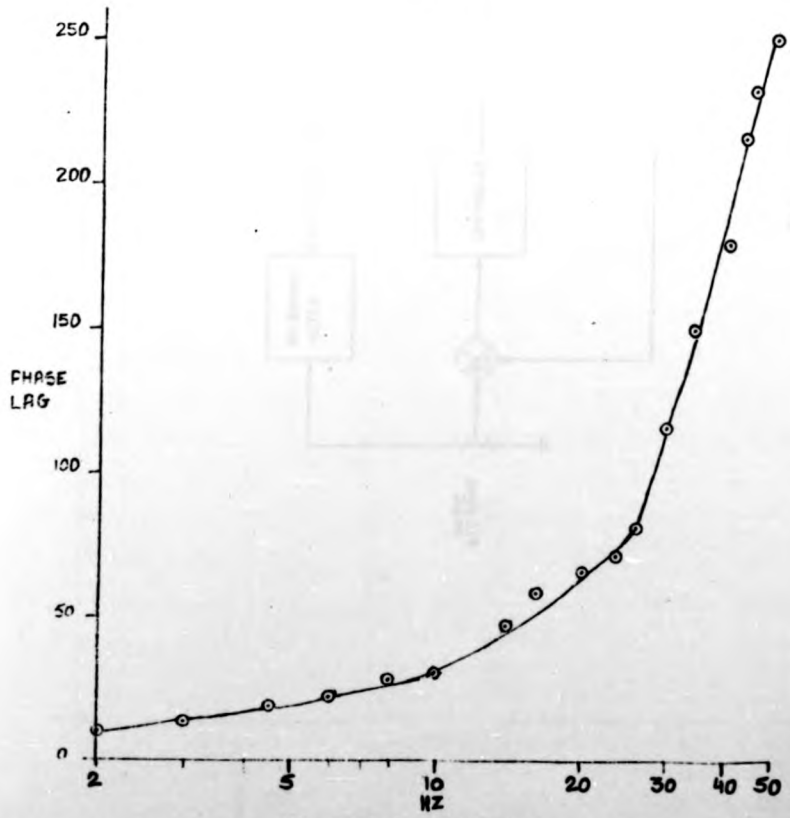

THROTTLE RESPONSE

FIG. 13

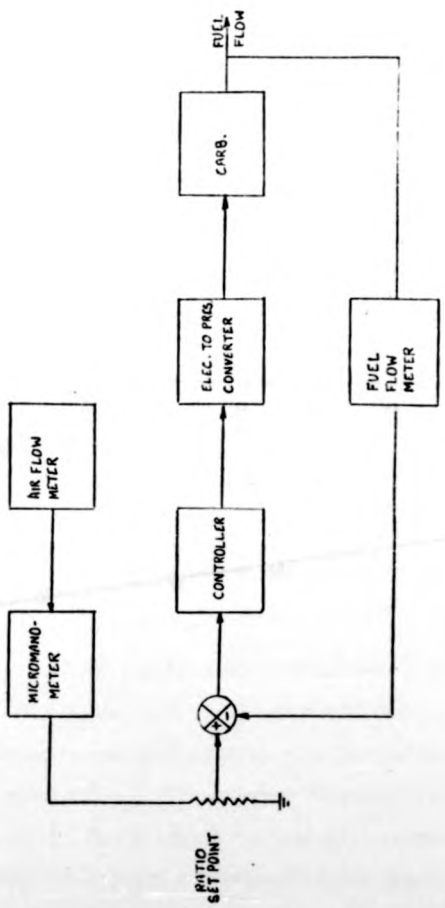

FUEL AIR RATIO CONTROL SCHEME

FIG.14

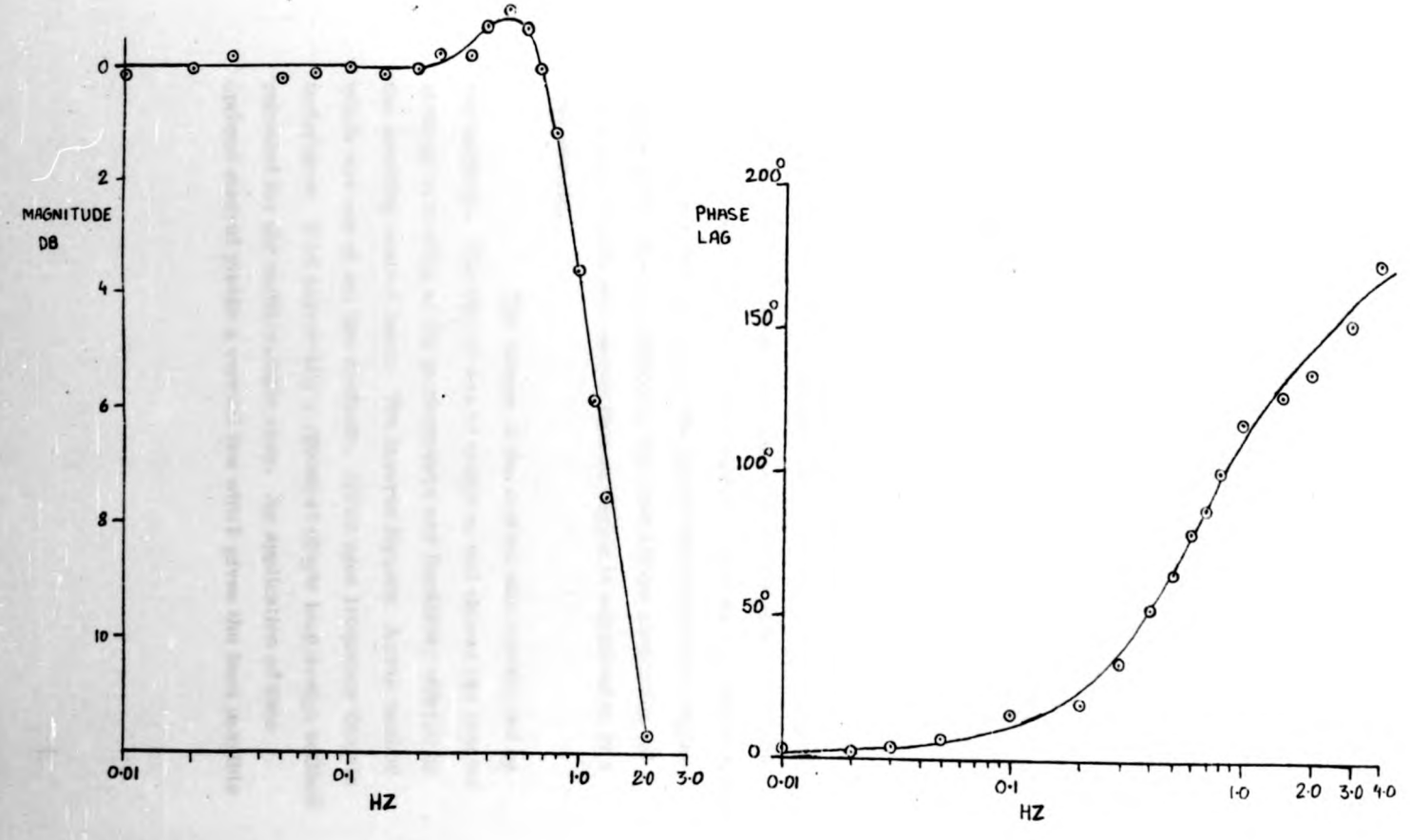

RESPONSE OF FUEL FLOW TO THROTTLE PERTURBATIONS
WITH CONSTANT FUEL AIR RATIO

FIG.15

CHAPTER 4 TEST-BED CONTROL STUDIES

4.1 Introduction

A mathematical modelling study of the test bed was thought to be necessary in order to understand the engine Ward-Leonard system. For testing and performance evaluation of an engine operating under dynamic conditions, the modelling study is vital. It not only provides an assessment of the limitations of the system, but also gives an insight into the behaviour of the engine.

Besides suggesting a solution to single loop engine test-bed control problem, mathematical modelling study is imperative when multivariable controls are considered for the engine test-bed. A controller designed to control the engine speed and torque not only increases the speed and accuracy of engine testing under steady conditions, but also allows simulation of the types of loads and speeds that an engine is subjected to in a real vehicle.

The design of the control was considered by two methods. The object was to compare and choose the control strategy according to the performance and flexibility offered by the resulting control laws. The Inverse Nyquist Array method which was one of the two methods, relies upon frequency domain techniques. It is essentially a classical single loop design method extended for the multivariable case. An application of time optimal control yields a control law which gives the best possible

performance. High performance is achieved through switching of controls to their extreme values, thus resulting in the so called "bang-bang" control.

In a simple design problem, it is usual to express the design criteria of the system by defining the desired performance of the system, when subjected to a step change. The criterion adopted for the engine test-bed control, was to achieve good performance of the system based on step changes. A need was also felt to obtain a simple and flexible control scheme, ideally requiring no "in between" adjustment to the controller, for any test schedule of the engine.

LIST OF SYMBOLS

T_e	Engine torque	Nm
T_d	Dynamometer torque	Nm
ω	Dynamometer speed	rad/s
θ	Throttle position	v
K_1	Throttle torque constant	21. Nm/v
C_e	Engine viscous damping	Nm.s/rad
C	Engine-dynamometer viscous damping	0.15 Nm.s/rad.
J	Engine-dynamometer moment of inertia	1.9 Kg m^2
E_g	Generator e.m.f.	v
E_d	Dynamometer e.m.f.	v
I_a	Loop current	A
R_a	Loop resistance	0.4 Ω
L_a	Loop inductance	3.4 mH
K_g	Generator field current/e.m.f. constant	160 v/A
K_b	Dynamometer speed constant	0.95 v.s/rad
K_t	Dynamometer torque constant	1.06 Nm/A
E_f	Generator field e.m.f.	V
R_f	" " resistance	51.5 Ω
L_f	" " inductance	38.5 H
I_f	" " current	A
K_p	" " controller gain	19.5

4.2. Test-bed Modelling Studies

Derivation of the model

Since the behaviour of the engine is non-linear, a small signal model linearized about an operating point was considered. Past workers have shown that the suitable operating point is in the middle of the torque/speed range of the engine characteristics (Ref.4.1). This is because the torque/speed curves remain substantially constant for the range of throttle settings.

A detailed structure of the engine was not considered, since the inclusion of reciprocating elements, pumping losses and service losses (oil and water pump, dynamo etc.) would lead to an excessively complicated model. Although combustion is a discrete process, the output from the engine appears continuous due to filtering effect of the flywheel of the engine. Further filtering is performed by the dynamometer rotor and casing. The shaft connecting the engine and the dynamometer was chosen to be such that it had a high stiffness. The load cell measuring the torque at the dynamometer casing was also stiff. The object was to move the dynamics of these elements outside the frequency range of interest.

The model considers the throttle position and the generator field voltage as inputs to the system and the dynamometer torque and speed as outputs. The model is derived with reference to figure 1.

Assuming that the load cell and the coupling shaft are stiff, the sum of the moments applied to the rotating parts of the engine and the dynamometer gives :-

$$T_e + T_d - C_d \omega = (J_d + J_e) \frac{d\omega}{dt} \qquad (1)$$

assuming that linearisation for "small" disturbances and operation of part throttle is appropriate then

$$T_e = K_1 \theta - C_e \omega$$

combining with eqn. (1) gives

$$K_1 \theta + T_d - C\omega = J\dot{\omega} \qquad (2)$$

where $C = C_e + C_d$

$J = J_e + J_d$

Application of Kirchoff's law to the dynamometer and generator loop gives

$$E_g - E_d = I_a R_a + L_a \frac{dI_a}{dt}$$

For small L_a this reduces to

$$E_g - E_d = I_a R_a \qquad (3)$$

also $E_g = K_g I_f \qquad (4)$

$E_d = K_b \omega \qquad (5)$

$T_d = K_t I_a \qquad (6)$

and

$$E_f = R_f I_f + L_f \frac{dI_f}{dt} \tag{7}$$

eqn. (3) to (6) give

$$T_d = \frac{K_g K_t}{R_a} I_f - \frac{K_b K_t}{R_a} \omega \tag{8}$$

The state variable form of the input and output variable given by eqn. (2), (7) and (8) is,

$$\begin{bmatrix} \dot{\omega} \\ \dot{I}_f \end{bmatrix} = \begin{bmatrix} -\frac{(K_b K_t + CR_a)}{JR_a} & ; & \frac{K_g K_t}{JR_a} \\ 0 & ; & -\frac{R_f}{L_f} \end{bmatrix} \begin{bmatrix} \omega \\ I_f \end{bmatrix} + \begin{bmatrix} \frac{K_1}{J} & ; & 0 \\ 0 & ; & \frac{1}{L_f} \end{bmatrix} \begin{bmatrix} T \\ E_f \end{bmatrix} \tag{9a}$$

$$\begin{bmatrix} \omega \\ T_d \end{bmatrix} = \begin{bmatrix} 1 & ; & 0 \\ -\frac{K_b K_t}{R_a} & ; & \frac{K_g K_t}{R_a} \end{bmatrix} \begin{bmatrix} \omega \\ I_f \end{bmatrix}$$

Taking the Laplace transform and ignoring initial conditions gives a transfer function relationship between the input and the output.

$$G(S) = \frac{1}{(1 + T_1 S)} \begin{bmatrix} \frac{K_{11}}{(1 + T_2 S)} & ; & K_{12} \\ \frac{K_{21}(1 + T_3 S)}{(1 + T_2 S)} & ; & K_{22} \end{bmatrix}$$

where

$$T_1 = \frac{JR_a}{CR_a + K_b K_t} \quad ; \quad T_2 = \frac{L_f}{R_f} \quad ; \quad T_3 = \frac{J}{C}$$

$$K_{11} = \frac{K_g K_t}{(CR_a + K_b K_t)} \quad ; \quad K_{12} = \frac{K_1 R_a}{(CR_a + K_b Kt)}$$

$$K_{21} = \frac{C K_g K_t}{R_f (CR_a + K_b K_t)} \quad ; \quad K_{22} = \frac{- K_1 K_b K_t}{(CR_a + K_b K_t)}$$

The gains of the measurement and control electronics are not included in the transfer function G (s) .

Verification of the model

The measured variables were dynamometer speed (ω) and Torque (T_d). The input variables were the voltages applied to the throttle position servo and the generator field control . Four transfer functions therefore defined the small signal dynamic performance of the plant. The technique adopted for the verification of the model was that of sine wave testing and step response tests.

Initially, steady state performance of the relevant parts of the plant was plotted to obtain the constants of the model. The resistance and inductance values of the armature loop and generator field circuits were measured using a commercial bridge. The time constants resulting from the armature loop inductance was found to be negligible relative to other time constants of the plant. An

where

$$T_1 = \frac{J R_a}{C R_a + K_b K_t} \quad ; \quad T_2 = \frac{L_f}{R_f} \quad ; \quad T_3 = \frac{J}{C}$$

$$K_{11} = \frac{K_g K_t}{(C R_a + K_b K_t)} \quad ; \quad K_{12} = \frac{K_1 R_a}{(C R_a + K_b K t)}$$

$$K_{21} = \frac{C K_g K_t}{R_f (C R_a + K_b K_t)} \quad ; \quad K_{22} = \frac{- K_1 K_b K_t}{(C R_a + K_b K_t)}$$

The gains of the measurement and control electronics are not included in the transfer function G (s) .

Verification of the model

The measured variables were dynamometer speed (ω) and Torque (T_d). The input variables were the voltages applied to the throttle position servo and the generator field control . Four transfer functions therefore defined the small signal dynamic performance of the plant. The technique adopted for the verification of the model was that of sine wave testing and step response tests.

Initially, steady state performance of the relevant parts of the plant was plotted to obtain the constants of the model. The resistance and inductance values of the armature loop and generator field circuits were measured using a commercial bridge. The time constants resulting from the armature loop inductance was found to be negligible relative to other time constants of the plant. An

examination of the dynamometer revealed a large value of rotor inertia. This was evaluated by carrying out simple mechanical tests. The constants for the engine torque and viscous damping were obtained from the slopes of engine torque/throttle and torque speed curves (Fig. 2). These slopes and hence the constants varied by 10% with speed in the mid range of engine speeds. At speeds less than 1500 R.P.M. the slopes were within 30% of those in the mid-speed region. As can be seen from figure 2, the torque throttle curve saturates at high throttle settings. With these observations, tighter bounds can be placed on the operating region. The characteristics of the dynamometer were not obtained since no ready means were available for loading the dynamometer. The viscous drag of the dynamometer was assessed from the speed run down tests with the dynamometer disconnected from the engine.

The dynamic behaviour of the system was identified by sinewave testing, using a digital transfer function analyser. The identification was done in the frequency range of 0.001 Hz to 10 Hz. Initially, significant dynamics of the engine were identified by obtaining frequency responses between the throttle and engine speed, with the engine disconnected from the dynamometer. The amplitude plot showed that the engine is predominantly a first order lag with time delay. The moment of inertia of the rotating masses of the engine was derived from the knowledge of viscous damping of the engine and the time constant of the first order system representing the engine. Time delay which is inversely proportional to the engine speed was given by (130/speed R.P.M.) in seconds. The measured time delay is composed of the time required to prepare and burn the fuel charge and also due to the parasitic lags.

Since the dynamometer was disconnected from the engine, it was thought advisable to verify the electrical side of the model. To this end, transfer functions between the generator

field control and the dynamometer speed as well as the torque were obtained. The results showed good agreement with the predicted behaviour of the dynamometer.

With the engine and the dynamometer connected, when the throttle was perturbed to obtain the transfer functions, it was found that the engine tended to operate with a "fuel rich" mixture. This necessitated frequent cleaning of the spark plugs. The cause of fuel rich operation was found to be the accelerator pump of the engine carburettor. Comparison of the transfer functions with and without the accelerator pump showed no difference. Therefore the accelerator pump was disconnected. The function of the accelerator pump is to provide a rich mixture, when the driver of the vehicle makes a large change in throttle position for rapid acceleration. The engine Ward-Leonard system has an inherent closed loop speed control, therefore changes in throttle only produce small changes in engine speed. The reason that the accelerator pump did not affect the dynamics of the system is thought to be the small changes in the throttle position and engine speed.

The amplitude plots of experimental and predicted results are shown in figures 3 to 6. The comparison in the time domain is shown in figure 7. It can be seen that there is a good agreement between the predicted and actual behaviour of the plant.

Comment on the model

Examination of the model shows that the eigenvalues of the system are negative in the operating region and as expected the system is stable. The eigenvalue due to the generator field can never be zero or positive because a practical field must have

resistance as well as inductance. The eigenvalue resulting from the engine dynamometer combination can be positive when the slopes of engine torque/speed curves are positive. However, the slopes have to exceed a value of 2.5 to render the system unstable. In practice large changes in torque can occur in case of severe misfiring of the engine, or if the torque dynamometer is started up with the throttle fully open, resulting in large changes in torque as soon as the engine begins to produce power. Much "gentler" starting up of the engine is therefore required and in practice this is usually achieved by an initial engine "warm up" procedure, necessary for other reasons.

The lead term occurring in the transfer function between the torque and the S.C.R. input, produces a zero in the open right half plane when the torque/speed curves have positive slope. This results in a non-minimum phase for this transfer function.

4.3. Multivariable Control Design Studies

Inverse Nyquist Array Design

The important feature of I.N.A. design method is that it makes the system diagonally dominant. This means that output i is predominantly dependent on the corresponding input i. Then on such a system, an extension of classical single loop inverse Nyquist stability criterion is applied. The only difference is that the stability criteria for a single loop system are valuable in the multivariable case, if referred to a set of bands instead of a single curve that is used in the classical inverse Nyquist plot (Ref. 4.3).

In its application to the engine test-bed problem, the design method consists of making the plant transfer function matrix diagonally dominant. Once dominance is achieved, then an extension

of classical design methods can be applied to each control loop. That is the speed loop and the torque loop.

Because the starting up of the system from rest is simplified, it was decided to control the speed of engine-dynamometer combination by perturbing the input to the S.C.R. controller and hence, torque was controlled by perturbing the throttle. Then the transfer function matrix for the system is as follows : -

$$G(S) = \begin{bmatrix} \dfrac{0.45}{(1+0.75\,S)(1+0.71S)} & ; & \dfrac{5.8 \times 10^{-2}}{(1+0.71S)} \\ \\ \dfrac{0.42\,(1+12.7S)}{(1+0.75S)(1+0.71S)} & ; & \dfrac{-0.93}{(1+0.71\,S)} \end{bmatrix}$$

Open loop step responses of the system show that the level of interactions present in the system, make independent settings of torque and speed unrealisable. Therefore a compensator was deemed to be necessary to reduce the interactions and improve the stability of the system.

The filters that were implemented to reduce the noise on the measured outputs are not included in the above-mentioned plant transfer function G(S), because their effects can be added on later, when dominance is achieved.

The matrix G(S) gives rise to the following inverse matrix:

$$\hat{G}(S) = \begin{bmatrix} 2.1\,(1+0.75\,S) & ; & 0.13\,(1+0.75\,S) \\ \\ 0.96\,(1+12.75S) & ; & -1.00 \end{bmatrix}$$

An examination of $\hat{G}(S)$ reveals that the first loop has a fair degree of dominance, whilst the second loop exhibits only marginal dominance at very low frequencies which is lost rapidly as the frequency is increased. The matrix $\hat{G}(S)$ was diagonalised at zero frequency by premultiplying it by G(O).

$$G(O) = \begin{bmatrix} 0.45 & ; & 5.8 \times 10^{-2} \\ 0.42 & ; & -0.93 \end{bmatrix}$$

This operation gave rise to the following matrix :

$$G(O)\hat{G}(S) = \begin{bmatrix} 1 + 1.42\,S & ; & 4.41 \times 10^{-2} S \\ -10.72\,S & ; & 1 + 4.2 \times 10^{-2} S \end{bmatrix}$$

As can be seen, the dominance of the first loop has improved, whilst the second loop does not show any sign of dominance at frequencies other than zero. Elementary row or column operations resulted in either high frequency or low frequency dominance in the second loop. A dynamic compensator was thought to be necessary to obtain dominance in the second loop. A compensator $\hat{K}(S)$ was chosen such that when it premultiplied $G(O)\hat{G}(S)$, the resulting matrix had its off-diagonal term in loop two equal to zero.

i.e.
$$\hat{K}(S) = \begin{bmatrix} 1 & ; & 0 \\ \dfrac{10.72S}{1 + 1.42S} & ; & 1 \end{bmatrix}$$

The I.N.A. plot of diagonal elements with Gershgorin band (Appendix II) superimposed is shown in Figure 8. The effect of the smoothing filters is also added to the plot. It can be seen that the first loop (speed loop) has a high degree of dominance and closed loop system would be stable for large values of feedback gains. However, if a very large gain is used then a much larger frequency range should be considered to ensure whether there is or there is not a Gershgorin band interception with the negative x axes. Since the off diagonal term in the second loop was made equal to zero by implementing $\hat{K}$ (S), the second loop should not display the Gershgorin band. The Gershgorin band on second loop as shown in figure 8 is due to the rounding off errors, for it was considered unrealistic to work beyond second figure after decimal when designing the compensator. From the artificially magnified plot of the second loop as shown in figure 9, it can be seen that the second loop is asymptotically stable for gains up to 14.2. Figure 10 shows the I.N.A. plot for both loops with a unity gain in the feedback path.

The necessity of large gains to reduce steady state off-sets was eliminated by implementation of proportional plus integral action. The time simulation of the closed loop system was carried out with integral time constant of one second and feed back gain of two in both the loops. Figure 11 shows the response of the speed loop and interactions on the torque loop with a unit step applied to the speed loop. Similarly figure 12 shows the response of the torque and interactions on the speed with a unit step applied to the torque demand. As can be seen, the interactions are minimal and the interaction on the torque loop due to a step demand in speed are solely due to the rounding off errors.

The I.N.A. plot of diagonal elements with Gershgorin band (Appendix II) superimposed is shown in Figure 8. The effect of the smoothing filters is also added to the plot. It can be seen that the first loop (speed loop) has a high degree of dominance and closed loop system would be stable for large values of feedback gains. However, if a very large gain is used then a much larger frequency range should be considered to ensure whether there is or there is not a Gershgorin band interception with the negative x axes. Since the off diagonal term in the second loop was made equal to zero by implementing $\hat{K}(S)$, the second loop should not display the Gershgorin band. The Gershgorin band on second loop as shown in figure 8 is due to the rounding off errors, for it was considered unrealistic to work beyond second figure after decimal when designing the compensator. From the artificially magnified plot of the second loop as shown in figure 9, it can be seen that the second loop is asymptotically stable for gains up to 14.2. Figure 10 shows the I.N.A. plot for both loops with a unity gain in the feedback path.

The necessity of large gains to reduce steady state off-sets was eliminated by implementation of proportional plus integral action. The time simulation of the closed loop system was carried out with integral time constant of one second and feed back gain of two in both the loops. Figure 11 shows the response of the speed loop and interactions on the torque loop with a unit step applied to the speed loop. Similarly figure 12 shows the response of the torque and interactions on the speed with a unit step applied to the torque demand. As can be seen, the interactions are minimal and the interaction on the torque loop due to a step demand in speed are solely due to the rounding off errors.

The sensitivity of the system to parameter changes was also simulated. The results showed that the system can tolerate up to $\pm$ 50% change in the eigenvalue resulting from the engine dynamometer combination without instability, although such large changes would result in a loop contactor blow out on the real system. However, the expected change in the eigenvalue was of the order of 15% only, due to the operation of the engine in the low speed high throttle region. Similarly, changes in torque/throttle gains in the low speed high throttle regime of the engine characteristic was also simulated. Once again the results showed that the system stability was not affected. The system stability was affected when torque/throttle gains were negative, resulting in positive feedback. It was thought that whilst operating under such conditions the saturation of torque at maximum level corresponding to fully open throttle and very low negative gains would suppress the slow drift resulting in instability.

The starting up procedure of the system from rest was simulated by applying small step inputs to the speed loop with throttle held at zero. The object was not only to assess the stability of the system, but also to assess whether the loop contactor "blow-out" would occur under starting conditions.

Optimal Control Design

The guiding principle of minimal time control is the so-called maximum principle, which simply states that subject to an amplitude constraint on the controls, the time optimal control is of the bang-bang type (Ref. 4.4). The problem is to find controls $u(t) = u$ such that the system is translated from an initial state to a given

final state in minimum time. Since for given controls the states of the system describe a locus in the phase plane, then the problem is to find controls such that the states of the system follow an optimum trajectory in translating the system from one state to the next.

In the context of the test bed control, the problem was to drive the torque and speed from an initial state to a given final state. In other words, the problem was to reduce the errors in torque and speed to zero as fast as possible.

The governing equations (eqn .9a and 9b) of the test bed system were scaled with respect to the maximum values of the states to provide a normalized representation of the system. The scaling of the system resulted in the following :

$$\begin{bmatrix} \dot{x}_1 \\ x_2 \end{bmatrix} = \begin{bmatrix} -1.4 & 1.33 \\ 0 & -1.34 \end{bmatrix} \begin{bmatrix} x_1 \\ x_2 \end{bmatrix} + \begin{bmatrix} 0.265 & 0 \\ 0 & 1.34 \end{bmatrix} \begin{bmatrix} u_1 \\ u_2 \end{bmatrix} \qquad (11a)$$

$$\begin{bmatrix} y_1 \\ y_2 \end{bmatrix} = \begin{bmatrix} 1 & 0 \\ -10.47 & 10.71 \end{bmatrix} \begin{bmatrix} x_1 \\ x_2 \end{bmatrix} \qquad (11b)$$

or in vector form

$$\dot{x} = Ax + Bu$$

$$y = Cx$$

In the above equations x_1 (speed) and y_2 (torque) were obtained by scaling to the maximum values of 4000 rev/min and 100 Nm respectively. The maximum value of the field voltage (u_2) and hence the field current (x_2) was chosen such that the power available from the generator was sufficient to drive the engine dynamometer system under steady conditions at the chosen maximum speed, without any assistance from the engine. The object was to minimize the peak value of the loop current during transients by imposing a limit on the field voltage. In the formulation of (11a) and (11b) the gains of the feedback transducers and the generator field voltage controller were omitted for simplicity.

Since the validity of the test bed model is limited to a frequency range of 0.001 - 10 Hz, the trajectories of system (11) under bang-bang control action were compared with those of the actual system. The object here was to ensure that at high frequencies excited by the bang-bang action, the test-bed behaved in a predictable manner. For the actual system, the plots of torque against speed were obtained by switching the throttle and the generator field voltage between two levels, within the linear operating region of the engine characteristics.

Since control of torque and speed was intended, writing the state equations (11) in vector form, in terms of the output variables gives :

$$\dot{y} = CAC^{-1}y + CBu \qquad (12)$$

where

$$|u| \leq 0.5 \; ; \quad |y| \leq 0.5$$

with the error

$$e = y_d - y$$

then

$$\dot{e} = CAC^{-1}e - CAC^{-1}y_d - CBu \qquad (13)$$

In the above equations it is assumed that C^{-1} exists.

At this stage it is recalled that the test bed control problem is to drive the states of the system from their initial values to the desired values in minimum time. That is, the terminal state of the system error vectors is the origin (Appendix II). However, due to the occurence of the demand term (y_d) in equation 13, the form of the system representation by this equation is that of a regulator, rather than a tracking problem. This is contrary to the requirements of the test-bed control system. The unsuitability of system (13) for the application of optimal control theory therefore necessitated a re-examination of the system representation. In re-formulation of the problem, it is necessary to observe that the need to drive system errors to the origin requires a symmetry in the control action about an origin. The problem was recast in the following manner.

Since the demand y_d is the desired steady state value then from equation 12 there exists a control $u = u_d$ such that

$$- CAC^{-1}y_d = CBu_d \tag{14}$$

is true under steady state conditions. Then equation 13 can be rewritten as ,

$$\dot{e} = CAC^{-1}e + CBu^*$$

where

$$u^* = u_d - u \tag{15}$$

and

$$|u^*| \leq \nu$$

The magnitudes of ν and u^* (as given by the difference between the required controls u_d and the controls u) changes with the demand y_d.

System (15) overcomes the shortcomings of the theory by translating the operating point of the states (i.e. the origin) to the demanded states with appropriate adjustments ν on the bang-bang levels. In other words, the proposed control scheme contains a proportional part due to u_d and a bang-bang part due to u^*. One of the consequences of changes in the levels of control u^* is that the system response depends on the operating point. This is due to practical constraints on the magnitude of controls.

Introducing a diagonalising transformation such that

$$e = Pz$$

where

$$P = \begin{bmatrix} 9.9633 \times 10^{-2} & ; & 9.5078 \times 10^{-2} \\ -0.99502 & ; & -0.99546 \end{bmatrix}$$

gives

$$\dot{z} = \begin{bmatrix} \lambda_1 & ; & 0 \\ 0 & ; & \lambda_2 \end{bmatrix} z + P^{-1}CBu^* \qquad (16)$$

$$|u^*| \leq \nu$$

In equation (16) $(\lambda_1 ; \lambda_2)$ are the eigenvalues of eqn. (15) and the matrix P was obtained by interchanging the columns of eigenvector matrix given by eqn. (15) so that

$$\lambda_2 < \lambda_1 < 0 \quad .$$

Putting $P^{-1}CB = D = \begin{bmatrix} d_1 & ; & d_2 \\ d_3 & ; & d_4 \end{bmatrix}$

and normalizing u^* by α gives

$$\frac{dZ_1}{dt} = \lambda_1 z_1 + \frac{d_1 \bar{u}_1}{\alpha_1} + \frac{d_2 \bar{u}_2}{\alpha_2}$$

$$\frac{dz_2}{dt} = \lambda_2 z_2 + \frac{d_3 \bar{u}_1}{\alpha_1} + \frac{d_4 \bar{u}_2}{\alpha_2} \qquad (17)$$

$$|\bar{u}| \leq 1$$

Since the independent variable time has not been subjected to the transformation, the optimal trajectories of system (17) are also the optimal trajectories of system (15). Setting

$$\frac{d_1 \bar{u}_1}{\alpha_1} + \frac{d_2 \bar{u}_2}{\alpha_2} = v_1$$

$$\frac{d_3 \bar{u}_1}{\alpha_1} + \frac{d_4 \bar{u}_2}{\alpha_2} = v_2 \qquad (18)$$

gives

$$\frac{dz_1}{dt} = \lambda_1 z_1 + v_1$$

$$\frac{dz_2}{dt} = \lambda_2 z_2 + v_2 \qquad (19)$$

The points v (v_1, v_2) for all possible values $\bar{u}$ then describe a parallelogram in the z (z_1, z_2) plane with vertices denoted by n_i $(i = 1, 2, 3, 4)$ (Ref. 4.4.). Then for all possible values of $\bar{u}$, the following values of n_i were obtained from equation 18, by setting $\alpha_1 = \alpha_2 = 0.5$ (i.e. $y_d = 0$).

n_1: 596.36, - 619.37; $\bar{u}_1 = +1$, $\bar{u}_2 = +1$

n_2: 596.36, - 630.5 ; $\bar{u}_1 = -1$, $\bar{u}_2 = +1$

n_3: -596.36, 619.37; $\bar{u}_1 = -1$, $\bar{u}_2 = -1$

n_4: - 596.36, 630.5 ; $\bar{u}_1 = +1$, $\bar{u}_2 = -1$

The numerical values of n_i clearly indicate that the resulting parallelogram would have one of its sides parallel to one of the co-ordinate axes (i.e. z_2 axis). The system thus violates the general position condition , which is imposed on the co-efficients of eqn. (17) (Appendix II). The difficulties were overcome by modifying the control matrix B such that

$$B = \begin{bmatrix} 0.265 & ; & 0 \\ b_2 & ; & 1.34 \end{bmatrix}$$

The off-diagonal term $b_2 = -0.1$ introduced in the control matrix B, can be reduced towards zero once the control laws are determined.

The magnitude of b_2 was chosen sufficiently large for ease of graphical construction.

The equilibrium position of the system for each control $\bar{u}$ can be obtained from equation 19 by setting the left hand side equal to zero. Then

$$z^1_1 = -\frac{v_1}{\lambda_1}$$
$$z^1_2 = -\frac{v_2}{\lambda_2} \qquad (20)$$

For all possible values of $\bar{u}$, four possible equilibrium points F_i^1 ($i = 1, 2, 3, 4$) are obtained. Then the phase portrait of system (19) can be obtained by translating the phase portrait of

$$\frac{dz_1}{dt} = \lambda_1 z_1$$
$$\frac{dz_2}{dt} = \lambda_2 z_2 \qquad (21)$$

to each equilibrium point. Thus, the construction of trajectories is simplified.

The parallelogram of the modified system (i.e. $b_2 = -0.1$) is shown in figure 13, with vertices F_i ($i = 1, 2, 3, 4$) given by equation 18. Normals to the sides of the parallelogram when drawn

through the origin, form angles ϕ_i ($i = 1, 2, 3, 4$). Also shown on the diagram are the equilibrium points F_i^1 of the modified system. The points F_i^1 indicate the direction of trajectories from any point under the control $\bar{u}$. The points F_i and F_i^1 were obtained by setting $\alpha_1 = \alpha_2 = 0.5$ in equations (18) and (20).

Before the optimal control can be determined for the test-bed system, it is necessary to investigate the behaviour of the auxiliary variable $\psi(t)$ and the Hamiltonian H (Appendix II). For the control law to be optimal, it is the behaviour of these functions that needs to be investigated. For the control process given by equation (19) the auxiliary variable takes the following form : -

$$\frac{d\psi_1}{dt} = -\lambda_1 \psi_1$$

$$\frac{d\psi_2}{dt} = -\lambda_2 \psi_2 \qquad (22)$$

whose general solution is

$$\psi_1 = K_1 e^{-\lambda_1 t} \quad ; \quad \psi_2 = K_2 e^{-\lambda_2 t} \qquad (23)$$

The solution of ψ indicates that vector ψ maintains a constant direction, parallel to one of the co-ordinate axes, if either of the constants of integration is zero. If not, then ψ rotates away from the axes of abscissas towards the axes of ordinates.

Since

$$\frac{\psi_2}{\psi_1} = \frac{K_2}{K_1} e^{(\lambda_1 - \lambda_2) t}$$

$\rightarrow \infty$ as t increases.

Now consider the Hamiltonian function which is given by

$$H = \ldots\ldots + \psi_1 v_1 + \psi_2 v_2 = \ldots\ldots + (\psi, v)$$

The dots indicate the terms which do not involve v_1 or v_2. The Hamiltonian H then attains its maximum at the vertex $F = F_i$ of the parallelogram (Fig. 13) when the auxiliary function ψ lies in the angle defined Φ_i and a switching of the controls is indicated when ψ is orthogonal to the parallelogram of figure 13 (Ref. 4.5).

The optimal controls can now be determined with reference to figure 13. Recalling what was said about the nature of ψ (eqn.22,23), if the initial value of ψ lies in the interior of the first quadrant within the region defined by angle Φ_i, then during the course of time as ψ rotates in an anti-clockwise direction towards the vertical axes z_2, it attains maximum at the vertex F_4 of the parallelogram. Consequently there is one switching. Similar conclusions are reached when the behaviour of ψ is considered in the third quadrant due to symmetry. Therefore every optimal control either has no switching or has one switching, in which case F coincides with either F_1 or F_3 before the switching and with either F_2 or F_4 after the switching. The number of switchings is verified by the related theorems (Appendix II).

Now allow b_2 to increase in magnitude so that it approaches zero. Then the points F_i will approach the points n_i . The optimal control laws deduced from the modified system remain unaltered, except for $F_i = n_i$, when the controls are indeterminate. For all practical purposes the optimal controls deduced from the modified system are also the optimal controls of the actual engine test bed system.

The "optimal" trajectories of the unmodified system (i.e. $b_2 = 0$) then are easily constructed. The trajectories of the unmodified system with $\tau_1 = \tau_2 = 0.5$ are shown in figure 14. Let OA be the trajectory of the system under control F_2 , and BO be the trajectory of the system under control F_4 , both terminating at the origin. Then the right hand side of curve BOA is filled by the trajectories of controls under F_1 and the left hand side by the trajectories of controls under F_3. The controls represented by F_i are as follows :-

$$F_1 : \quad \bar{u}_1 = +1, \quad \bar{u}_2 = +1$$

$$F_2 : \quad \bar{u}_1 = -1, \quad \bar{u}_2 = +1$$

$$F_3 : \quad \bar{u}_1 = -1, \quad \bar{u}_2 = -1$$

$$F_4 : \quad \bar{u}_1 = +1, \quad \bar{u}_2 = -1$$

Equation 9 on integration gives the trajectories of the system that terminate at the origin.

Controls F_2 give trajectory AO which is

$$z_2 = \left[\left[1 + \frac{z_1 \lambda_1}{\frac{-d_1}{\tau_1} + \frac{d_2}{\tau_2}}\right]^{\frac{\lambda_2}{\lambda_1}} - 1\right]\left[\frac{-d_3}{\tau_1} + \frac{d_4}{\tau_2}\right]\frac{1}{\lambda_2} \qquad (24)$$

and the control F_4 gives trajectory BO which is

$$z_2 = \left[\left[1 + \frac{z_1^{\lambda_1}}{\frac{d_1}{\alpha_1} - \frac{d_2}{\alpha_2}}\right]^{\frac{\lambda_2}{\lambda_1}} - 1\right]\left[\frac{d_3}{\alpha_1} - \frac{d_4}{\alpha_2}\right]\frac{1}{\lambda_2} \qquad (25)$$

The switching trajectory ACBas defined by equations (24) and (25) depends on the control level α. This implies that the optimal switching law is maintained throughout the engine torque/speed plane.

The behaviour of the control scheme was investigated in the time domain by simulation. It was found necessary to place a tolerance of $\pm$ 0.1% on the switching trajectories AOB (eqn.(24) and (25)) to obtain a rapid translation of the states to the origin, otherwise the controls switched the states from one side of curve AOB to the other side, resulting in excessive switching of controls and thus in slow recovery to the origin. The response of the system to a small step input is shown in figure 15. For a step change in speed of 200 rev/min the output settles to the desired value in 280 ms and results in a maximum torque level of 77 Nm. The torque settles to a step demand of 20 Nm in 30 ms and results in a peak change of 4 R.P.M. in speed.

Since the bang-bang level changes with the demand or the initial values of the states, the response of the system depends upon the initial conditions. The non-linearity of the system was investigated by applying a ramp change on the system input. Figure 16 shows the behaviour of the system to a ramp change of 920 R.P.M./sec. in the speed, which was just sufficient to blow the loop contactor. The

output lags the input by 66 ms at the output speed of 920 R.P.M. and at the maximum speed the output lags by 600 ms due to the reduction in the bang-bang level. The reduction in control level results in a reduction in the interaction of the torque loop which reduces to zero 0.5 sec. after the speed reaches the maximum value. The torque loop on the other hand can follow a ramp change of 400 Nm/s with a negligible interaction of the speed loop.

Sensitivity of the system to changes in the parameters of the system was investigated . Simulation showed that changes in the eigenvalues of up to 30% were tolerated without any signs of instability. However, motion of the states along the switching trajectory resulted in some switching of the controls and a limit cycle resulted at the origin. The operation of the system in the engine torque saturation region was simulated by putting the throttle gain to zero. This also resulted in rapid switching of the generator field control for small changes in torque demand.

4.4. Implementation of Control

Although the control scheme suggested by the optimal control theory offers a much higher performance system, it was decided to implement the controls obtained by I.N.A. method. By implementation of linear control, limit cycles (switching of controls in the vicinity of the origin) that result from non-linear control are avoided.

The final controller resulting from I.N.A. design technique is as follows :

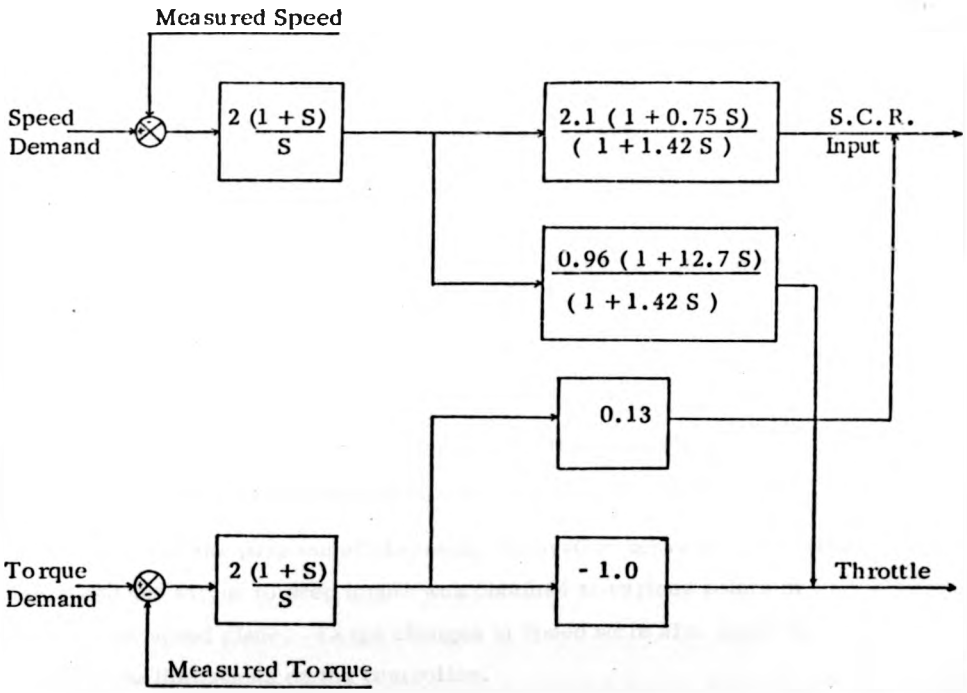

A controller given by the above was designed and is shown in figure 17. The parameters associated with the compensator were made adjustable to facilitate the commissioning of the controller. The integrators were physically implemented after the compensator to prevent saturation of the amplifier when operating in the non-linear region of the engine torque/speed plane and also to reduce the effects of noise between the two loops due to the cross-coupling terms

of the compensator. The consequences of implementing the integrators after the compensator are that torque demands in excess of engine capability will not only result in steady state offset on the torque loop, but also an offset will result in the speed loop. This also necessitated a careful choice and adjustment of electronic components to reduce the drift and offsets on individual amplifiers. In the operating temperature range the components were chosen to reduce the offsets to the order of 1 mV. In addition automatic switching of integrators was employed so that prior to starting of the system the integrators were ineffective. Also, an initial condition, on the final stage of the input to the S.C.R. was employed, as a fail safe measure in case of integrator switch failure.

Finally, analogue computer simulation of the controller was carried out to test the circuit and assess the performance of the controller when subjected to noise. Small lags had to be incorporated in the compensator to minimize the effects of noise.

For the purpose of assessing the system behaviour, response of speed and torque to step inputs was obtained at various points in the torque speed plane. Large changes in speed were also made to assess the limitations of the controller.

Initially the parameters of the controller were trimmed to give desired responses in the operating region of the torque-speed plane. It was found impossible to obtain zero interactions on the torque loop for a step change in speed. This is partly due to the time delays involved in mixture preparation and successive firing in the cylinder and also due to the exclusion of shaft dynamics from the model. Difficulties were encountered whilst trimming the controller due to noise on the measured outputs.

The step inputs applied in the linear region consisted of a 200 rev/min. change in speed and a 21.25 Nm change in torque. These values correspond to the Peak to Peak perturbations that were applied to the speed and throttle whilst identifying the system dynamics. The response of the system to a "unit" step input to the speed and torque is shown in figure 18 and figure 19 respectively. Figure 18 also shows the interactions on the torque loop due to a unit step in the speed in decreasing speed direction. This figure was obtained by setting the steady state torque such that throttle excursions when the speed was disturbed did not decrease to a fully closed throttle. As can be seen, the characteristics of the interactions on the torque loop due to disturbances of speed are direction dependent to some extent. Similar behaviour was observed with the removal of fuel measurement transducer and the accelerator pump. It is thought that this direction dependence is due to the preparation of mixture being direction dependent.

The results show that the speed loop has a time constant of 0.75 seconds and the torque loop has a time constant of 0.3 seconds. The peak to peak level of interactions on the torque loop due to a step change in speed correspond to a change of 2 Nm in torque. Figure 20 shows the response of both the loops with a 500 rev/min step change in speed, with steady state torque held in the linear region. In this case the time constant of the speed loop has increased to 1.2 seconds with an overshoot of 7.5%. Similarly figure 21 shows the response of both the loops to a 200 rev/min change in speed with the torque demand set at the maximum capability of the engine prior to a change in speed.

In this case the time constant of the speed loop was of 1.9 seconds and an overshoot of 13.6%. The above results show that the time constant of the speed depends upon the level of interactions on the torque loop and hence on the region of operation in the engine torque speed plane.

Observations similar to those described above were made at various speed settings in the operating range of the test bed. The results did not show marked deviations from the above discussed results. Speed changes (step) of 1000 rev/min. showed that the peak to peak level of interactions on the torque loop was 80 Nm.

Tests showed that a torque demand of 1% in excess of engine capacity results in a 3 rev/min. drop in the speed due to the physical implementation of integrator after the compensator. This means that if maximum possible output torque of engine is demanded at initial speed setting of 1300 rev/min. , then the engine speed will fall by approximately 40 rev/min.

4.5. Conclusions

The modelling studies of engine Ward-Leonard system show that experimental results of the plant compare favourably with those predicted by the model. This indicates that the simplified model is valid in the frequency range of interest. The plant step responses bring to attention a lead term between generator field voltage and torque. The lead term results from the inherent closed loop speed control of the Ward-Leonard system due to the back E.M.F. of the dynamometer. The effect of time delays of the engine is not significant , as can be seen on the phase plots; therefore time delays can be neglected in control design studies.

The I.N.A. control design study has resulted in a compensator which reduces the interactions to such an extent that independent setting of engine torque and speed was made possible. Due to the inherent closed loop speed control of the Ward-Leonard system, a dynamic compensator was found to be necessary. Simulation studies indicated that the control scheme resulting from I.N.A. design study is more suited for test-bed applications than the bang-bang control scheme. Therefore the controller resulting from the I.N.A. method was implemented.

The behaviour of the system in the linear region was found to be as predicted by the design study. However, it was found that the level of interactions on the torque loop due to a step change in speed was in excess of that predicted by the design study. This is due to inadequate identification and characterisation of the system by a linear model. In real terms the level of interactions is low enough to be considered negligible, thus rendering more accurate representation of the system unnecessary. Tests have shown that the speed loop time constant and overshoot are affected by the level of interactions present on the torque loop . This is the direct consequence of I.N.A. design technique that results in a compensator, which is why the behaviour of the system in the non-linear region is agreeable from the point of view of interactions.

Although the time constants of both the loops can be further reduced by increasing the feedback gains, it is thought unwise to do so for the result would be an increase in the level of interactions when operating in the non-linear region. Also due to the excursions of throttle into the non-linear region when initially operating in the linear region the interactions would increase.

Interactions combined with the increased sensitivity of the controller to noise would result in unnecessary overstressing of the test bed components. Because the system behaviour was not markedly different throughout the test bed speed range, scheduling of the controller to compensate for parameter variations was not necessary.

Large step changes in speed have shown that the likelihood of loop-contactor failure is not present. The restraint required on torque demands in excess of engine capability are reduced by physically implementing the integrators after the compensator.

In conclusion the I.N.A. design technique has resulted in a flexible control scheme whose performance was predictable to a reasonable degree. The flexibility and assured asymptotic stability renders I.N.A. design technique suitable for non-linear systems.

Application of the optimized bang-bang control strategy results in a rapid response control scheme for the test-bed system. The practical limitations on the maximum levels of the controls has resulted in sub-optimality. Consequently, a workable control is necessarily of proportional plus bang-bang type. The analysis showed that the test bed system is not particularly well conditioned for the application of this type of control. However, certain modifications to the system parameters to obtain the control laws and subsequent application of the deduced control laws to the actual system has resulted, for practical purposes, in an optimal control scheme.

The results of simulation studies show that the step changes in the speed are limited to small values due to large interactions with the torque loop. Simulation also indicates that

torque demands greater than the engine capacity would result in rapid switching of controls.

Spurious switching of the controls due to noise can be prevented by placing large tolerances on the origin in the phase plane. A dual mode of control with non-linear control for large errors and linear control for small errors offers a better possibility. Since the level of interaction on the speed loop due to step change in torque is low , the change over with respect to the torque loop can be a small percentage of the demand, say 5%. The interactions on the torque due to a change in speed are large, and when the speed is 95% of the demanded value the torque error of 10 Nm exists (Fig.15) , which can take up to 1 sec for the linear controller (I.N.A.) to reduce to zero. Therefore the change over point needs to be 1% for the system to settle to steady state within 0.5 seconds. Operation in the saturation region will require careful scheduling of the controller. Therefore engine maps will be required to schedule the control such that the linear controller takes over when the engine is operated in the non-linear region.

The above-discussed control scheme is best implemented by the use of microprocessor , because the scheduling necessary would result in complicated electronics if discrete components are used.

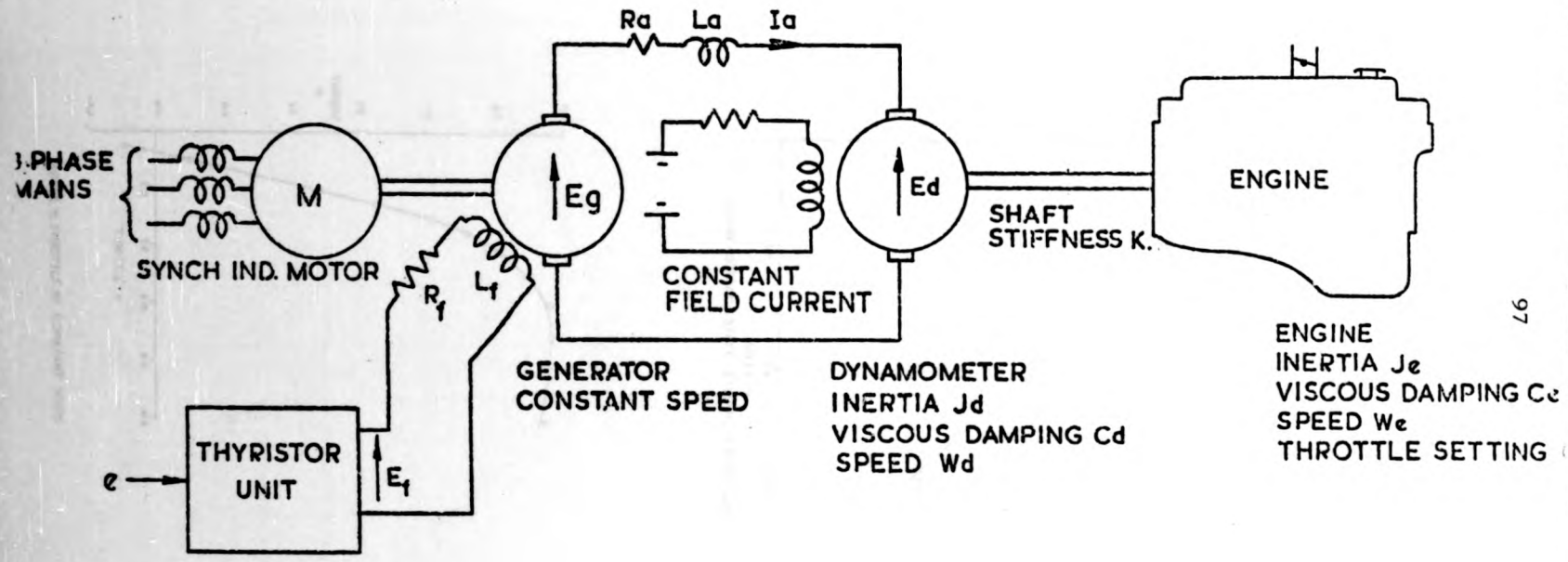

MAIN ELEMENTS OF ENGINE DYNAMOMETER MODEL.

FIG.1.

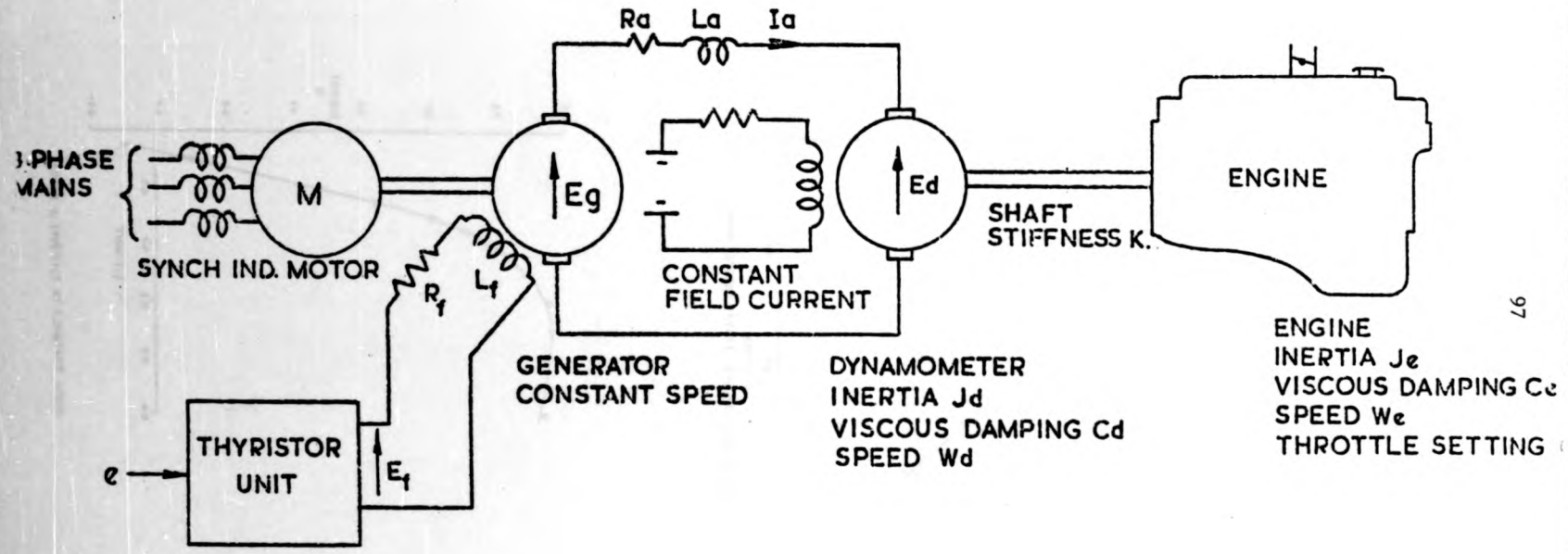

MAIN ELEMENTS OF ENGINE DYNAMOMETER MODEL.

FIG.1.

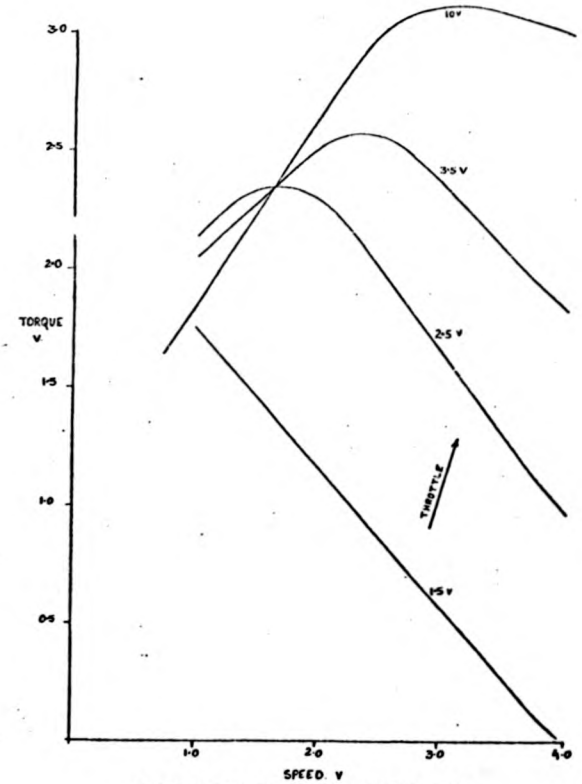

ENGINE STEADY STATE CHARACTERISTICS

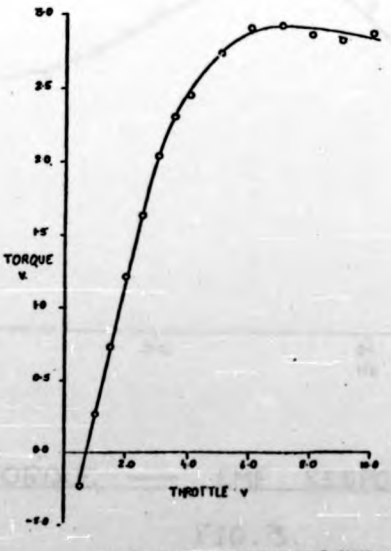

TORQUE Vs. THROTTLE AT CONSTANT SPEED

FIG. 2

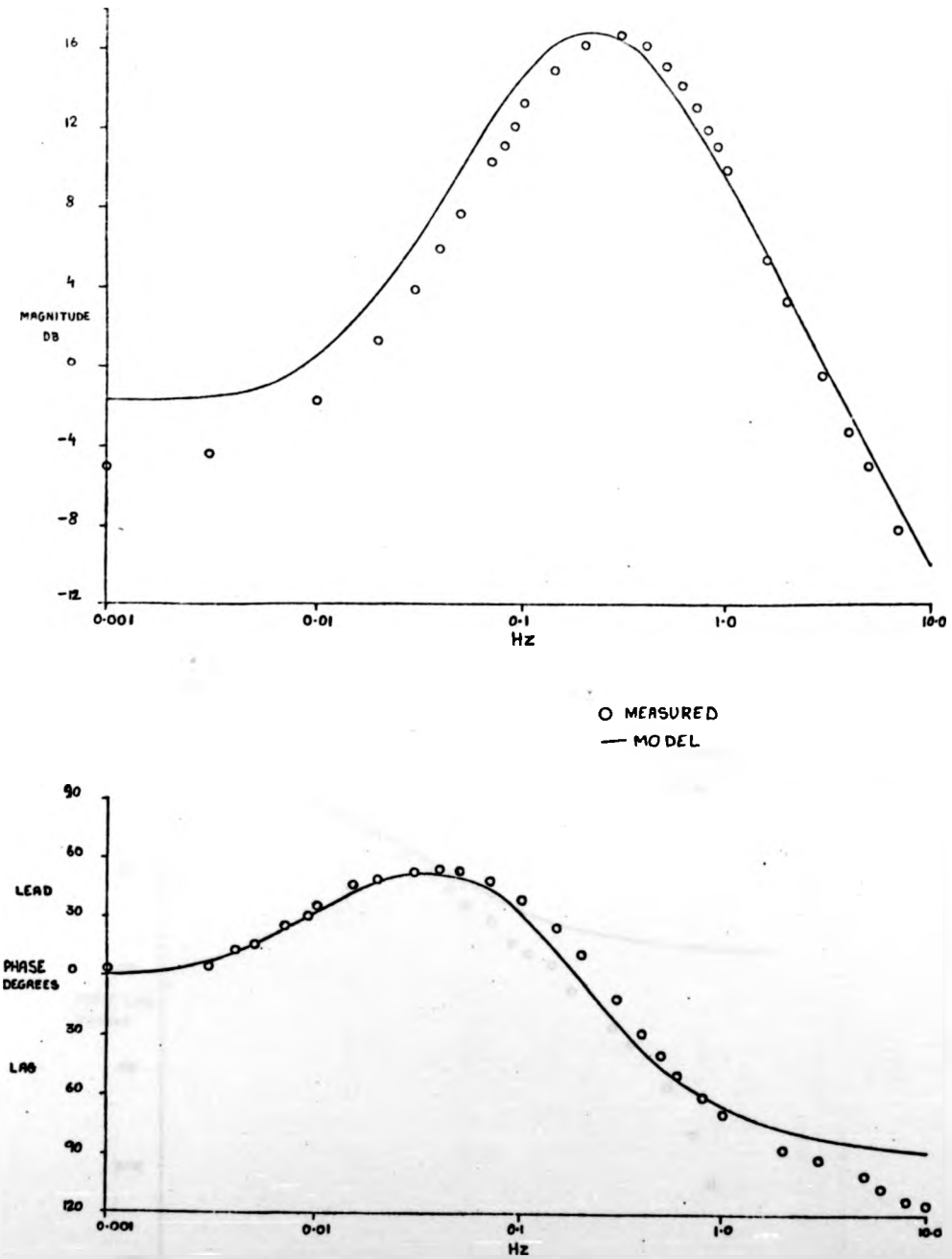

TORQUE — EMF RESPONSE

FIG.3.

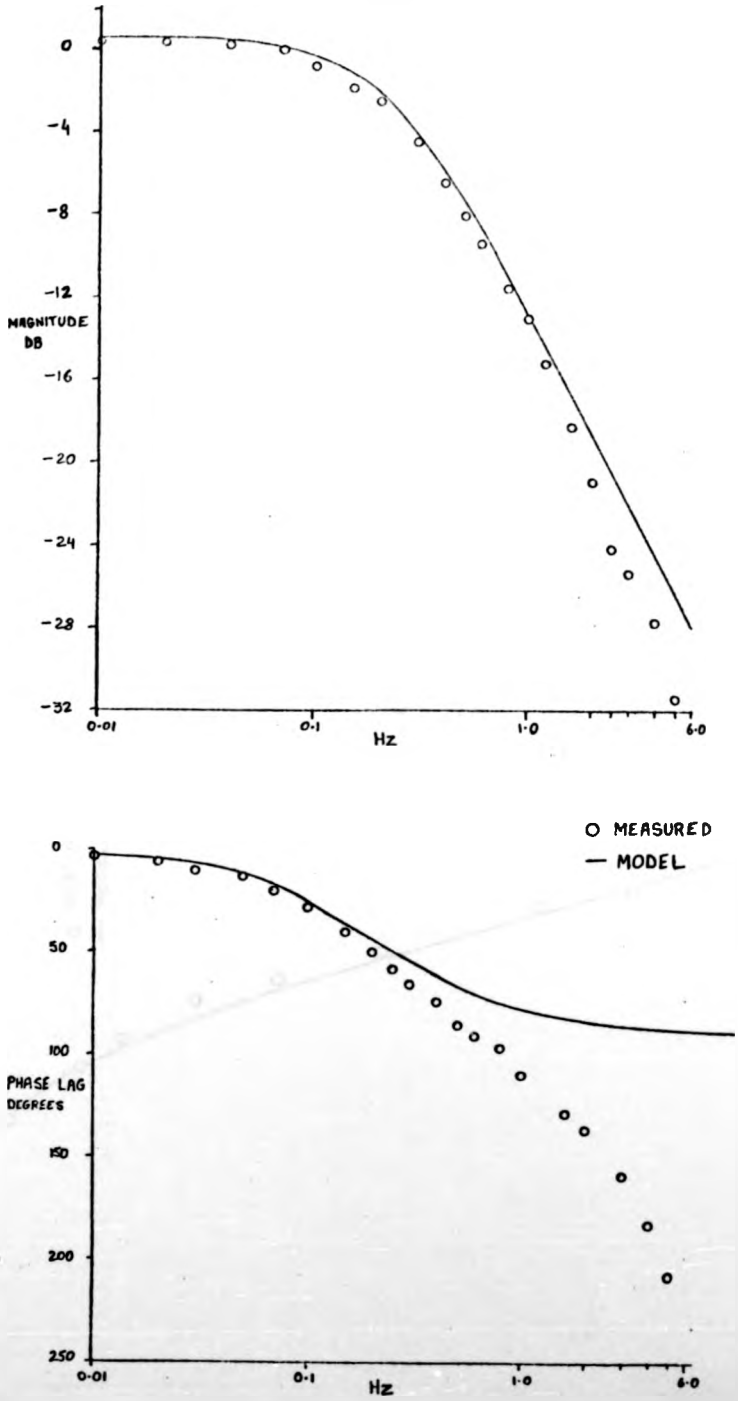

TORQUE – THROTTLE RESPONSE

FIG. 4

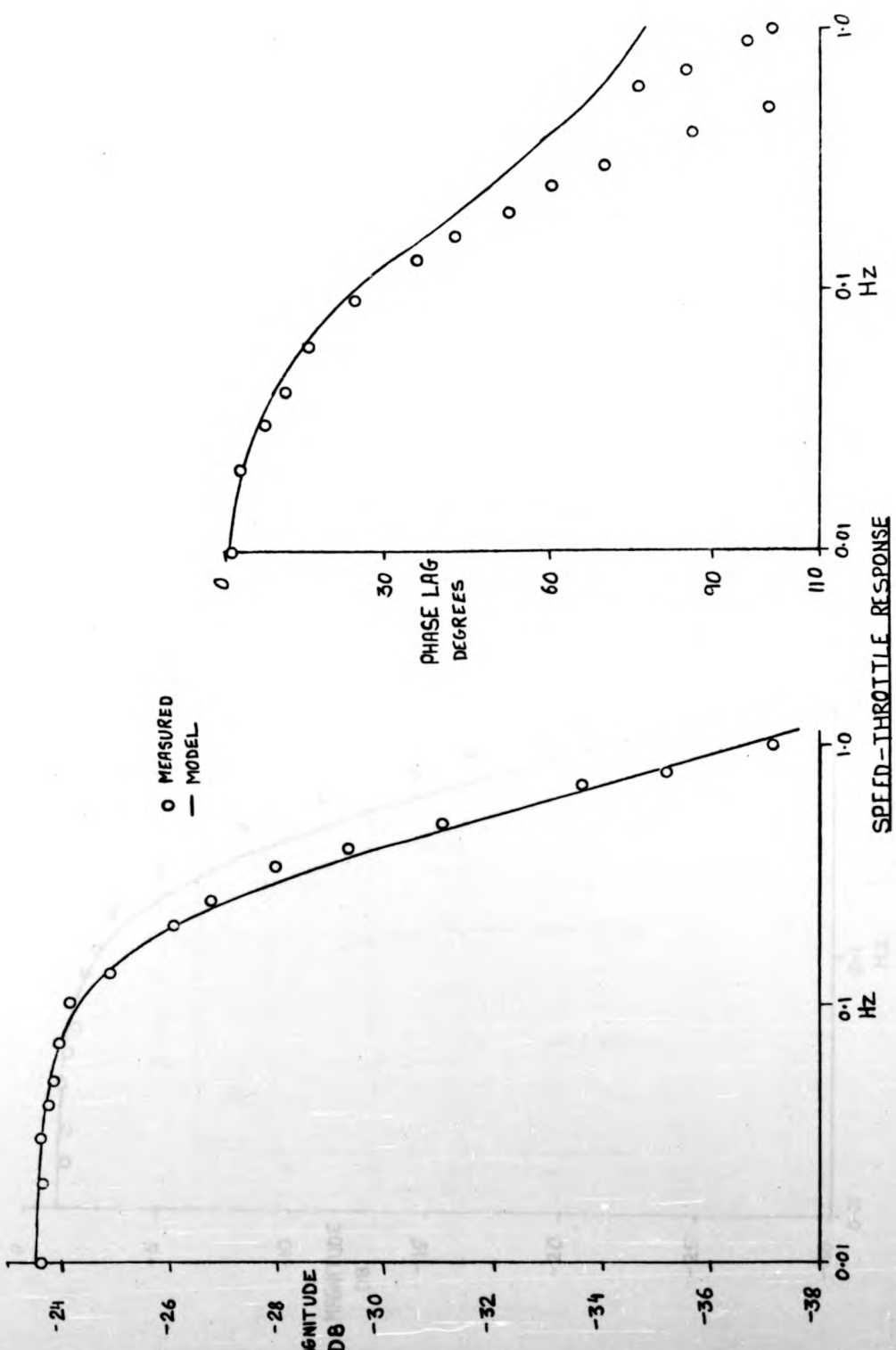

SPEED-THROTTLE RESPONSE

FIG.5.

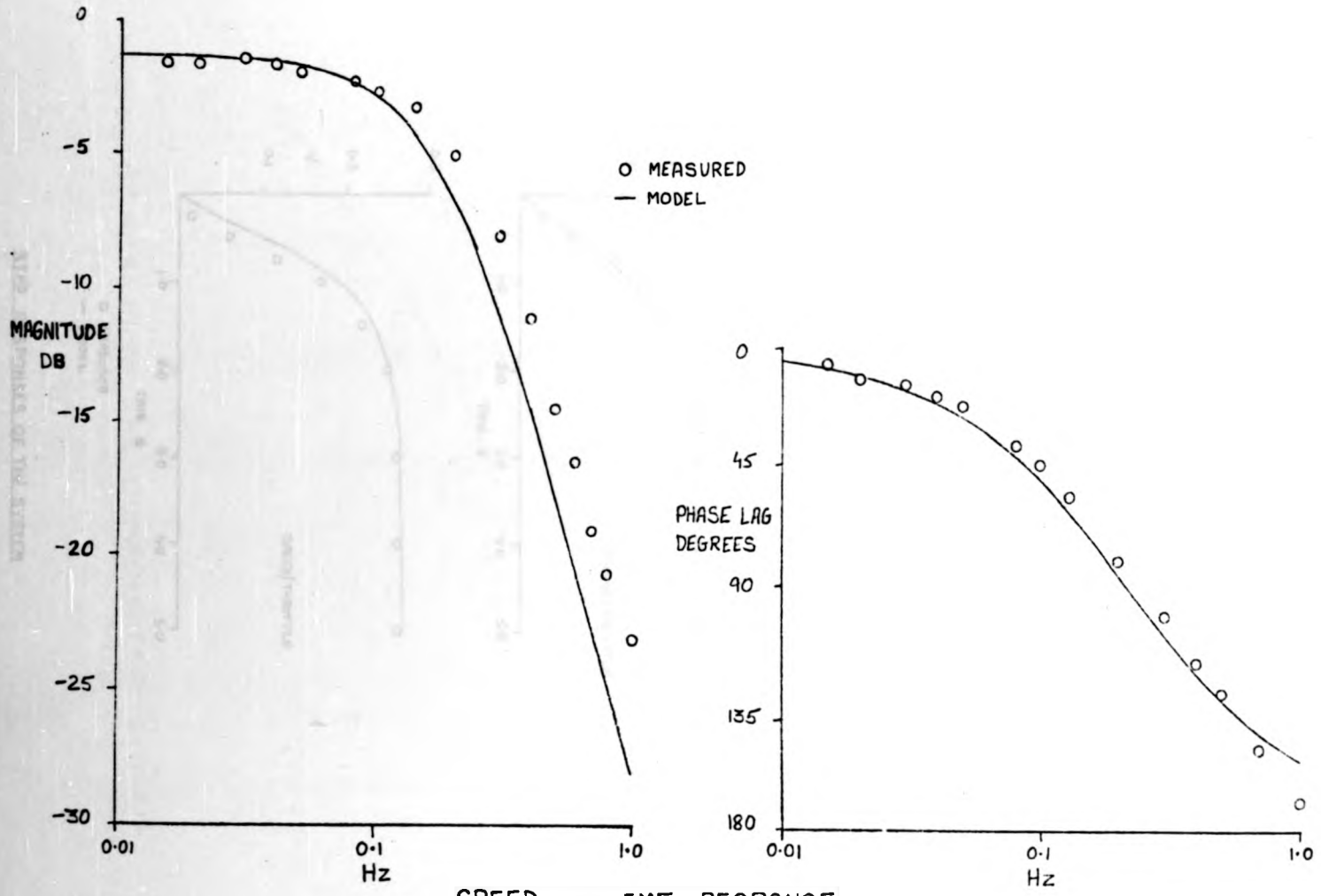

SPEED — EMF RESPONSE

FIG.6

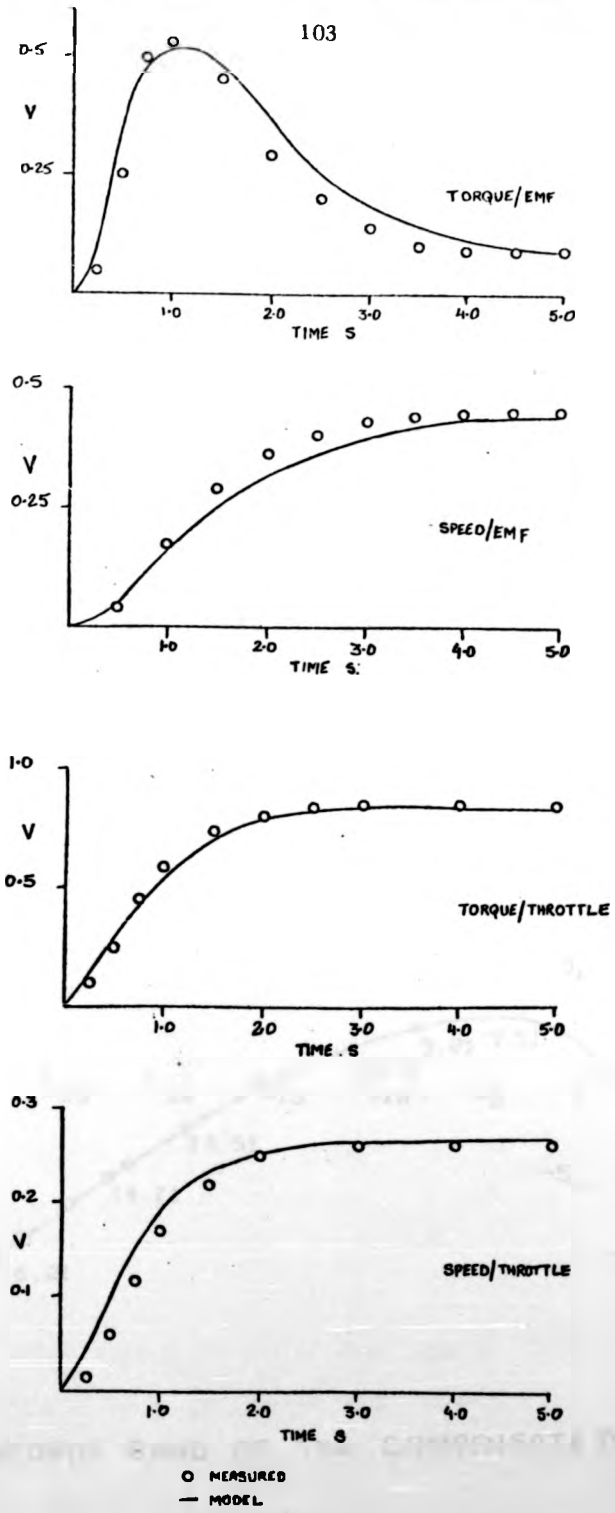

STEP RESPONSES OF THE SYSTEM

FIG. 7

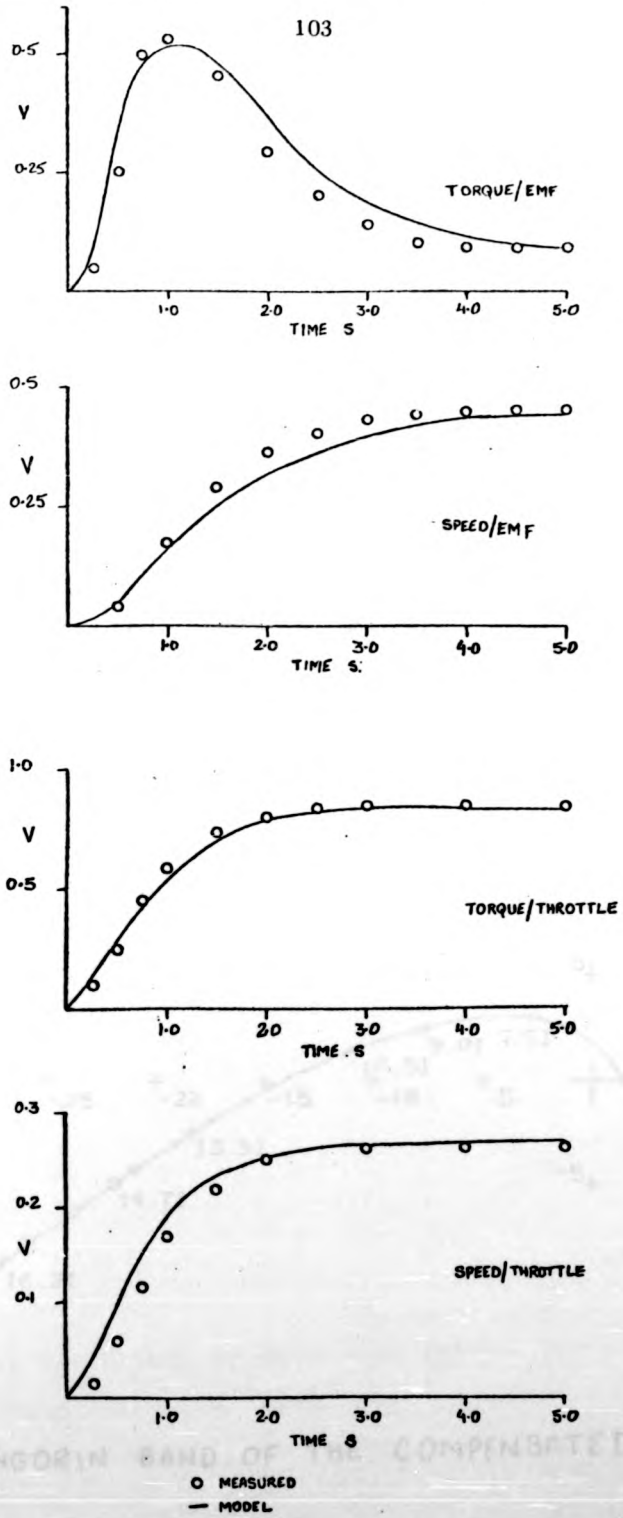

STEP RESPONSES OF THE SYSTEM

FIG. 7

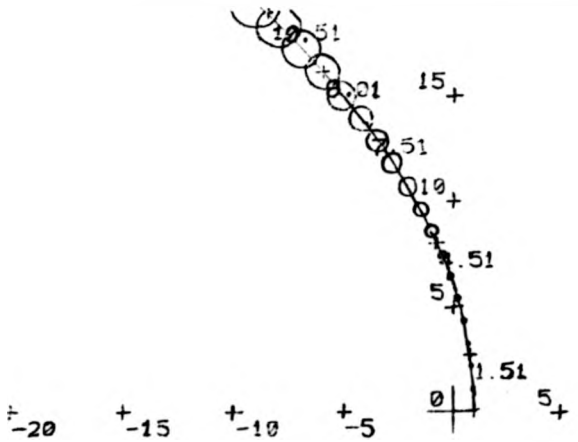

SPEED LOOP

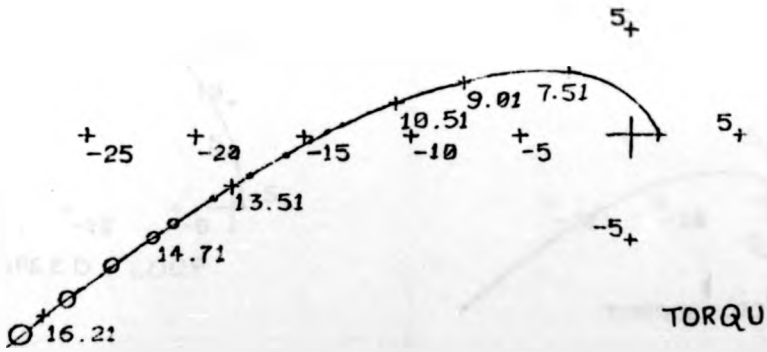

TORQUE LOOP

GERSHGORIN BAND OF THE COMPENSATED SYSTEM

FIG. 8.

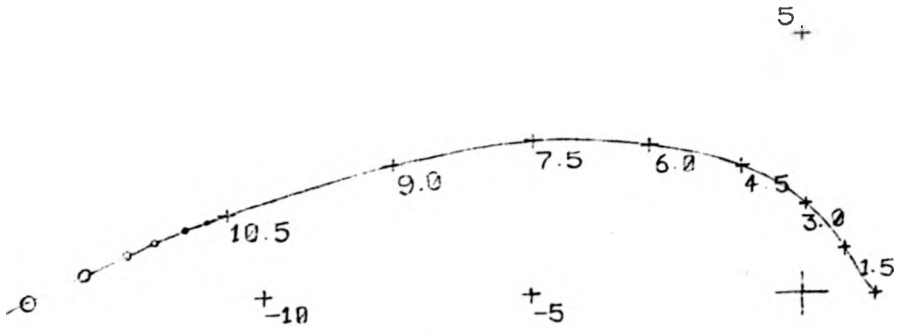

MAGNIFIED GERSHGORIN BAND OF THE TORQUE LOOP

FIG.9

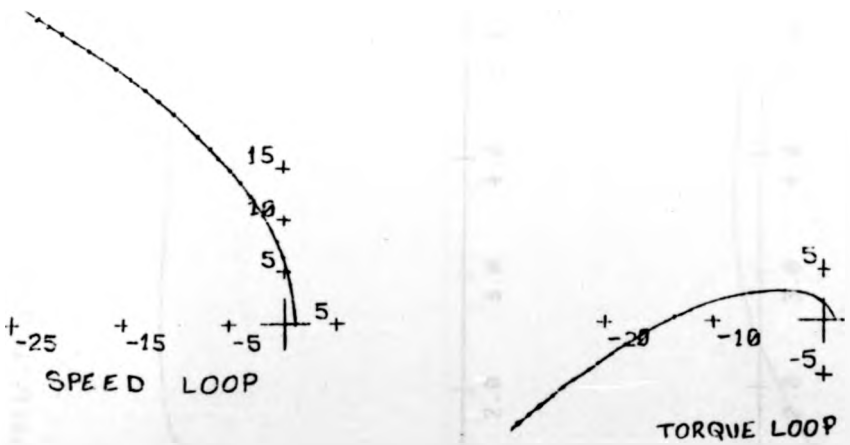

OSTROWSKI BAND OF BOTH THE LOOPS WITH UNITY FEEDBACK GAINS IN BOTH THE LOOPS

FIG.10

PREDICTED RESPONSE TO A UNIT STEP IN SPEED

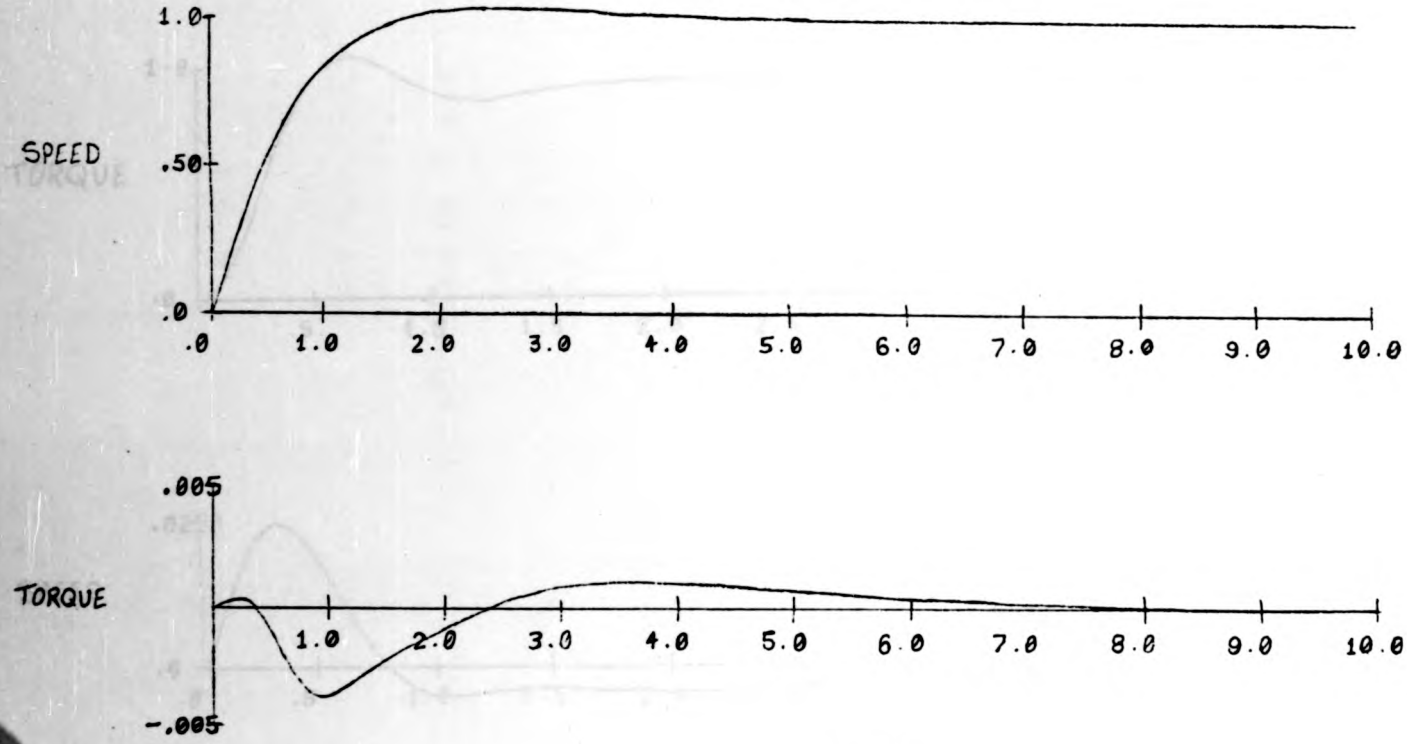

FIG.11

PREDICTED RESPONSE TO A UNIT STEP IN TORQUE

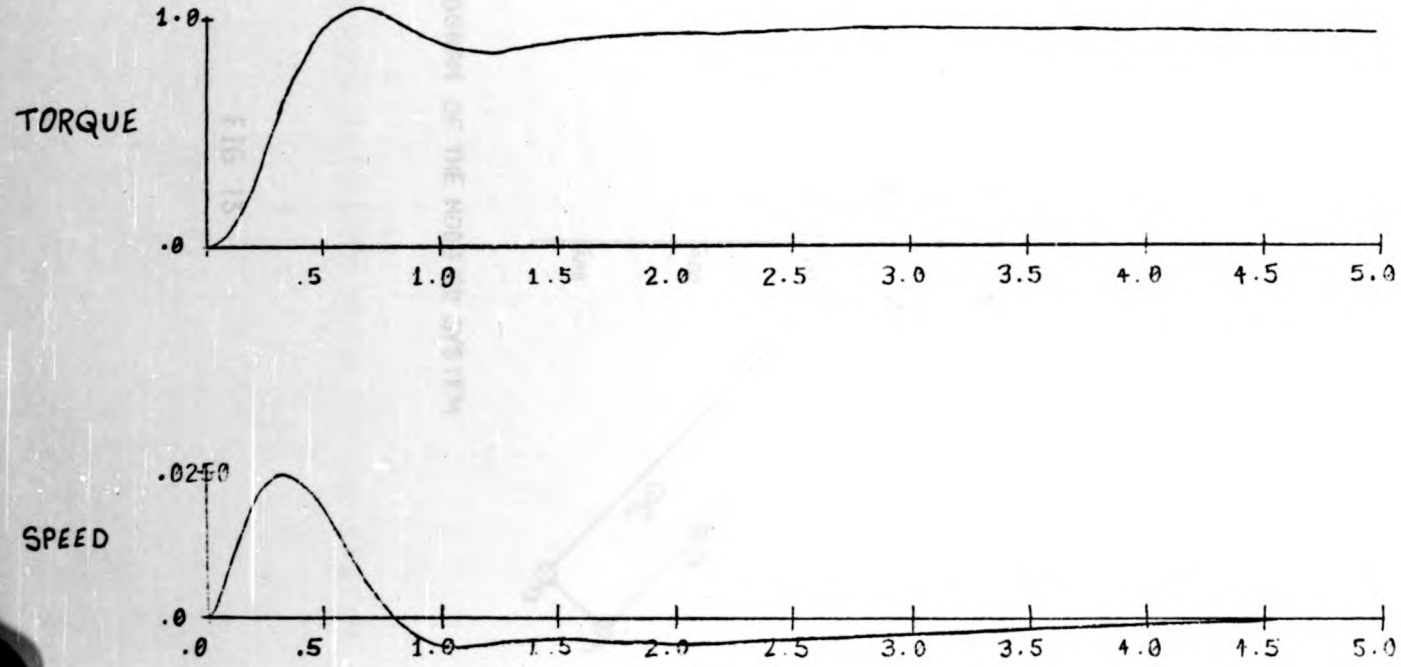

FIG. 12

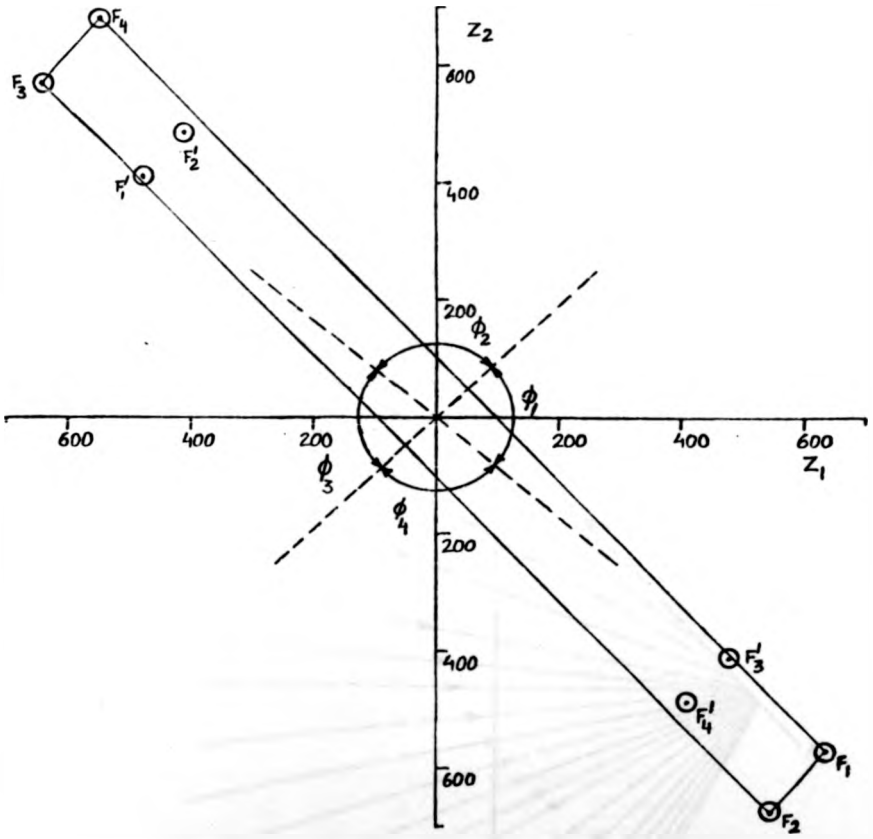

PARALLELOGRAM OF THE MODIFIED SYSTEM.

FIG. 13

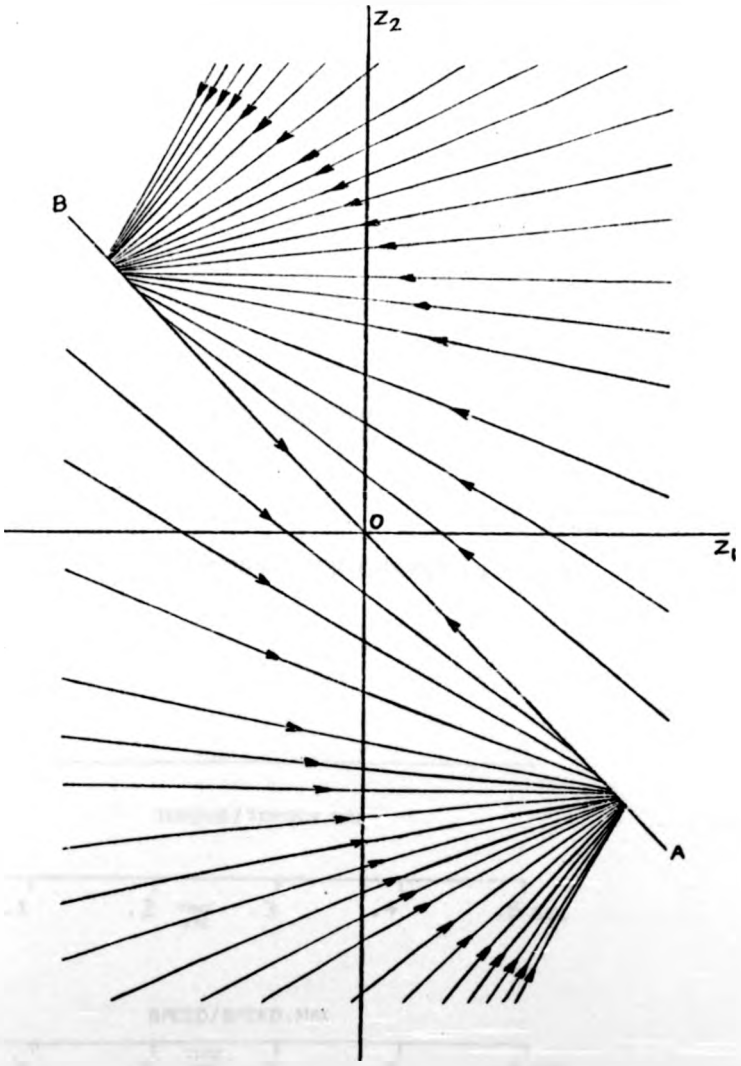

OPTIMAL TRAJECTORIES OF THE TEST BED SYSTEM

FIG. 14

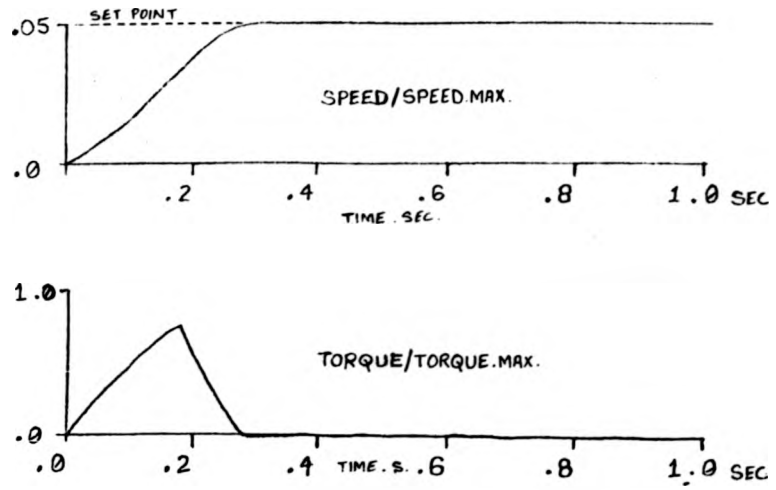

RESPONSE OF THE SYSTEM TO A STEP CHANGE IN SPEED

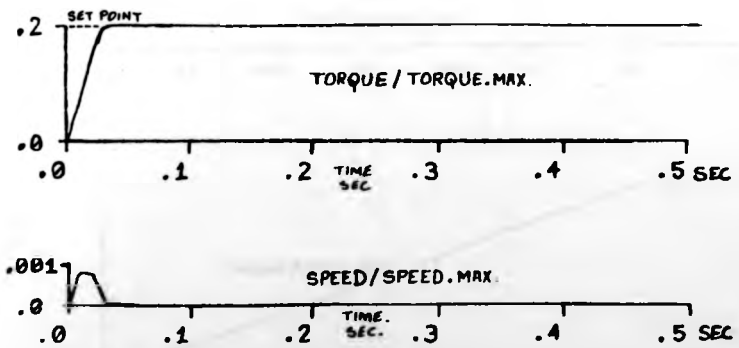

RESPONSE OF THE SYSTEM TO A STEP CHANGE IN TORQUE

SYSTEM BEHAVIOR WITH TIME OPTIMAL BANG-BANG CONTROL

FIG. 15

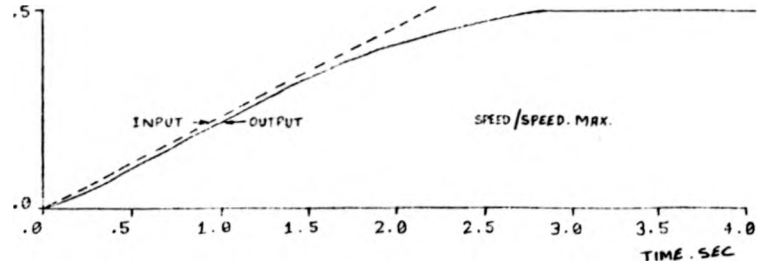

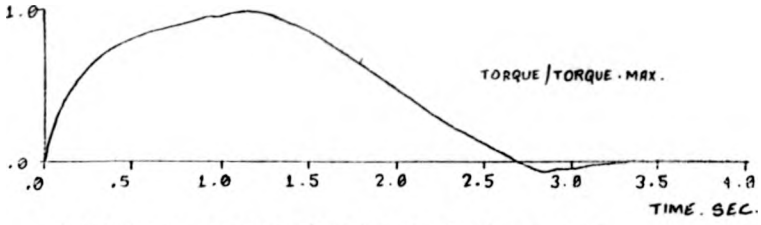

RESPONSE OF THE SYSTEM TO A RAMP CHANGE IN SPEED

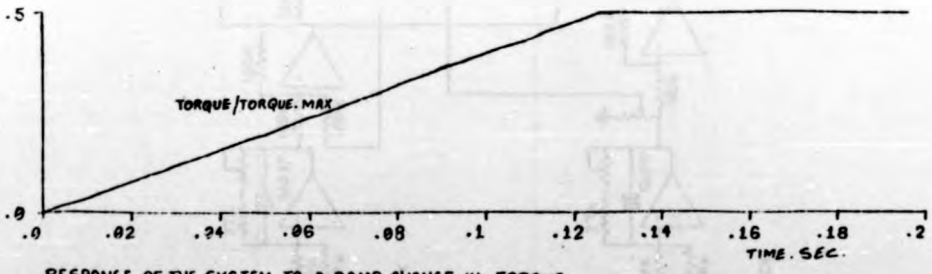

RESPONSE OF THE SYSTEM TO A RAMP CHANGE IN TORQUE

FIG. 16

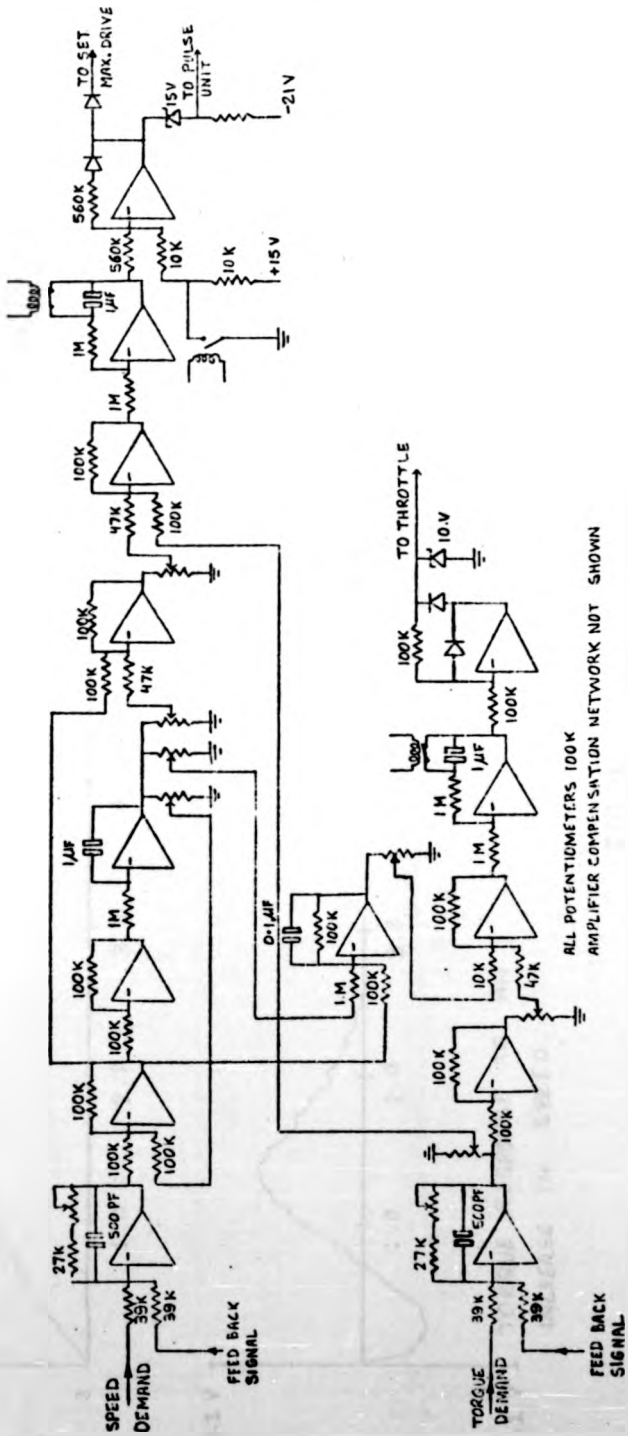

CIRCUIT DIAGRAM OF THE MULTIVARIABLE CONTROLLER

FIG.17

MEASURED RESPONSE TO A UNIT STEP IN SPEED

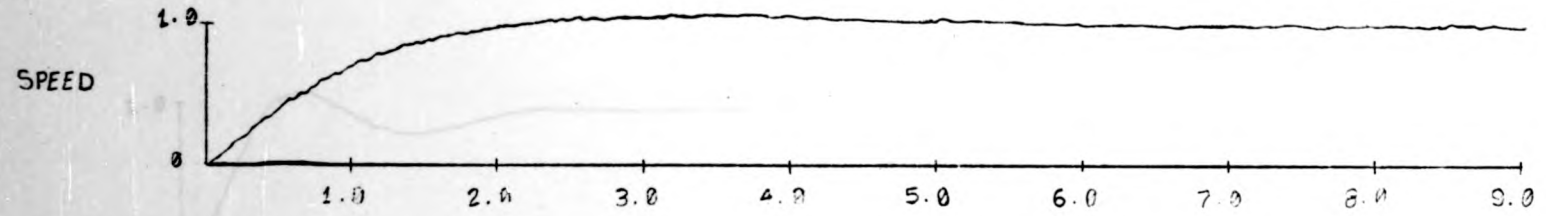

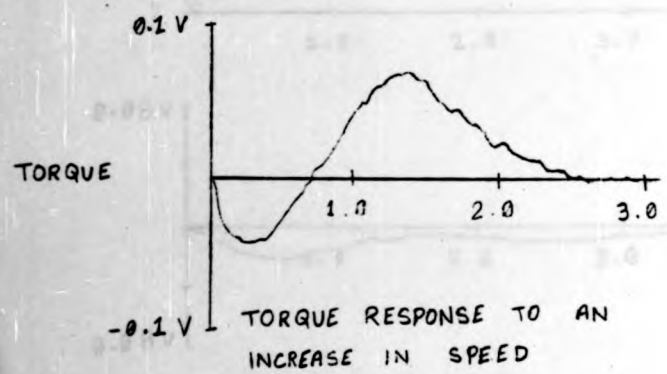

TORQUE RESPONSE TO AN INCREASE IN SPEED

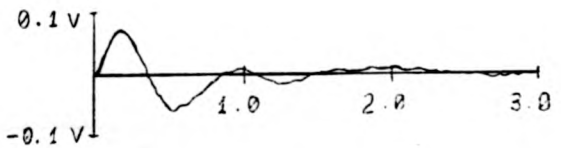

TORQUE RESPONSE TO A DECREASE IN SPEED

FIG. 18

MEASURED RESPONSE TO A STEP CHANGE IN TORQUE

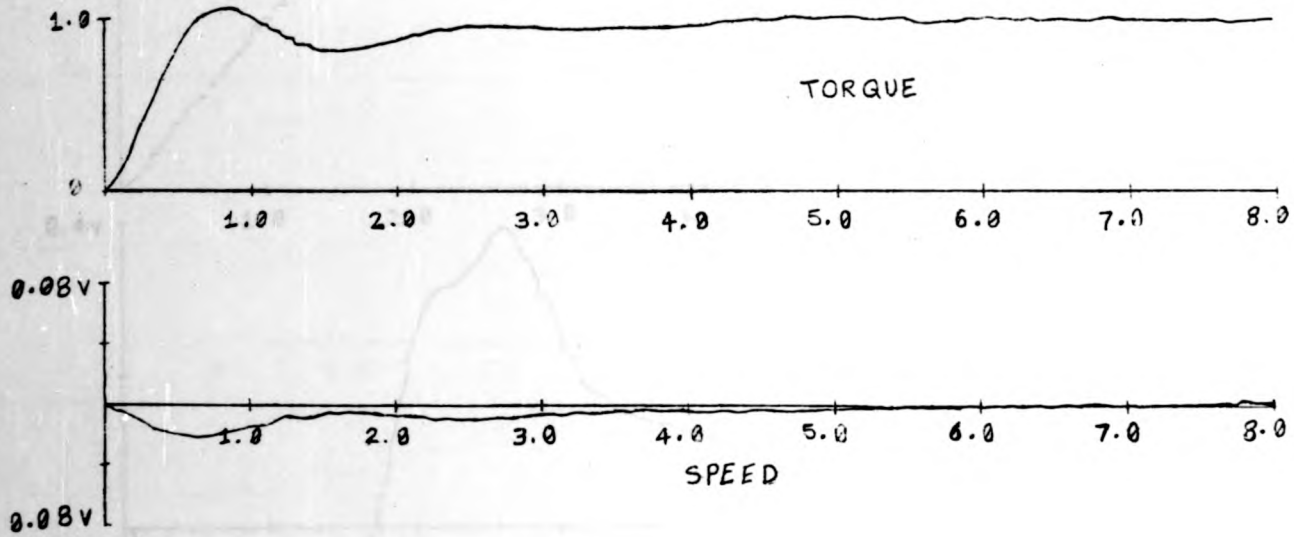

FIG. 19

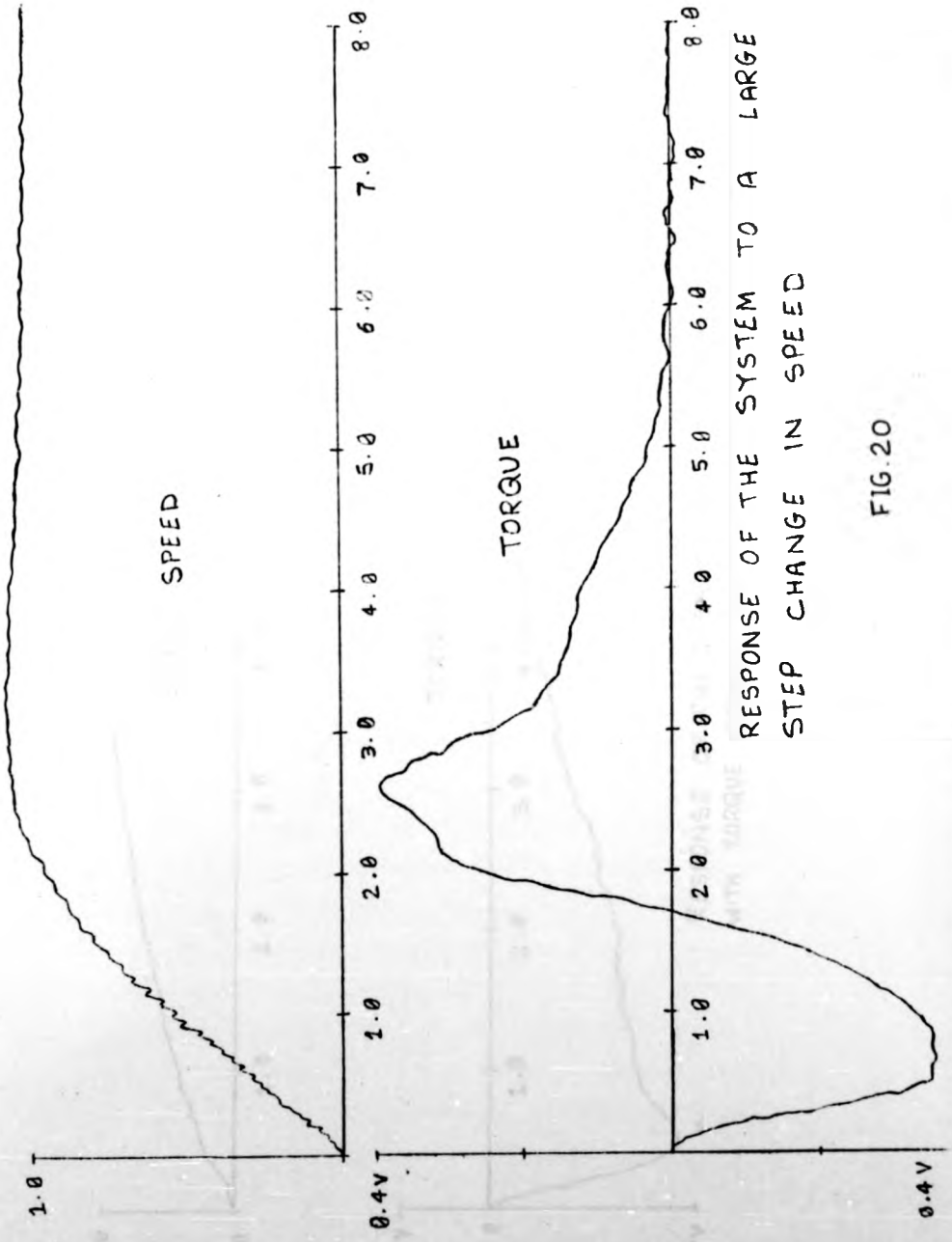

RESPONSE OF THE SYSTEM TO A LARGE STEP CHANGE IN SPEED

FIG.20

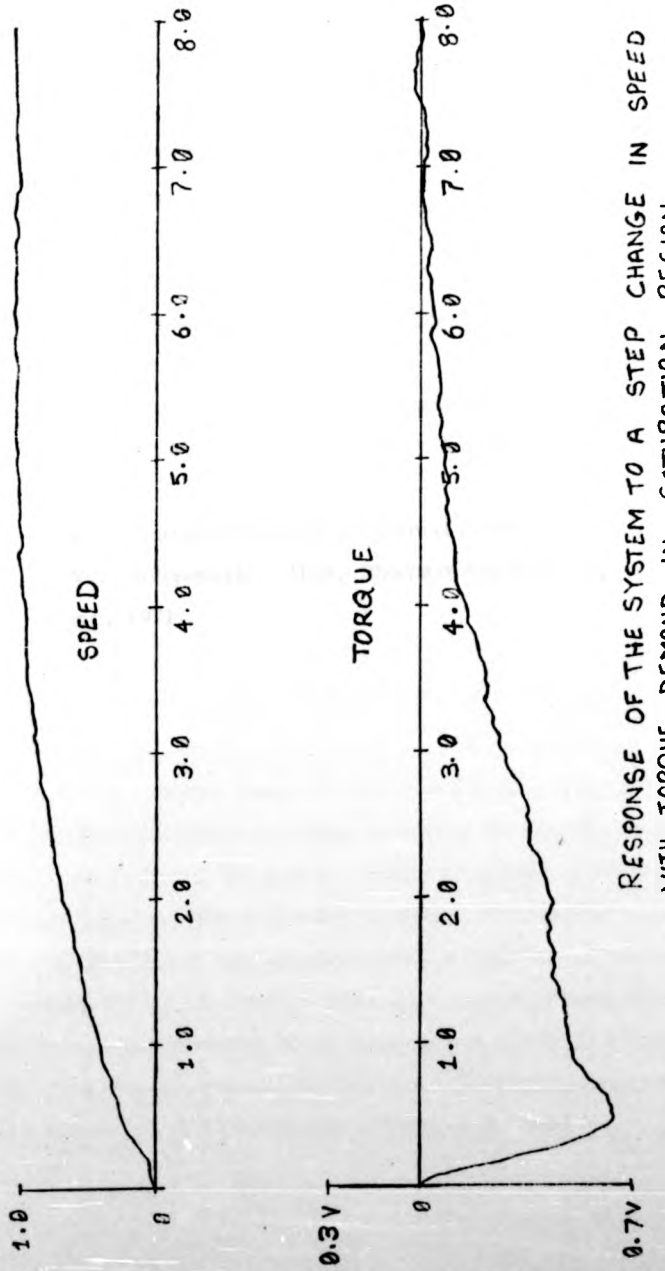

RESPONSE OF THE SYSTEM TO A STEP CHANGE IN SPEED WITH TORQUE DEMAND IN SATURATION REGION

FIG.21

References

4.1. ' Studies in Engine Test Bed Automation.'
J.V.Comfort,University of Warwick Ph.D.thesis
Nov. 1970.

4.2. ' Control of Engine/Dynamometer Test Rig .'
R.Romano. M.Sc. Dissertation. UMIST. 1975

4.3 ' Computer-Aided Control System Design .'
H.H.Rosenbrock, Academic Press, 1974.

4.4. ' The Mathematical Theory of Optimal Processes. '
L.S.Pontryagin et al., J.Wiley & Sons , 1962

4.5. ' Mathematical Methods of Optimal Control . '
V.G.Boltyanskii . Holt, Rinehart and Winston,
Inc. 1971 .

CHAPTER 5 STUDIES OF THE TRANSIENT BEHAVIOUR OF ENGINE

5.1. Introduction

In the evaluation of the behaviour of vehicle power trains , simulation plays an increasingly important role. It has been normal practice up to the present to characterise the engine by steady state maps. Simulation studies indicate that the steady state maps are inadequate to describe the behaviour of the emissions. The available evidence suggests that the transient effects should be considered. Much work has been done to investigate the behaviour of emissions and conflicting conclusions are drawn from the results (Ref.5.1, 5.2). However, it is generally agreed that predicted emissions by using steady state maps do not agree with the actual emissions obtained from dynamometer simulation. This has led to models that describe the 'average dynamic' behaviour over some well defined drive cycle (Ref.5.3). The models obtained in this manner are complicated due to the lack of knowledge of the processes involved and are only valid for fixed trajectories of the engine states.

More recent developments in this area (Ref.5.4) suggest that the mixture preparation system of the engine plays an important role in determining the transient behaviour of the engine. It has been suggested that impaction of fuel on the manifold wall results in a thin film of fuel which presents a 'hold-up' in the fuel supply during engine transients. That is, a sudden opening of the throttle results in weakening of the mixture and similarly a sudden closure of the throttle richens the mixture. Convincing arguments based on this idea can be developed to indicate the need for an

accelerator pump which is normally fitted to the carburettors.

The above discussions indicate that knowledge of the transient behaviour of the engine is vital for vehicle simulation studies. The increased understanding of the engine processes that results from the knowledge gathered also assists in a better control of the engine. To this end experiments were carried out on the engine to investigate the transient behaviour of exhaust emissions.

In the analysis of the transient behaviour of exhaust emissions, two important factors need to be considered. One is that the emissions analysis equipment has slow response time and therefore the dynamics of the gas analysis system need to be considered. Secondly, the engine system is a non-linear device and hence care is necessary when deciding the form of test signals. For the purposes of the study it was convenient to consider the emissions system in two parts. One was concerned with the production of pollutants and the other with the measurement. As is obvious, the need here was thought to be the isolation of emissions generation process. Some of the ideas resulting from the emissions study were extended and applied to the case of engine efficiency. The transient emissions that result from engine on-off operation were also investigated because this form of engine control has a possible application in a hybrid vehicle.

5.2. Transient behaviour of gas analysis system

Initial enquiries revealed that the instantaneous measurement of emissions was not possible due to the slow response of available gas analysis equipment. The use of continuous measurement of emissions necessitated the identification of the system dynamics. The system was identified in the time domain by

step responses and in the frequency domain by spectral analysis methods.

Since the behaviour of the sampling line was not known, it was included in the system. A positive displacement pump was used to pump the sample because it has low residual gases. However, the input to the analysis system is quantised at the pump frequency (50 Hz). Thus a low displacement pump running at high speeds is necessary to reduce the quantisation effects and the transport delays. The size of the water trap also needs to be small to reduce the hold up (Chapter 3, Fig.5).

Since it was impractical to apply a continuous change in the concentration levels at the inlet to the system, Pseudo-Random-Binary-Sequence was chosen as an input signal. To this end a three-way spool valve was constructed which allowed the calibrating gases to be switched between two cylinders (Fig.1). The signal from the P.R.B.S. generator was used to switch the solenoid operated spool valve via a suitable signal conditioning circuit.

The input P.R.B.S. signal and the system output signal were recorded on computer via fourth order butterworth filters with cut-off frequency set at 0.3 the sampling frequency (Fig.2). The time delay of the exhaust sample line was assessed from the cross correlation functions (Appendix III) and the recorded signals were aligned accordingly (Fig.3). The magnitude and the phase plots suggested that each analysis equipment was a damped second order system over the frequency range considered . Transfer functions were fitted to the results and the comparison is shown in figures 4A → C.

The transfer functions of the system are apparently as follows :

$$\frac{Y_{co}}{X_{co}} = \frac{K_{co}}{(1 + 0.5s)(1 + 0.6S)}$$

$$\frac{Y_{no}}{X_{no}} = \frac{K_{no}}{(1 + 0.5S)(1 + 0.6S)}$$

$$\frac{Y_{HC}}{X_{HC}} = \frac{K_{HC}}{(1 + 0.4S)(1 + 0.25S)}$$

The comparison of the step responses is shown in figure 5.

Due to the complicated nature of the analysis system, contributions to the overall dynamics by various components of the system are difficult to assess. The response of the N.D.I.R. analyser was measured by applying a small step change to the infrared light entering the sample tube. This was accomplished by obstructing the light beam with a thin wire. The response of the analysis equipment was that of a first order lag with a time constant of 0.6 seconds. This indicated that the second lag was due to the diffusive elements in the gas handling system. If perfect mixing is assumed in the hold up volumes, then

The transfer functions of the system are apparently as follows :

$$\frac{Y_{co}}{X_{co}} = \frac{K_{co}}{(1 + 0.5s)(1 + 0.6s)}$$

$$\frac{Y_{no}}{X_{no}} = \frac{K_{no}}{(1 + 0.5s)(1 + 0.6s)}$$

$$\frac{Y_{HC}}{X_{HC}} = \frac{K_{HC}}{(1 + 0.4s)(1 + 0.25s)}$$

The comparison of the step responses is shown in figure 5.

Due to the complicated nature of the analysis system, contributions to the overall dynamics by various components of the system are difficult to assess. The response of the N.D.I.R. analyser was measured by applying a small step change to the infrared light entering the sample tube. This was accomplished by obstructing the light beam with a thin wire. The response of the analysis equipment was that of a first order lag with a time constant of 0.6 seconds. This indicated that the second lag was due to the diffusive elements in the gas handling system. If perfect mixing is assumed in the hold up volumes, then

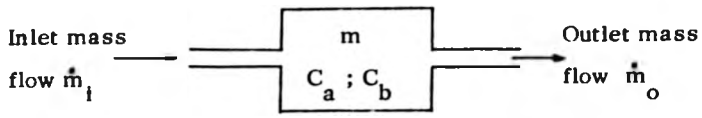

The total mass held up is

$$m = m_a + m_b$$

and the composition of constituent a

$$Ca = m_a / m$$

Then for small changes

$$dm_a = dC_a \cdot m$$

$$dm_a = \dot{m}_{ai} - \dot{m}_{ao}$$

$$\frac{m}{\dot{m}} \frac{dCa}{dt} = \frac{\dot{m}_{ai}}{\dot{m}} - \frac{\dot{m}_{ae}}{\dot{m}}$$

$$T \frac{dCa}{dt} = C_{ai} - C_{ao}$$

but $C_{ao} = Ca$ since perfect mixing

$$\therefore \quad \frac{Ca}{C_{ai}} = \frac{1}{1 + TS}$$

Using the perfect mixing model the time constants of the individual elements of the sample line for the N.D.I.R. analyser are as follows :

Condensate trap	0.064 seconds
Sample pump	0.02 seconds
Filter	0.5 seconds
Analyser sample tube	0.2 seconds

The above analysis indicates that the second time constant in the N.D.I.R. model is predominantly due to the mixing in the sample filter. Since the diffusion or mixing process is essentially a distributed parameter system it is thought that the measured time constant is due to the contributions from the various hold ups and duc to the mixing in the sample line. However, the simple analysis gives a valuable insight into the processes involved.

5.3. Transient behaviour of exhaust emissions

Since the engine is a discrete process the dynamic changes in the emissions can be expected to take place at the firing frequency of the engine. The identification because of the limitations imposed by the measurement system can only be done by discrete sampling of exhaust gases. The practical constraints and the high frequency nature of the process led to the idea of representing the process by average changes in pollutants with frequency of perturbation of an engine state. To this end experiments were carried out in which sine wave perturbations were applied to the engine throttle at a constant engine speed. The output of the pollutants was continuously recorded whilst the perturbation frequency was altered. From these experiments it soon became apparent that the mean level of the output did not alter with frequency, but the amplitude increased with frequency. Moreover,

the maximum change in the amplitude occurred at frequencies well below one Hertz. Because air leaks into the engine manifold can cause changes in fuel air ratio, the system was checked for air leaks and the excess fuel drain pipe fitted to the inlet manifold was plugged. From subsequent tests it was concluded that significant dynamics of the process can be measured and represented by the traditional frequency domain methods.

Since the engine system is a non-linear device with many variables affecting the production of emissions, it was decided to investigate the system with respect to a fixed reference state, namely the optimum engine efficiency state. Therefore the air/fuel ratio and the ignition timing were controlled to give the optimum efficiency at the operating point. The temperature of the inlet air was measured and controlled to less than 5% of deviation about the operating point. The object here was to control the thermodynamic states of the inlet system and hence prevent drifts of the emissions signals. In this respect a measure of the mixture temperature in the manifold would have been more appropriate. Attempts were made to measure the mixture temperature but the noise due to the impaction of fuel on the probe seriously impaired the accuracy. However, it was found that with steady engine operation the mean value of mixture temperature followed the changes in the inlet air temperature as measured at the air flow meter. Therefore a check on the inlet air flow was thought to be sufficient to fix the operating point of the inlet system.

The magnitude of the throttle perturbation signal was determined by using a transfer function analyser . A signal at a fixed frequency was applied to the throttle and the changes in the gain and phase were observed with the changes in the input magnitude. The value of the input at which gain and phase of the

system altered from a constant value indicated the maximum value of perturbation amplitude that can be applied to the throttle position without departing from linearity. A signal level with peak to peak value of one volt satisfied the chosen linearity criterion.

Transfer functions between the pollutants and the throttle position were obtained by a transfer function analyser. The experiments were repeated at different engine speed settings to ensure that the effects observed were not local. To ensure that the observed phenomenon was not due to the measurement and control of air and fuel, experiments were carried out with the standard engine. One of the consequences of the presence of the liquid fuel in the manifold is the maldistribution between the cylinders, which can cause variations of the air fuel ratio between the cylinders (Ref.5.5). The maldistribution varies with engine speed and the standard design of the engine tries to minimize maldistribution. Hence, the checks carried out were thought to be necessary. The maldistribution with a fixed jet carburettor, which the test engine utilized, tends to be greater than that due to a variable jet (constant vacuum) type of carburettor. An engine with approximately twice the test engine capacity, fitted with a variable jet type of a carburettor, was available at the school which as regards the transient emissions,showed similar behaviour.

Spectral analysis with random perturbations of throttle was used as an alternative method of identification (Appendix III). The experimental set up is shown in figure 6. Initially, the engine was run under steady state conditions and the emissions output was recorded on the computer to assess the noise levels on the system. The auto spectrum (Fig.7) of the pollutants show that the noise is essentially confined to low frequencies. The peak

in the hydrocarbon spectrum at 1.5 Hz is due to the F.I.D. pressure regulating bubbler. The area occupied by the peak was found to be 6% of the total area. Since the noise level was low and occurred in the frequency range of interest, it was concluded that guard filters were not essential.

The transfer functions obtained by the two methods between the throttle position and pollutants are compared in figures 8A → C. The measurement dynamics and the time delays (3.2 secs) are removed from the results shown. The time delay was obtained from step responses and more accurately by the cross-correlation functions. The results obtained by the transfer function analyser have the confidence limits (± 5% for magnitude and phase) marked, which indicate the repeatability of the measured points. Scatter limits are large at very low and high frequencies, the regions which also exhibit low coherencies. Identification of the system was carried out in the time domain by step responses (Fig. 9). As an approximation to the step responses the cross-correlation function between throttle and emissions was integrated (Fig. 10). The object here was to compare the actual step responses with those obtained by spectral analysis and thus validate the identification method. The differences bet ween the actual and the predicted responses, particularly near steady state conditions, can be attributed to low coherencies at low frequencies.

The results suggest that the emissions system has a lead term with a low cut off frequency and lag terms at a higher frequency. The time responses and the phase behaviour suggests that the carbon monoxide system has a non-minimum phase behaviour which is thought to be due to the steady state engine tuning. The phase behaviour of hydrocarbons obtained by T.F.A.

suggests a non-minimum phase,whilst that obtained by spectral methods suggests otherwise. The step responses (Fig.9) indicate that the steady state change in hydrocarbons is very small and is dominated by noise. This is thought to be the reason for low coherency and the discrepancy between the T.F.A. and spectral analysis results.

Since the throttle position modulates the fuel air mixture induced into the engine, a more direct representation of the system can be obtained by considering the air as an input to the engine system. The representation of the process would be complicated due to the non-linearities of the engine system and lack of definition of the processes involved. With the air as an input, the engine can be viewed as a process that converts fuel-air mixture and external load into mechanical and chemical outputs.

The pollution system can be simplified by quasi-linearisation by considering small perturbations about a given steady state. This form of representation would be suitable for a hybrid vehicle. In the case of the conventional vehicle operation and on-off strategies, the above considerations do not apply , because the changes are no longer small in practice.

The gas analysis equipment limits the analysis to comparison of exhaust gas properties with reference to standard gases. This consideration leads to the following model of the system

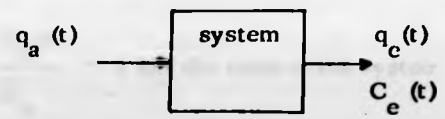

i.e. $q_p(t) = q_e(t).\ C_e(t)$

where $q_a(t)$ and $q_e(t)$ are the inlet and exhaust mass flow rates, $q_p(t)$ is the pollutant mass flow rate, and $C_e(t)$ is the composition of a product in the exhaust gases.

Then for small changes

$$\delta q_p(t) = \bar{q}_e \delta C_e(t) + \bar{C}_e \delta q_e(t) \qquad (2)$$

The bar in the above represents the average quantities.

Also at steady state

$$\bar{q}_e = \bar{q}_a$$

and suppose that (operationally, in terms of Laplace Transforms)

$$\frac{\delta qe}{\delta qa} = G(s) \qquad (3)$$

then

$$Q_p(s) = \bar{Q}_a C_e(s) + \bar{C}_e \; Q_a(s) \; G(s) \qquad (4)$$

$$\frac{Q_p(s)}{\bar{Q}_a \bar{C}_e} = \frac{Q_p(s)}{\bar{Q}_p} = \frac{C_e(s)}{\bar{C}_e} + \frac{Q_a(s)}{\bar{Q}_a} \; G(s) \qquad (5)$$

Let

$\frac{Q_a(s)}{\bar{Q}_a}$ = x (s) the input to the system

$\frac{Q_p(s)}{\bar{Q}_p}$ = Y (s) the output from the system

$$\frac{C_e(s)}{\overline{C}_e} = C(s) \text{ the normalised composition change}$$

Then $$Y(s) = C(s) + X(s)\ G(s) \quad (6)$$

Let $$C(s) = A(s)\ X\ (s) \quad (7)$$

$$Y(s) = A(s)X\ (s) + X(s)\ G(s) \quad (8)$$

$$\frac{Y(s)}{X(s)} = G(s) + A(s) \quad (9)$$

and A(s) is measurable such that

$$A(s) = \frac{Ce\ (s)}{\overline{C}_e} \quad \frac{\overline{Q}_a}{Q_a(s)}$$

The suggested representation requires the knowledge of relationship G(s) between the inlet and exhaust gases. Because only the dynamics were of interest since it is known that at steady state $G(0) = 1$, it was sufficient to compare the phases of inlet and exhaust gases resulting from perturbations applied to the throttle. The exhaust gas flow was measured by monitoring the pressure in the exhaust pipe which can be related to the gas flow rates and for small changes the relationship can be assumed to be linear. The difference in the phase between the inlet and exhaust gases is shown in figure 11. The results show that at low frequencies within the bandwidth of the

emissions system the exhaust and inlet gases are in phase. The results also show a resonance in the exhaust system with a 90 degree change over at 10 Hz. The results are not surprising at low frequencies for a hold up of the exhaust gases (in the form of residual gases within the cylinder) reduces the inlet charge. In other words a negative feedback exists between the inlet and exhaust gases.

The transfer functions depicting the behaviour of normalised quantities are shown in figures 12A → C. Also shown are the plots of fitted equations. In the case of hydrocarbons, normalisation has resulted in a discontinuity in the transfer function at very low frequency and is thought to be due to low coherencies in this region. A gain term was included in the fitted model to allow for this. The functions A(s) are as follows :

$$A_{NO}(S) = \frac{1 + 11.5S}{(1 + 0.6S)(1 + 0.3S)} \quad (10)$$

$$A_{co}(S) = \frac{1 - 11.5S}{(1 + 0.6S)(1 + 0.3S)} \quad (11)$$

$$A_{HC}(S) = \frac{(-0.22)(1 + 11.5S)}{(1 + 0.6S)(1 + 0.3S)} \quad (12)$$

Although a gain term was included for the hydrocarbon responses (eqn.12),the functions A(s) for the three pollutants show that the dynamics of the pollutants are similar. This suggests a

emissions system the exhaust and inlet gases are in phase. The results also show a resonance in the exhaust system with a 90 degree change over at 10 Hz. The results are not surprising at low frequencies for a hold up of the exhaust gases (in the form of residual gases within the cylinder) reduces the inlet charge. In other words a negati ve feedback exists between the inlet and exhaust gases.

The transfer functions depicting the behaviour of normalised quantities are shown in figures 12A → C. Also shown are the plots of fitted equations. In the case of hydrocarbons, normalisation has resulted in a discontinuity in the transfer function at very low frequency and is thought to be due to low coherencies in this region. A gain term was included in the fitted model to allow for this. The functions A(s) are as follows :

$$A_{NO}(S) = \frac{1 + 11.5S}{(1 + 0.6S)(1 + 0.3S)} \quad (10)$$

$$A_{co}(S) = \frac{1 - 11.5S}{(1 + 0.6S)(1 + 0.3S)} \quad (11)$$

$$A_{HC}(S) = \frac{(-0.22)(1 + 11.5S)}{(1 + 0.6S)(1 + 0.3S)} \quad (12)$$

Although a gain term was included for the hydrocarbon responses (eqn.12), the functions A(s) for the three pollutants show that the dynamics of the pollutants are similar. This suggests a

emissions system the exhaust and inlet gases are in phase. The results also show a resonance in the exhaust system with a 90 degree change over at 10 Hz. The results are not surprising at low frequencies for a hold up of the exhaust gases (in the form of residual gases within the cylinder) reduces the inlet charge. In other words a negative feedback exists between the inlet and exhaust gases.

The transfer functions depicting the behaviour of normalised quantities are shown in figures 12A → C. Also shown are the plots of fitted equations. In the case of hydrocarbons, normalisation has resulted in a discontinuity in the transfer function at very low frequency and is thought to be due to low coherencies in this region. A gain term was included in the fitted model to allow for this. The functions A(s) are as follows :

$$A_{NO}(S) = \frac{1 + 11.5S}{(1 + 0.6S)(1 + 0.3S)} \quad (10)$$

$$A_{co}(S) = \frac{1 - 11.5S}{(1 + 0.6S)(1 + 0.3S)} \quad (11)$$

$$A_{HC}(S) = \frac{(-0.22)(1 + 11.5S)}{(1 + 0.6S)(1 + 0.3S)} \quad (12)$$

Although a gain term was included for the hydrocarbon responses (eqn.12),the functions A(s) for the three pollutants show that the dynamics of the pollutants are similar. This suggests a

common controlling process. The behaviour of the emissions can be attributed to the changes in the fuel-air ratio due to the hold ups in the mixture preparation system. It is thought that the changes in manifold pressure due to changes in the air flow result in evaporation or condensation of fuel at the manifold walls. The system then can be represented by the following block diagram.

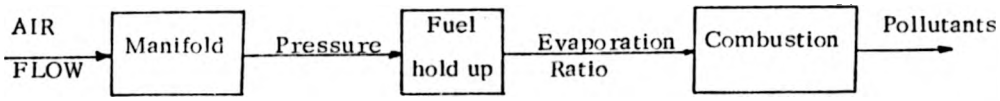

5.4. Exploratory studies into the behaviour of engine efficiency

The work done for control purposes on the test bed modelling show that at low frequencies the dynamics of the system are described adequately by the test bed models (Chapter 4). This indicates that in the frequency range considered the efficiency generating process of the engine does not exhibit significant dynamic effects. That is, the engine torque is proportional to the throttle position for small changes about on operating point. Similar work carried out in the past (Ref. 5.6) over a wider frequency range also indicates that steady state engine maps are adequate for simulation studies. Since the behaviour of emissions under transient operating conditions is different from that under steady state operation due to the mixture preparation system, it was decided to explore this idea for the case of efficiency by changing the air fuel ratio such that the effects of the liquid fuel in the manifold would inrease.

Transfer functions between the throttle and the torque were obtained with fuel flow and the speed held constant. The consequences of the constant fuel flow were such that increase in the throttle position resulted in weakening of the mixture and reduction in the throttle position resulted in richening of the mixture. Mixture changes were kept within 10% of the optimum value at the operating point, for it was thought that greater changes would result in misfiring during transient operation.

The consequences of keeping the speed constant by applying a closed-loop speed control is that the perturbations on the throttle act as disturbance on the speed loop and hence the measured torque. The transfer function between the throttle and the measured torque for the operating conditions can be derived from the test bed models. The transfer function between torque and throttle with a closed-loop engine speed control was obtained from the test bed models discussed in Chapter 4. The resulting transfer function is given by :

$$\frac{\text{Torque}}{\text{Throttle}} = \frac{1 + 8.16\,S + 7.47\,S^2 + 1.33\,S^3}{1 + 8.14S + 9.1\,S^2 + 4.1\,S^3 + S^4}$$

The comparison of the experimental results and those given by the model are shown in figure 13. It is clear that the model describes the behaviour of the system adequately over the frequency range considered. Therefore the efficiency generating process does not exhibit significant dynamic effects as do the pollutants. The reason is thought to be the insensitivity of the efficiency to the fuel air ratio changes near the optimum SFC settings.

5.5. Emission transients during on-off engine operation

In a hybrid vehicle it is desirable to operate the engine at maximum efficiency. Integration of the engine with the energy storage device requires deviation of the engine power away from the optimum efficiency point. In this case an on-off strategy of engine operation can be employed to provide a better integration of the package. The behaviour of the emissions during the on-off transients is not known. The knowledge of the transients is necessary for optimum design strategy.

To assess the behaviour of emissions the engine was run at a constant speed and the fuel supply was turned on and off at the inlet to the jets of the carburettor. Because of the limitations of the test bed system, the air flow into the engine was constant, thus during the fuel off conditions, the cylinders were cooled. The practical situation which the tests simulate is the one where the engine of a hybrid vehicle would be run up to the required speed with external drive and started up as soon as the speed is attained, thus avoiding the transient emissions as well as the operation in the inefficient region.

In the tests carried out the fuel off period was varied between five and thirty seconds. The behaviour of the pollutants for fuel on condition is shown in figure 14 and for fuel off condition in figure 15. The dynamics of the measurement equipment were removed by performing deconvolution (Appendix III). The results indicate that both the hydrocarbon and nitric oxide exhibit an overshoot, whilst the carbon monoxide response is over damped. As the fuel off period is reduced the two responses (fuel off and fuel on)

approach each other keeping their structure.

Since the changes in the emissions occur at relatively slow rates, the result suggest a slow process. Such a process can result from the thermal lags due to the heating of the cylinder walls or the lags in the fuel preparation system. Because the wall temperature mainly affects the hydrocarbons and not nitricoxides, the results suggest that the mixture preparation system is the controlling mechanism. The fueling system can affect the response in the following manner. As the fuel is turned off, the engine relies upon the liquid fuel in the manifold and the jets to sustain combustion. The mixture weakens and results in misfiring. Consequently the nitric oxides go through their peak as mixture weakens and further 'leaning' of the mixture results in misfiring, thus increasing hydrocarbons. The little fuel which is left in the system is released over a period of time. Similarly, as the fuel is turned on, the wetting of the manifold wall and the lags in the fuel flow result in a change in the air-fuel ratio from very lean to its steady state value. Thus the hydrocarbons increase due to misfires and oxides of nitrogen go through their peak with respect to the fuel-air ratio. Carbon monoxide on the other hand does not exhibit a peak with respect to the fuel-air ratio as oxide of nitrogen does , nor does it increase with misfiring like the hydrocarbons. Consequently the carbon monoxide responses appear to be over damped. The situation, however, is more complex due to maldistribution between the cylinders. It is very likely that under transient conditions some cylinders may be misfiring , whilst others can be running at weak mixtures.

The results imply that optimisation can be performed such that the transient effects are averaged out by choosing duration of the 'fuel off' period. The engine, however, needs to be braked rapidly when the fuel is turned off to eliminate continuing hydrocarbon emissions. The use of a fuel injection system on the other hand would eliminate the mixture preparation dynamics. In such cases, thermal lags in the cylinder would dominate the responses.

5.6. Conclusions

Identification of gas analysis system in the time domain by step responses and in the frequency domain by spectral analysis shows that the system essentially consists of two lags in cascade. These lags result from the time constant of the measurement part of the system and from the time constant associated with mixing of gases in the gas flow system. Reduced 'hold up' volumes coupled with high throughput of sample gas therefore reduce the response time as well as the pure time delay of the system.

Studies of the transient behaviour of emissions show that pollutant levels as measured in the exhaust depend upon the perturbation frequency of the throttle. The two types of perturbations of the throttle give similar results. The results indicate that the changes in emission levels occur at low enough frequencies to affect the predictions of pollutants based on steady state performance maps of the engine. Implications are that the rate of change of the engine states as well as the change of states needs to be considered. Representation of the engine as a chemical reactor results in simple models suitable for vehicle drive train simulation studies. The models, however, are applicable only for small changes in the

states of the engine. In practice one such case might be the continuous hybrid vehicle. Further extension of the model by the inclusion of disturbances on the system such as engine or environmental temperature changes can be made to simulate cold engine operation.

Similar dynamic behaviour of the three major pollutants suggests (eqn. 10 - 12) a common controlling mechanism under transient engine operation. It is thought that the behaviour of fuel in the inlet manifold during transients causes the emissions to differ from their steady state values. Further understanding of the two phase behaviour of fuel in the inlet system is therefore necessary for the development of pollution reducing devices.

The studies of the transient behaviour of engine efficiency indicate that over the frequency range considered (0.01-5.0Hz), the transient behaviour of fuel in the inlet system does not affect the engine efficiency. The reason is thought to be the insensitivity of specific fuel consumption to the air-fuel ratio in the vicinity of optimum setting. For the limited frequency range encountered in computer simulation studies, steady state maps are therefore adequate to characterise the engine. The case may be different, however, as perturbation frequencies approach engine firing frequency.

Engine power control by on-off operation results in higher emissions of hydrocarbons and nitric oxides during the transient period than those encountered during steady state operation. Application of this form of engine operation to a hybrid vehicle will require rapid deceleration of the engine speed to standstill to prevent continuing emissions of hydrocarbons. Also engine scheduling will be necessary such that engine "off" periods are of sufficient duration to achieve an average level of emissions.

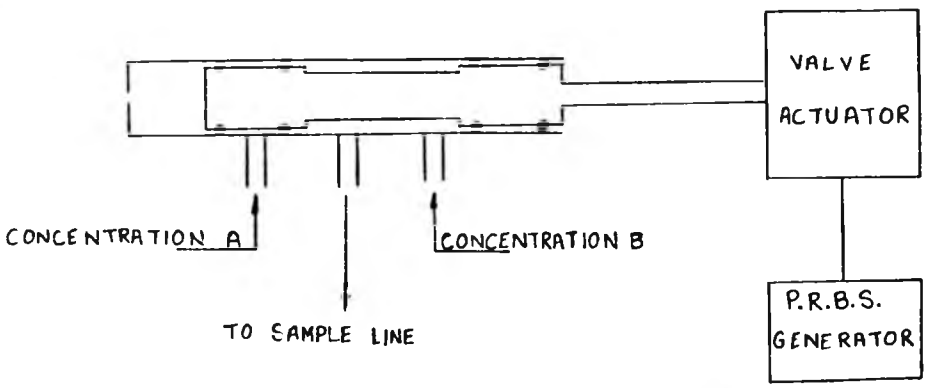

CONCENTRATION LEVEL SWITCHING MECHANISM

FIG.1

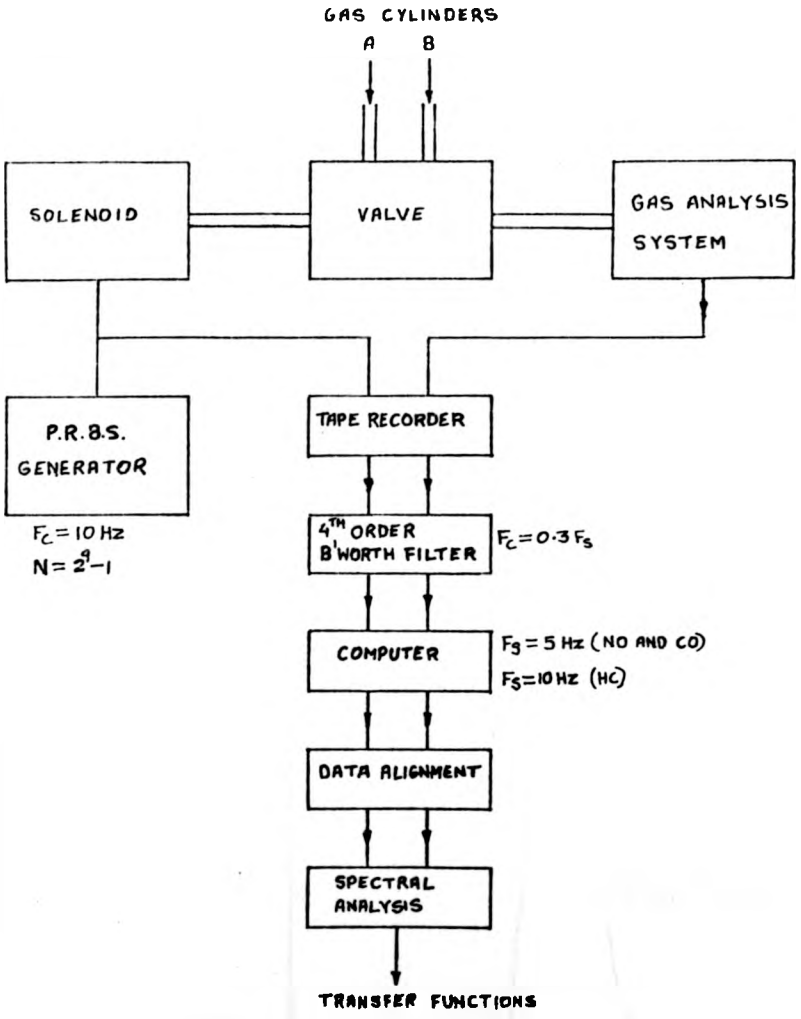

EXPERIMENTAL SET UP TO ASSESS THE DYNAMICS OF EXHAUST GAS ANALYSIS SYSTEM

FIG.2

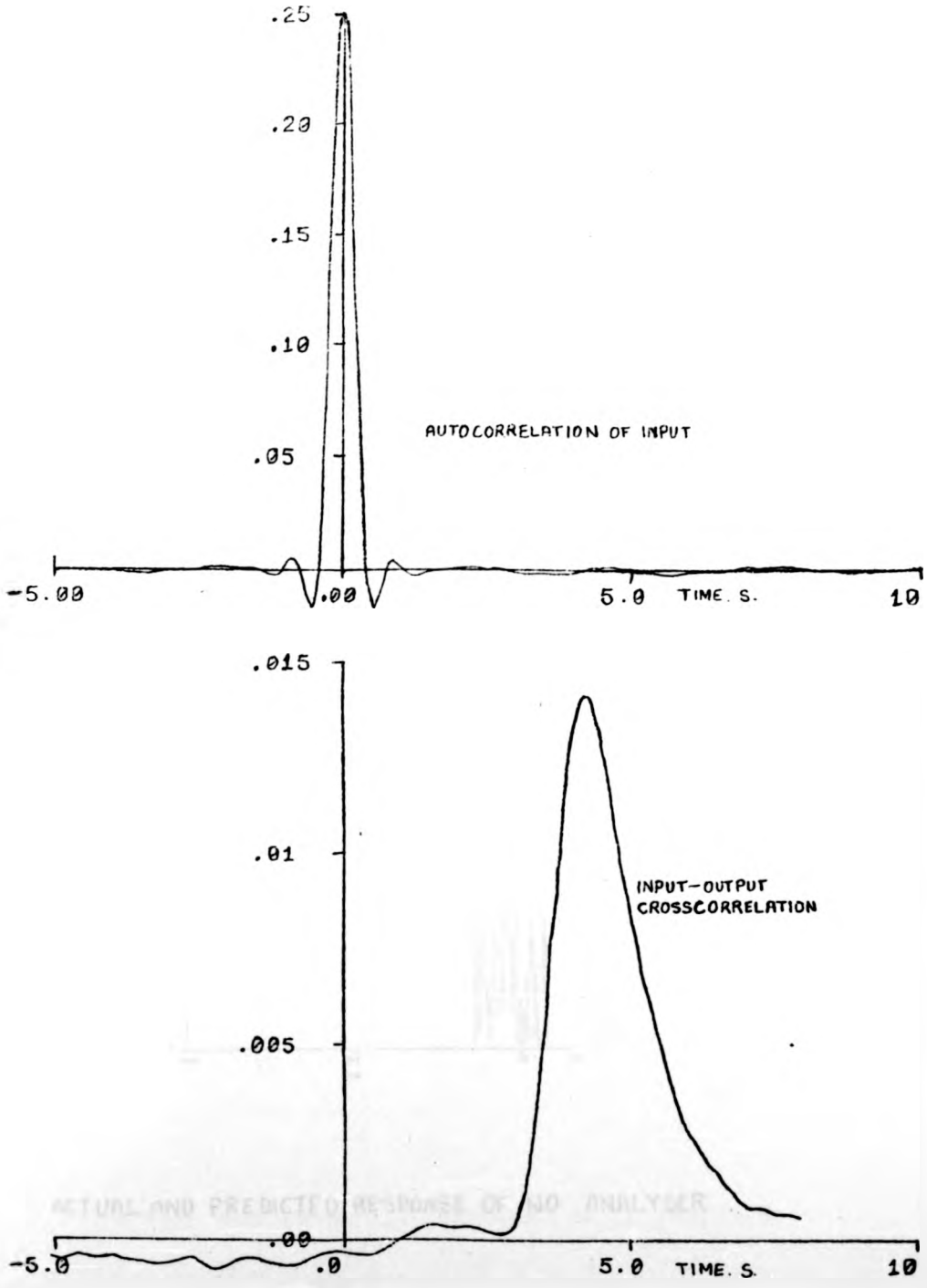

EXAMPLE OF CORRELATION FUNCTIONS OF EXHAUST GAS ANALYSIS SYSTEM

FIG.3

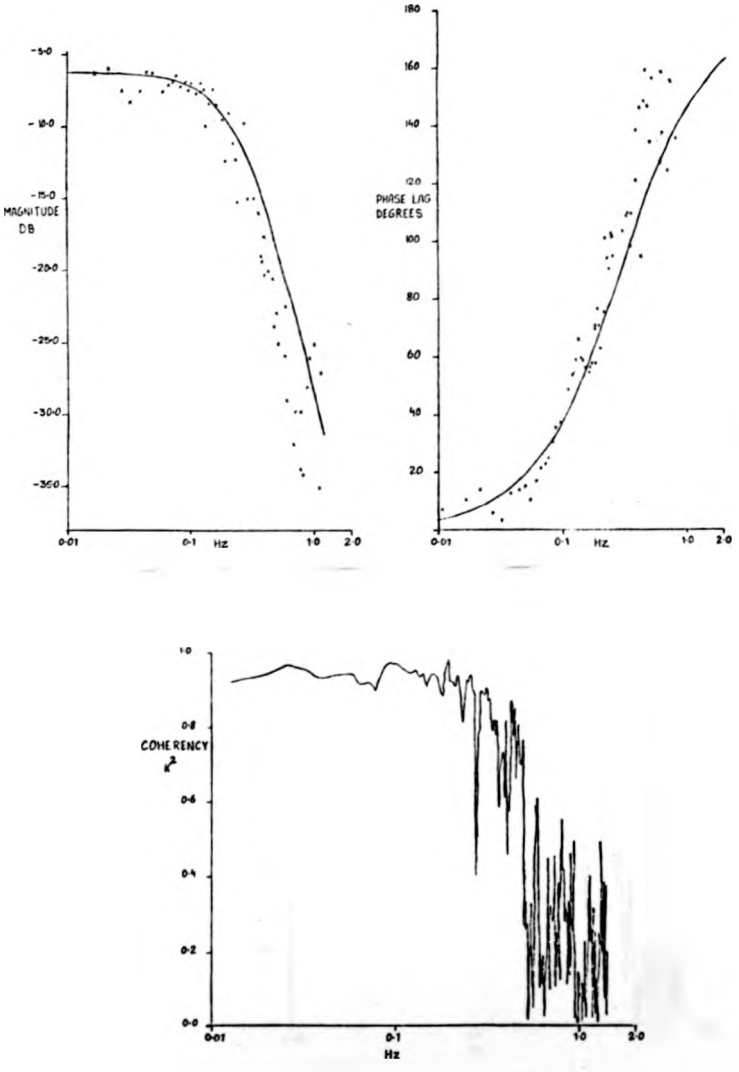

ACTUAL AND PREDICTED RESPONSE OF NO ANALYSER

FIG. 4A

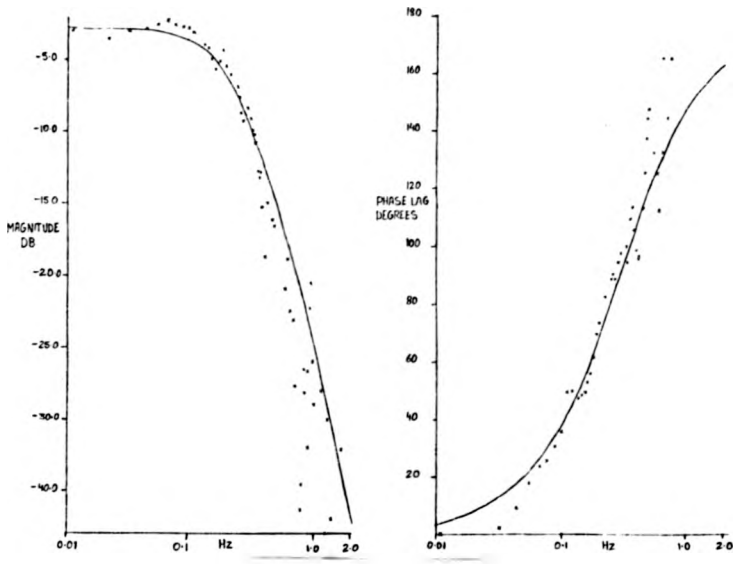

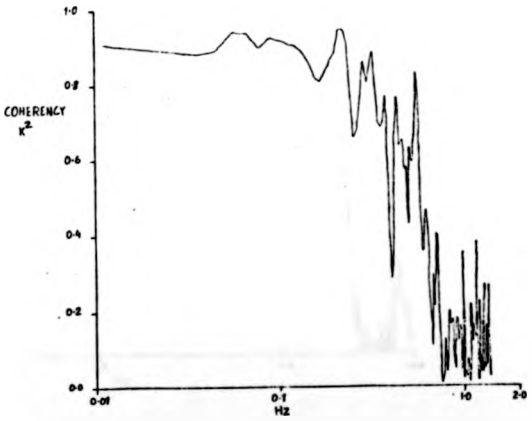

ACTUAL AND PREDICTED RESPONSE OF CO ANALYSER

FIG.4B

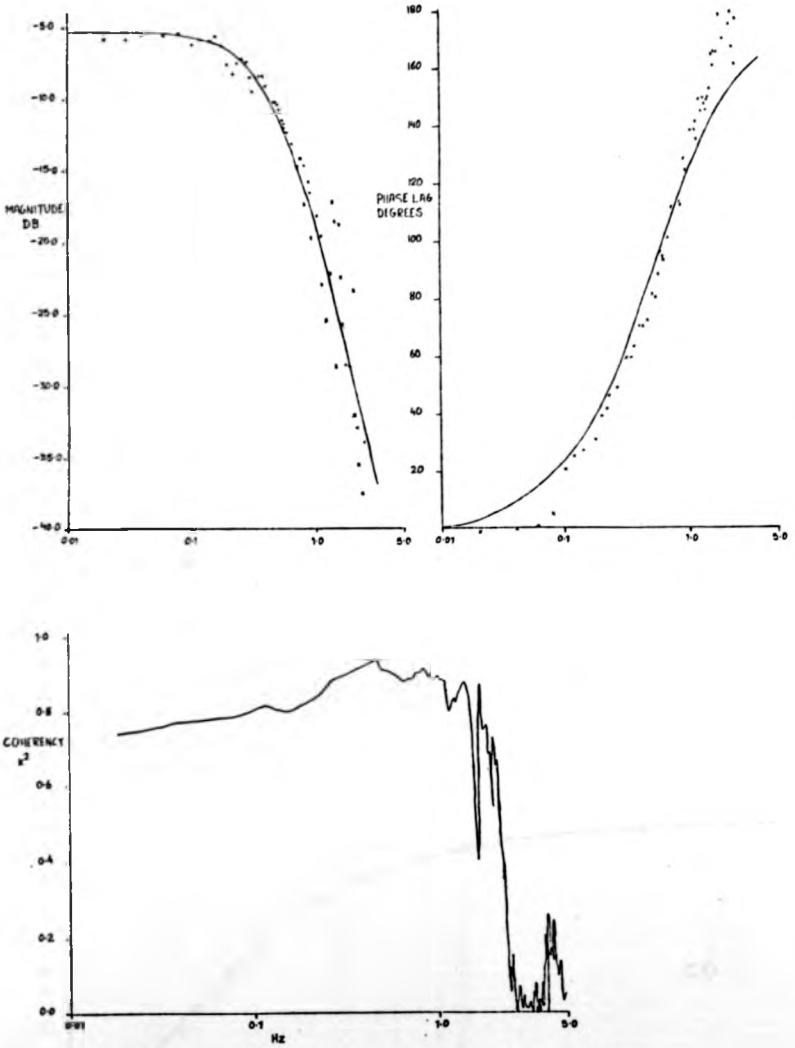

ACTUAL AND PREDICTED RESPONSE OF HC ANALYSER

FIG.4C

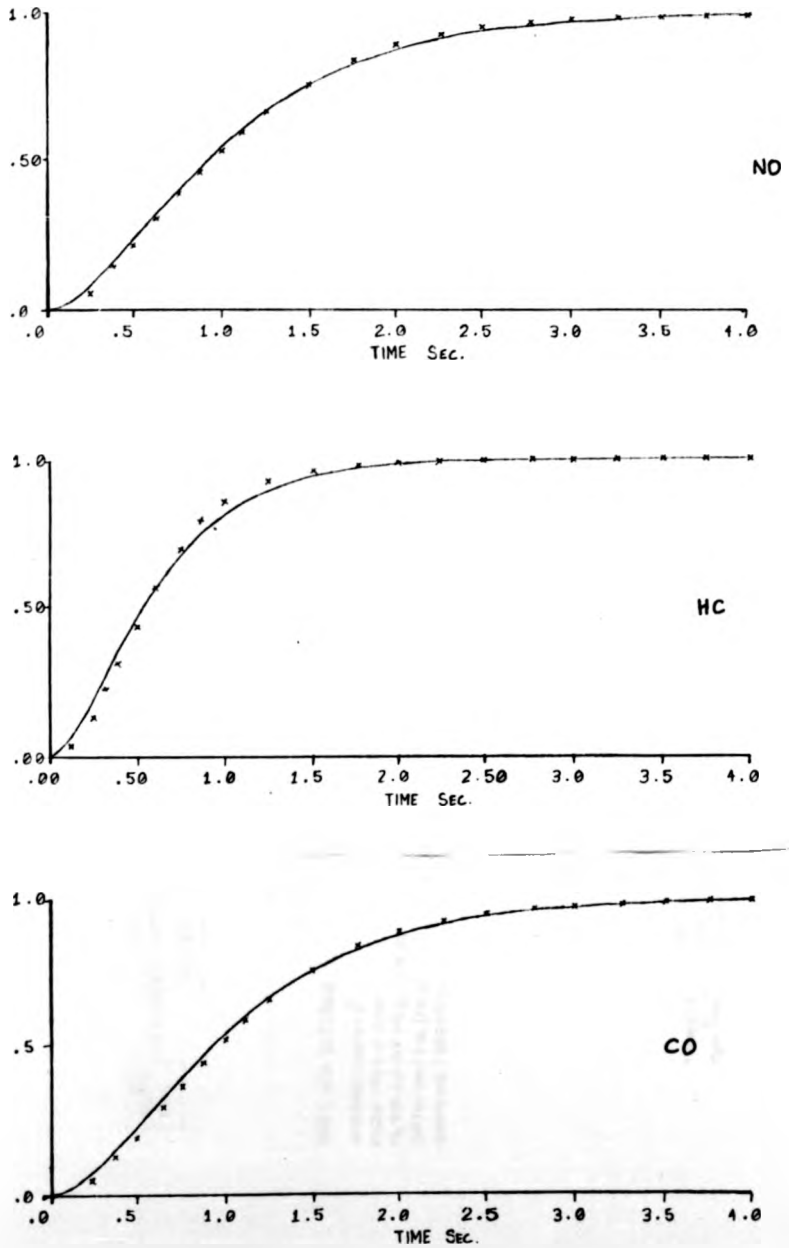

ACTUAL AND PREDICTED GAS ANALYSIS SYSTEM RESPONSE

FIG.5

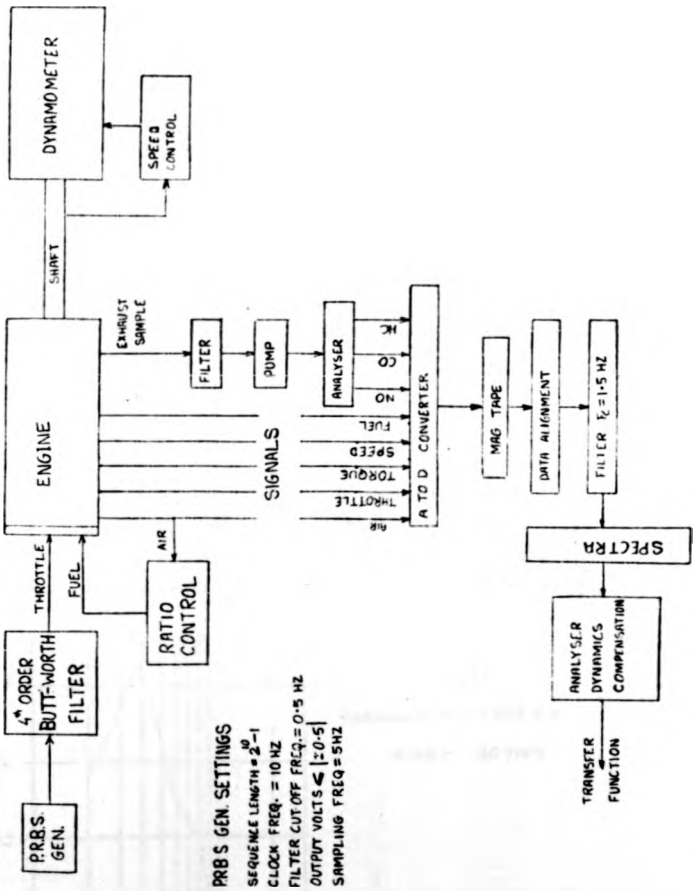

FIG.6

EXPERIMENTAL ASSESSMENT OF POLLUTANT BEHAVIOUR

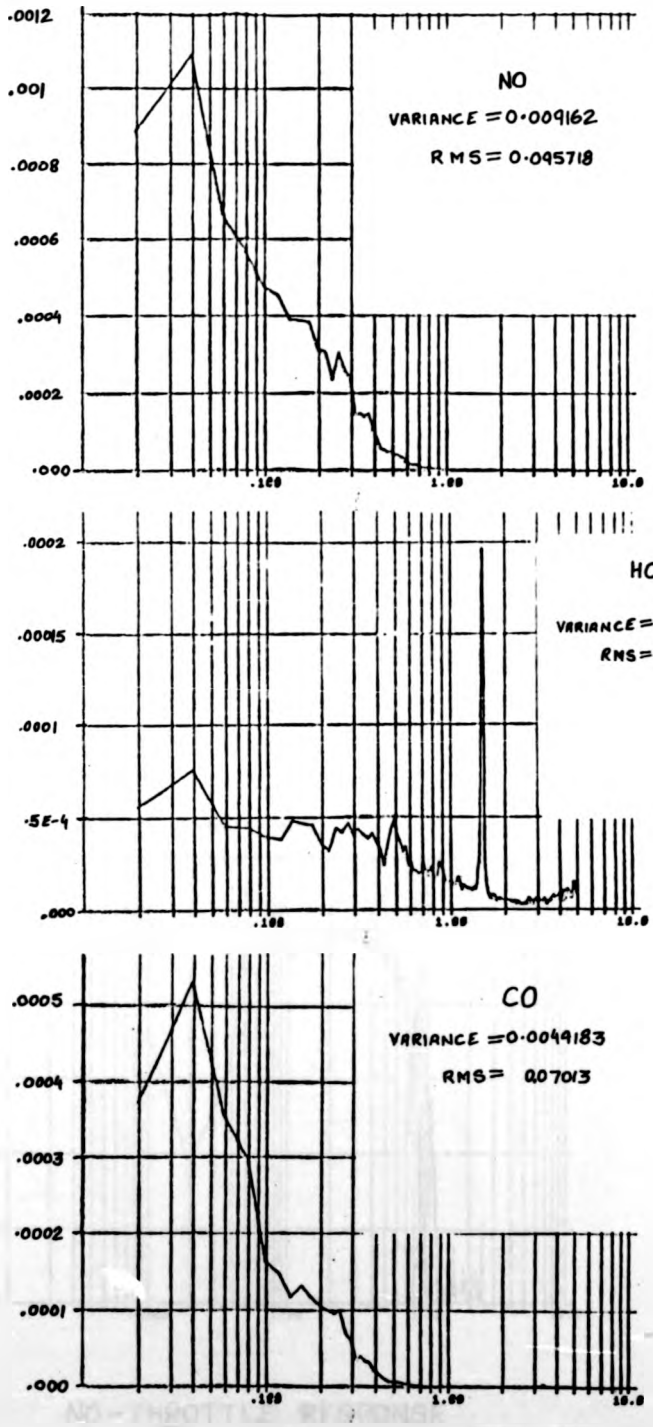

AUTOSPECTRUM OF NOISE ON EMISSIONS

FIG.7

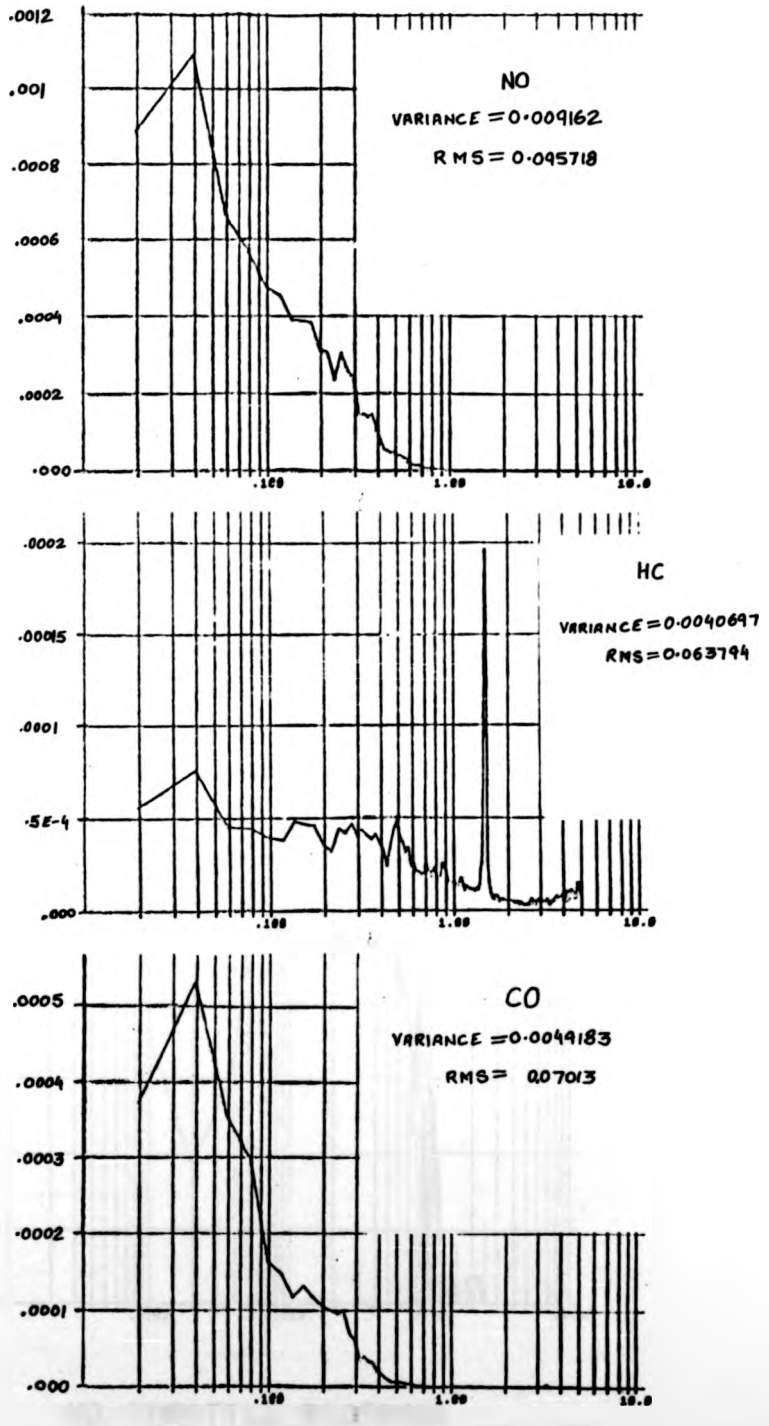

AUTOSPECTRUM OF NOISE ON EMISSIONS

FIG.7

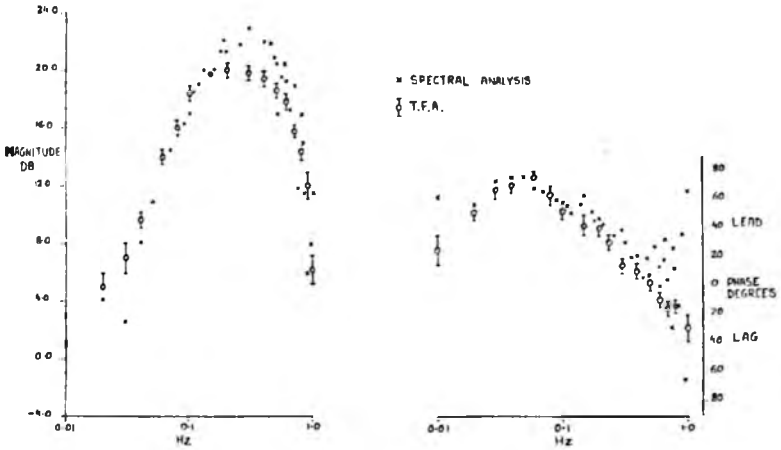

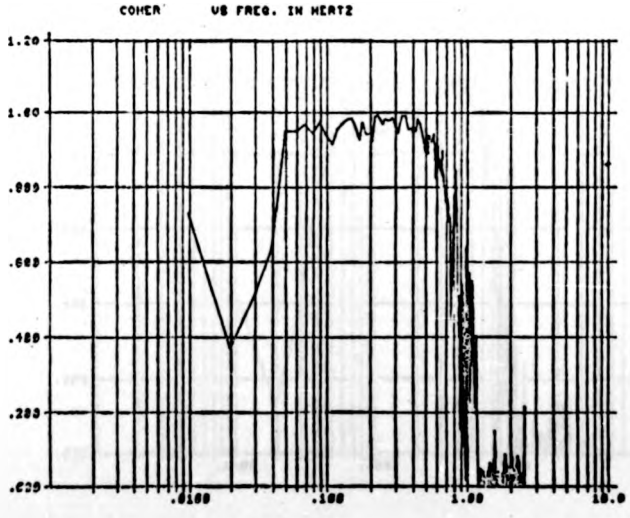

NO-THROTTLE RESPONSE

FIG. 8A

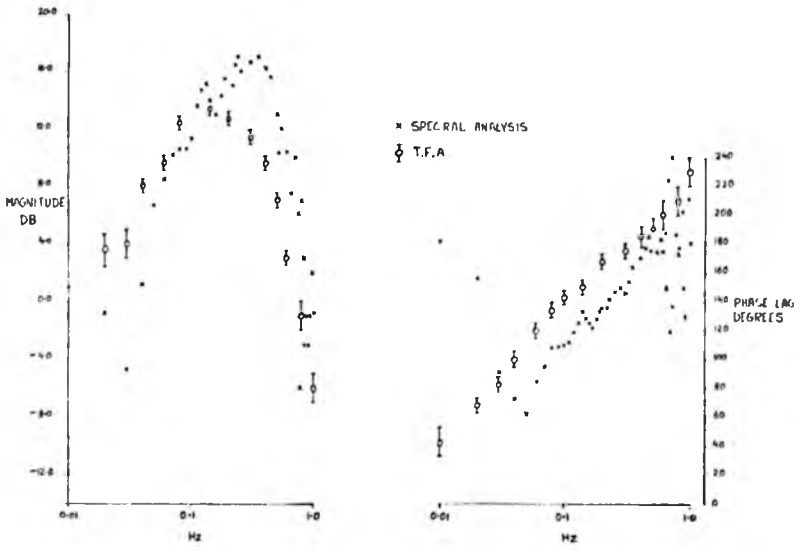

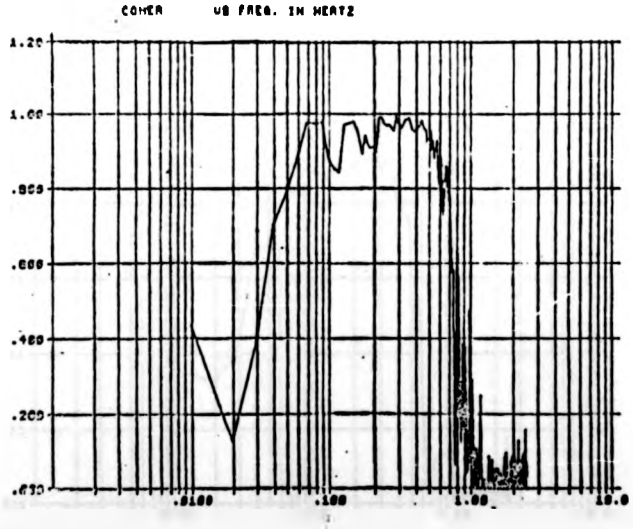

CO-THROTTLE RESPONSE

FIG.8B

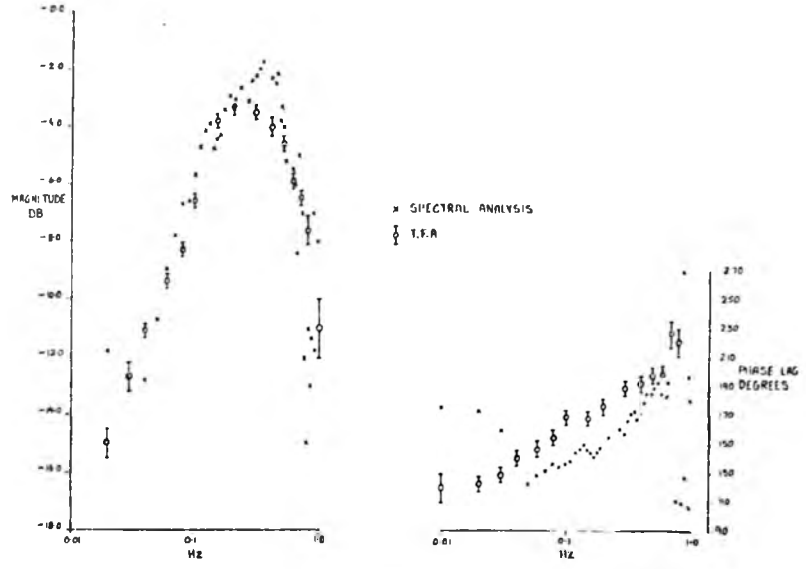

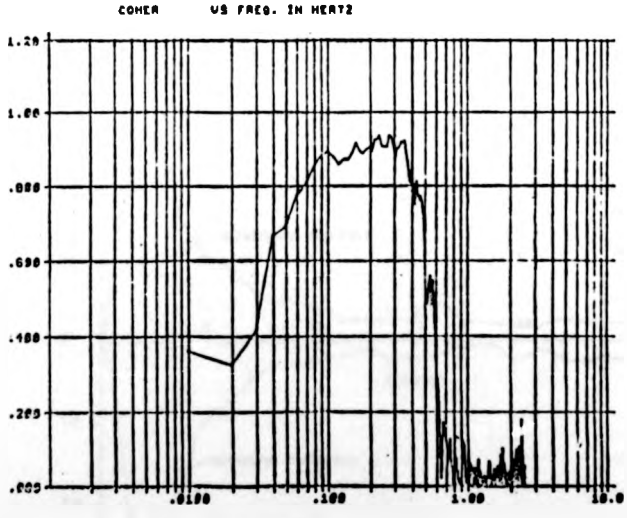

HC-THROTTLE RESPONSE

FIG.8C

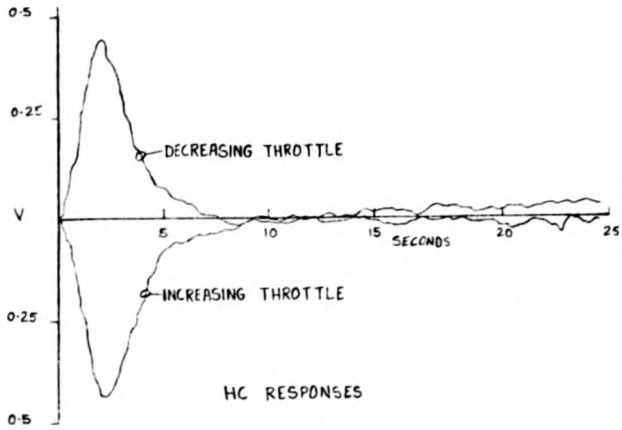

HC RESPONSES

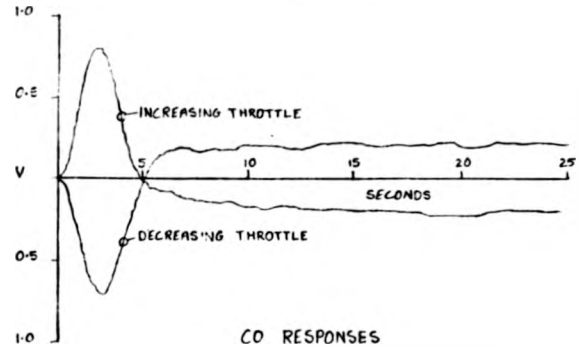

CO RESPONSES

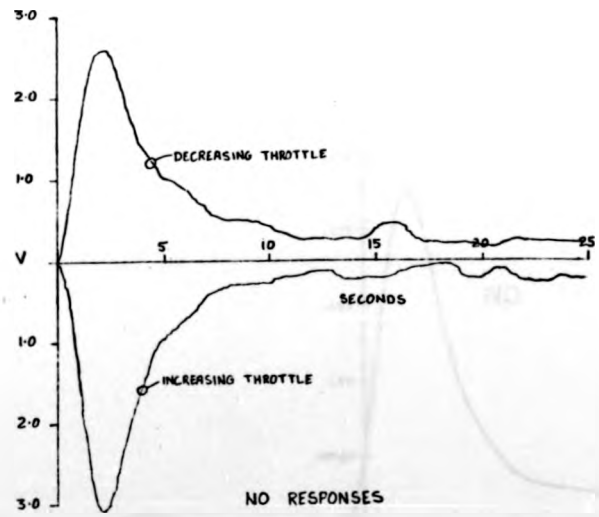

NO RESPONSES

EMISSIONS STEP RESPONSES

FIG.9

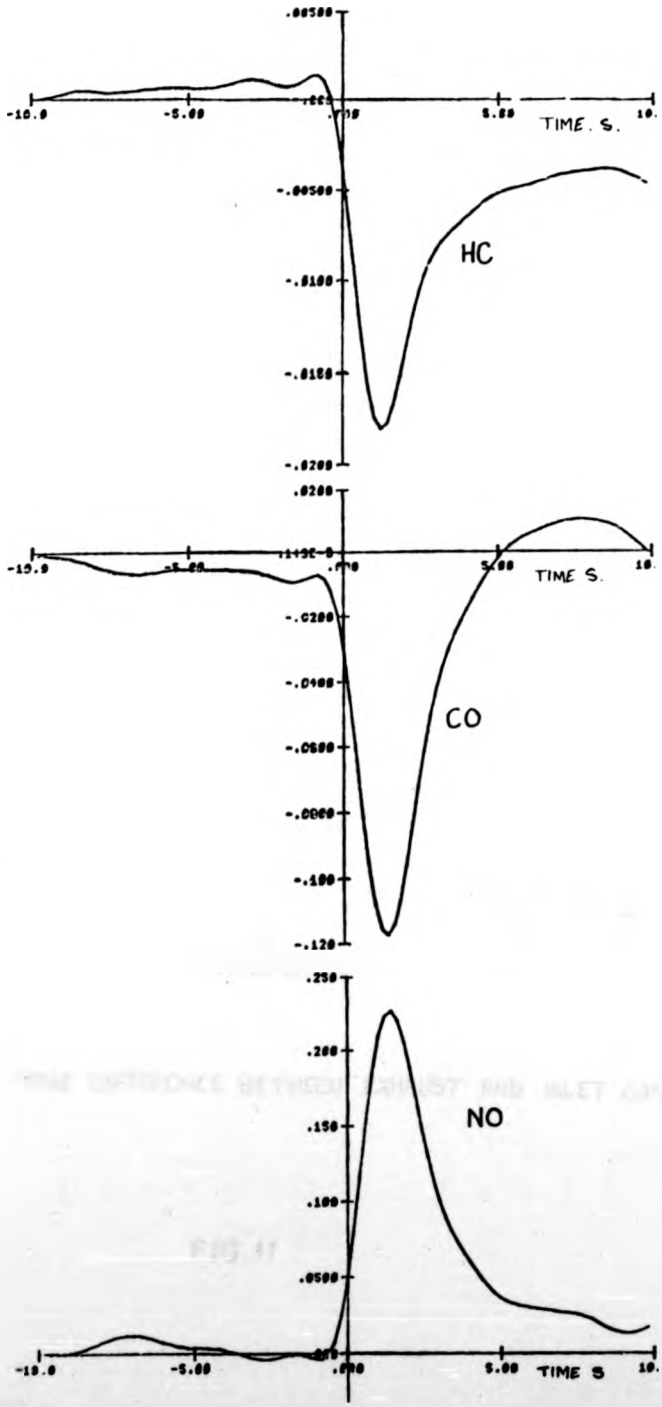

APPROXIMATIONS TO EMISSIONS STEP RESPONSES

FIG. 10

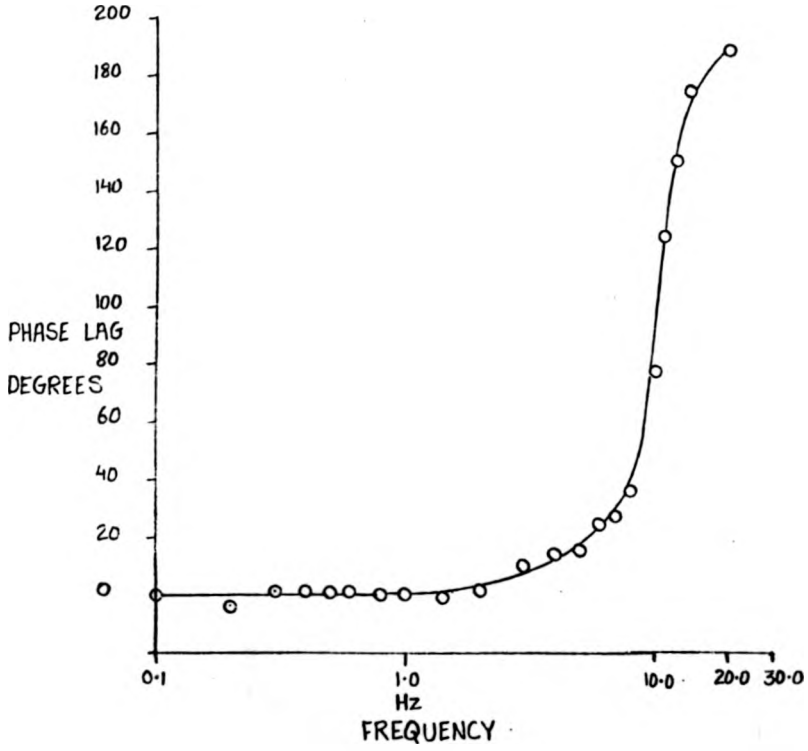

PHASE DIFFERENCE BETWEEN EXHAUST AND INLET GASES.

FIG.11

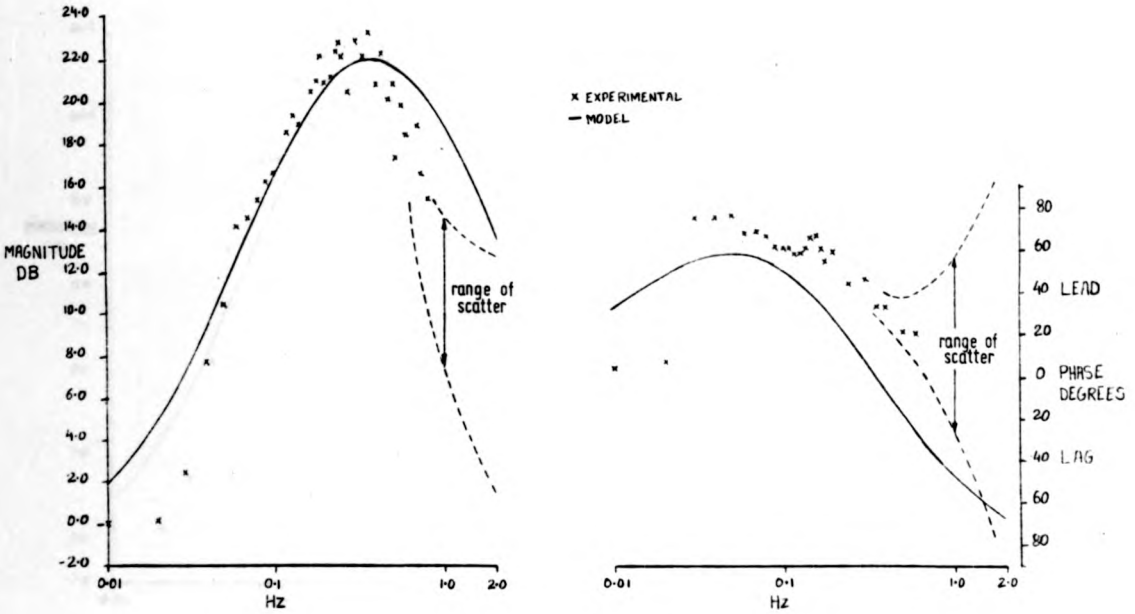

NORMALISED NO-INLET AIR RESPONSE

FIG. 12 A

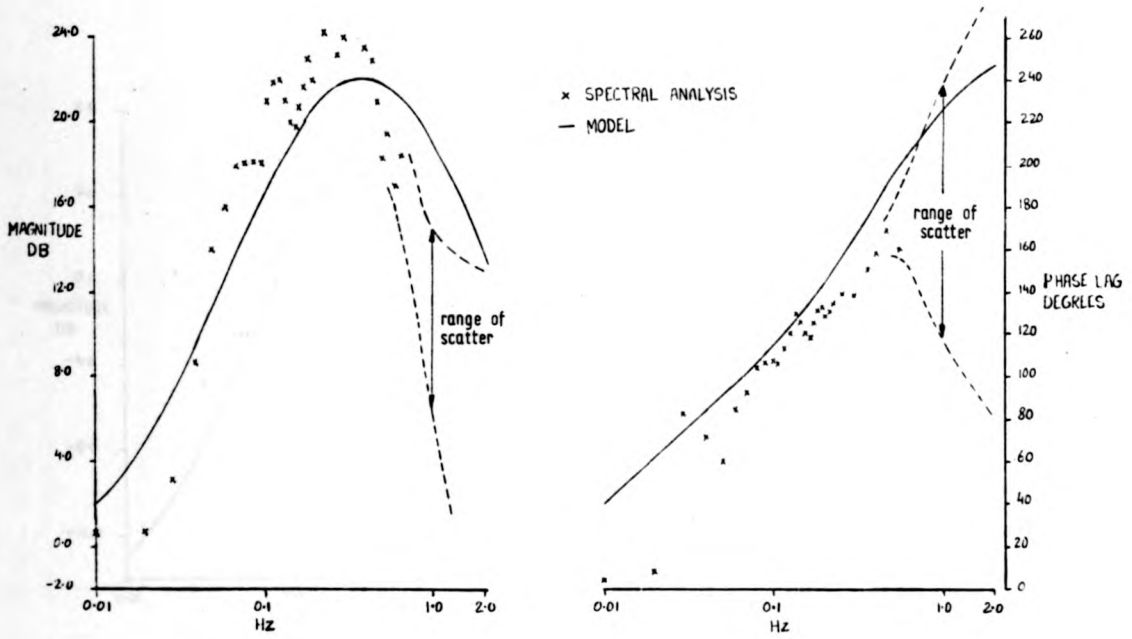

NORMALISED CO-INLET AIR RESPONSE

FIG.12B

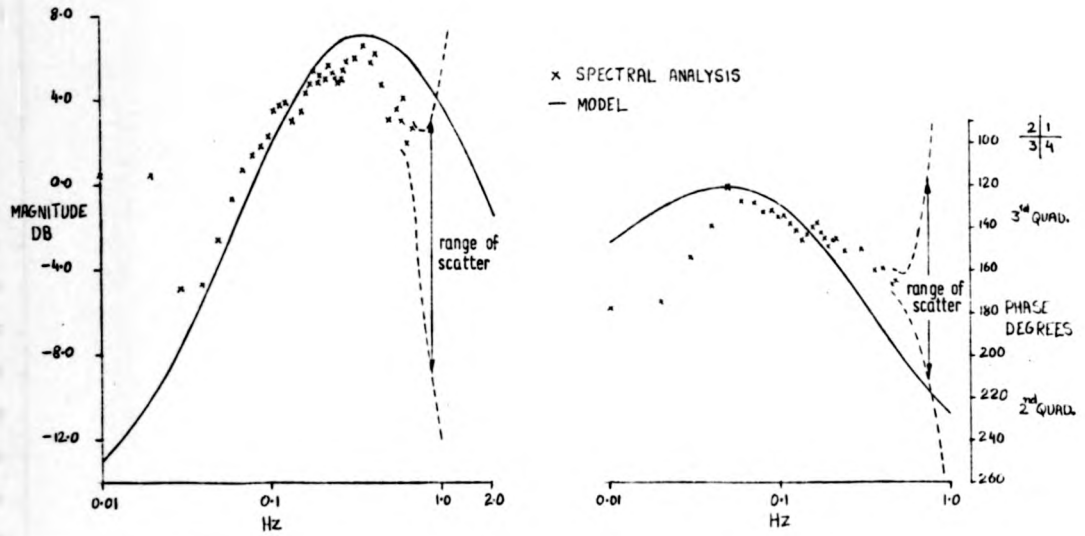

NORMALISED HC-INLET AIR RESPONSE

FIG.12C

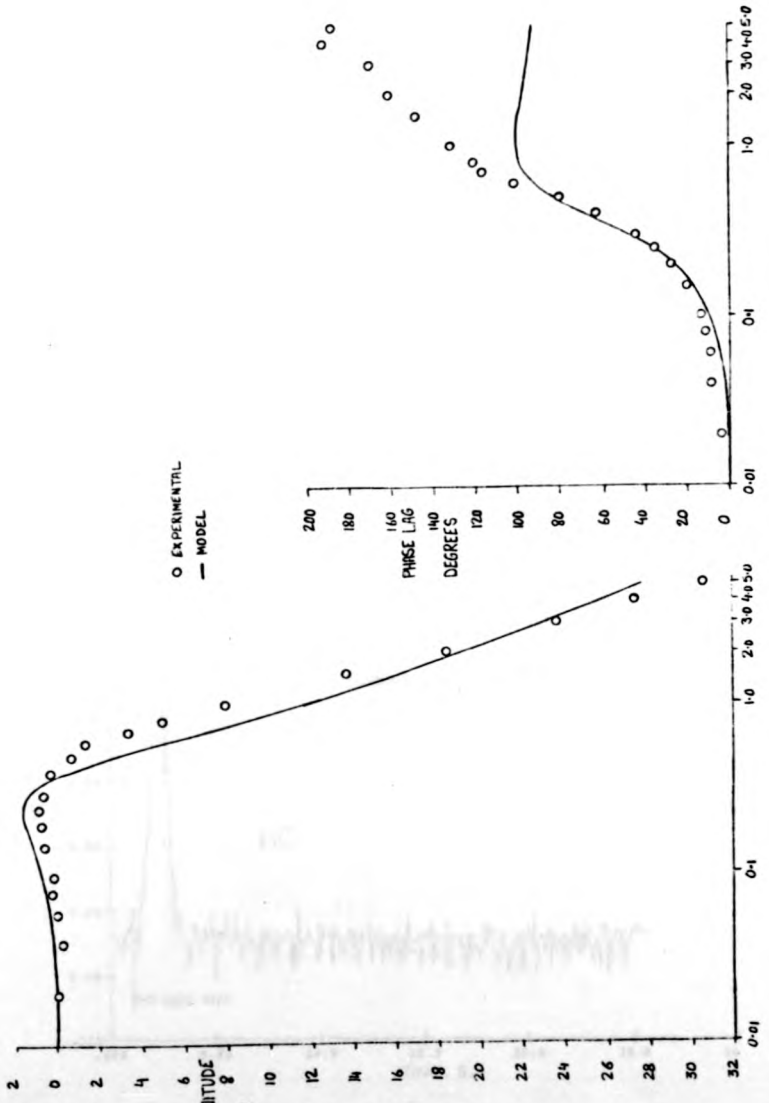

TORQUE–THROTTLE RESPONSE AT CONSTANT FUEL FLOW

FIG. 13

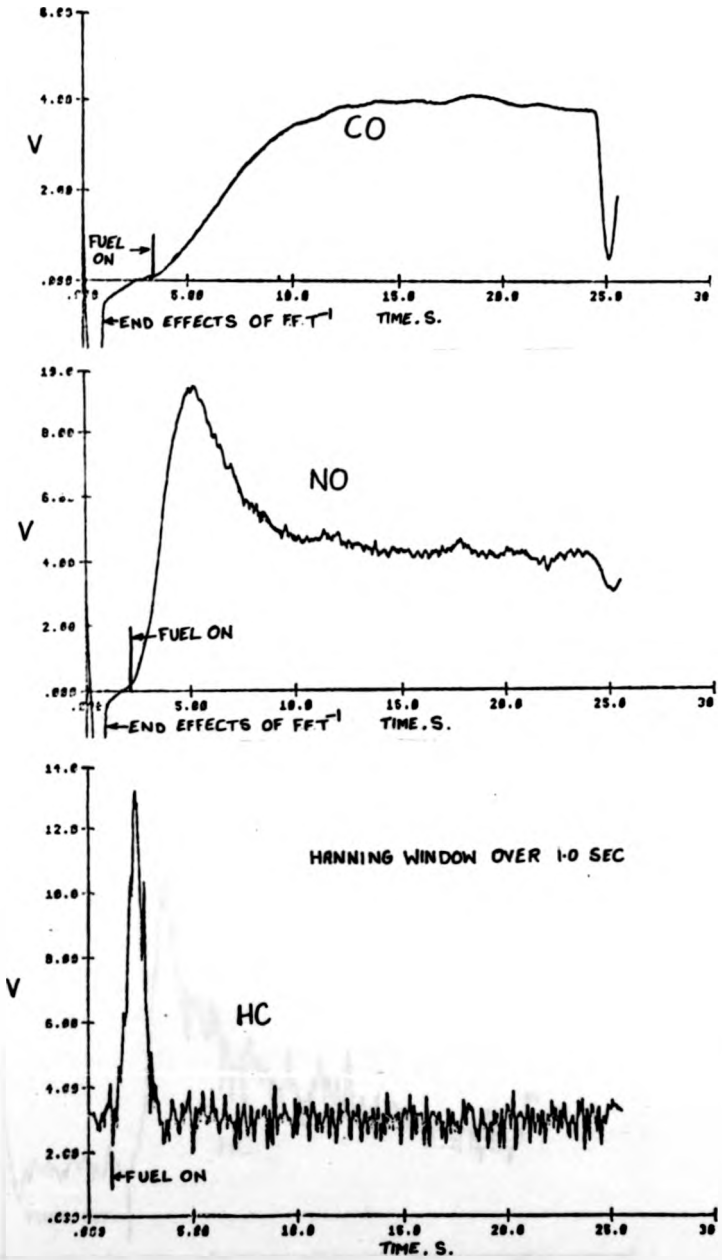

TRANSIENT EMISSIONS DURNG ENGINE START

FIG.14

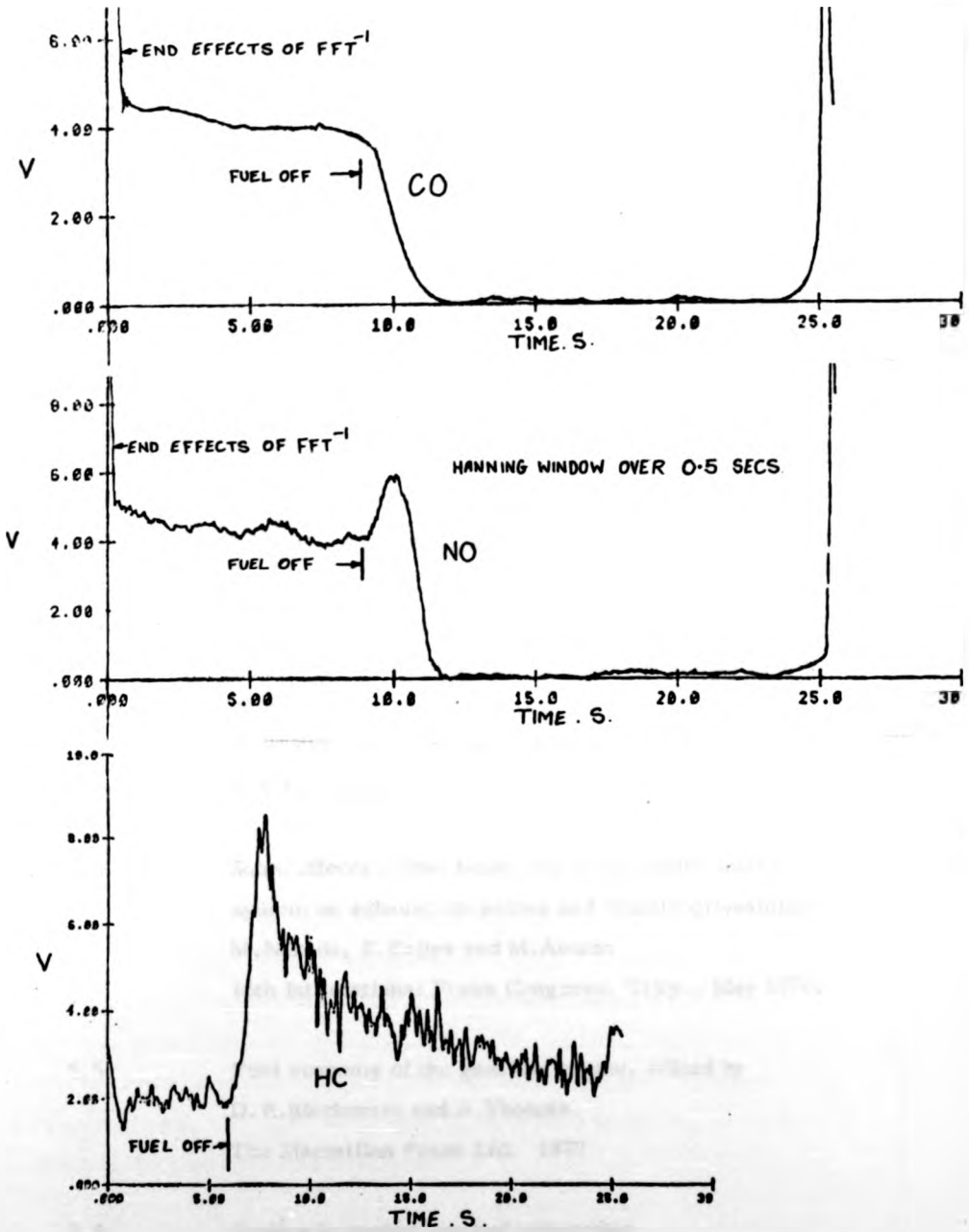

TRANSIENT EMISSIONS DURING ENGINE OFF CONDITION

FIG.15

REFERENCES

5.1. The influence of transient conditions on the operation of an S.I. engine, especially with respect to exhaust emissions.
K.Zeilinger and A.W.Hussmann, 1975.
S.A.E. 750053

5.2. Emission characteristics of a prime mover for hybrid vehicle use.
J.R.Allsup and R.D.Fleming
INT-BU. of Mines, PGH, PA 19767

5.3. A Technique for obtaining an engine emissions model based on continupus EPA-CVS test data and a dynamic vehicle model.
R. Radtke, A.Frank and N.Beachley, 1976.
S.A.E. 760156.

5.4. Some effects of fuel behaviour in the engine intake system on exhaust emissions and vehicle driveability
M.Nakada, S.Kajiya and M.Amano
16th International Fisita Congress, Tokyo, May 1976.

5.5. Fuel economy of the gasoline engine, edited by
D.R.Blackmore and A.Thomas.
The Macmillan Press Ltd. 1977

5.6 Studies in engine test bed automation.
J.V.Comfort
Ph.D. thesis, 1970.

CHAPTER 6 INVESTIGATIVE STUDIES OF MODULAR ENGINE CONTROL

6.1 Background

In general, the spark ignition engine operating on the Otto cycle exhibits a high specific fuel consumption at part loads under steady operating conditions, except when the full load economy is sacrificed for performance, in which case the full load efficiency is reduced by richening of the mixture to provide higher power levels. The need for reserve power means that the operation of the engine is confined to the inefficient part load region (Reg. 6.1). The behaviour of the engine at part loads is therefore of significant importance in terms of fuel economy.

The design of the conventional vehicle is such that power available from the engine at low vehicle speeds is much higher than the power required for propulsion of the vehicle. This design strategy is deliberate to ensure that the engine has a "good" power reserve for the acceleration of the vehicle.

The main reason for high S.F.C. at part loads is due to the pumping losses. These result from the fact that to obtain power from an engine the cylinders have to be filled with fresh charge at every inlet stroke and the necessity for the engine to interact with the surroundings means that the cylinders have to be emptied every exhaust stroke. The process results in work done by the engine on the gases at the expense of the shaft work.

The pumping work consists of two components, one due to the work required to overcome the inlet and exhaust system throttling losses which arise from the pressure differences between the inlet and exhaust systems. The other component is the work required to move the gas at high velocities past the valves. The valve flow work therefore increases with the speed and the mass of the gases. The dilution of fresh charge by the residual gases is probably another source of losses, particularly at partly closed throttle where the low pressures in the intake manifold would increase the residual gases (Ref.6.1). The result is that there is a reduction in combustion efficiency (flame-speed).

Although valve flow losses are not retrievable, throttling losses can be minimized by operating the engine without throttling as is the case for some diesel engines. The power then is controlled by varying the fuelling rate. Hitherto this has not been a practical proposition for the spark ignition engine for the reduction of fuelling in this case leads to lean misfiring problems. One possible solution is the variable displacement engine, the main feature of which is that the power output of the engine is controlled by varying the displacement, thus dispensing with the need for throttling except for idling where throttling may be retained. This method not only minimises pumping losses but it also reduces friction at low power levels due to reduced piston speeds . However, the implementation is very complex, requiring extensive redesign of the basic engine unit. Moreover, the problems are intensified by the need for rapid response from the engine to provide power for acceleration of the vehicle. These factors make widespread adoption of the variable displacement engine unlikely in the foreseeable future.

The throttling can be reduced by cylinder disabling, a strategy of engine operation in which a given number of cylinders are disabled by deactivating both the inlet and exhaust valves, according to the power demand of the vehicle. The simplicity of the controls and minimum alterations to the basic unit makes cylinder disabling strategy of engine operation more attractive than the variable displacement engine .

Disabling of an engine cylinder can be achieved by various methods. The simplest method of disabling a cylinder is by an induction of fuel free air into the cylinder. This can be accomplished with a valve after the carburettor to divert fresh air into the cylinder, or by turning the fuel injectors off at the unused cylinders. The use of this method will result in cooling of the cylinders, and hence the restarting problems of the type discussed in Chapter 6 will be created. Closing the inlet valve and holding the exhaust valve open will maintain the cylinders at exhaust gas temperatures, and thus reduce the magnitude of restarting problem. In the methods discussed above, inlet pressures of the disabled cylinders are increased and therefore pumping work is reduced. However, work required to transport gases in and out of the cylinder results in losses, particularly at high engine speeds. Sealing the disabled cylinder by deactivating both the inlet and exhaust valves is the best method for minimizing pumping losses.

The mechanism necessary to perform valve deactivation needs to be precisely controllable with fast response time . One such mechanism is shown in figure 1 (A). This type of mechanism is limited to low speed range of engine operation because the increased mass of the rocker mechanism would result in "valve bounce" at high engine speeds. Another device (Fig.1B) overcomes the valve bounce problems

by transferring the excess masses from the rocker to the centre studs. In the enable mode (Fig.1B), the selector body is restrained from moving upward by the contact between projections on the body and the blocking plate above it. The rocker arm fulcrum point is held down by the blocking plate and the body, and the valves operate normally. Deactivation of the valves results when the blocking plate is rotated, by the solenoid, to align small windows in the blocking plate with corresponding projections on the body. The rocker arm then pivots about its valve tip, since the fulcrum point is raised by the push rod action and the valves remain closed. Because a single solenoid is used to deactivate both inlet and exhaust valves simultaneously, the products of combustion are trapped inside the cylinder. The use of individual solenoids is therefore necessary, if shock and possible damage to the engine is to be avoided.

Past work in the field of engine cylinder disabling has been concentrated in the demonstration of the benefits of the concept regarding fuel consumption, with large capacity engines having high power reserves (Ref.6.2 to 6.6.). Also the work mainly deals with a so called dual displacement concept, in which only half of the engine cylinders are disabled. Clearly, limited disabling of the engine does not realise the full fuel economy benefits of the cylinder disabling concept. Therefore, it was decided to investigate the concept for the full range of possible cylinder disabling. That is, from zero to four cylinder operation.

The disablement was achieved in practice by grinding the camshaft lobes because lack of resources prevented the design and development of valve deactivating mechanism. The study therefore does not consider the transient emissions and restarting problems associated with cylinder disabling. However, if it is valid to assume that a disabled cylinder can be reinstated rapidly without misfiring, then

steady state fuel consumption maps are adequate to predict the fuel economy of a vehicle by computer simulation. For the purposes of simulation studies, engine fuel consumption and emissions of pollutants were obtained experimentally for each state of engine disablement, under steady operating conditions. Measurement of exhaust emissions was thought to be valuable in indicating the trends of emissions throughput due to disabling. Friction characteristics of the engine were also measured to obtain a better insight into the pumping losses of the engine and to predict the fuel consumption of the disabled engine.

6.2. Measurement of Engine Friction

The object of the motoring tests was to determine the pumping behaviour, and the frictional characteristics of the engine with cylinder disabling. The pumping work of motoring test when compared with that of running the engine on a P.V.diagram shows that the pumping work of the running engine is less than that of the motored engine (Ref.6.8). The differences are due to the absence of exhaust blowdown and lower exhaust temperature during the motoring process. The results of the pumping tests are therefore valuable only for the comparisons of a disabled engine with a standard engine.

For the measurement of engine friction, the cooling water and lubricating oil temperatures were maintained at preset reference levels. Although for the case of three and four active cylinders the temperatures were relatively easy to maintain, after initial warm-up and slightly extended motoring at high speed, it was found that with further deactivation, this strategy became too time consuming due to

the reduction in the work done on the engine. A heating system was therefore built to heat the water and the oil, to maintain the required temperature.

The results of the motoring tests (Fig. 2 and 3) at various stages of engine disablement show that the motoring power reduces with an increase in the throttle position. It can be seen that the difference of power required to motor the engine between full throttle and fully shut throttle reduces with speed (Fig.2). Also, the difference reduces with the level of cylinder deactivation at constant speed (Fig.3). The reduction with speed is due to an increase in valve flow losses because the mass flow rates and velocities of the gases increase with speed. The volumetric efficiency which is the ratio of actual mass of air induced to the actual capacity of the engine is shown in figure 4. The drop in volumetric efficiency at high speed (Fig.4) results in reduced intake pressure which increases throttling. The reduction of the difference of the motoring torque between fully open and fully shut throttle is also due to the reduction in the volumetric efficiency at high speeds. This is noticeable for the case of one and two active cylinder operation. In this case the volumetric efficiency (Fig.4) begins to reduce at higher engine speed than for the case of three and four active cylinders. The result is that the rate of reduction (for one and two active cylinders) of the difference in motoring power, between fully shut and fully open throttle, with the engine speed is low.

6.3. Measurement of Engine Characteristics

Tests were carried out on the engine to obtain the fuel consumption and emissions characteristics of the engine under steady state conditions. The steady state performance maps of the engine, under various stages of cylinder disablement were obtained to assess the external effects of the disabled engine. These maps were also necessary for simulation studies. Deactivation of the cylinders was

once again carried out, in a similar manner to the engine friction tests, by grinding of the camshaft lobes.

The engine crankshaft and its supports are designed to withstand the dynamic and the firing forces. In the case of cylinder disabling, the cylinders were deactivated such that firing pulses were evenly spaced over the ignition timing cycle. Consultations with the manufacturer of the engine indicated that the natural modes of the crankshaft were outside the speed range of interest, therefore special precautions in the form of dampers were not thought to be necessary. Although the deactivated cylinders act as dampers to some extent, it was thought prudent to retain as short a length as possible of the "dead" crankshaft between the flywheel and the first active cylinder. Also, since the induction system plays an important part in the performance of an engine (Ref.6.1), it was thought advisable to observe the continuity of the induction system, as well as the symmetry of firing. These observations led to the deactivation of the following cylinder through stages of cylinder disabling.

1. Cylinder No.2 disabled
2. Cylinders Nos. 2 and 3 disabled.
3. Cylinders Nos.1, 2 and 3 disabled.

Prior to serious testing, the behaviour of the disabled engine was observed at "no load", with the engine disconnected from the dynamometer, and also with the engine under load. The object here was to assess the behaviour of the engine under reduced firing frequencies. Particularly, the behaviour of the instrumentation system was checked. Also the physical well being of the disabled engine was considered. Fuel consumption and emissions

characteristics of the disabled engine were then obtained with the ignition and the mixture adjusted to obtain the most economical fuel consumption.

The fuel consumption of the engine was also measured at no load. The fuel consumption in this case was measured with a positive displacement type of fuel flow meter for the accuracy of the continuous flow meter was suspected at very low flow rates. In these tests, the criteria for setting the mixture and ignition timing was to obtain the maximum engine speed for a minimum fuel flow at a given throttle setting. This method ensures that the tickover is smooth with the lowest fuel consumption.

The results of no load fuel consumption tests indicate an improvement in fuel consumption with cylinder disabling (Fig. 5). The improvement at 1000 R.P.M. is shown in the following table (Table 1).

TABLE 1

Fuel consumption and emissions of pollutants at idle

No. of Cyls. Operating	Fuel L/HR	Savings in Fuel %	NO G/HR	CO G/HR	HC G/HR
1	0.35	35.2	0.197	187.9	5.79
2	0.43	20.4	0.116	88.1	3.36
3	0.48	11.1	0.363	128.8	6.48
4	0.54	-	1.974	314.28	14.58

The optimisation of fuel consumption, necessary to obtain high engine efficiency, was carried out using the multivariable controller. The desired torque and speed were demanded, and adjustments to the mixture control and ignition timing were made to read the lowest fuel flow. Since the power is held constant by the controller, the method adopted then minimises the S.F.C. At full power the fact that excessive torque demands cause a reduction in speed (Chapter 4) was used to keep the power constant. Figure 6 shows the change in S.F.C. and emissions at constant power and speed. It was found that the controller was sensitive to very lean air-fuel ratios and excessive ignition timing retard. The misfires that occurred at these extreme settings caused large throttle openings, resulting in cutting out of the engine due to the transients. Therefore the adjustments to the mixture and timing require some care. For the case of the disabled engine the feedback gains (Chapter 4) of both the torque and speed loops were reduced to unity. Under these circumstances of changed engine behaviour, adjustments to the compensator of the multi-variable controller were not found to be necessary.

The plots of engine S.F.C.(Fig.7) show that cylinder disabling results in a definite improvement in S.F.C., especially at low speed and load settings. The results suggest that improvements in S.F.C. are realized throughout the entire speed and load range considered with two active cylinders, whilst the improvement with three active cylinders depends on the load. One active cylinder offers improvement only at low speeds, and the gain in S.F.C. is lost rapidly at higher speeds. As can be seen, the improvement over the standard engine is a function of both the load and speed.

At constant speed, as the load is increased, the pumping losses of the fully active engine decrease,therefore the SFC of the disabled engine (three active cylinders) progressively approaches that of the fully active engine, and at full loads the disabled engine is worse than the fully active engine due to the friction of the disabled cylinder. Disabling from three active cylinders to two active cylinders results in further fuel savings due to a further reduction in pumping losses. The change in improvement due to speeds is due to an increase in friction torque with speed and also reduction in volumetric efficiency (Fig.4) of the engine. The S.F.C. with one active cylinder also indicates gains at low engine speeds. However, the gain in this case is lost rapidly with speed, and at high speeds, operation with one active cylinder is less efficient than the standard engine.

The behaviour of emissions with cylinder disabling also indicates significant changes (Fig.8, 9 and 10). The change in S.C.O. with one disabled cylinder is small when compared with fully active engine. However, a significant drop in S.C.O. results with further disabling, and furthermore much reduced levels of this emittant are maintained throughout the engine power range considered. The S.H.C. behaviour (Fig. 10) for the disabled engine suggests an improvement in the low speed region and little or no improvement at higher speeds. The actual values of S.H.C. are also similar for all cases of cylinder disabling modes, indicating that further disabling from one cylinder does not produce as significant an improvement in S.H.C. as it does for S.C.O. The behaviour of S.N.O. is similar to that of S.C.O. but in the opposite sense, that is S.N.O. increases with disabling in a similar manner to S.C.O. which reduces with disabling. This behaviour of S.N.O. is apparently

inconsistent with the idle data (Table 1), where NO together with CO and HC outputs decrease with disabling. For the case of engine idle the decrease in total quantity of exhaust gases reduce with disabling, and thus the quantity of the pollutants also reduces.

Engine maps (Appendix IV) of S.F.C. show that the behaviour of the disabled engine is similar to that of the fully active engine, in the sense that the engine maps have low and high S.F.C. regions. The overall trends in the behaviour of emissions for a disabled engine are also similar to those of a fully active engine. That is S.N.O. emissions are low at low power, and they increase at high power. Similarly S.H.C. and S.C.O. emissions are high at low power and low at high power. These trends ,however, do not seem to apply to S.N.O. for the case of one active cylinder, where the S.N.O. map indicates a strong correlation with S.F.C. That is S.N.O. emissions are high at high S.F.C. and low at low S.F.C. This would be consistent with the occurrence of high temperatures at low power levels.

6.4. Analysis of Modular Engine Control

Engine Fuel Consumption

When some engine cylinders are disabled within the active throttle region of the engine, the indicated power produced by the active cylinders, per cylinder basis, is higher than in the fully active engine due to the friction load imposed by the disabled cylinders. The discussion can be extended further by saying that for a given indicated torque level, the brake torque of the disabled engine is reduced by the amount of added friction of the disabled cylinders. Assuming that the fuel-air mass required to produce a given

indicated torque is the same for the disabled and fully active engine then knowing the fuel consumption of the fully active engine, the fuel consumption of the disabled engine can be predicted. That is, for a fixed fuel consumption the brake torque of the disabled engine is given by

$$T_{bn} = T_{b4} - (4 - n)\, T_f; \quad n = 1, 2, 3, 4 \qquad (1)$$

where T_{bn} is the brake torque per cylinder of the disabled engine.

T_{b4} is the brake torque per cylinder of the fully active engine.

T_f is the friction torque per cylinder of the fully disabled engine.

n is the number of active cylinders.

The description of the engine on a "per cylinder" basis, as indicated in the above analysis, assumes that each cylinder operates independently of the others.

The procedure used in prediction of the fuel consumption was to fix the fuel flow and the brake torque (per cylinder) of the standard engine at a given speed. The brake torque of the disabled engine was then calculated using equation (1). The total fuel flow and torque was given by multiplying these quantities by the number of active cylinders.

The comparison of measured and predicted fuel consumption is shown in figure 11 and 12. The prediction for three active cylinders was found to be within 10% of the actual fuel flow throughout

the engine speed range. For the case of two active cylinders, the predicted fuel flow is lower than the measured fuel flow at the high engine speeds considered, and is greater than the measured fuel flow at the lowest engine speeds. In the mid-speed regions (i.e. 1500 to 3800 R.P.M.) the comparison was found to be better than 10%, and the discrepancy at the extreme speeds is less than 25% . However, the simple analysis does not predict the fuel consumption of one active cylinder case with reasonable accuracy.

The failure of analysis for one active cylinder case was investigated by reconsidering the pumping work and volumetric efficiency of the engine during motoring tests.

Comparison of pumping torque (difference between the motoring torque and friction torque of fully disabled engine) per active cylinder (Fig. 13) shows that disabling reduces the pumping torque up to two active cylinders; but a further increase in disabling increases the pumping work. Also, the reduction occurs most at part throttle, whilst at full throttle the pumping work is relatively constant. These results show that cylinder disabling, especially at part throttle, not only eliminates the pumping work of the disabled cylinders but also reduces the pumping work of active cylinders. This explains the observations of past workers (Ref. 6.4), where it was found that disabling of the engine at idle, from eight to four cylinder operation, increased the engine idle speed.

The volumetric efficiency (Fig. 4) which indicates the effectiveness of the engine as an air pump, shows that disabling increases volumetric efficiency at part throttle whilst it reduces for the full throttle case. The reduction at full throttle results from low air speeds due to disabling. This is because the induction

system is designed for four active cylinders. The increase in the volumetric efficiency at part throttle indicates increased inlet manifold pressure. The behaviour of volumetric efficiency with one and two active cylinders, together with the motoring results (Figs. 2 and 3) for these two modes of cylinder disabling, indicates that externally the two cases are very much alike. This similarity in the motoring torque and the volumetric efficiency is explained when the volume of the induction system, between the throttle butterfly and valves, is considered.

The volume of "active" induction path between the throttle and the valves for various modes of cylinder disablements was measured, and is shown in Table 2 at the end of the present chapter. It can be seen that the ratio of active volume to the swept volume of the engine changes from approximately 0.4 to 0.6 between the two extremes of active cylinders. This small increase in the active volume of the induction system represents a decrease in the inlet pressure with cylinder disabling. The increase in the active induction system volume with disabling is relatively small when the "dead" volume of the induction system is also considered. If assumptions regarding the similarity of the engines are valid (Ref. 6.8), then it is possible to obtain some idea about the size of the induction system required for the disabled engine relative to the standard engine. Column C of Table 2 is then obtained by assuming that the ratio of the induction system volume to the engine displacement is 0.39. The design of the induction system obtained in this manner indicates that the excess volume of the induction system (Column C, Table 2) increases rapidly with disabling. This indicates why the motoring torque with one active cylinder is similar to that with two active cylinders (Figs. 2 and 3). The

increase in the volume of the induction system also explains the high pumping torque (per cylinder) with one active cylinder (Fig.13).

The above discussions indicate that the volume of the induction system plays an important role in minimization of pumping losses. In other words, if a large tank is placed between the throttle and the inlet valves of a single cylinder engine, then the pumping diagram of a single cylinder engine can be made to look like the pumping diagram of a multi-cylinder engine, simply by increasing the size of the tank (Ref.6.8).

The failure of the analysis to predict the fuel consumption of the one cylinder engine is simply due to the large inlet manifold volume. The size of the manifold also explains the small discrepancies between the predicted and measured values of fuel flow with two and three active cylinders.

Engine Exhaust Emissions

The increase in S.N.O. (Fig.8) is thought to be due to higher i.m.e.p. that results from cylinder disabling. The resulting high temperature (Ref.6.5) due to high i.m.e.p. results in an increase in S.N.O. Since throttling losses are reduced, that is, inlet pressures are increased, the residual gases are reduced at low power levels with cylinder disabling. The reduction in the residual gases implies that the internal "E.G.R." is reduced. This is thought to be another cause for an increase in S.N.O. with disabling.

The behaviour of S.H.C. (Fig.10) also suggests that high cylinder temperatures with disabling results in an increased oxidation of the quench layer gas as it mixes with the bulk gas, during expansion and exhaust stroke (Ref.6.9). For the case of S.H.C., the reduction in residual gases imply an increase in

hydrocarbon output because part of the sheared layer, rich in hydrocarbons, that is ejected during the final phase of the exhaust stroke, is no longer trapped inside the cylinder. It is believed that for the case of hydrocarbons these two mechanisms (i.e. increased temperature and decreased residuals) tend to cancel each other. That is, after initial disablement there is little reduction in S.H.C. with further disabling (Fig. 10).

At high combustion temperatures the carbon monoxide which is formed oxidises to carbon dioxide as products expand and cool. However, at lower temperatures during expansion the chemical reaction rates lag behind the equilibrium values, thus resulting in carbon-monoxide output at the exhaust (Ref. 6.9). The higher temperatures that result from disabling ensure that departure from the equilibrium line occurs relatively further down the expansion stroke, thus S.C.O. (Fig. 9) is reduced with disabling. Also the decrease in residual gases ensures a more uniform mixture in the combustion chamber. That is, local rich or weak mixture regions in the combustion chamber are reduced, resulting in more uniform burning. Carbon monoxide formation which is attributable to local fuel rich regions is also reduced with disabling.

Subjective Aspects of Disabled Engine Operation

One of the qualities of a well designed engine is thought to be the "subjective smoothness" during operation. In this respect, it was thought necessary to discuss the observed behaviour of the disabled engine.

The smoothness at idle of the disabled engine was compared qualitatively with the standard engine. It was noticed that with three active cylinders, there was a slight deterioration in smoothness due to unbalanced firing. However, with further disabling, including one active cylinder, the engine idle was very smooth down to 500 R.P.M. The reluctance of the engine to start at room temperature was found only for the case where three cylinders were disabled. The "cold" engine in this case required some choke and a number of tries with the starter before it fired. Also, the cold engine was very sensitive to throttle change such that an increase in throttle setting caused the engine to cut-out. This type of behaviour persisted up to the lubricating oil temperature of approximately 50 degrees celcius, above which the behaviour of the engine rapidly returned to normal. In vehicle applications a cold start schedule will therefore be necessary to overcome the cold running problems of the engine operating with one active cylinder.

The disabled engine required adjustments to the carburettor setting for each mode of disabling. Furthermore, the settings had to be altered for speed changes at no load. With one active cylinder it was found that the standard mixture adjusting screw did not provide an adequate range of adjustment. In this case, the mixture screw had to be screwed almost tight before the mixture setting approached the "correct" value. This difficulty was overcome by lowering the float level by approximately

three sixteenth of an inch. As a consequence the response of the engine indicated a "flat spot" when rapid changes in throttle position were made.

Although the operation of the engine under load was tolerably smooth, there was a distinct change in the exhaust noise due to low firing frequencies. The noise, however, was thought to be acceptable in the laboratory environment with the given exhaust system. The type and level of exhaust noise indicated that noise emissions from a vehicle would be acceptable. However, at low engine firing frequencies, the internal noise of the vehicle may increase due to the excitation of body work panels.

6.5 Conclusions

It has been demonstrated that disabling of engine cylinders, by valve deactivation, increases the part load efficiency of the conventional Otto engine. The short duration of tests indicated that disabling of cylinders does not have any detrimental effects on the engine. However, it is felt that durability tests are necessary to investigate the long term effects on the engine.

The engine motoring tests showed that motoring power reduces with disabling due to a reduction in pumping losses. As a result, fuel savings of up to 35% with an added reduction in emission levels is possible at idle. The cold starting difficulties associated with one cylinder operation will require a cold start schedule in the actual vehicle. Therefore the indicated fuel savings are not possible under all idling conditions. Tests at idle also showed that mixture settings of the carburettor had to be adjusted for each mode of cylinder disabling. This indicates that a variable venturi

type of carburettor that meters the fuel according to the air flow, or a fuel injection system are more suitable than the fixed jet carburettor because in practice automatic metering adjustments are easily realized with these devices.

Further tests showed that cylinder disabling results in a significant reduction in S.F.C. at low power levels due to a decrease in throttling losses. The gains in efficiency, as the results indicate, depend upon the engine speed and load. This is because the friction of the engine depends on speed, and at high loads the throttling losses of the conventional engine are low. The results suggest that in the application of the cylinder disabling concept to a vehicle, optimisation of fuel consumption will be required in such a way that the number of operating cylinders will depend on the power required for the propulsion of the vehicle.

The analysis showed that fuel consumption of the disabled engine can be predicted with reasonable accuracy by a very simple method. The technique , however, breaks down for the case of one active cylinder due to the large volume of the inlet manifold. The indication here is that the size of the manifold needs to be reduced to minimise pumping losses. With the given system, engine models which consider the details of each element of the engine system are necessary to predict the fuel consumption of the engine with three disabled cylinders.

The results also show that steady state emissions of carbon monoxide and unburnt hydrocarbons are significantly reduced with cylinder disabling. The emissions of oxides of nitrogen on the other hand show a significant increase. The measured behaviour of the exhaust emissions is thought to be due to the high combustion

temperatures and reduced residual gases which result from cylinder disabling. The increased combustion temperatures and reduced residual gases increase the emissions of the oxides of nitrogen and reduce the emissions of carbon monoxide. It is believed that reduction of unburnt hydrocarbons due to increased combustion temperatures is offset by the reduced residual gases. Thus the reduction in hydrocarbons in a similar manner to carbon monoxide is not realised with cylinder disabling. Formation of pollutants, especially the hydrocarbons, is very complicated. It is felt that further work is necessary to establish the exact dependence of pollutant formation on combustion temperature and residual gases with engine cylinder disabling.

TABLE 2

Active Cylinders	Volume of active flow path (cc) (A)	Active Volume / Engine Disp. (B)	Required Volume cc . (C)	Excess Volume. / Design Volume (345 -C/C) (D)
4	345	0.39		
3	291	0.44	256	0.35
2	237	0.54	170.6	1.02
1	127	0.58	85.3	3.04

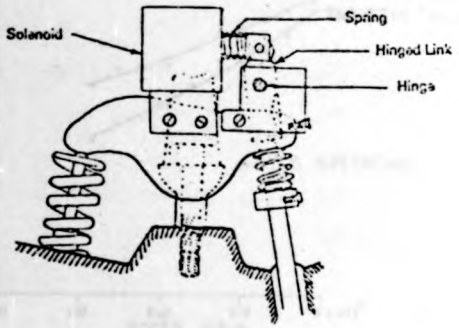

(a) Rocker arm activated

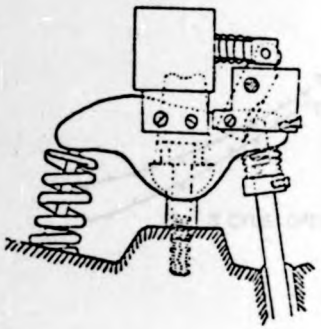

(b) Rocker arm deactivated (REF. 6-3)

(A).

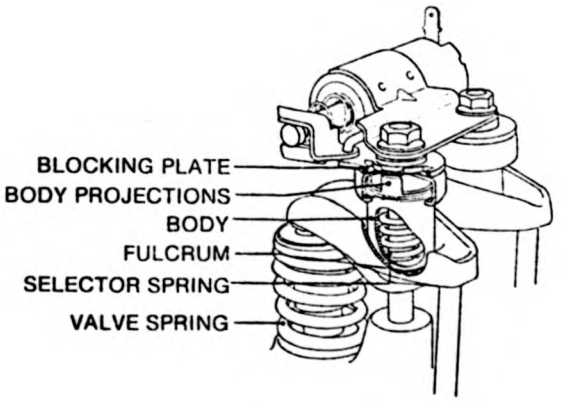

Valve operating

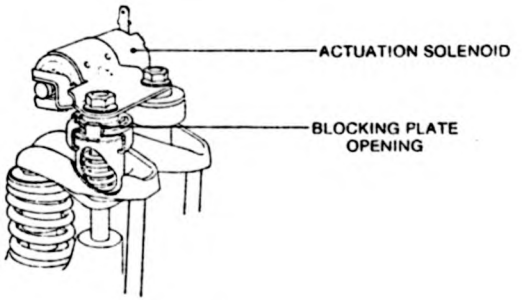

Pivot released (REF. 6-7)

(B)

FIG. 1

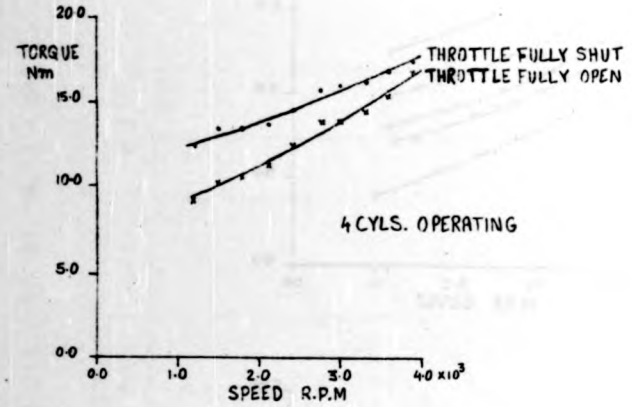

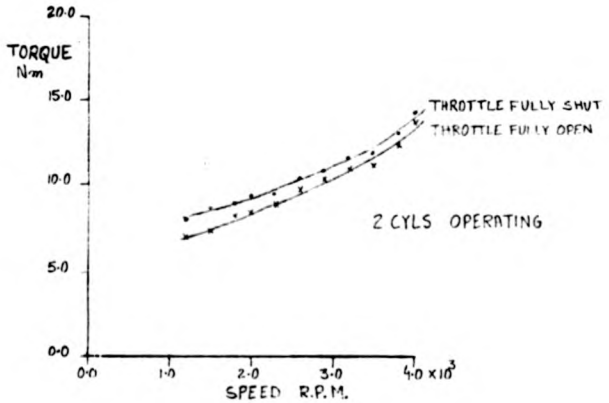

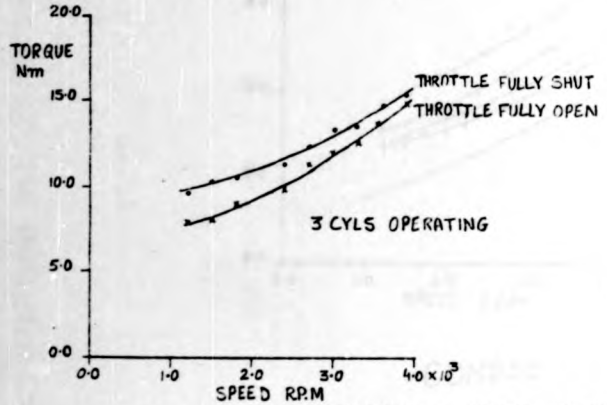

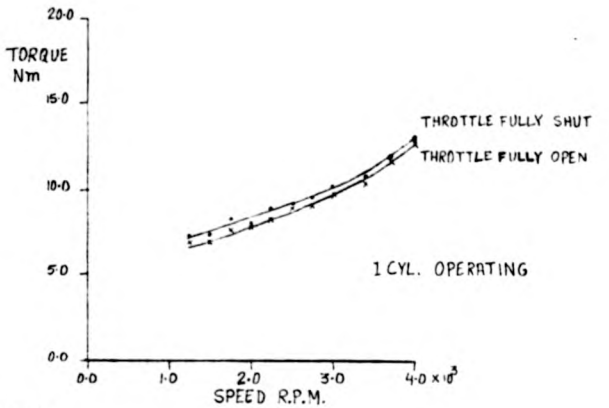

MOTORING TORQUE WITH DISABLING

FIG. 2

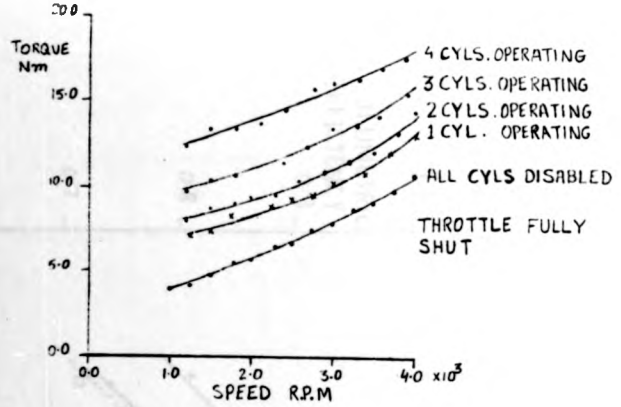

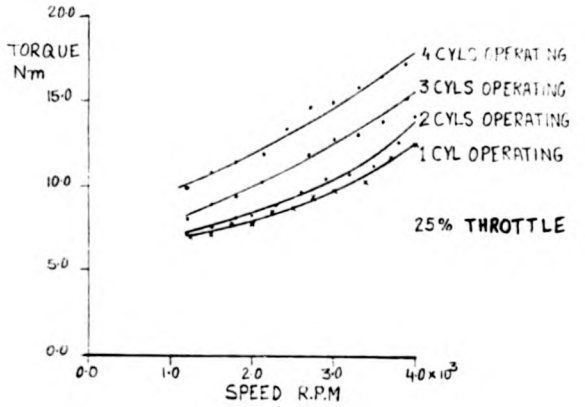

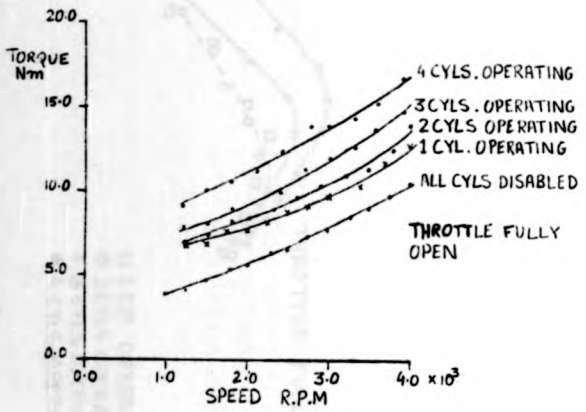

COMPARISON OF MOTORING TORQUE

FIG.3

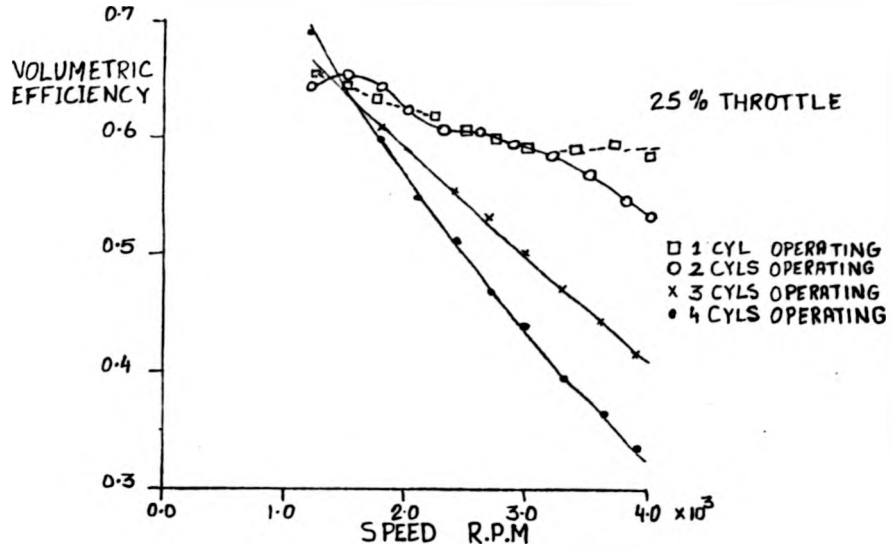

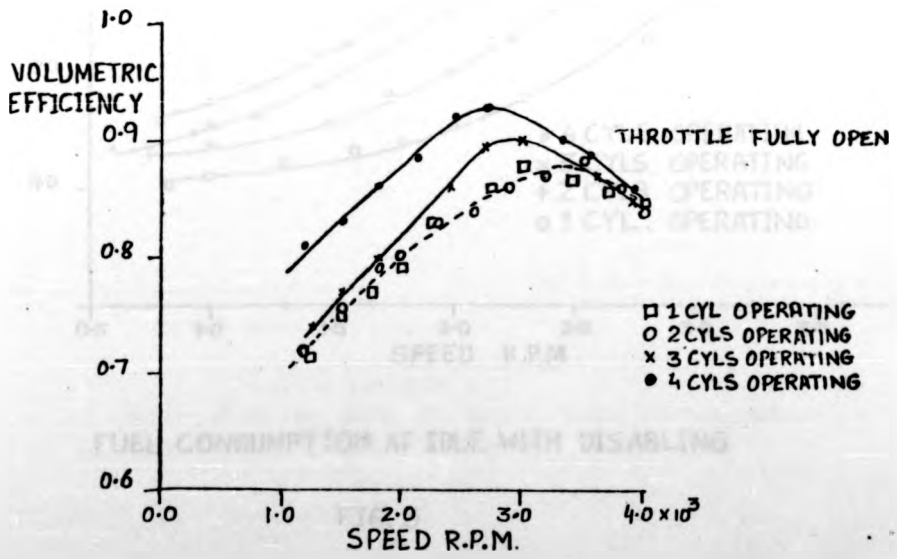

CHANGE IN VOLUMETRIC EFFICIENCY OF THE MOTORED ENGINE

FIG.4

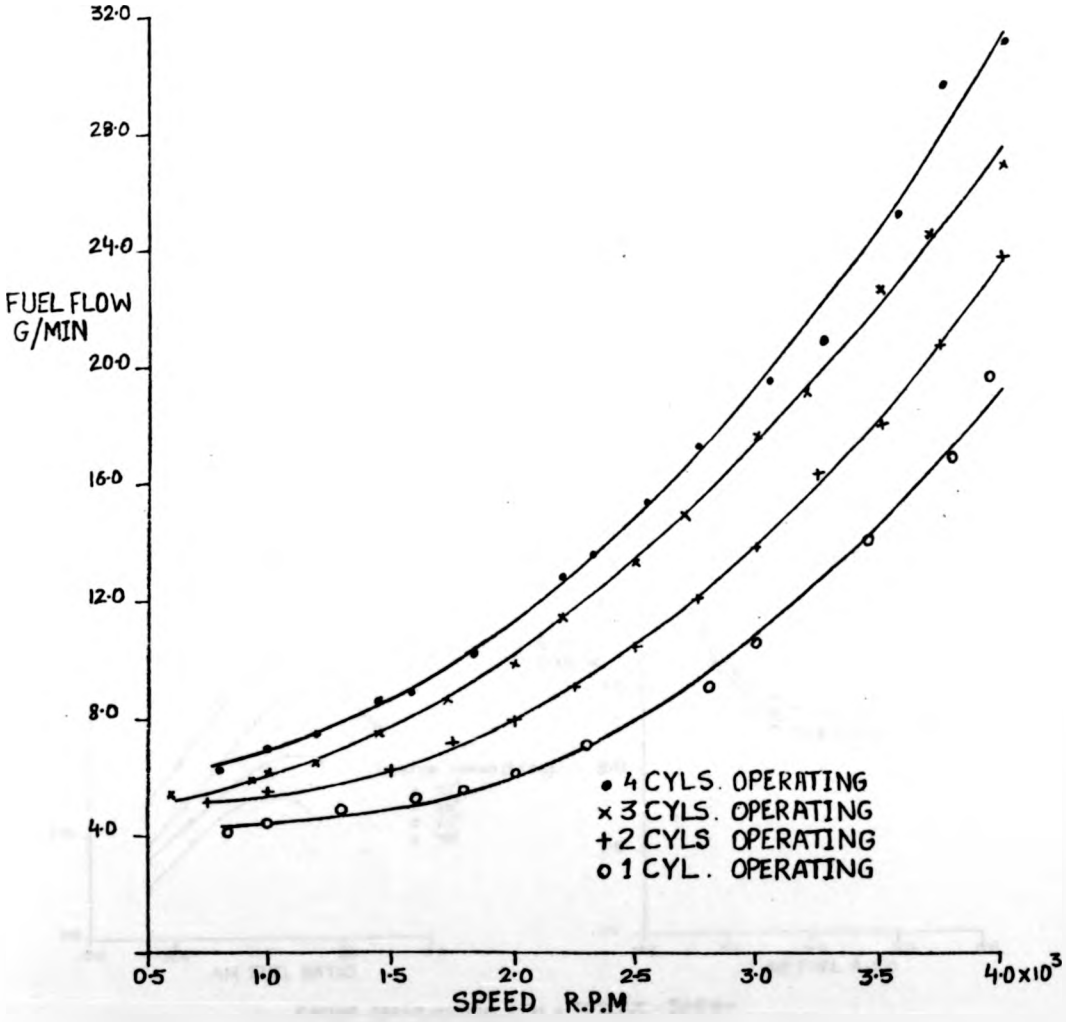

FUEL CONSUMPTION AT IDLE WITH DISABLING

FIG. 5

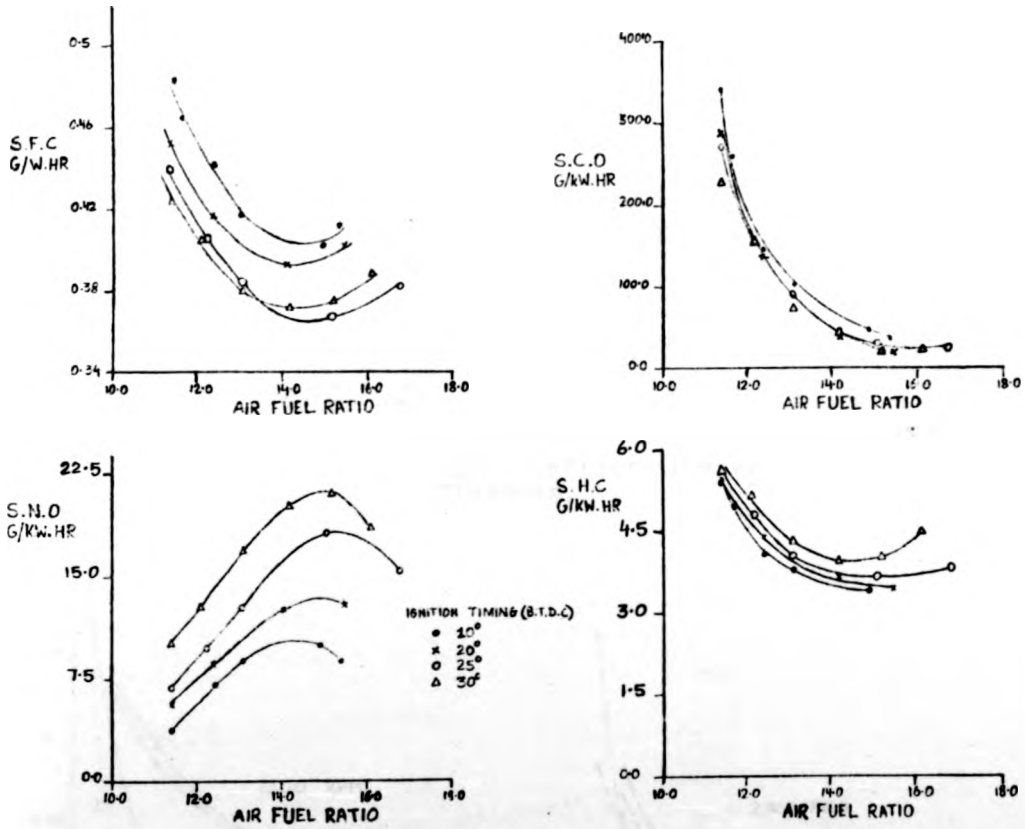

ENGINE SPEED = 2500 R.P.M ; TORQUE = 30·0 Nm.
4 ACTIVE CYLINDERS.

EFFECT OF AIR FUEL RATIO AND IGNITION TIMING ON EFFICIENCY AND EMISSIONS AT CONSTANT SPEED AND POWER.

FIG. 6

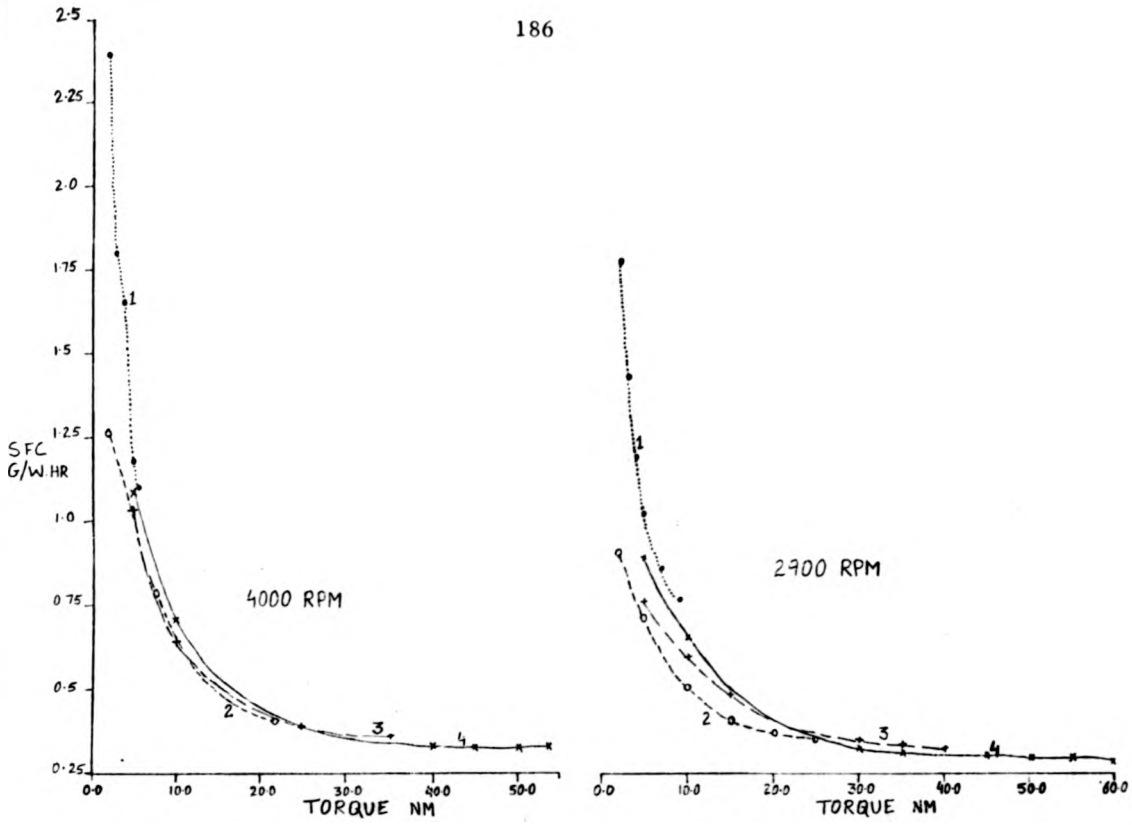

LABELS INDICATE ACTIVE CYLINDERS.

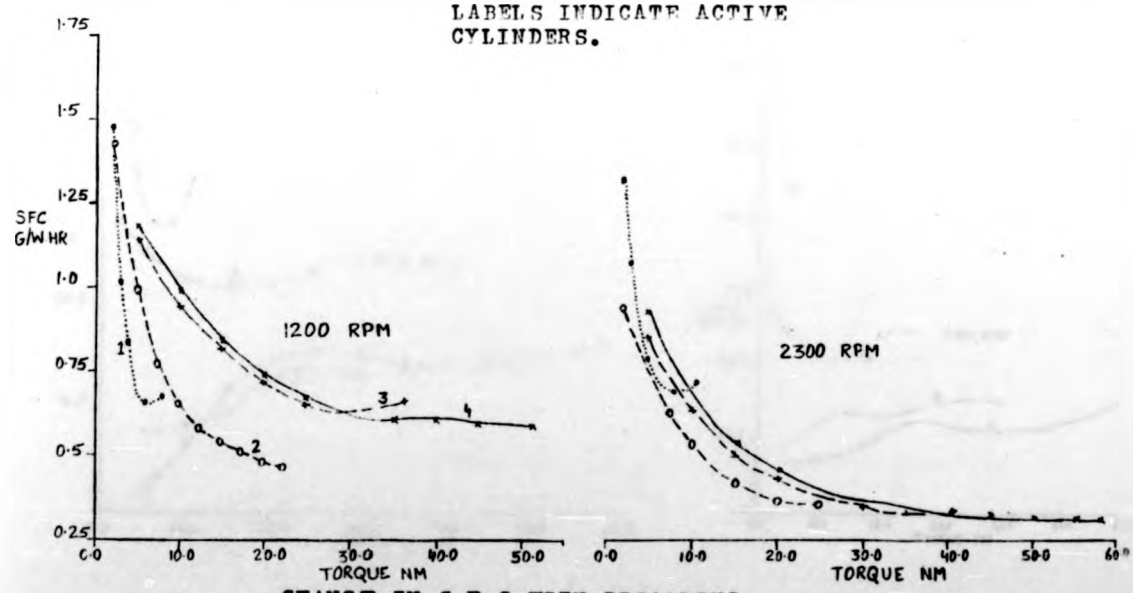

CHANGE IN S.F.C WITH DISABLING

FIG. 7.

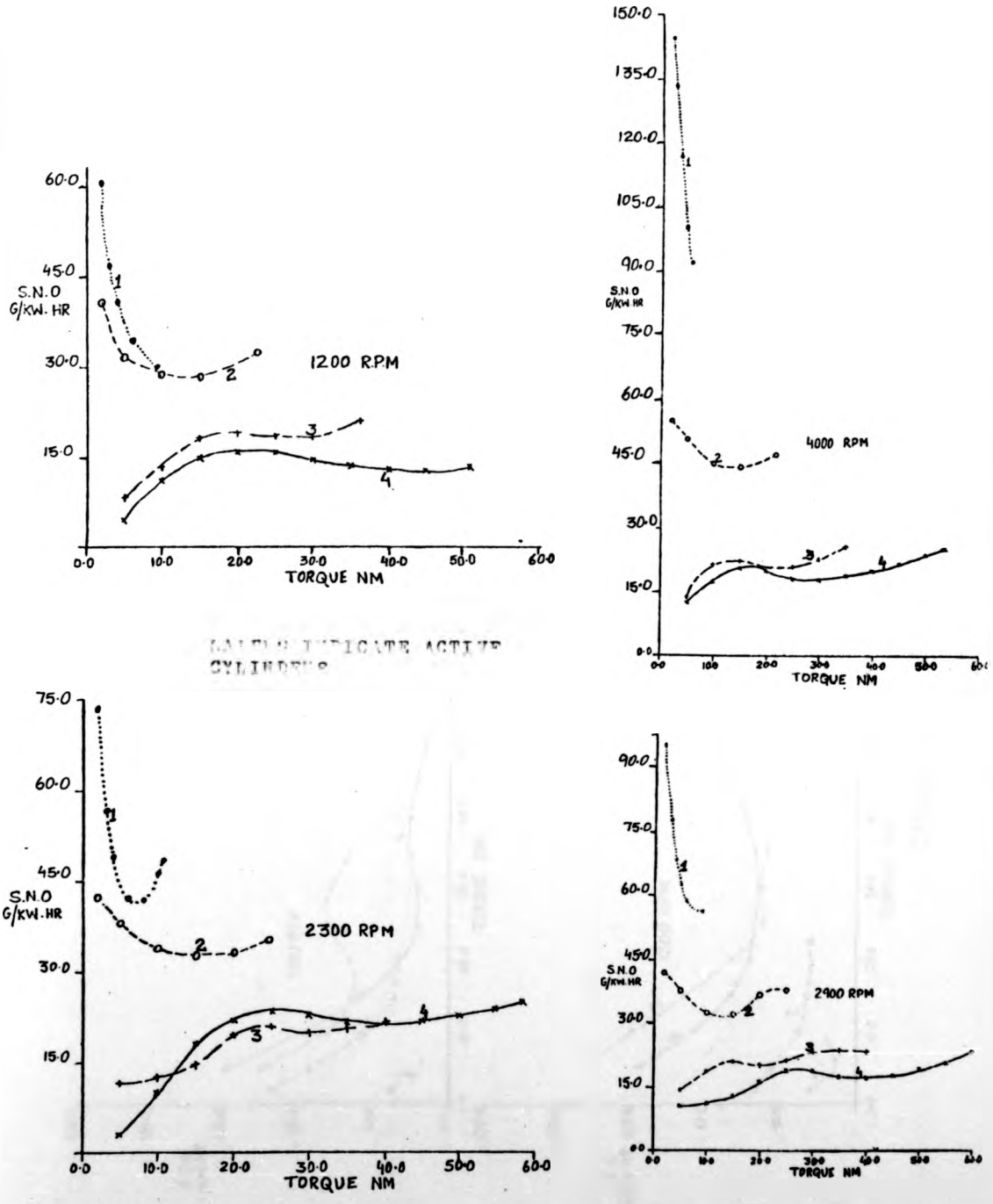

CHANGE IN S.N.O WITH DISABLING

FIG. 8

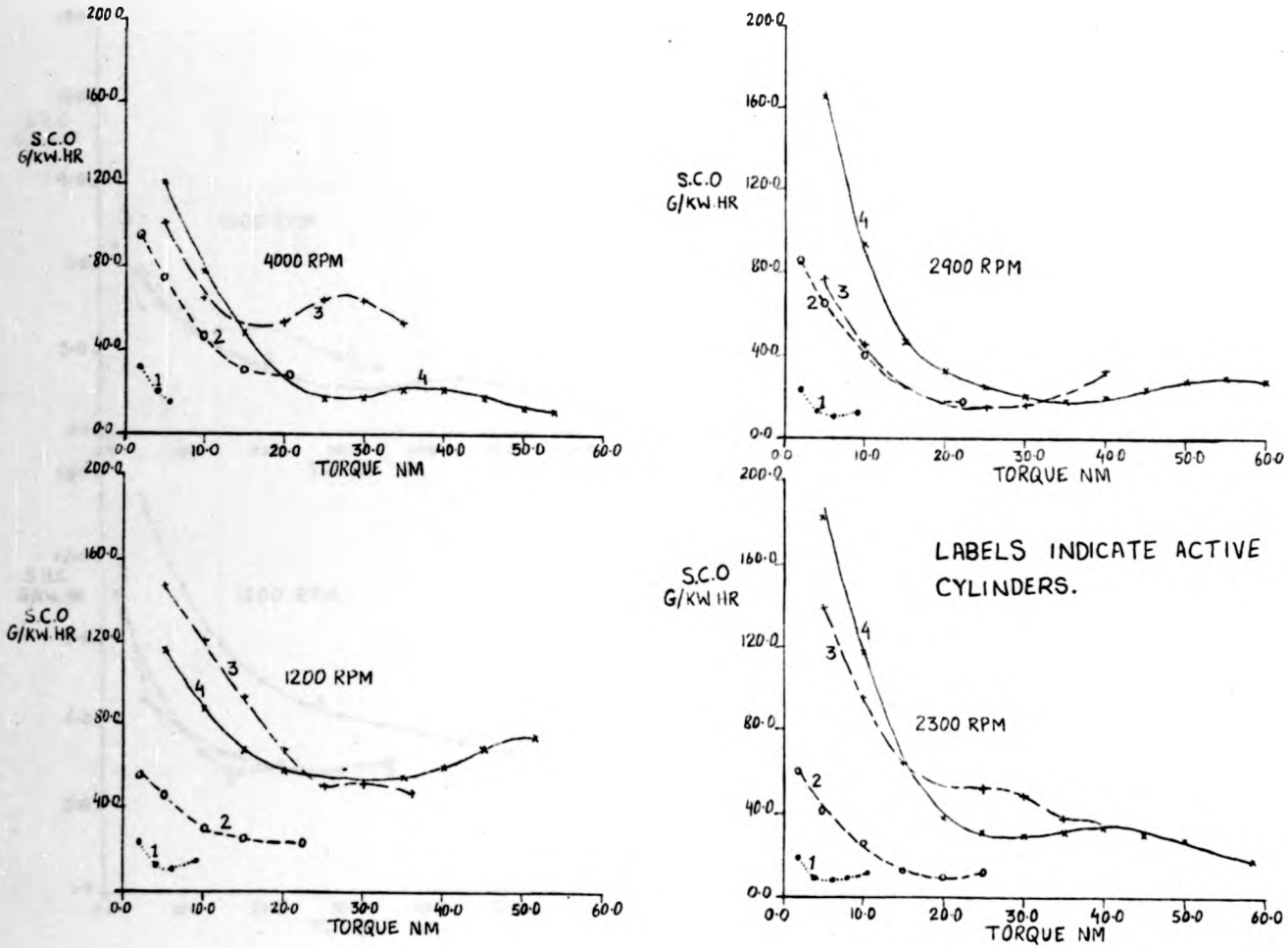

CHANGE IN S.C.O WITH DISABLING

FIG.9

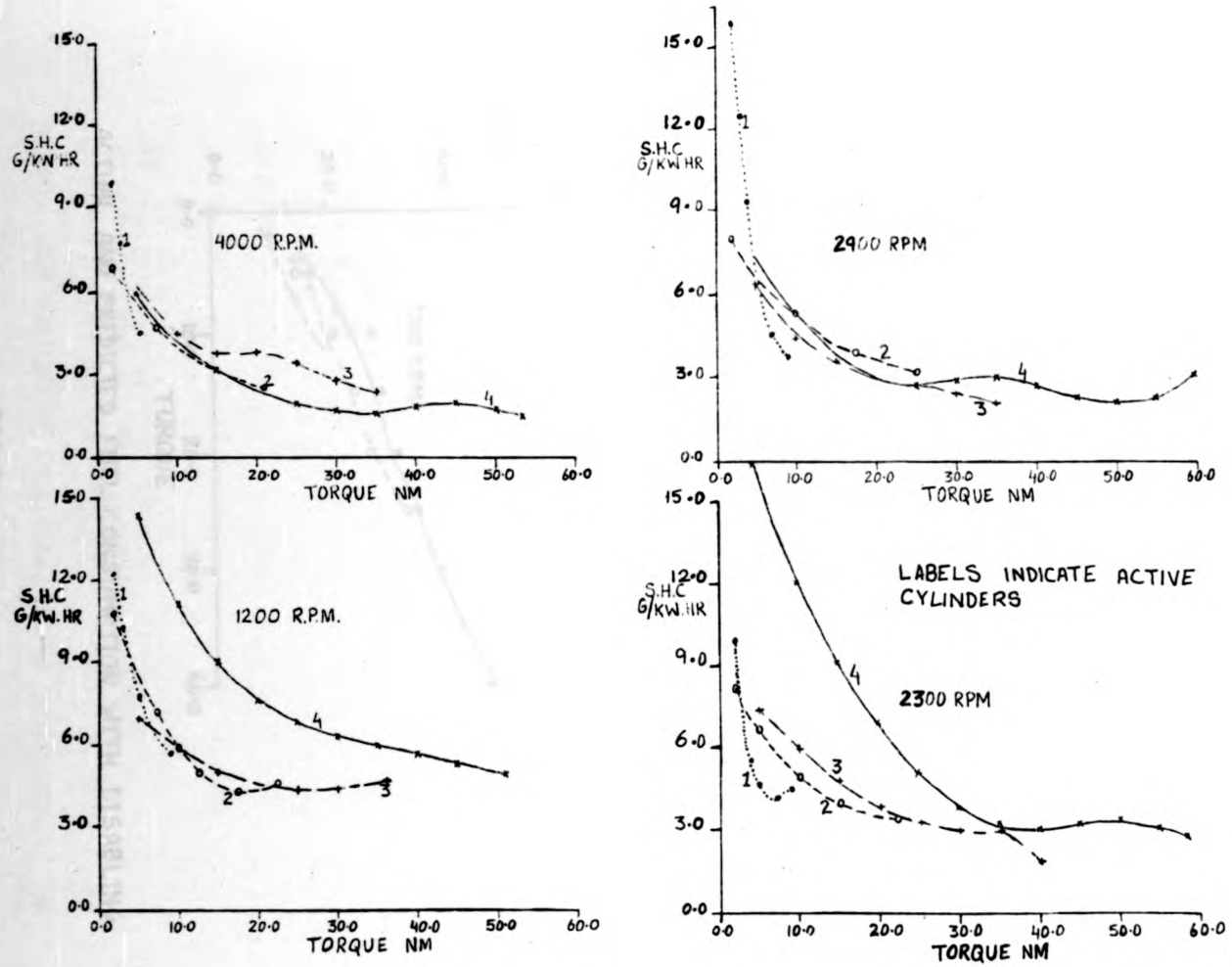

CHANGE IN S.H.C WITH DISABLING

FIG. 10.

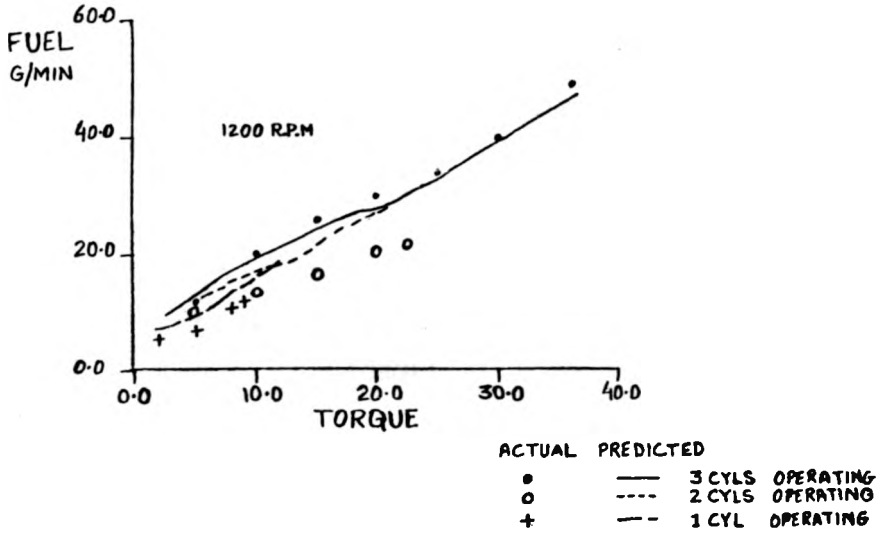

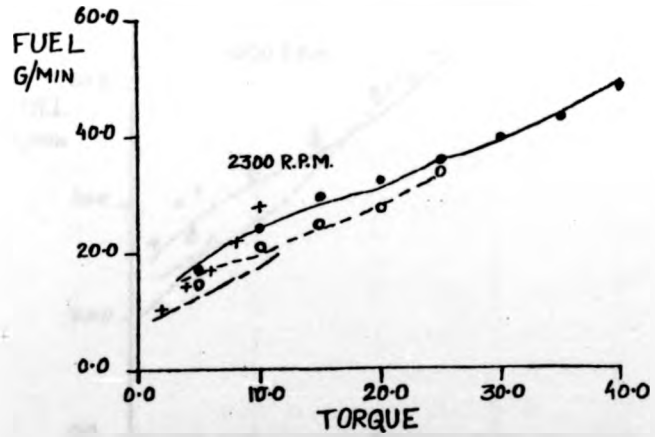

ACTUAL AND PREDICTED FUEL CONSUMPTION WITH DISABLING.

FIG. 11

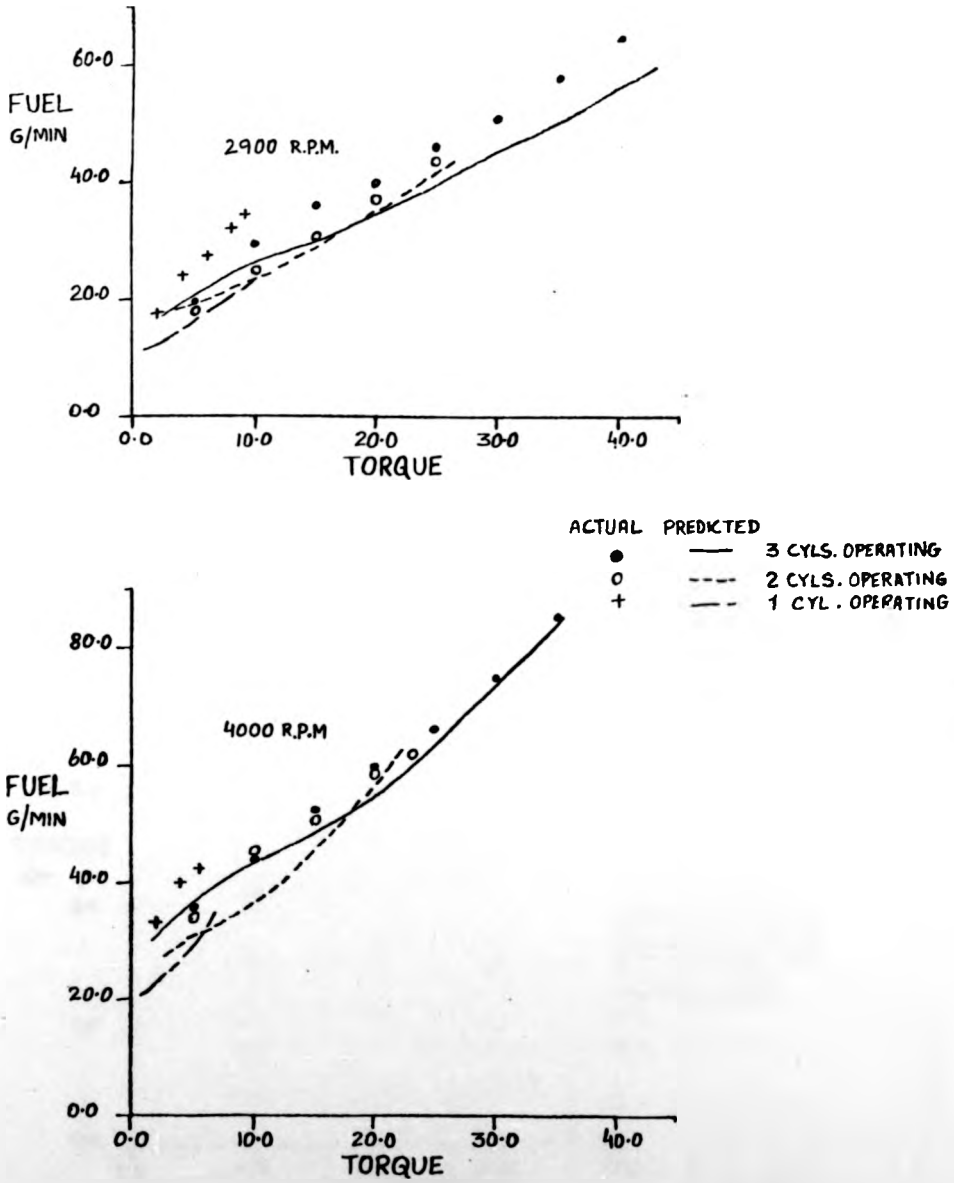

ACTUAL AND PREDICTED FUEL FLOW WITH DISABLING.

FIG. 12

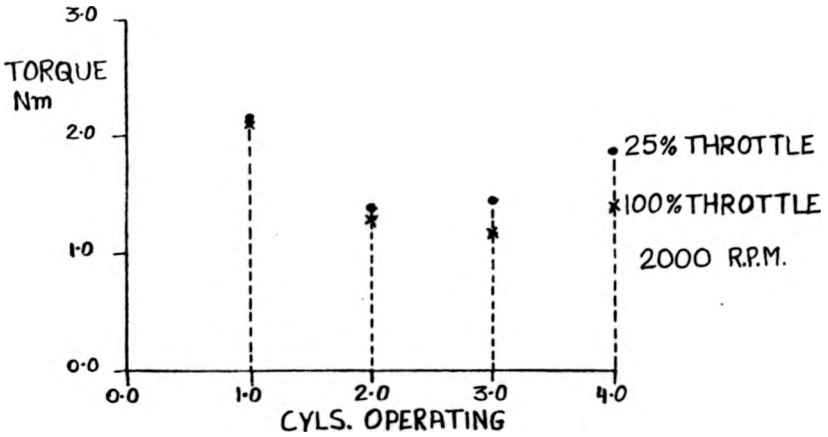

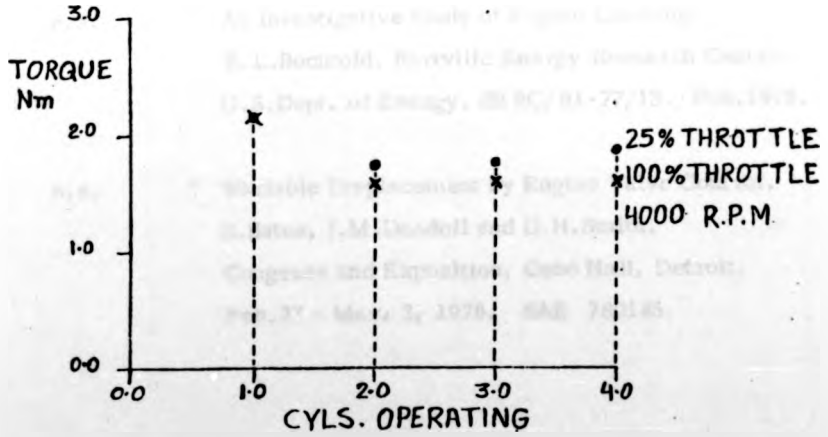

CHANGE IN PUMPING TORQUE PER CYLINDER WITH DISABLING

FIG. 13

REFERENCES

6.1 ' Fuel Economy of the Gasoline Engine '
D. R. Blackmore and A. Thomas. Macmillan Press 1977.

6.2. ' Fuel Savings by Deactivating 8 Power Cylinders on a V-16 Engine. ' A.S.M.E. Publication. Presented at Diesel and Gas Turbine Power Conference and Exhibition, Chicago Ill , April 4.8.76.

6.3. ' The Eight Cylinder Engine : A Respite for Four ? '
Mohammad Loghavi , Robert H. Wilkinson.
Agricultural Engineering, June 1977.

6.4. ' A New Approach to Variable Displacement'
Editorial Report. Automotive Engineering. May 1977.

6.5. ' An Investigative Study of Engine Limiting.'
R. L. Bechtold. Bartville Energy Research Centre.
U.S. Dept. of Energy. BERC/R1-77/13. Feb. 1978.

6.6. ' Variable Displacement by Engine Valve Control. '
B. Bates, J.M. Dosdoll and D.H. Smith.
Congress and Exposition, Cobo Hall, Detroit.
Feb. 27 - Mar. 3, 1978. SAE 780145.

6.7 ' Valve Selector Hardware ' R.S.Mueller, M.W.Uitvlugt. Congress and Exposition, Cobo Hall, Detroit. Feb.27 - Mar. 3rd,1978 SAE 780146.

6.8. ' The Internal Combustion Engine in Theory and Practice.' Vol. I , C.F.Taylor, M.I.T.Press .1966.

6.9 ' Pollutant Formation and Control in Spark-Ignition Engines.' J.B.Heywood .Prog.Energy Combust. Sci. Vol.1 , pp 135-164 , 1976, Pergamon Press.

CHAPTER 7 VEHICLE SIMULATION STUDIES

7.1. Introduction

Meaningful comparisons of the control strategy of the engine must go beyond looking at merely the engine characteristics and consider the performance of the engine in a vehicle. To this end computer simulation studies were undertaken to assess the benefits of cylinder disabling as a means of engine control over various drive cycles.

Simulation was carried out on the standard E.P.A. urban and highway drive cycles. Because fuel consumption of a vehicle is affected by the type of driving, it was also decided to carry out simulation over a cycle that represented the type of driving encountered in United Kingdom. For this purpose the speed time profiles measured by the Department's research vehicle over 'route 1400Y' were chosen to represent typical urban driving encountered in United Kingdom. The basic statistics of above three drive cycles are shown in Table 1, whilst the time profiles are shown in Figure 1. The acceleration profiles shown were obtained by differentiating the speed profiles.

For the purpose of simulation studies an engine operating mode was chosen to maximize the fuel economy, thus the idealised principle of a perfect continuously variable transmission was involved.

The technique of simulation involves simplifying assumptions that result in errors in predicting the absolute values of the quantities of interest. However, if the assumptions are not random, then prediction of the changes of quantities due to alteration of the vehicle specifications are relatively accurate. Therefore simulation is a useful tool in assessing the benefits of different drive train configurations.

LIST OF SYMBOLS

F_i	Fuel flow g/min
ω	Engine speed rad/s.
T	Torque Nm
F_p	Propulsion force N
V	Vehicle speed m/s
$\dot{V}$	Vehicle Acceleration m/s^2

Suffix i refers to the number of active cylinders.

7.2. VEHICLE CHARACTERISTICS

Engine performance model

The fuel consumption of the engine was modelled by fitting an equation to the experimental data using the 'least squares' technique. The model represented the fuel consumed to overcome the internal losses of the engine due to changes in speed and the fuel used to generate power from the engine. Attempts to model the emissions proved unsuccessful due to lack of consistency with speed variations. The fuel consumption models were as follows :

Four active cylinders :

$$F_4 = 40.57 - 0.27\,m + 0.61\,m^2 + mT\,(0.17 \times 10^{-2} + \frac{0.5}{m} + 0.13 \times 10^{-4}\,T) \quad (1)$$

Three active cylinders :

$$F_3 = 39.21 - 0.28\,m + 0.64 \times 10^{-3}\,m^2 + 0.685T + 2.04 \times 10^{-3}\,mT \quad (2)$$

Two active cylinders :

$$F_2 = 18.48 - 0.125\,m + 0.32 \times 10^{-3}\,m^2 + 4.59 \times 10^{-3}\,mT \quad (3)$$

One active cylinder :

$$F_1 = 3.58 - 2.12 \times 10^{-2}\,m + 1.83 \times 10^{-4}\,m^2 + 7.47 \times 10^{-3}\,mT \quad (4)$$

The fuel consumption maps (Appendix IV) suggest that there is an optimum engine control strategy for a given disablement mode and it is reflected in selection of speed such that for each level of power, the operating strategy yields the best fuel economy. The best fuel consumption schedule was found by differentiating the fuel consumption (equations 1 - 4) with respect to speed at a constant power. This necessitated an evaluation of a cubic polynomial in speed (Ref.7.1) for the case of three and four active cylinders, whilst the minimum fuel consumption for one and two active cylinders occurred at a constant speed. The solution for the one active cylinder occurred at an unrealistically low speed. Therefore the lowest engine speed at which the engine was tested was chosen.

Transmission system

The definition of engine operation resulting from earlier discussions is simplified by the assumption of a continuously variable transmission. With a continuously variable transmission a single required vehicle speed and driving torque can be achieved by means of an infinite number of combinations of gear ratio and engine speed. The problem therefore, is to determine the ideal gear ratio to achieve the desired performance of the vehicle.

If the maximum possible economy is demanded at all times, the engine must operate always at constant speed and throttle settings: but since the engine power would then be constant, it follows that no acceleration would be possible to raise the vehicle speed from a lower value to a higher one, so that absolute maximum economy is only attainable under steady state conditions or with a regenerative system. Hence there is a need to vary the power output from the engine.

There are presently at least two types of continuously variable transmission concepts at various stages of development. The hydrostatic type of transmission employs a hydraulic pump and motor with variable displacement to provide power transmission. The load matching and control capabilities of the hydrostatic system are very good but serious problems have been encountered in areas of transmission efficiency and noise. These problems can be overcome to some extent by blending the hydrostatic unit with planetary gear system (Ref. 7.2). The matching of the hydrostatic unit and gearing is such that the power handled by the hydrostatic unit is relatively low. However, the efficiency and noise problem still persists at high overall gear ratios of the unit. A second type of system is generally described as "traction drive." This technique employs power transmission through rolling elements that are arranged in such a way that variable contact radius can be obtained. High contact pressures are used in the power transmission elements and function depends on the use of special fluids. The efficiencies of the traction drive transmission are reportedly much better than those employing hydrostatic units and it has no serious noise problem (Ref. 7.3). Most of the traction type and hydromechanical type of systems require planetary system to achieve adequate ratio range. The popularity of the dry belt type of system has declined due to an increased number of belts required for satisfactory transmission of high powers and also due to maintenance problems.

Since the state of the art of continuously variable transmission is not clear, for the purposes of simulation transmission efficiency of 100% was assumed. Thus, the resulting fuel economy predictions will provide useful information in a trendwise, rather than an absolute sense.

Vehicle performance model

The size of the engine required for a vehicle depends upon the desired performance of the vehicle. The performance is affected by size and weight of the vehicle, type of tyres and the terrain over which the vehicle is driven. For simplicity, the vehicle was represented by inertia and drag forces, implying that the vehicle was driven over a level surface with no wind present. The representation of the vehicle was obtained by scaling an available model of a larger (1150 kg) vehicle (Ref.7.4) such that the resultant model represented a suitable vehicle (708 kg) for the size of engine used for cylinder disabling studies. The resulting scaled model was as follows:-

$$F_p = 92.35 + 0.6\,V^2 + 729.55\,\dot{V} \qquad (5)$$

The constant term in equ (5) represents the rolling resistance of the vehicle due to tyres and bearings. The tyre rolling resistance results from the deformation of the tyre on the rough road surface and due to imperfect release of brakes,. Any external influence that increases the tyre deformation therefore increases the rolling resistance. The losses in the bearing oil seals and oil churning for a given weight of vehicle is constant , except at very high speed where bearing losses and tyre ripple become significant (Ref.7.5). The rolling resistance therefore was obtained by a scaling factor dependent on vehicle weight.

The second term in the model represents the air drag and as can be seen, it depends upon the square of velocity and therefore power depends on cube of velocity. This term arises from the resistance of the atmosphere to the motion of the vehicle.

The magnitude of the drag constant in the equation is proportional to the drag co-efficient and the frontal area of the vehicle. For recent vehicle types, typical values of drag co-efficient lie in the range of 0.45 - 0.55 and the frontal area of a smaller vehicle increases by less than 5% (Ref. 7.6) . Because the drag co-efficient and the frontal area of a vehicle changes by small amounts, the drag term was not scaled.

The third term in the model represents the force required to accelerate the vehicle and the constant associated with it is due to the mass of the vehicle and the second moment of mass of the rotating parts referred to the vehicle mass. Assuming that the second moment of mass of the rotating parts is proportional to the mass of the vehicle, this term was also scaled. The scaling of the rotating parts is strictly true only for a fixed gear ratio. It was found that inertia term varies by a maximum of 12% for the range of typical gear ratios encountered in a small vehicle. The above mentioned figure of 12% for the variations in inertia was arrived at by considering only the moment of inertia of the engine and mass of the vehicle.

7.3. The Method of Simulation

The simulation of the vehicle was carried out in two parts, one with the "normal" engine operation and the other with the disabling strategy.

The program used the drive cycle information , i.e. speed and acceleration (obtained from speed) as an input at time intervals of one second. For each time interval the fuel and emission rates were determined on the assumption that these rates occur at the midpoint of the interval. Since the maximum acceleration during the drive cycle corresponding to route 1400Y

was only of 4 m/s^2, this represents a negligible source of error. The quantities of interest for each time interval were summed over the drive cycle and finally expressed as average quantities for the cycle under consideration.

For each time interval the power inputs required for rolling resistance, aerodynamic drag and vehicle acceleration were added to define the power required from the engine. The required speed of the engine was then calculated to give the minimum fuel consumption at that power level. The data for the emissions was stored in tabular form and linear interpolation routines were used to evaluate the flow rates of emissions. When the power required exceeded the engine capacity due to high acceleration of the vehicle, the difference of the engine power and the demanded power was stored and added to the power required from the engine in the following time interval. Thus the energy demand in terms of fuel consumption was met over the drive cycle.

The large accelerations of the vehicle resulting from braking creates an engine 'overrun' condition demanding negative power from the engine. In this situation the engine was operated along the minimum fuel consumption line with the fuel consumption given by the no load fuel requirements of the engine, and the emissions were extrapolated to the no load case. In the normal driving condition the driver of a vehicle utilizes the engine braking by making gear changes according to his needs. In case of simulation, the needs are met by operating the engine along the minimum fuel consumption line. Maximum advantage of engine braking is obtained if the engine is operated at high speeds during braking. However, this requires a predefined engine braking schedule and rapid response gear ratio change. For the case where the vehicle was stationary, the engine was idled.

The simulation of the vehicle with cylinder disabling was similar to that of the conventional vehicle. In this case the fuel consumption was minimized by cylinder disabling. The number of active cylinders depended upon the fuel consumption at the required power level. Under the overrun conditions the engine was completely disabled and the engine was idled with one active cylinder whilst the vehicle was stationary.

7.4. Results and Discussions

Initially the simulation of the vehicle was carried out at steady speeds to validate the characterisation of the vehicle. It was found that the predicted fuel consumptions were unrealistically low, particularly at low vehicle speeds. The accuracy of the fuel consumption predicted by the model was suspected and the actual data in tabular form was used to characterise the engine. Although the models of the fuel consumption of the engine were felt to be unacceptable for the prediction of fuel consumption, it was thought that errors in the minimum fuel consumption trajectories as defined by the models were negligible. This point was validated by graphical means.

The steady speed fuel consumption (fig.2) was found to be realistic. It can be seen that at very low and high speeds the fuel economy of the vehicle is poor. At low vehicle speeds and therefore at low engine power, the efficiency of the engine is low. At high vehicle speeds the power required to overcome the aerodynamic drag is significant. At low vehicle speeds the advantages of cylinder disabling are clearly illustrated. Improvement in fuel economy of 54% is possible at 30 m.p.h. with two active cylinders and an improvement of 130% results at 12 m.p.h. with

one active cylinder. The gains offered by three active cylinders are low relative to those that result from further disabling. However, the speed range with three active cylinders is increased.

The behaviour of emissions at steady speeds (fig.3) indicate that hydrocarbon emissions are approximately halved by cylinder disabling. The carbon monoxide reduces by large amounts with similar increases in the nitric oxides. The results for fuel consumption and emissions are qualitatively predictable from the discussions in the previous chapter.

The vehicle was simulated over the EPA cycles and route 1400Y to obtain a comparison with more realistic driving. The results of the simulation (table 2) runs show that the cylinder disabling strategy is most effective in increasing fuel economy in the urban mode of driving due to the operation of the engine at low loads (fig.4) and hence the number of active cylinders (fig.5). The average fuel consumption for route 1400Y is better than that of EPA urban cycle due to slightly higher times spent at idle and much higher time spent at low power levels or at higher level of disablement. The poor improvement with the highway cycle is due to the operation of the engine at higher power levels. The joint probability of fuel consumption and speed (fig.6) shows that the sectional mean is lowered for the disabled engine.

The improvements in the average emission rates of carbon monoxide and hydrocarbon are also significant over the urban type of drive cycles. However, there is an increase in nitric oxide levels. The improvements in the emissions and fuel economy over the highway drive cycle are low due to the operation of the engine at higher power levels. The increase in the carbon monoxide emissions for the highway cycle becomes clear after

examination of the carbon monoxide emissions at steady speeds (fig. 2) and the probability distribution of the active cylinders (fig. 4).

A sectional mean through the joint probability of gear ratio and vehicle speed (fig. 7) shows the average required gear ratios. At very low vehicle speeds the gear ratios are very large, suggesting a need for an infinitely variable transmission or a clutch mechanism. For the range of ratios considered the transmissions employing hydraulic elements would exhibit high losses at low vehicle speeds. The traction type of transmission appears to have an advantage over the hydraulic system. The necessity for the clutch mechanism or planetary gears may cause driveability problems at crawling speeds with a traction type of transmission, which may require a special schedule of engine operation for low vehicle speeds. The disabling of the engine results in lower gear ratios due to the operation of the engine at relatively lower speeds, thus permitting lower vehicle speeds with a given ratio range. Although the sectional mean through the X and Y axes for the fully active engine case approximately lie on top of one another, for the disabled engine operation this is not so. In the case of the disabled engine operation the acceleration of the vehicle alters the number of active cylinders, thus distorting the mean levels of the gear ratios. The ratio changes approximately from 17 : 1 to 20 : 1 at vehicle speed of 2 m/s and from 3:1 to 1.5:1 at vehicle speed of 20 m/s. The changes in the gear ratios, although small, indicate the need for a rapid-response transmission ratio changing system.

7.5. Conclusions

The simulation studies show that the use of cylinder disabling as a means of engine control offers considerable fuel savings and reduced HC and CO emissions over urban type of driving. The advantages in large measure stem from the disabling of the engine to one active cylinder at idle and cutting off the fuel supply on the engine overrun. More efficient operation of the engine at part loads as encountered in the city driving results in further savings. For the realistic case the reduction in emission levels (particularly of unburnt hydrocarbons) may be offset due to the disabling transients. However, it is thought that with better fuelling system and possibly with after "burners" the problem can be reduced. The engine on-off control strategy discussed in Chapter 5 qualitatively suggests that nitric oxides can be expected to increase during cylinder reactivation transients. This, coupled with the increases indicated by simulation studies, means that control of nitric oxides will be necessary. Some trade off with the engine efficiency and other pollutants may have to be tolerated for a simple and effective control of nitric oxides.

The benefits of cylinder disabling are maximized through the use of a continuously variable transmission. The traction type of continuously variable transmissions appears to have an advantage over the hydrostatic types due to their better efficiency at high gear ratios and absence of noise. The driveability problems at low vehicle speeds may require the operation of the engine to be suboptimal. An important requirement of the transmission system is for a fast response time of the ratio change.

The possibility of instability in cylinder disabling will result in driveability problems when the vehicle system is under fully automatic control. That is when the vehicle speed is controlled by the pedal position. The situation can be further aggravated by the slow response of the transmission system because the optimum fuel economy line is unique in torque speed space for each disablement mode of the engine. The instabilities will have a more serious effect on the emission levels. Scheduling of the engine and transmission system required to overcome driveability problems may result in some trade offs with fuel economy.

The need to retain engine braking requires the cutting off of fuel supply, rather than deactivation of valves for maximum pumping losses to occur at closed throttle. Special engine and transmissions schedules required will be costly and the potential reinstatement problems make engine braking schedules of the type discussed unattractive.

TABLE 1

BASIC STATISTICS OF THE DRIVE CYCLES

Speed (m/s)

	Maximum	Minimum	Mean	Variance
Route 1400Y	25.807	0.0	7.3318	39.644
EPA Urban	25. 15	0.0	8.8	40.161
EPA Highway	26.8	0.0	21.604	17.324

Acceleration (m/s^2)

	Maximum	Minimum	Mean	Variance
Route 1400Y	4.05	- 3.85	0.1×10^{-4}	0.368
EPA Urban	2.5	- 3.55	-0.108×10^{-8}	0.4336
EPA Highway	1.45	- 1.5	-0.78×10^{-9}	0.08

TABLE 2

Effects of Cylinder disabling on fuel consumption and emissions

	Route 1400 Y		EPA URBAN	
	Normal mode	Disabled mode	Normal mode	Disabled mode
Fuel (M.P.G.)	45.0	66.24	46.8	64.35
NO g/mile	2.7	3.29	2.63	3.27
CO g/mile	11.23	5.46	10.02	6.15
HC g/mile	2.96	0.54	2.21	0.59

	EPA Highway	
	Normal mode	Disabled mode
Fuel m.p.g.	55.64	58.44
No g/mile	3.7	3.78
CO g/mile	4.83	5.8
HC g/mile	0.6	0.58

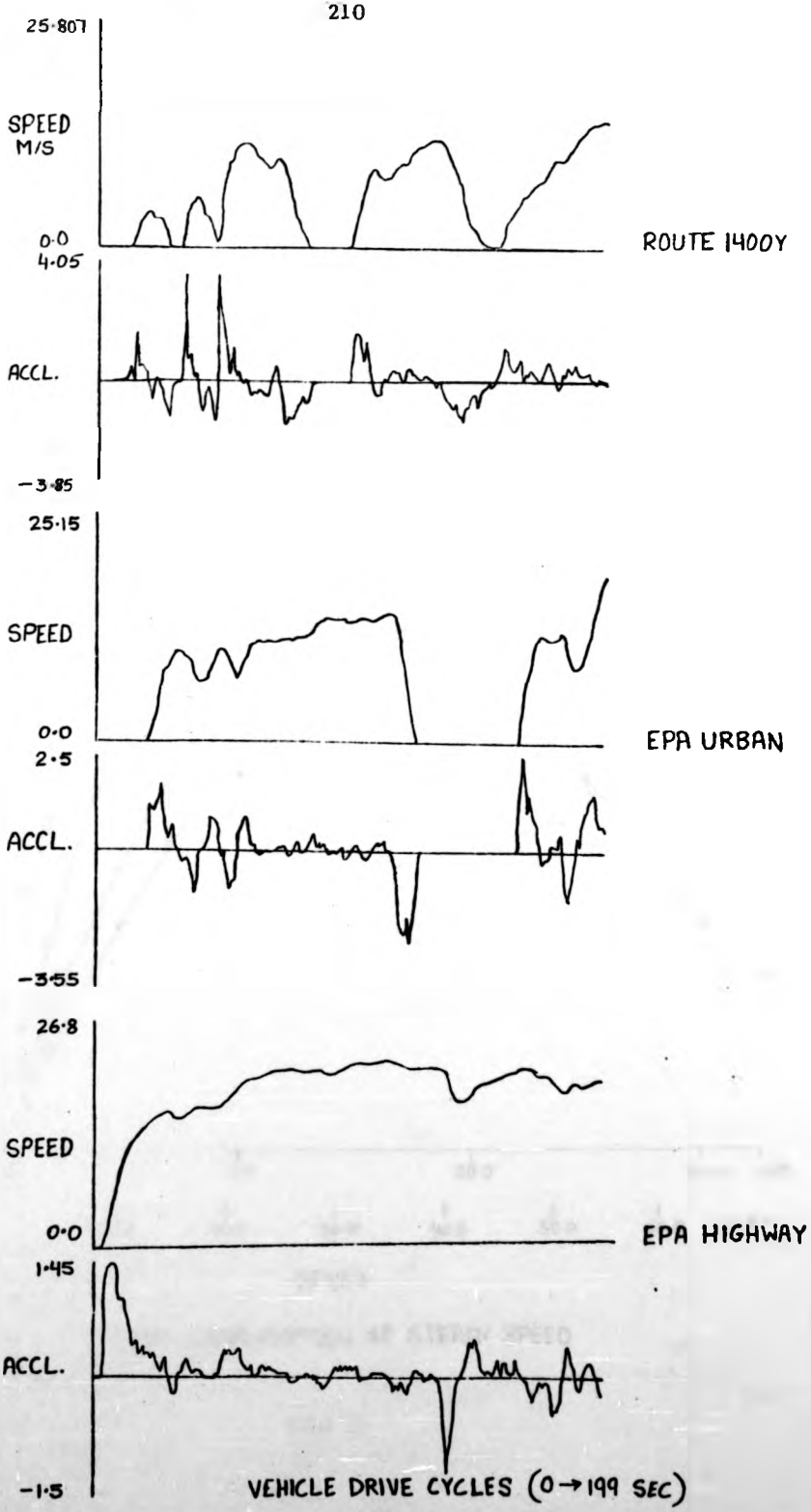

VEHICLE DRIVE CYCLES (0→199 SEC)

FIG.1

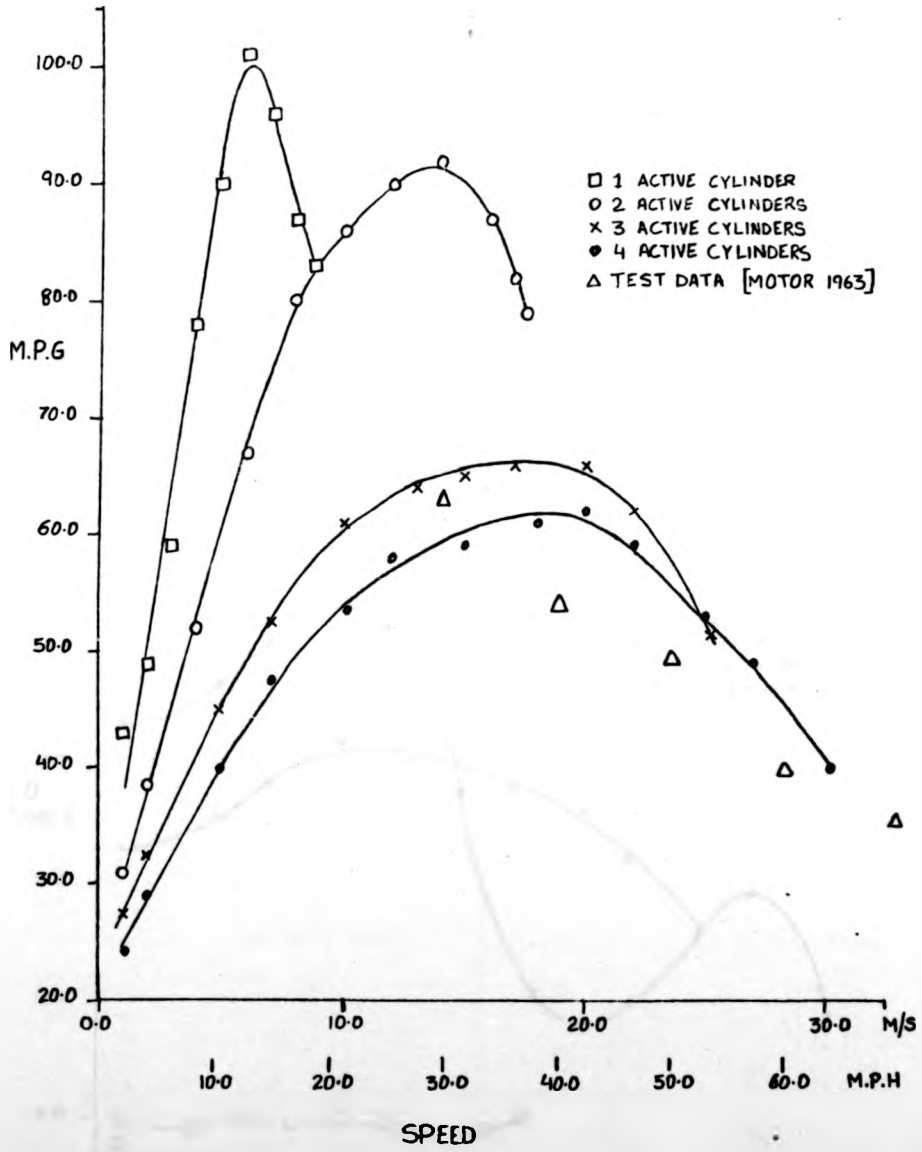

FUEL CONSUMPTION AT STEADY SPEED

FIG.2

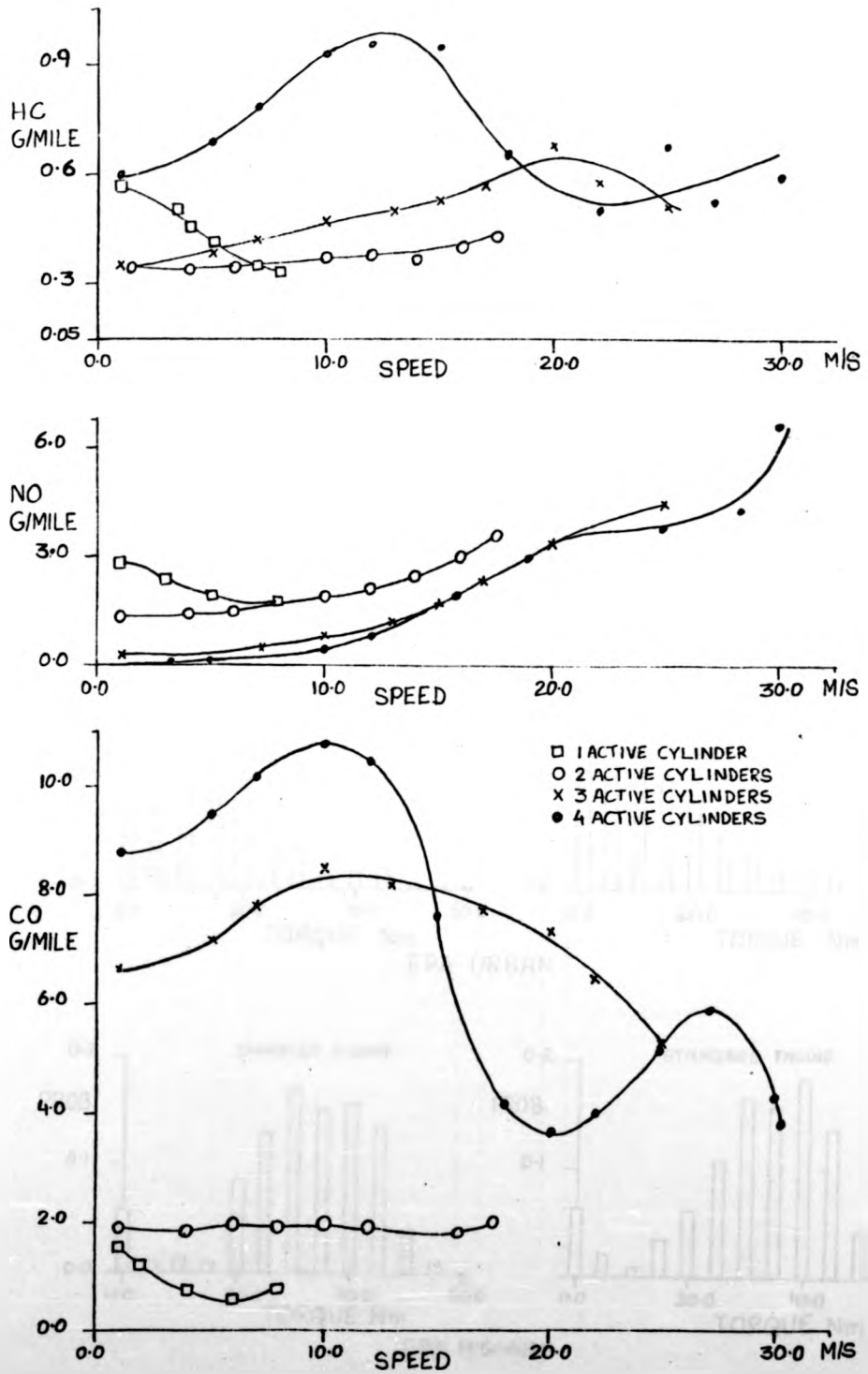

EMISSIONS AT STEADY SPEED

FIG.3

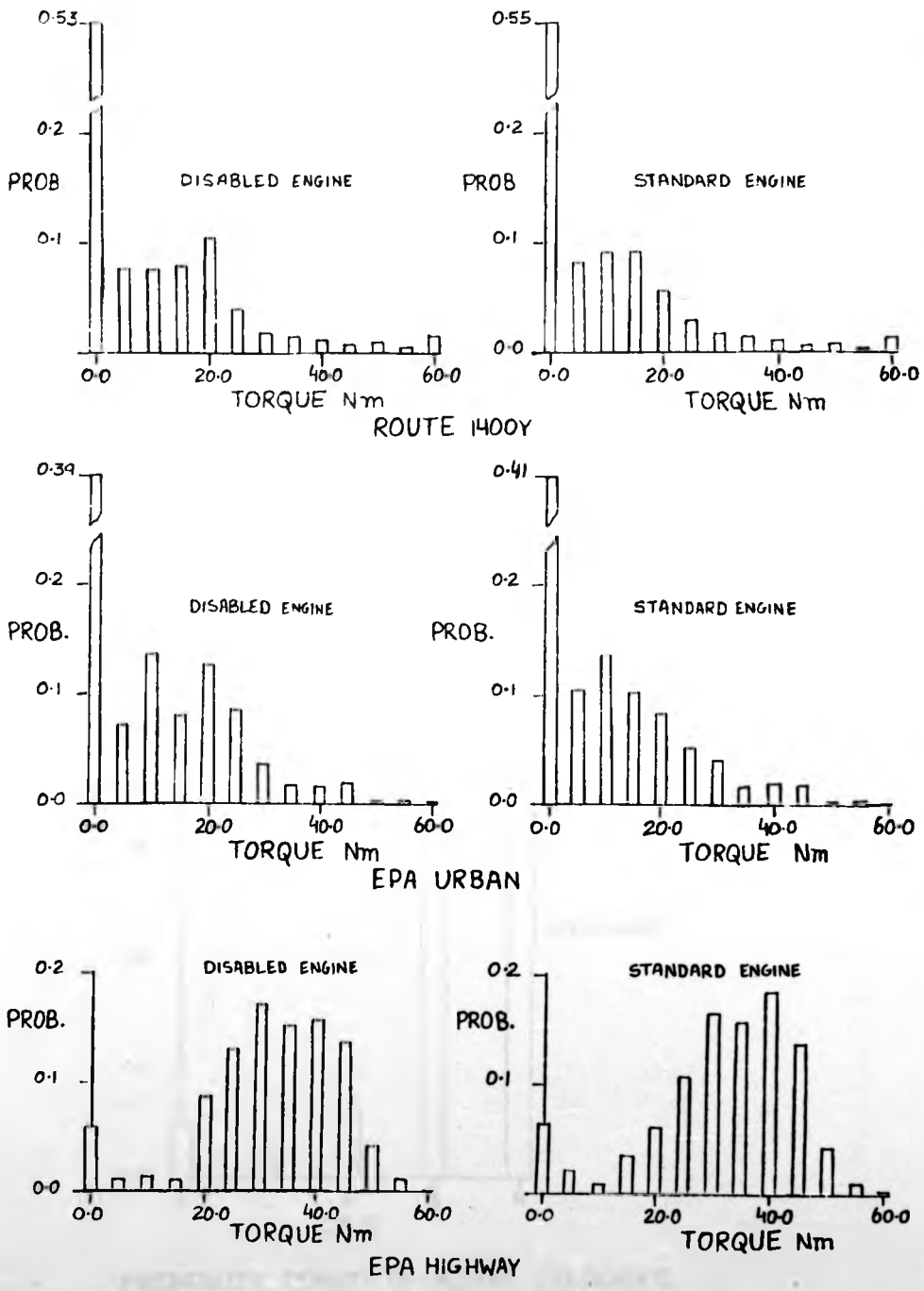

PROBABILITY DENSITY OF ENGINE TORQUE

FIG.4

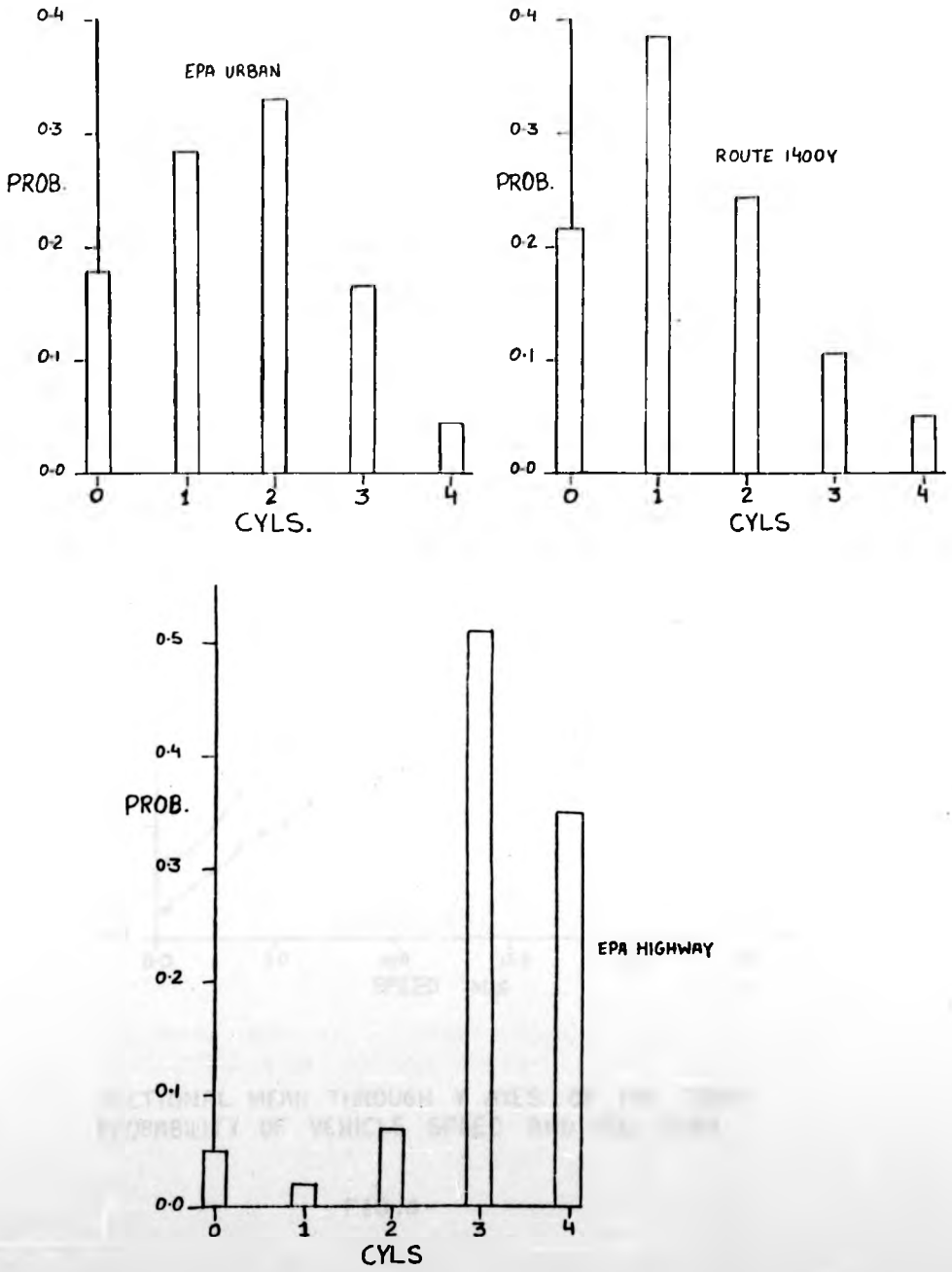

PROBABILITY DENSITY OF ACTIVE CYLINDERS.

FIG.5

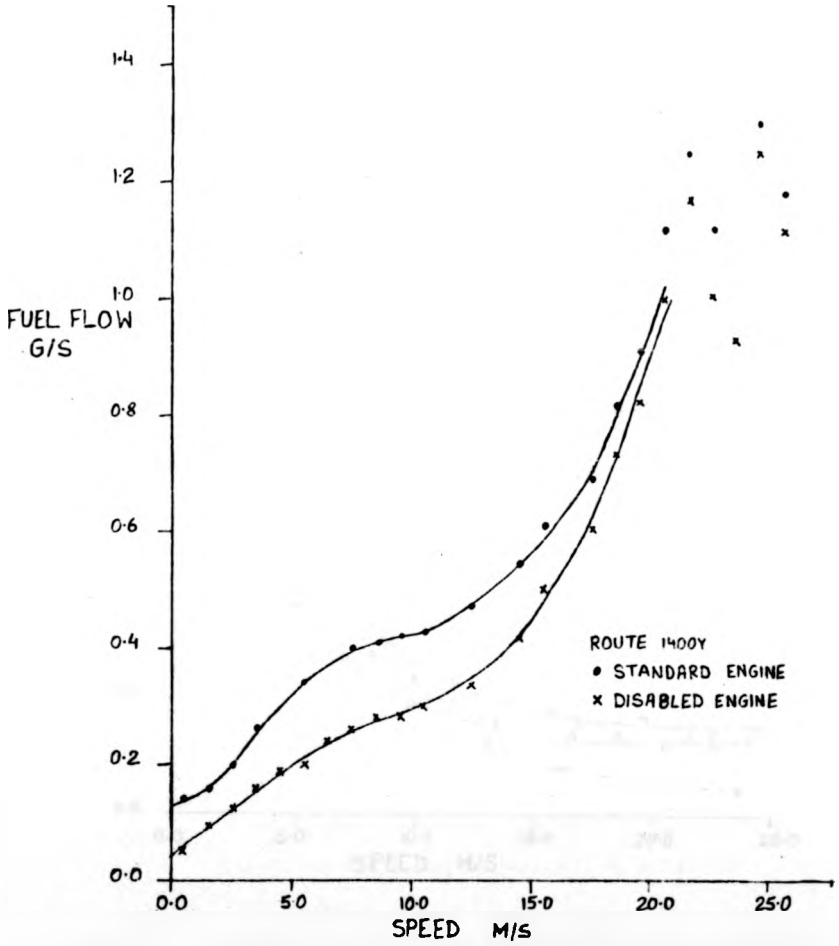

SECTIONAL MEAN THROUGH Y AXES OF THE JOINT PROBABILITY OF VEHICLE SPEED AND FUEL FLOW

FIG.6

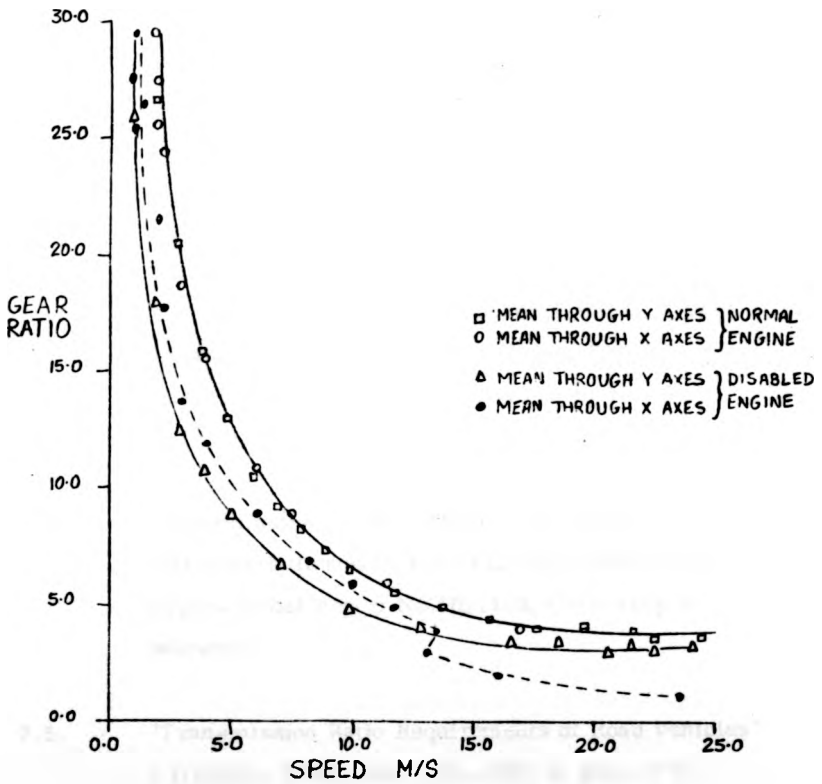

SECTIONAL MEAN OF THE JOINT PROBABILITY OF GEAR RATIO AND VEHICLE SPEED

FIG.7

REFERENCES

7.1. 'Compendium of Mathematics and Physics'
D.S.Meyler, The English Universities Press Ltd., 1958

7.2. 'Automobile Fuel Economy with Hydromechanical Transmission by Simulation Studies.'
E.Orshansky, P.Huntly and W.E.Weseloh, 1974
S.A.E. 740308.

7.3. 'Perbury Continuously Variable Ratio Transmission.'
T.G.Fellows, D.Dowson, F.G.Perry and M.A.Plint
Advances in Automobile Engineering, Part II,
Carter, N.A. editor, Pergamon Press, New York, 1964,
(P 123 - 142)

7.4. 'Determination of the Dissipative Resistance Characteristic and Inertia of Cortina Test Vehicle'
Departmental Report No.HEV103, University of Warwick.

7.5. 'Transmission Ratio Requirements of Road Vehicles'
J.G.Giles, MIRA Report No.1957/4, June 1975.

7.6. 'Should We Have a New Engine? An Automotive Power Systems Evaluation.' Vol.II. Jet Propulsion Laboratory CIT. Aug.1975.

CHAPTER 8 CONCLUSIONS AND SUGGESTIONS FOR FURTHER WORK

8.1. Engine Test Bed System

The engine test bed facility based on the Ward-Leonard system, although complex, is very versatile. Although much of the author's time was spent on development of the test facility , the reliability of the final product proved it worthwhile. Experiences with the instrumentation showed that methods of performing calibration checks need to be considered at the initial design stages.

The problem of engine-dynamometer coupling shaft failure was overcome by introducing flexibility into the coupling. It is felt that there is scope for a further increase in the flexibility whilst maintaining the constraints of the control system.

In the design of the interface required for testing of the engine, it was found necessary to make the interface compatible with the school's computer (for data logging). There is scope for the application of computer controlled testing by extending the facilities.

8.2. Control Systems

A small-signal linearized model of the test bed system described the behaviour of the system adequately over the frequency range considered (Chapter 4). The resulting multi-variable controller based on the Inverse Nyquist Array design method coped with the non-linearities of the system satisfactorily. Limitations in the performance of the control system were imposed by the inertia of the dynamometer and the time constant of the generator field winding. Further limitations were imposed by the non-linear behaviour of the engine. The gains of the controller were chosen to provide minimum interactions (in the operating region) , on the torque loop for small step changes in speed (200 R.P.M.). The design of the compensator, although

complicated, is such that a replacement of the engine to be tested can easily be accommodated. The information necessary for compensator adjustment can be obtained from steady state engine maps and from tests to establish the engine time constant.

Time optimal control design studies indicated the feasibility of a higher performance control system. In practice, the application of "bang-bang" control requires switching of controls even at steady state to maintain the system states at the desired values. This feature makes the non-linear control undesirable for test-bed applications. However, combination of non-linear control resulting from optimal control theory with the linear control due to Inverse Nyquist Array method overcomes the switching problems of the non-linear control. The resulting control scheme will have a performance suitable for dynamometer simulation studies of vehicles.

Under large power changes which can occur during simulation of vehicles on engine test-bed, the engine coolant control system may prove to be inadequate. There is scope in this area for optimization of the control system using feed forward techniques.

8.3. Engine dynamics

The dynamic studies of the gas analysis system showed that the bandwidth of the system is limited due to the lags of the equipment as well as the exhaust gas sampling system. Therefore care is necessary in the design of the sampling system. The resulting transfer functions offer an alternative method of measuring vehicle emission to the conventional exhaust gas collection method over a limited bandwidth. There is a serious need in this area for better gas analysis techniques.

The studies of exhaust emissions during transient operating conditions have identified a problem area. The results show that dynamics are significantly slow and need to be considered in computer simulation studies of vehicle systems. The resulting models are not adequate for predicting emissions under all engine operating conditions because they contain no information about the effects of ignition timing, air fuel ratio and temperature changes. The indicated information is necessary for simulation studies over the Federal drive cycles.

The mechanism controlling the exhaust emissions during transient engine operation is thought to be "wetting" of the inlet manifold wall by impaction of fuel droplets . There is considerable scope in this area for further work.

The behaviour of engine efficiency under transient engine operation indicates that steady state maps are adequate for the prediction of engine fuel consumption by computer simulations of the vehicle.

8.4. Cylinder Disabling Concept

Engine cylinder disabling by valve deactivation shows a potential for an improvement in fuel economy of the vehicles (Chapter 7). It is also clear that the concept requires an advanced technology transmission system to realise its full potential. Certainly it would be impossible to match the conventional "fixed" ratio transmissions to an engine for maximum economy. Independent control of throttle position is also desirable for optimisation of efficiency. The result is an increase in complexity and cost.

The valve deactivating mechanism needs to be fast-acting so that deactivation can be performed precisely at a defined point towards the end of the exhaust stroke to ensure low pressure in the cylinders. In practice it may be advantageous to trap some exhaust gases in the cylinder to prevent oil pumping by the piston rings, especially in a worn engine. Also the resulting gradual leakage of the exhaust gases into the crankcase can be fed into the engine intake to provide E.G.R.action. Reactivation of the exhaust valve will depend upon the method adopted for deactivation. If no gases are present then the exhaust valve will need to be reactivated near the end of the exhaust stroke,and if gases are present near the beginning of the exhaust stroke. The exact point of reactivation will depend on the amount of exhaust gas . The case of the inlet valve is not so complex for it can be activated at the beginning of the inlet stroke and deactivated at the end of the stroke. In the preceding discussions activation and deactivation implies that the valves are in position to follow the camshaft. In view of the nature of the strokes , both the inlet and exhaust valve disabling mechanism can be energised simultaneously.

The complicated functions such as engine efficiency optimisation and precise valve deactivation can be performed satisfactorily by an on board microprocessor. The microprocessor can be utilized to perform other tasks such as control of ignition timing, fuel-air ratio and engine coolant temperature.

Because the transient effects due to cylinder disabling and those resulting from the dynamic operation of the throttle were not considered in vehicle simulation studies, the predicted values of exhaust emissions (Chapter 7) are inaccurate. However,

the results are valuable in indicating the trends. The indications are that oxides of nitrogen increase, whilst the unburnt hydrocarbons and carbon monoxide decreases with cylinder disabling. The results of engine on-off tests (Chapter 5) indicate that emissions of carbon monoxide will not be affected by the cylinder disabling transients. However, oxides of nitrogen and unburnt hydrocarbons are expected to increase with disabling transients. The increase in hydrocarbons is expected to be less than the levels indicated by the results of on-off tests because some of the hydrocarbons will be oxidized in the exhaust system by the hot gases from active cylinders. Control of pollutants may prove to be a serious problem and may require costly fuel injection systems.

Due to the short duration of tests and the general condition of the test engine, "oiling up" of the spark plugs of the disabled cylinders was not present. In a worn engine the case is likely to be otherwise. Also cooling of the disabled cylinder may aggravate the transient emissions. The cylinders in this case can be disabled in a random manner. This process will also assist to even out the cylinder wear. The frequency of the random process will be such as to optimize the oiling up and cooling problems with the transient emissions which will result on cylinder activation.

The behaviour of the test engine indicated that noise and vibration is not a problem. These observations may be due to the laboratory conditions. In a vehicle low firing frequencies associated with the reduced engine may excite body work panels. The vibration problems of the bodywork and the engine are easily solved by increasing the stiffnesses or by introducing damping.

The preceding discussions indicate some of the problems with possible solutions associated with the concept of cylinder disabling. Proposals for further work in this field deal with concepts of engine control and vehicle application.

The valve deactivation can be thought of as a limiting process of valve lift control which offers a possibility of intake valve throttling. The resulting shock wave at the intake valve should produce a more homogeneous mixture. Combination of valve lift and timing control would then allow optimization of efficiency over the engine disabled state as well as engine speed. Also, trade off with exhaust emissions and particularly with the oxides of nitrogen is possible due to the internal E.G.R. resulting from changes in valve timing.

The gains in fuel economy with cylinder disabling depend upon the reserve engine power available for acceleration. In this respect, high performance vehicles such as large saloons or sports cars will derive the most benefits. An obvious application of the concept is to a hybrid vehicle. Since the high efficiency range of the engine is broadened with disabling, the problems associated with engine turn-off are reduced considerably. The resulting "continuous" engine operation and hence power control offers a better coupling with the energy store. Such a system will derive benefits from regenerative braking as well as better efficiency of the engine.

8.5. The Future of the cylinder disabling concept

Clearly the days of vehicles as we know them today are numbered. The use of lighter materials for weight reduction and a change in shape to reduce aerodynamic drag will alter the external appearance of the vehicle. In this area, the motor industry has an

opportunity to make a contribution to society by redeploying the redundant expertise from the ailing aircraft industries. The use of innovative concepts and modern electronic technology will also produce some changes under the bonnet.

Although the vehicle may differ in appearance and level of technology, the basic characteristics required in a vehicle are not expected to alter. For convenience the objectives discussed in Chapter 1 are reproduced again, together with an extra requirement.

1. Fuel economy
2. Low emissions
3. High performance
4. Good driveability
5. Comfortable ride
6. Economy of production and maintenance.

The requirements, although listed separately, have strong interrelationships with one another. The final acceptability of any alternative system will be based on the overall "goodness" of the compromise of the listed properties. The cylinder disabling concept has an advantage over the other alternatives because the support technologies it requires are either developed or are in stages of advanced development. In the short term the prospects seem bright, but whether in the long term it can compete with the alternatives remains to be seen.

APPENDIX I

A. OPERATION OF THE WARD LEONARD SYSTEM FOR ENGINE TESTING

The motor generator set of the Ward-Leonard system is used to service a test bed in cell DO20, a bank of batteries in cell D106, as well as the test bed in cell D102. The control system used consisted of safety relay controls to prevent accidental damage to the system. The control relay scheme is shown in figure 1.

The control system also serviced the battery stack in which case the dynamometer is replaced by the battery stack. Therefore the start-up procedures need to be followed with care.

OPERATING THE WARD-LEONARD SYSTEM FOR ENGINE TESTING

INITIAL CHECKS

1. Ensure that the change over switch in M.G. room (D100) is set to dynamometer No.1 position. Also check that the generator field change over switch in the control cell (D101) is switched to dynamometer No.1.
   The field change over switch is located near the light switch in the control cell (D101).

2. Switch on the mains isolator in D100.

3. Switch on the mains 240V supplies in control cell (D101) and in the engine cell (D102).

4. Select the dynamometer/battery change over switch in the engine cell (D102) to the dynamometer position.

5. Start up the M.G. set .

6. Ensure that the cooling water is switched on.

7. Close the cell (D102) doors.

8. Check that the dynamometer field rheostat located in the control cell (D101) is turned fully clockwise.

9. Start up the throttle servo and turn the throttle demand to close the throttle.

   At this stage the following lights should be on :

   a) Throttle
   b) Dynamometer field
   c) Generator field
   d) M.G. set running
   e) Cell door
   f) Dynamometer selected

   The cooling water light should be off.

SINGLE LOOP SPEED CONTROL OPERATION

1. Plug in the original S.C.R. board No.4
2. Select the Torque/speed switch to the speed position.
3. Select the mimo/siso switch to the siso position.
4. Ensure that the throttle switch located on shalf 4 is in the off position.
5. Ensure that the speed demand is zero.
6. Press the start button.
   G1, D1 and L1 closed lights should turn on.
7. Turn the speed demand to the desired speed.
8. Switch on the ignition.
9. Operate the throttle to the desired load.

MULTIVARIABLE CONTROL

1. Replace the original S.C.R. board No.4 with the multivariable board.
2. Select the Torque/speed switch to the speed position.
3. Select the mimo/siso switch to mimo position.
4. Ensure that the throttle switch is in the 'off' position.
5. Turn current/Torque demand to No.5 position (i.e. zero torque).
6. Ensure that speed demand is zero.
7. Press the start button
   G1, D1, and L1 lights should turn on.
8. Turn the speed demand to the desired speed.

MULTIVARIABLE CONTROL (Cont'd..)

9. Switch on ignition.

10. Adjust the throttle demand to obtain power from the engine.

11. After the engine has reached its normal operating temperature, close the throttle.

12. Select the throttle switch to 'on' position

13. Demand desired torque and speed.

Note that prior to Step 12, the multivariable controller operates in a single loop speed control mode with "current limit" due to the compensator.

To turn the system off, whether operating in a simple input output mode or multivariable mode, reduce the load and speed of the engine and follow the start up steps in reverse order.

B. OPERATION OF GAS ANALYSIS SYSTEM

1. Switch on the power supply to the equipment

2. Replace filter paper

3. Leave the system to warm up for approximately 3 - 4 hours

One hour before use :

4. Switch on the sample pump.

5. Fill cooler with ice.

6. NO Analyser

6.7. Turn on the oxygen supply and adjust the pressure to 5 p.s.i.

6.2. Switch on the Ozoniser.

7. HC Analyser

7.1. Turn on the air supply and adjust to obtain a flow of 230 ml/min.

7.2. Turn on the hydrogen supply and adjust to obtain a flow rate of 15 ml/min.

7.3. Turn on the sample flow and adjust to bring the pressure level up to the mark on the manometer.

7.4. Press ignite button. The flow as indicated by the rotameter reduces considerably when ignition is established.

8. CO Analyser

8.1. Adjust sample flow to 1.5 l/min.

CALIBRATION

Initial calibration of the analysers is carried out by applying the appropriate calibrating gases to obtain the calibration curves. Before each test, point checks of the calibration are necessary to safeguard against drifts and flow settings. The CO analyser has a built in calibration check, whilst the HC and NO analyser require an application of calibrating gases. In the case of the HC analyser, care is necessary whilst applying the gas and the following procedure is recommended to prevent blow out of the flame.

1. Turn on the calibrating gas at the cylinder and adjust the pressure to approximately 5 p.s.i.

2. Turn on the valve to allow the calibrating gas to flow to the analyser and simultaneously turn off the sample valve.

A periodic calibration check through the sampling line is necessary to ensure that the characteristics have not altered.; if they have, then cleaning of the system may be necessary. Whilst operating the system for engine tests it is advisable to maintain a regular check on the calibration. A regular change of the filter paper is also necessary.

C. CONVERSION OF EMISSIONS DATA

For the purposes of the conversion of emissions from concentration to the mass flow rates, the following equations were used (Instrumentation and techniques for exhaust gas emissions measurement. S.A.E. J254)

$$CO\left(\frac{g}{hr}\right) = (\text{air flow} + \text{fuel flow})\frac{28}{\text{mol.wt.exh.}}\ \%\ CO \times 10^{-2} \times 453.6\left(\frac{lb}{hr}\ \frac{g}{lb}\right)$$

$$NO_2\left(\frac{g}{hr}\right) = (\text{air flow} + \text{fuel flow})\ \frac{46}{\text{mol.wt.exh.}}\ NO\ ppm \times 10^{-6} \times 453.6\left(\frac{lb}{hr}\ \frac{g}{lb}\right)$$

$$HC\left(\frac{g}{hr}\right) = (\text{air flow} + \text{fuel flow})\ \frac{13.85}{\text{mol.wt.exh.}}\ HC\ ppm\ C \times 10^{-6} \times 453.6\left(\frac{lb}{hr}\ \frac{g}{lb}\right)$$

Molecular weight of exhaust = (34.67 - 83.3 F/A)

where F/A is the fuel air ratio.

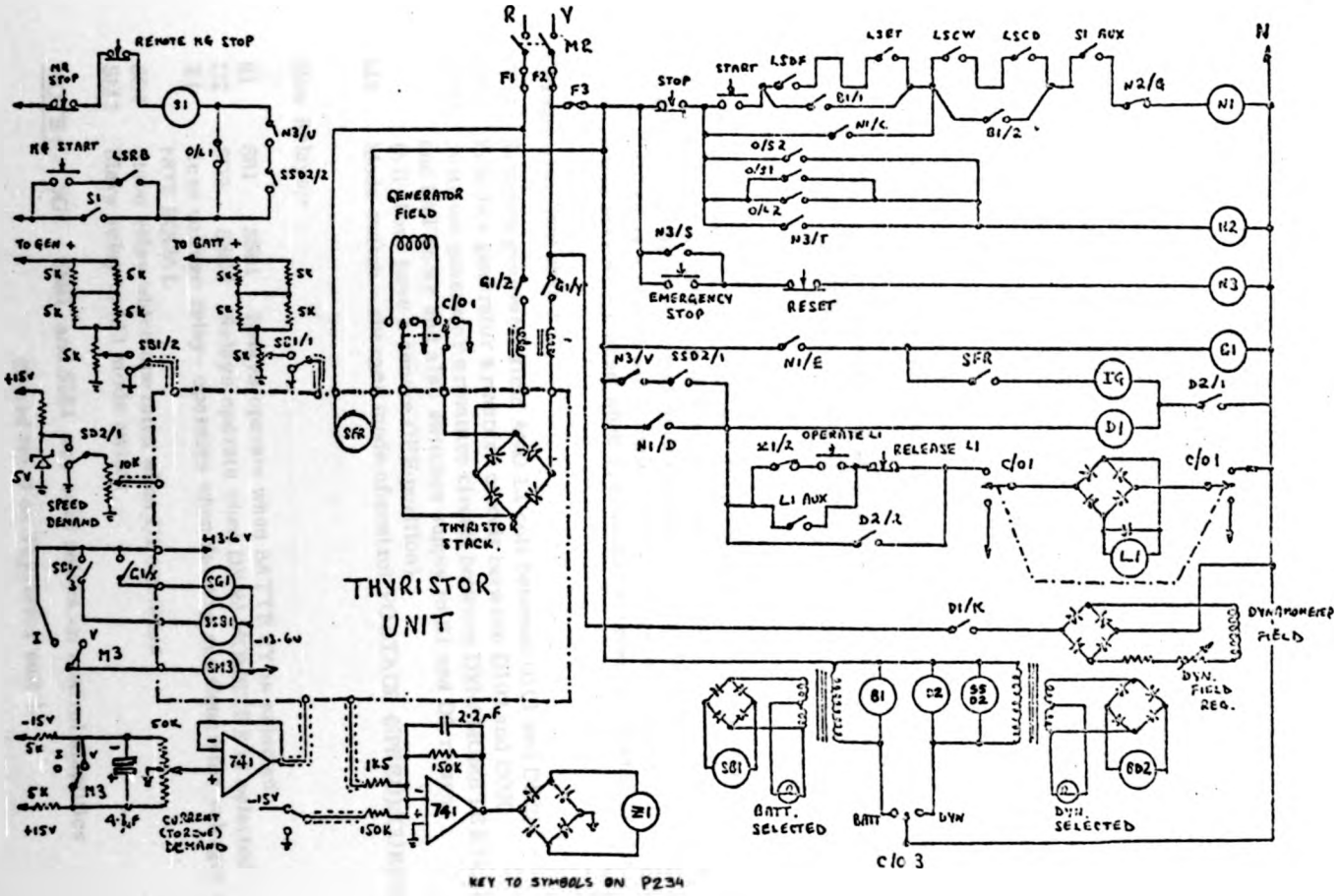

RELAY CONTROL SYSTEM

FIG.1

KEY TO RELAY AND SWITCH SYMBOLS

M1	Main 415 V, 3 ph. Isolator
M2	Mains 415 V , ON/OFF Switch on Control Panel
S1	Contactor feeding 3 ph. Motor
L1	Contactor switching armature loop circuit
N1	START Relay - initiates sequence to build up generator voltage
N2	STOP Relay - releases N1 and hence initiates normal shut-down
G1	Generator Field relay - switches supply to thyristor bridge only.
SFR	Supply Failure Relay - operates when mains is applied to thyristor unit
IG	Ignition Relay - controls the 12 V d.c. supply to engine ignition
D1	Dynamometer field supply relay
N3	EMERGENCY STOP relay - see text

Overloads : -

O/L1	Current overload on a.c.motor
O/L2	Generator armature current overload
O/S1	MG Set Overspeed relay
O/S2	Dynamometer Overspeed relay (contacts on electric tachio indicator)
CB1	Battery Circuit Breaker and Isolator.

Limit Switches :-

LSDF	Dynamometer Field - closed when regulator set for maximum field
LSET	Engine Throttle - closed when throttle closed
LSCW	Cooling Water - closed when cooling water is flowing.
LSCD	Cell Door - closed when engine cell (D102) door is closed.
LSRS	Rotor Starter - closed when a.c. motor starter resistance is all-in.

Change-over Switches :

C/01	Switches generator field AND L1 coil between D101 and D020
C/02	Switches generator armature circuit between D102 and D020
C/03	Switches generator armature circuit between DYNAMOMETER No.1 and BATTERY and also switches supply to B1 and D2 relays. (All above have a centre OFF position).
M3	Mode switch - charges mode of control VOLTAGE (SPEED)/CURRENT (TORQUE

New Relays:-

B1	SB1	SSB1	Relays operate when BATTERY is selected
D2	SD2	SSD2	Relays operate when DYNAMOMETER is selected
Z1	Zero voltage relay- operates when Battery and Generator voltages are NOT EQUAL		
SG1	Slave relay which operates when G1 operates		
SM3	Slave relay to M3 mode switch		

NOTE: SG1 SSB1 and SM3 are reed relays on control amplifier (Board No.4 on Thyristor unit).

APPENDIX II

INVERSE NYQUIST ARRAY DESIGN METHOD

Consider a least order multivariable system described by linear time-invariant differential equations, having the same number of outputs as inputs. The general representation of the system is given by :

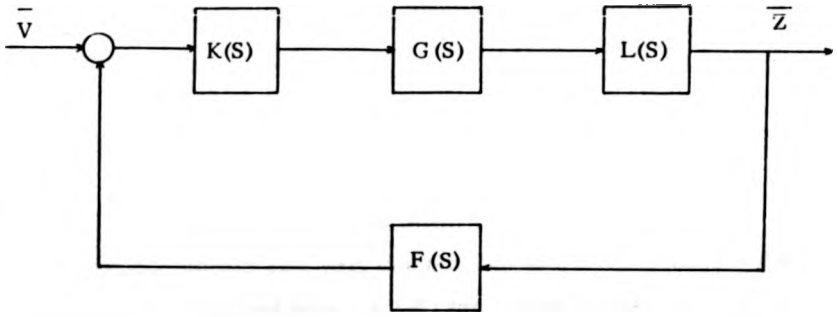

Where

G (S) is the transfer function of the plant.

K (S) is the input compensator

L (S) is the output compensator

F (S) is the feedback matrix

$\bar{V}$ and $\bar{Z}$ are the input and output vectors

The close loop transfer function relating output to input is :

$$H(S) = (I + QF)^{-1} Q = Q(I + FQ)^{-1} \qquad (1)$$

where $Q = LGK$

and $|I + QF| \neq 0$

when inverted eqn. (1) becomes

$$\hat{H} = F + \hat{Q} \qquad (2)$$

where $\hat{H}$ and $\hat{Q}$ are the inverse close loop and open loop transfer functions.

Stability Criterion for a multivariable System

In its more general form, the stability theorem for multivariable system is a very complicated one, even when $F = \text{diag}(f_i)$. However, if $K(S)$ and possibly $L(S)$ are chosen so that $\hat{Q}$ is dominant on a suitable Nyquist contour, then a much simpler stability criterion is obtained (Ref. II.1)

Dominance is defined in the following way :

Definition

A matrix $\hat{Q}(S)$ is dominant on a contour D if

$$\text{either} \quad \left|\hat{q}_{ii}(S)\right| - \sum_{\substack{j=1 \\ j \neq i}}^{m} \left|\hat{q}_{ij}(S)\right| > 0, \; i = 1, 2 \ldots m$$

$$\text{or} \quad \left|\hat{q}_{ii}(S)\right| - \sum_{\substack{j=1 \\ j \neq i}}^{m} \left|\hat{q}_{ji}(S)\right| > 0, \; i = 1, 2 \ldots m \qquad (3)$$

where the first inequality holds for row dominance and the second holds for column dominance.

Theorem 1

Let $\hat{Q}(S)$ be dominant on D and let there be no pole of $\hat{q}_{ii}(S)$ on D, (i = 1 ... m). As S goes once (clockwise) round D, let the image of the Nyquist plot of D under $|\hat{Q}|$ go $\hat{N}$ times (clockwise) around the origin and let the image of the Nyquist plot of D under $\hat{q}_{ii}$ go $\hat{N}_i$ times (clockwise) round the origin. Then

$$\hat{N} = \sum_{i=1}^{m} N_i$$

This is the result obtained if $\hat{Q}$ were diagonal. The theorem shows that dominance achieves the same result with less restrictive conditions.

This theorem leads to a very useful stability theorem which is ,

Theorem 2

Let $\hat{Q}$ and $\hat{Q} + F$ be dominant on D. Let the image of the Nyquist plot of D under $\hat{q}_{ii}$ go $\hat{N}_{oi}$ times around the origin and $\hat{N}_{ci}$ times around the critical point $(-f_i, O)$, i = 1, 2 ..m. Let the open loop system have P_o poles in the open right half plane. Then the closed-loop system is asymptotically stable if and only if

$$\sum_{i=1}^{m} N_{oi} - \sum_{i=1}^{m} N_{ci} = P_o$$

Here D consists of imaginary axis from $-i\alpha$ to $+i\alpha$, indented into the left hand plane to avoid any imaginary poles or zeros of $|\hat{Q}|$ or $|\hat{Q} + F|$ and any imaginary poles of

$\hat{q}_{ii}$, i = 1 ..... m, and completed by a semicircle in the right hand plane. The radius r of the semi-circle is chosen large enough to ensure that all finite poles and zeros, lying in the closed right half plane of $|\hat{Q}|$ and $|\hat{Q} + F|$, lie inside D. Let F = diag(f_i) with f_i independent of S.

Graphical interpretations

The above stability theorem leads to simple graphical interpretations. The procedure is to draw Nyquist plot of $\hat{q}_{ii}$ and circles of radius $\hat{d}_i$ or $\hat{d}_i^1$ are superimposed with $\hat{q}_{ii}(S)$ for each S as S goes round D. Where $\hat{d}_i$ and $\hat{d}_i^1$ are defined as

$$\hat{d}_1 = \sum_{\substack{j=1 \\ j=i}}^{m} |\hat{q}_{ij}(S)|$$

and

$$\hat{d}_i^1 = \sum_{\substack{j=1 \\ j+i}}^{m} |\hat{q}_{ji}(S)|$$

These circles, known as Gershgorin circles, sweep out a band as S goes round D. If this band does not include the origin or the critical point (- f_i , 0) , and if this is true for i = 1, 2 .....m, then $\hat{Q}$ and $\hat{Q}$ + F are dominant on D. If $\hat{Q}$ is dominant on D then $\hat{N}_{oi}$ is the number of times the Gershgorin band encircles the origin, while $\hat{N}_{ci}$ is the number of times it encircles the critical point (-f_i, 0).

The Gershgorin bands do not only give the stability criterion but they also set bounds on the transfer function $h_{jj}^{-1}(S)$ seen in the jth loop as the gains in the other loop are varied.

Theorem 3

Let the dominance criterion (3) for $\hat{Q} + F$ be satisfied for $i = 1, 2 \ldots j-1, j+1 \ldots m$. Then the inverse transfer function $h_{jj}^{-1}(S)$ between input i and output j of the plant, when $F = \text{diag}(f_1, f_2 \ldots f_{j-1}, O, f_{j+1} \ldots f_m)$ lies inside the j Gershgorin band.

That is to say, so long as dominance is maintained in the other loops, $h_{jj}^{-1}(S)$ is trapped inside the j Gershgorin band.

For a fixed set of gains $f_1 \ldots f_{j-1}, f_{j+1} \ldots f_m$ the above result is refined by construction of narrower Ostrowski band. Ostrowski circles are defined in a similar way to the Gershgorin circles but with radius of $\mu_j(s)\, d_j(S)$ or $\mu_j^1\, d_j^1$ where

$$\mu_j(S) = \max_{\substack{j \\ i \neq j}} \frac{d_i(S)}{\left|f_i + \hat{q}_{ii}(s)\right|}$$

or $$\mu_j^1(S) = \max_{\substack{j \\ i \neq j}} \frac{d_i(S)}{\left|f_i + \hat{q}_{ii}(S)\right|}$$

For the given $f_1, f_2 \ldots f_{j-1}, f_{j+1}, \ldots f_m$, $h_{jj}^{-1}(S)$ lies inside the jth Ostrowski band. The width of the Ostrowski band depends on the chosen gains, whereas Gershgorin band is independent of the gains. From the Ostrowski band subject to small uncertainty, phase margin and gain margin can be estimated, leading to the design of phase advance or phase lag compensation as desired.

Achieving Dominance

A system can be made dominant in the following ways :

1. Elementary row and/or column operations.

These operations include multiplication of a row (column) by a constant and addition or subtraction of a multiple of row (column) to another row (column). These operations performed on the rows of the system transfer function matrix result in a precompensator and when performed on the column, they result in a post compensator.

2. Pseudo-diagonalisation

This results in a pre- or post-compensator which nearly diagonalises the system transfer function matrix at a specified frequency. That is, for each row (column) of the compensator system matrix, the sum of the squares of the magnitudes of the off-diagonal elements at this frequency is minimised in comparison with the diagonal element.

An extension of pseudo-diagonalisation would be the minimisation of a weighted sum of squares at frequencies $\omega_1, \omega_2 \ldots\ldots \omega_n$, of the off diagonal elements in a row (column) of transfer function matrix.

TIME OPTIMAL CONTROL

The design of time optimal control laws for the test-bed system was carried out using the Pentryagin's maximum principle (Ref.II.2). Consider a linear system represented by the following differential equations :

$$\frac{dx^i}{dt} = \sum_{\nu=1}^{n} a^i_\nu x^\nu + \sum_{\rho=1}^{r} b^i_\rho u^\rho \qquad (1)$$

$$i = 1, 2, \ldots\ldots n$$

where x^i are the phase co-ordinates of the controlled object which define its state at each instant of time; u^ρ are the control parameters which determine the course of the process. The subscripts and superscripts associated with a and b define the elements of matrices operating on co-ordinates x and controls u. The determination of optimal controls laws depends upon the behaviour of the Hamiltonian H which is really the sum of kinetic and potential energy of the system. The Hamiltonian then is :

$$H(\psi, x, u) = \sum_{\alpha=1}^{n} \psi_\alpha f^\alpha(x,u) \qquad (2)$$

where the auxiliary variable ψ, sometimes referred to as Pontryagin function, is given by :

$$\frac{d\psi_i}{dt} = -\sum_{\alpha=1}^{n} \frac{\partial f^\alpha(x,u)}{\partial x^i} \psi_\alpha \quad , i = 1, 2, \ldots n \qquad (3)$$

Then the Hamiltonian canonical equations are as follows :

$$\frac{dx^i}{dt} = \frac{\partial H}{\partial \psi_i}$$

$$\frac{d\psi_i}{dt} = -\frac{\partial H}{\partial x_i} \qquad (4)$$

Theorem 1

Let $u(t)$, $t_0 \leq t \leq t_1$ be an admissible control such that the corresponding trajectory $x(t)$ and $u(t)$ is optimal if there exists a non-zero continuous function $\psi(t)$ corresponding to $x(t)$ and $u(t)$ such that

1) for every t, $t_0 < t_1$, the function $H(\psi(t), x(t), u(t))$ of the variable u attains its maximum at the point $u = u(t)$:

$$H(\psi(t), x(t), u(t)) = M(\psi(t), x(t))$$

2) at terminal time t_1 the relations

$$\psi(t_1) \leq 0 ; \quad M(\psi(t_1), x(t_1)) = 0$$

are satisfied.

In equation (1), the matrix A defines a linear transformation of n dimensional space in n dimensional space, and matrix B defines a transformation of r dimensional space into n dimensional space.

Hence, $A : X \to X$ and $B : E_r \to X$

Writing equation (1) in vector form gives

$$\dot{x} = A x + B U \tag{5}$$

In the solution of linear time optimal control the following three conditions need to be satisfied:

(1) the equations of motion of the system are linear;

(2) the prescribed terminal state x^i, coincides with the origin of $x^1, \ldots x^n$ space

(3) the control region U is an r -dimensional polyhedron; moreover, the origin of $u^1 \ldots u^r$ space belongs to , but is not a vertex of, this polyhedron.

Apart from the above-mentioned conditions, a further condition known as the general position condition is applied on the co-efficients of equation (5), which states that , for every vector ω which has the direction of one of the edges of U , the vector $B\omega$ has the property that it does not belong to any proper subspace of X which is invariant under the operator A; i.e. the vectors

$$B\omega, \quad AB\omega, \quad \ldots\ldots\ldots \quad A^{n-1}\omega$$

are linearly independent in X.

In this case the function $H(\psi, x, u)$ has the form

$$H = (\psi, Ax) + (\psi, BU)$$

and the auxiliary variable can be written as :

$$\frac{d\psi_j}{dt} = -\sum_{\nu=1}^{n} a_j^{\nu} w_{\nu}, \quad j = 1, \ldots n$$

or in the vector form

$$\frac{d\,\psi}{dt} = A^{*}\,\psi \qquad (6)$$

where A^{*} is the matrix obtained from A by transposition. H, considered as the function of u attains its maximum with the function (ψ, Bu). If $u(t)$ is an optimal control, then there exists a solution of $\psi(t)$ of equation

$$(\psi(t), Bu(t)) = P(\psi(t)) \qquad (7)$$

The above discussions then leads to the following theorems :

Theorem 2

Relation 7 uniquely determines the control function $u(t)$ for each non-trivial solution of $\psi(t)$. In addition $u(t)$ is piecewise constant and all its values are the vertices of polyhedron U.

Theorem 3

Suppose the control region U is a parallelopiped and all eigenvalues of the system are real, then theorem 2 is true, and the control function $u(t)$ does not have more than n - 1 switchings where n is the order of the system.

References

II.1. ' Computer-Aided Control System Design '
H.H. Resenbrock , Academic Press 1974

II.2. ' The Mathematical Theory of Optimal Processes '
L.S. Pontryagin et al. J.Wiley & Sons , 1962.

II.3. ' Mathematical Methods of Optimal Control.'
V.G. Boltyanskii. Holt, Rinehart and Winston, Inc. 1971.

APPENDIX III

System Identification

A non-repetitive signal x (t) can be expressed by the Fourier transform :

$$x(t) = \frac{1}{2\pi} \int_{-\infty}^{\infty} X(j\omega).e^{j\omega t} \, d\omega \qquad (1)$$

where

$$x(j\omega) = \int_{-\infty}^{\infty} X(t).e^{-j\omega t} \, dt \qquad (2)$$

$X(j\omega)$ is called the Fourier spectrum of x (t).

If the input x (t) to a system is represented by a series of impulses and the impulse response h (t) of the system is known , then the output of the system is given by summing the response of all the impulses. Then convolution or superposition integral is

$$y(t) = \int_{0}^{\infty} h(\tau) \; x(t-\tau) \; d\tau \qquad (3)$$

It is assumed that the input x (t) to the system has commenced in the remote past. The lower limit of the integrand may be changed to $-\infty$, since $h(\tau) = 0$ for $\tau < 0$ for a physically realisable system. Taking the Fourier transform of eqn. (3) gives

$$Y(j\omega) = \int_{-\infty}^{\infty} \left[\int_{-\infty}^{\infty} h(\tau) \; x(t-\tau) \; d\tau \right] e^{-j\omega t} \, dt$$

Interchanging the order of integration and multiplying the inner bracket by $e^{j\omega t}$ gives

$$Y(j\omega) = \int_{-\infty}^{\infty} h(\tau) \left[\int x(t-\tau)\, e^{-j\omega(t-\tau)} dt \right] e^{-j\omega\tau} d\tau$$

Changing the variable of integration results in

$$Y(j\omega) = \int_{-\infty}^{\infty} h(\tau)\, e^{-j\omega\tau}\, d\tau \int_{-\infty}^{\infty} x(z)\, e^{-j\omega z}\, dz$$

$$Y(j\omega) = G(j\omega)\, x(j\omega)$$

$$\therefore \quad X(j\omega) = \frac{Y(j\omega)}{G(j\omega)} \qquad (4)$$

The Autocorrelation function $R_{xx}(\tau)$ of a stationary (time invariant probability characteristics) random signal is

$$R_{xx}(\tau) = E\left[x(t) \cdot x(t+\tau) \right]$$

$$= \lim_{T \to \infty} \frac{1}{2T} \int_{-T}^{+T} x(t).\, x(t+\tau)\, d\tau \qquad (5)$$

Similarly cross correlation function $R_{xy}(\tau)$ of two signals is

$$R_{xy}(\tau) = \lim_{T \to \infty} \frac{1}{2T} \int_{-T}^{+T} x(t)\, y(t+\tau)\, d\tau \qquad (6)$$

The power spectral density of a random signal x (t) is defined as the Fourier transform of the auto correlation function

$$\Phi_{xx}(\omega) = \int_{-\infty}^{\infty} R_{xx}(\tau)\, e^{-j\omega\tau}\, d\tau \qquad (7)$$

and the cross spectrum is

$$\Phi_{xy}(j\omega) = \int_{-\infty}^{\infty} R_{xy}(\tau)\, e^{-j\omega\tau}\, d\tau \qquad (8)$$

A useful measure of the statistical independence of two signals x (t) and y (t) is given by the coherency function defined by

$$K_{xy}^{2}(\omega) = \frac{|\Phi_{xy}(j\omega)|^{2}}{\Phi_{xx}(\omega)\,\Phi_{yy}(\omega)} \qquad (9)$$

Convolution integral can be written as

$$y(t) = \int_{-\infty}^{\infty} h(s)\, x(t-s)\, ds$$

Then substitution in eqn. (b) gives

$$Rxy(\tau) = \lim_{T\to\infty} \frac{1}{2T} \int_{-T}^{\tau} x(t) \left[\int_{-\infty}^{\infty} h(s)\, x(t+\tau-s)\, ds \right] dt$$

$$Rxy(\tau) = \int_{-\infty}^{\infty} h(s)\, R_{xx}(\tau - s)\, ds \qquad (10)$$

Equation 10 implies that if the input signal approximates to white noise so that the autocorrelation is an impulse, then the cross correlation function is proportional to the impulse response of the system. This provides a practical method for determining the impulse response of a system.

From definitions in eqn (8) and (10)

$$\Phi_{xy}(j\omega) = \int_{-\infty}^{\infty}\int_{-\infty}^{\infty} h(s)\left[R_{xx}(\tau - s)\, e^{-j\omega(\tau - s)}\right] e^{-j\omega s}\, d\tau\, ds$$

Where the inner bracket has been multiplied by $e^{-j\omega s}$.

Changing the variable of integration gives

$$\Phi_{xy}(j\omega) = \int_{-\infty}^{\infty} h(s)\, e^{-j\omega s}\, ds \int_{-\infty}^{\infty} R_{xx}(z)\, e^{-j\omega z}\, dz$$

The first term on the right hand side is the frequency response function $G(j\omega)$ and the second term is the power spectral density $\Phi_{xx}(\omega)$. Hence

$$G(j\omega) = \frac{\Phi_{xy}(j\omega)}{\Phi_{xx}(\omega)} \qquad (11)$$

The above expression provides a useful method for system identification.

REFERENCES

III.1 " Continuous and Discrete Signal and System Analysis . " C.D.McGillen, G.R.Cooper. Holt, Rinehart and Winston Inc. 1974.

III.2 " Measurements and Analysis of Random Data. " J.S.Bendal , A.G.Piersol. Wiley , 1966

APPENDIX IV

ENGINE PERFORMANCE MAPS

This appendix contains the steady state fuel consumption and emissions maps of the engine (Fig. 1 to 8). These maps were drawn by a computer and therefore it was necessary to arrange the data in the form of an mxm matrix. This necessitated an extrapolation of the data beyond the maximum power outputs at some engine speed. The contour lines in the performance maps that occur beyond the maximum engine torque levels should be ignored.

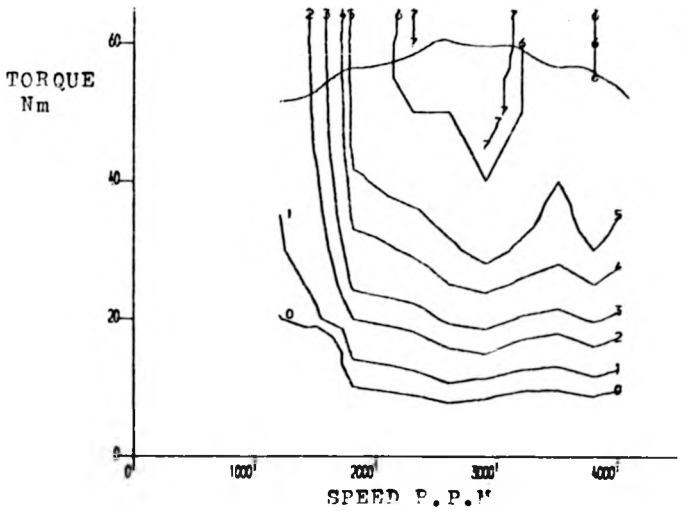

CONTOUR NO.	S.F.C (LB/BHP.HR)
0	1.2
1	1.0
2	0.8
3	0.7
4	0.6
5	0.55
6	0.5
7	0.49

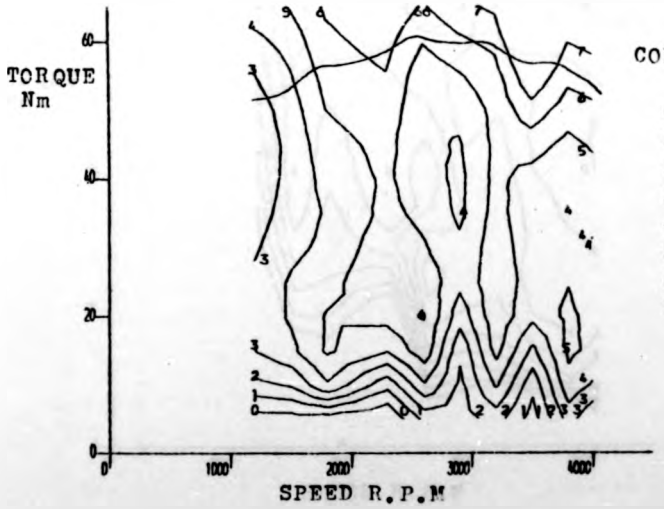

CONTOUR NO.	S.N.O (G/kW.HR)
0	6
1	9
2	12
3	15
4	18
5	21
6	24
7	27

CONTOUR MAPS OF S.F.C AND S.N.O WITH FOUR CYLINDERS OPERATING.

FIG. 1.

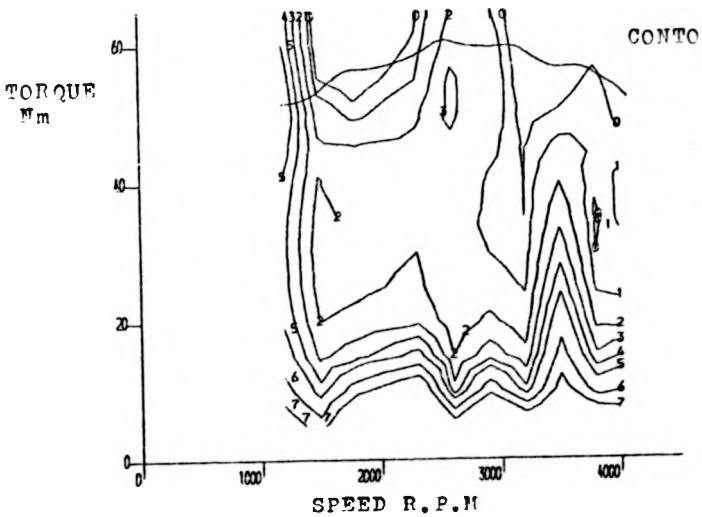

CONTOUR NO.	S.C.O (G/kW.HR)
0	15.0
1	20.0
2	30.0
3	40.0
4	50.0
5	60.0
6	80.0
7	100.0

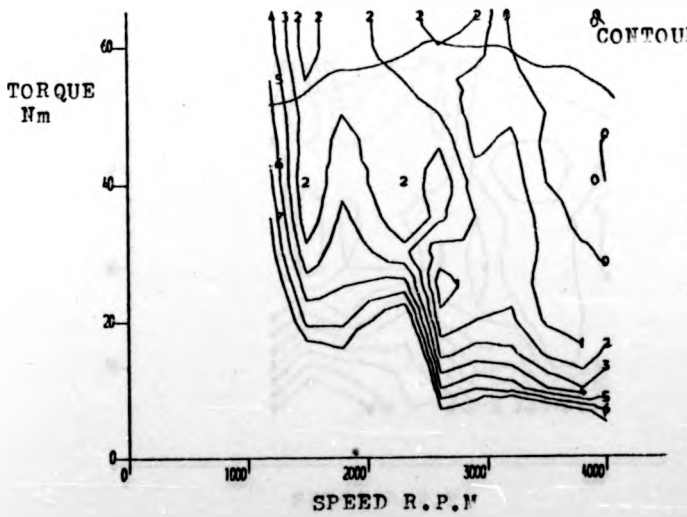

CONTOUR NO.	S.H.C (G/kW.HR)
0	1.8
1	2.4
2	3.0
3	3.6
4	4.2
5	4.8
6	5.4
7	6.0

CONTOUR MAPS OF S.C.O AND S.H.C WITH FOUR CYLINDERS OPERATING.

FIG.2

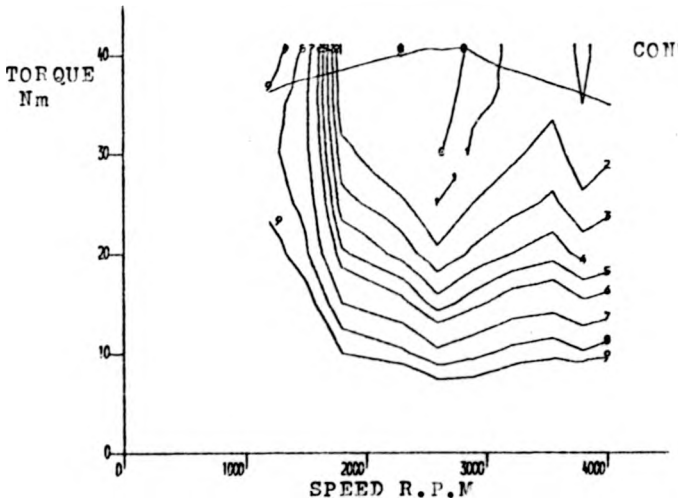

CONTOUR NO.	S.F.C (LB/BHP.HR)
0	0.5
1	0.55
2	0.6
3	0.65
4	0.7
5	0.75
6	0.8
7	0.9
8	1.0
9	1.1

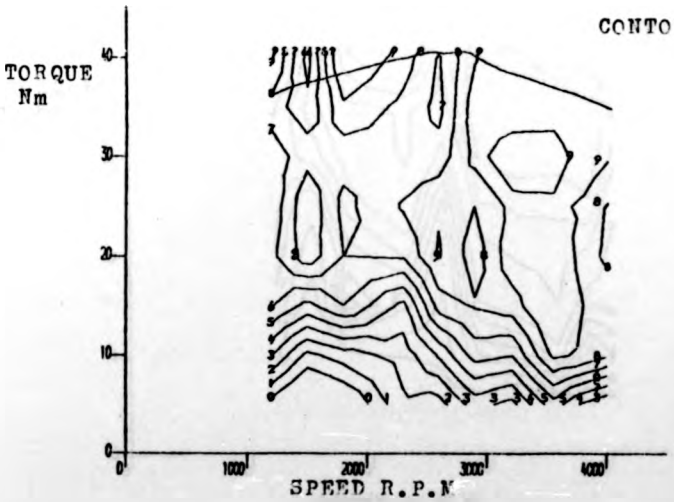

CONTOUR NO.	S.N.O (G/kW.HR)
0	9.0
1	10.5
2	12.0
3	13.5
4	15.0
5	16.5
6	18.0
7	19.5
8	21.0
9	22.5

CONTOUR MAPS OF S.F.C AND S.N.O WITH THREE CYLINDERS OPERATING.

FIG.3

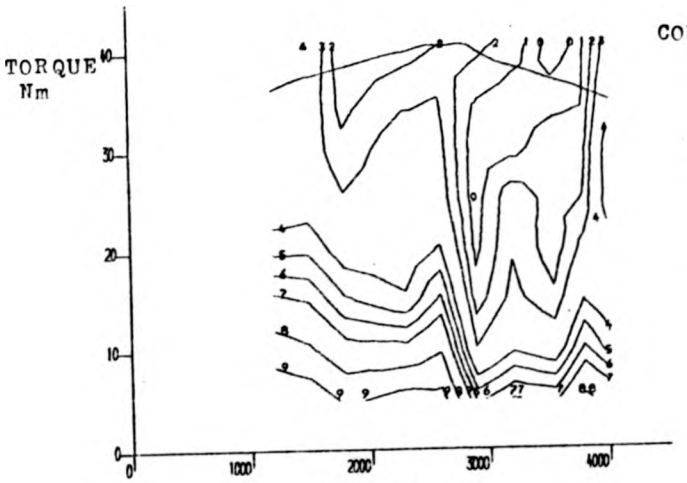

CONTOUR NO.	S.C.C (G/kW.HR)
0	15.0
1	20.0
2	30.0
3	40.0
4	60.0
5	70.0
6	80.0
7	90.0
8	110.0
9	130.0

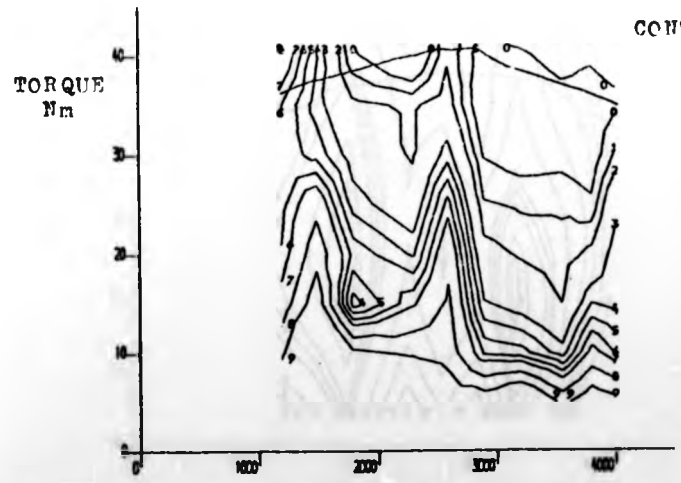

CONTOUR NO.	S.F.C (G/kW.HR)
0	2.4
1	2.7
2	3.0
3	3.6
4.	3.9
5	3.2
6	4.5
7	4.8
8	5.4
9	6.0

CONTOUR MAPS OF S.C.C AND S.F.C WITH THREE CYLINDERS OPERATING.

Fig.4.

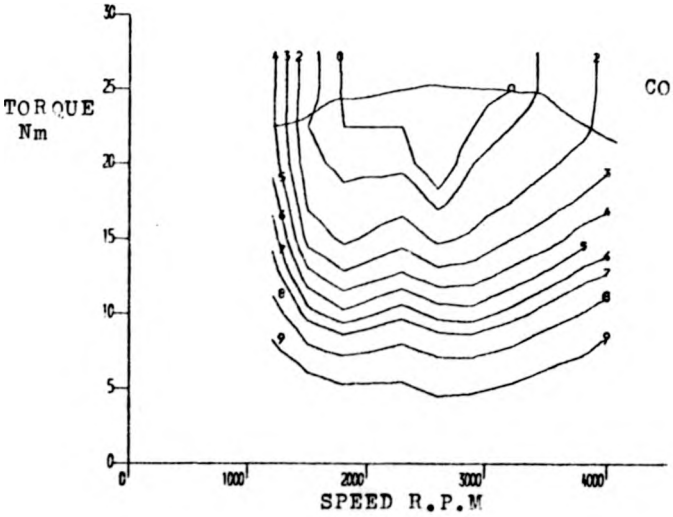

CONTOUR NO.	S.F.C (LB/BHP.HR)
0	0.58
1	0.6
2	0.65
3	0.7
4	0.75
5	0.8
6	0.85
7	0.9
8	1.0
9	1.2

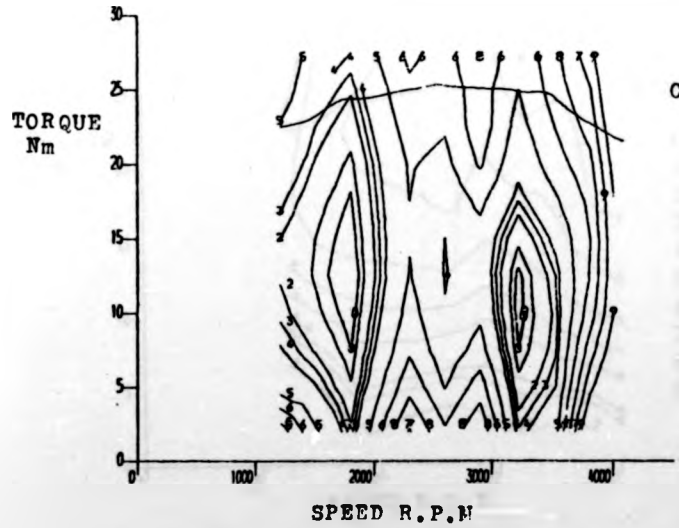

CONTOUR NO.	S.F.C (G/kW.HR)
0	26.25
1	27.00
2	28.50
3	29.25
4	30.00
5	33.00
6	36.00
7	42.00
8	39.00
9	45.00

CONTOUR MAPS OF S.F.C AND S.F.C WITH TWO CYLINDERS OPERATING.

Fig.5.

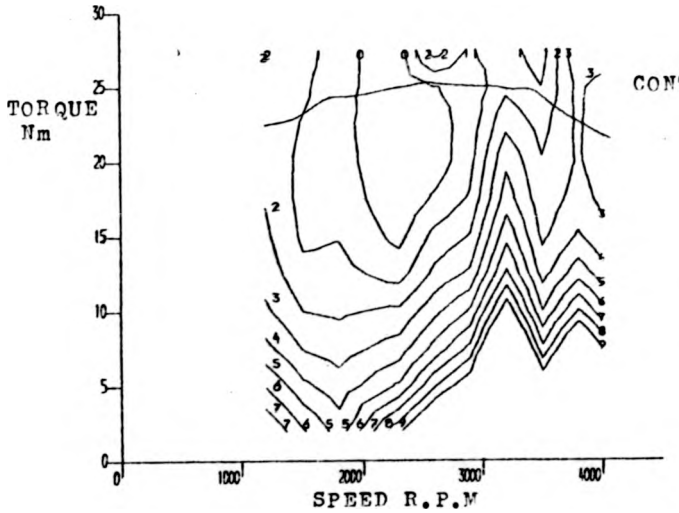

CONTOUR NO.	S.C.O (G/kW.HR)
0	15.0
1	20.0
2	25.0
3	30.0
4	35.0
5	40.0
6	45.0
7	50.0
8	55.0
9	60.0

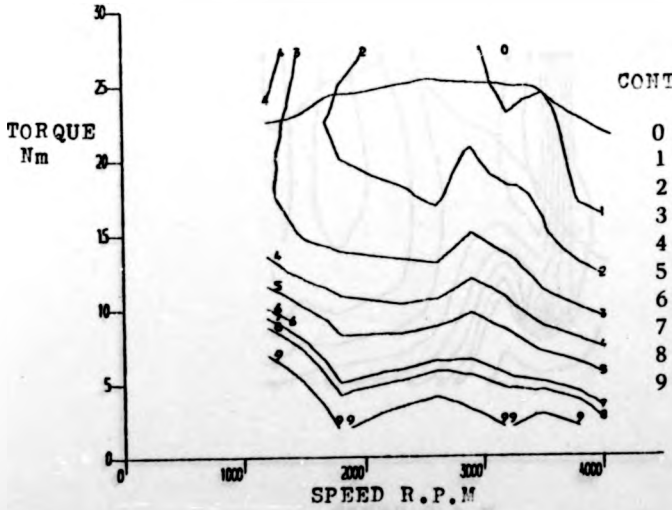

CONTOUR NO.	S.H.C (G/kW.HR)
0	2.85
1	3.00
2	3.6
3	4.2
4	4.8
5	5.4
6	6.0
7	6.3
8	6.6
9	7.5

CONTOUR MAPS OF S.C.O AND S.H.C WITH TWO CYLINDERS OPERATING.

Fig.6.

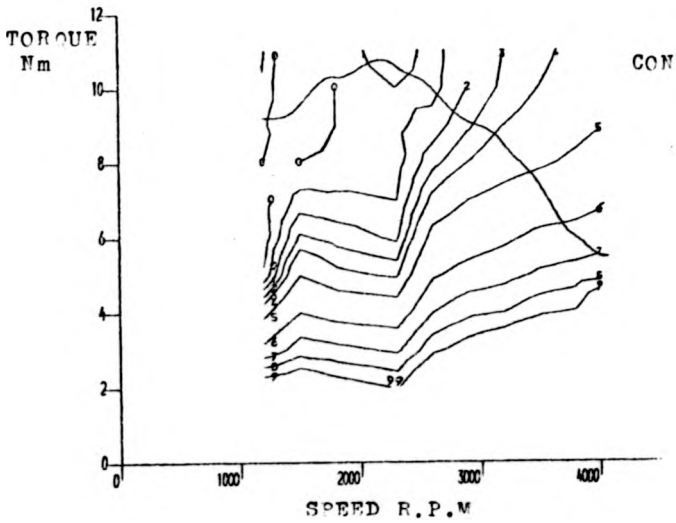

CONTOUR NO.	S.F.C (LB/BHP.HR)
0	1.1
1	1.15
2	1.2
3	1.25
4	1.3
5	1.4
6	1.6
7	1.8
8	2.0
9	2.2

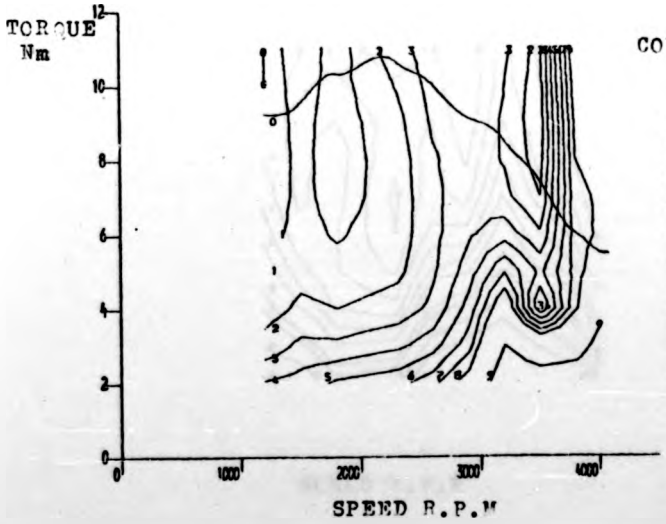

CONTOUR NO.	S.N.O (G/kW.HR)
0	30.0
1	37.5
2	45.0
3	52.5
4	60.6
5	67.5
6	75.0
7	82.5
8	90.0
9	120.0

CONTOUR MAPS OF S.F.C AND S.N.O WITH ONE CYLINDER OPERATING.

Fig.7

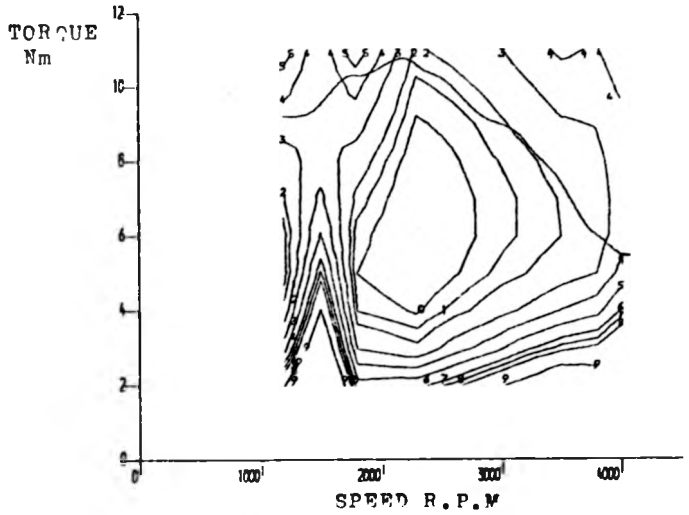

CONTOUR NO.	S.C.O (G/kW.HR)
0	10.0
1	11.0
2	12.0
3	14.0
4	16.0
5	18.0
6	20.0
7	21.0
8	22.0
9	25.0

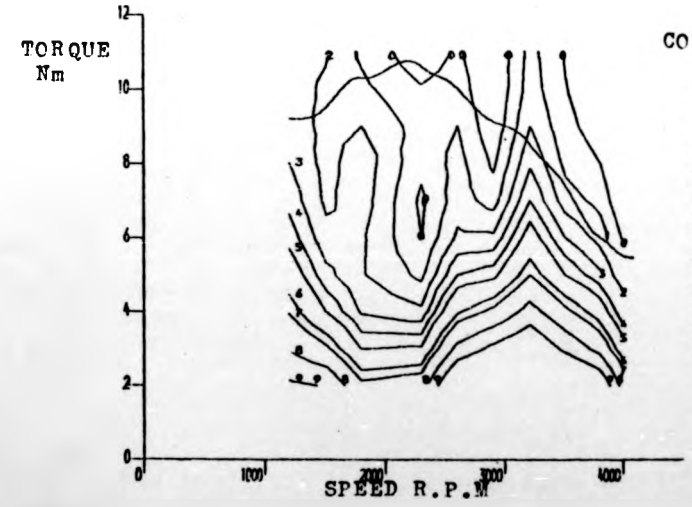

CONTOUR NO.	S.H.C) (G/kW.HR)
0	4.2
1	4.8
2	5.4
3	6.0
4	6.6
5	7.2
6	8.4
7	9.0
8	10.5
9	12.0

CONTOUR MAPS OF S.C.O AND S.H.C WITH ONE CYLINDER OPERATING.

Fig. 8